

# **The paracrine effect of normoxic and hypoxic cancer secretions on blood-brain barrier endothelial cells**



**By**

**Mariam Abobaker.M.Rado**

MSc Integrative Cellular biology

Student number: 3580480

A thesis submitted in fulfillment of the requirements for the degree of Doctor of  
Philosophy in the Department of Medical Bioscience, Faculty of Science,  
University of the Western Cape

**Supervisor**

Prof. David W Fisher

**Co-supervisor**

Dr. Brian T Flepisi

**January 2022**

# Abstract

Cancer is the most common leading cause of death worldwide. Glioblastoma and breast cancer are the most aggressive solid tumour. The survival rate of these tumours depends on their ability to progress and spread. These cancers use their high proliferative capabilities for survival, increasing their malignancies. Glioblastoma is considered the most aggressive tumour initiated in the brain, whereas breast cancer is the most common metastatic cancer in the brain, both types of cancer are known as high infiltrated cancer and their invasiveness due to their capability to release factors that can alter the neighbouring cells to facilitate their progression.

On the other hand, the brain remains a vital organ where the blood-brain barrier (BBB) plays a protective and homeostasis role, thus ensuring optimum brain function. The endothelial cells are the functional site of the BBB; these cells, with assistance from other brain cells such as astrocytes and pericytes, maintain the BBB protective function. The literature revealed perturbations and disruption in the BBB integrity in glioblastoma and metastatic breast cancer. The endothelial cells and other components of the BBB have been morphologically altered, resulting in impacting the BBB integrity.

The interaction between cancer cells and brain endothelial cells is a complex scenario that is not entirely illustrated; however, a vital role in the crosstalk between cancer cells and endothelial cells is played by signalling mediated by soluble factors that can further promote cancer progression. This study aimed to investigate whether the secretions from glioblastoma and breast cancer cells could influence the brain endothelial cells.

Brain endothelial cells (bEnd.3) were cocultured with glioblastoma (U-87) or breast cancer (MCF7) cells or subjected to their conditioned media. To mimic the heterogeneous

physiological conditions of the solid tumour such as glioblastoma and breast cancer, U-87 and MCF7 cells were cultured under normoxia (to reflect cancer cells exposed to oxygen levels in the perivascular regions of the tumour) or hypoxia (to reflect the hypoxic tumour area where invasive cancer cells are detached and invade the surrounding tissue forward to the blood vessels).

Our findings underlined the involvement of paracrine secretion of cancer cells in modulating brain endothelial cells' properties. Our data suggested that both cancer secretions derived from normoxia and hypoxia rendered changes in the brain endothelial cells at the level of mitochondrial activity. To investigate whether the exerted effects were associated with the acquisition of the brain endothelial resistance, we screened the trans-electrical endothelial resistance (TEER) of brain endothelial cells after exposure to cancer secretions. Our findings revealed a decrease in TEER of the exposed brain endothelial cells. Moreover, gene expression of the tight junction (Claudin-5 and Occludin) were quantified in brain endothelial cells (bEnd.3) after exposure to normoxic and hypoxic cancer secretion using real-time qPCR; results showed upregulation of Claudin-5 after exposure to normoxic and hypoxic cancer secretion. Occludin gene expression was also upregulated after exposure to normoxic cancer secretion; however, the exposure to hypoxic cancer secretion decreased Occludin gene expression.

In addition, the proliferation of endothelial cells (bEnd.3) exposed to cancer secretion was measured by cell counting, followed by analyzing the cell cycle; results showed that long-term exposure to cancer secretion suppressed the proliferation of brain endothelial cells (bEnd.3), mostly after exposure to hypoxic cancer secretion. Cells were accumulated in the G1 phase. Overall, data suggest that factors secreted from normoxic and hypoxic cancer cells modulate brain endothelial cells, affecting their function.

## Keywords

Blood-brain barrier

Glioblastoma

Breast cancer

Hypoxia

Normoxia

Cancer secretions

Brain endothelial cells

Mitochondrial activity





## Declaration

I declare that “The paracrine effect of normoxic and hypoxic cancer secretions on blood-brain barrier endothelial cells” is my original work that has not been submitted before for any degree or examination in any other university. During the review of published data and literature, all the sources I have used or quoted have been indicated and acknowledged by complete references.



Mariam Abobaker.M.Rado

Signature

A handwritten signature in black ink, followed by the initials "MR" in red.

January 2022

# Acknowledgements

I wish to return all glory to the Almighty ALLAH, who has been my Ultimate source of inspiration and strength through the journey to the completion of this work

My profound gratitude goes to my supportive Supervisor and Co-supervisor, Prof. David W. Fisher and Dr Brian T Flepisi . I am grateful for their guidance, and I am fortunate to grow as a researcher under their supervision.

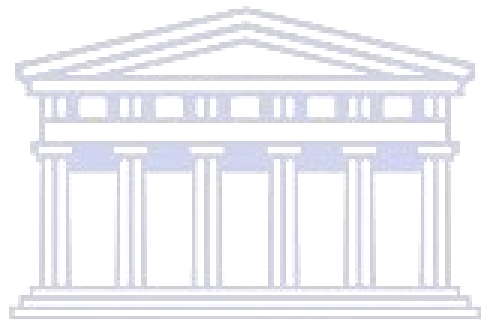
I wish to show appreciation to my laboratory colleagues in the Neurobiology laboratory and my friends and companions in the Department of Medical Bioscience.

I am grateful for the support of my immediate and close family members, my brothers and sisters, for their support throughout my stay far away from home to complete the work of this study.

Finally, my deepest and most sincere appreciations go to my husband, Mr Saleh abdulnabi and our lovely children Miss. Ghufra abdulnabi and Mr Ali abdulnabi, and Miss Patool abdulnabi for their immense support.

## Dedication

To my children Miss. Ghufraan abdulnabi and Mr. Ali abdulnabi, and Miss Patool abdulnabi.



UNIVERSITY *of the*  
WESTERN CAPE

## List of Publications/conferences

- Olufemi Alamu, Mariam Rado, Okobi Ekpo, and David Fisher (2020). Differential Sensitivity of Two Endothelial Cell Lines to Hydrogen Peroxide Toxicity: Relevance for in Vitro Studies of the Blood-Brain Barrier. <https://doi.org/10.3390/cells9020403>
- Rado, M.; Flepisi, B.; Fisher, D. Differential Effects of Normoxic versus Hypoxic Derived Breast Cancer Paracrine Factors on Brain Endothelial Cells. *Biology* **2021**, *10*, 1238. <https://doi.org/10.3390/biology10121238>
- Rado, M.; Flepisi, B.; Fisher, D. The Effect of Normoxic and Hypoxic U-87 Glioblastoma Paracrine Secretion on the Modulation of Brain Endothelial. *MDPI Cells Journal* 2022. <https://www.mdpi.com/2073-4409/11/2/276>
- Rado, M.; B.; Fisher, D. The Paracrine Effect of Hypoxic and Normoxic Cancer Secretion on the Proliferation of Brain Endothelial Cells (bEnd.3). *MDPI Cells Journal* 2022. <https://www.mdpi.com/2073-4409/11/7/1197>.
- Conference Presentation: Glioblastoma and breast cancer alter the mitochondrial activity in brain endothelial cells: *in vitro* study. First Conference of Physiology society of SouthAfrica (PSSA) (12-15 September 2021).

## List of abbreviations

AA	Anaplastic astrocytoma
ABC	ATP-binding cassette
ACLY	ACLY
ACs	Astrocytes
AD	Alzheimer's Disease
AJs	Adherent junction
ANG-1	Astrocytic angiopoietin 1
AO	Anaplastic oligodendroglioma
AQP4	Aquaporin-4
AQP5	Aquaporin-5
ATP	Adenosine triphosphate
BCRP	Breast cancer resistance protein
BCSFB	Brain-cerebrospinal fluid barrier
BECs	Brain endothelial cells
BLBC	Basal-like breast cancers
BM	Basement membrane
BTB	Brain tumour barrier
CIS	Carcinoma in situ
CMTs	Carrier-mediated transporters
COXs	Cyclooxygenases
CP	choroid plexus
CSF	Cerebrospinal fluid
CSF	Cerebrospinal fluid
CSF1	Colony stimulating factor 1
DA	Diffuse astrocytoma
DCIS	Ductal carcinoma in situ
DO	Diffuse oligodendroglioma
E2F	E2 transcription factor
ECs	Endothelial cells
E-face	Exocytosplasmic fracture face
EGFR	Epidermal Growth Factor Receptor
EGFR	Epidermal growth factor receptor
EGFR	Epidermal Growth Factor Receptor
ER	Estrogen receptors
ET-1	Endothelin-1
FADH2/3	Flavin adenine dinucleotide
GABRA1	Gamma-Amino Butyric Acid A Receptor
GBM	Glioblastoma multiforme
GDNF	Glia-derived neurotrophic factor
GFAP	glial fibrillary acidic protein
GJs	Gap junctions

GLUT1	glucose transporter
GUK	guanylate kinase-like
HGF	Hepatocyte Growth Factor
HGFR	Hepatocyte growth factor receptor (HGFR)
HIF-1 $\alpha$	Hypoxia-inducible factor-1 $\alpha$
HO-1	Heme oxygenase-1
HP	Horseradish peroxidase
IDCs	Invasive ductal carcinomas
IDH	Isocitrate dehydrogenase
IL-1 $\beta$	Interleukin-1 $\beta$
IL-6	Interleukin-6
ILC	Invasive lobular carcinoma
INF- $\gamma$	Interferon gamma
ISF	Interstitial fluid
JAMs	Junctional adhesion molecules
LAMs	Leukocyte adhesion molecules
LCIS	Lobular carcinoma in situ
LOH	Loss of heterozygosity
MAGUKs	Membrane-associated guanylate kinase-like proteins
MAPK	Mitogen-activated protein kinase
MCT1/4	Monocarboxylate transporters
MDM	Murine double minute proteins
MDR	Multidrug resistance proteins
MET	Mesenchymal-epithelial transition factor
MET	Mesenchymal-epithelial transition factor
MHC II	Histocompatibility complexes
MLC	Myosin light chain
MLCK	Myosin light chain kinase
MMP	Metalloproteinase
MS	Multiple sclerosis
NADPH	NADPH
NADPH	Nicotinamide adenine dinucleotide phosphate
NF1	Neurofibromin 1
NF-K $\beta$	Nuclear Factor kappa-light chain enhancer of activated B cells
NO	nitric oxide
NOS	Nitric oxide synthase
NVU	Neurovascular unit
O <sub>2</sub>	Oxygen
PCs	Pericytes
PDGF/R	Platelet-derived growth factor /receptor
PDGFR-b/ $\beta$	Platelet-derived growth factor-b / $\beta$
PKD1/2	Phosphatidylinositol dependent kinase-1/2
PDZ-1/3	{Post synaptic density protein, Drosophila disc large tumor suppressor, and Zonula occludens protein}
PECAM-1	Platelet endothelial cell adhesion molecule-1
P-gp	P-glycoprotein

PHDs	prolyl hydroxylase domain family proteins
PIK3CA	Phosphatidylinositol-3-kinases
PKB	protein kinase B
PLC	Pregnancy and lactation cycle
PPP	Pentose phosphate pathway
PTEN	Phosphatase and Tensin Homolog
qRT-PCR	Real-time reverse transcription-polymerase chain reaction
RB	Retinoblastoma
RMT	Receptor-mediated transcytosis
ROS	Reactive oxygen species
RTK	Receptor tyrosine kinase
Shh	Sonic hedgehog
SLC12A5	Solute carrier family 12 members 5
SYT1	Synaptotagmin 1
TAM	Tumor associated macrophages
TCA	Tricarboxylic acid
TCGA	Cancer Genome Atlas
TECs	Tumour endothelial cells
TGF- $\beta$	Transforming growth factor-beta
TJs	Tight junctions
TME	The tumour microenvironment
TNBC	Triple-negative breast cancer
TNF $\alpha$	Tumor necrosis factor-alpha
TP53	Tumor protein 53
TSPs	Thrombospondins
VAP1	Vascular adhesion protein 1
VCAM1	Vascular cell adhesion molecule 1
VEGF	Vascular endothelial growth factor
WHO	The World Health Organization
ZO-1/2	Zonula occludens
$\alpha$ -KG	alpha-ketoglutarate
$\gamma$ -GTP	$\gamma$ -glutamyl transpeptidase

## List of figures

Figure 1. Cancer hallmarks where normal cells transform to cancerous cells (Fouad and Aanei, 2017). .....	8
Figure 2. A summarization of Receptor tyrosine kinase (RIK) and retinoblastoma (RB) signalling pathways involved in cancer. The binding of RIK receptors EGFR, PDGFR, and MET with their ligands EGF, PDGF, and HGF activate various signalling pathways of many cellular processes, such as cell growth, proliferation, and motility. These activations are mediated by a series of pathways, including PI3K/AKT, MAP Kinase, STAT3, Ras and JAK/STAT(Ozawa et al., 2010; Cruickshanks et al., 2017). PTEN regulates the AKT activity by inhibiting the phosphorylation of PI3K and controlling the conversion of PIP3 to PIP2. PTEN influences gene expression (Hopkins et al., 2014). PI3K is coded by PIK3CA and PIK3RI genes. Cell cycle portions (CDK/Cyclin) induce phosphorylation of RB to bind to the transcription factor E2F, which influences the transcription of growth genes needed for DNA synthesis. Ink4 family portions negatively regulate the RB activation(Crespo et al., 2015). Created by Biorender.com .....	11
Figure 3. A summarization of P53 pathway: Cells are exposed to different sources of stress, including endogenous and exogenous stresses, that activate P53 via a series of cellular responses that rely on the type and degree of insults. P53 activate the expression of genes responsible for cell cycle arrest, DNA repair. MDM2 binding to P53 to inhibit its activity. The P53 pathway is vital to maintaining cellular homeostasis. This pathway is either mutated or lost in cancer cells, thus promoting cancer progression. Modified from (Hu et al., 2021). ...	13
Figure 4. Genetic alterations involved in glioblastoma (GBM). Modified from (Joshi, 2015). .....	19
Figure 5. The anatomy of the female breast, the areola, lobules, and ducts are indicated. ....	21
Figure 6. The classification of breast cancer. HER2: human epidermal growth factor receptor 2 (Sharma et al., 2019). .....	23
Figure 7. Metastatic cascade through the blood capillary: At the primary tumour site, cancer cells are highly proliferated, and have the ability to detach from the tumour and invade into the surrounded tissues. Some of the cancer cells successfully invade the extracellular matrix and reach the blood vessel. Cancer cells enter the blood vessel through the endothelial cell-cell connection (via the endothelial tight junction). Cancer cells use the blood vessel to spread into new locations. Cancer cells are arrested at the endothelial surface and preparing to extravasate into the new place; at this step, a cross-talk occurs between cancer cells and endothelial cells via soluble factors and the physical endothelial-cancer cells adhesion to facilitate the extravasation between the endothelial cells (also called endothelial migration	



(TEM)). After the extravasation, a few cancer cells adapt to the new place and proliferate to arise the secondary tumour tissue. However, some metastatic cancer cells enter into the dormancy, but the majority of metastatic cancer cells die after the extraversion (Reymond et al., 2013).	26
Figure 8. Schematic diagram representing the neurovascular unit (NVU): (EC)endothelial cell is lined at the luminal side of the capillary and connected by the tight junction. On the abluminal side, pericytes (PC) incompletely covers the endothelial cell separating (BL) basal lamina of the basement membrane. Astrocytes (AC) endfeet envelop the capillary and are connected to the basement membrane(MG) macroglia cells, the immune defence agent in the brain(Islam and Mohamed, 2015).	31
Figure 9. The above scheme shows examples of the correlation between NVU components which result in the BBB function. 5-HT:5-hydroxytryptamine, Ach: Acetylcholine, NE: norepinephrine. GABA: neurotransmitter $\gamma$ -aminobutyric acid. Modified from (Arshad et al., 2010).	32
Figure 10. Comparison between the brain and systemic capillary. Endothelial cells are tightly connected by tight junctions in the brain capillary and entirely covered by astrocytes endfeet. In the peripheral capillary, tight junctions also hold endothelial cells; however, they are less tighter and permeable for large types of substances and cells. The astrocytes cover is absent (Boonstra et al., 2015).	34
Figure 11. location of pericyte in the NVU, Pericyte is embedded in the basal membrane. It is the cellular mediator between endothelial cells and astrocytes (Yang et al., 2017).	35
Figure 12. Interaction between cellular components in the neurovascular unit(NVU). Endothelial cells link each other by tight junctions (Claudins, Occludin and JAMs (junctional adhesion molecules), the adherent junction (VE-cadherin (bind to F-actin by catenins), and gap junction, PECAM-1 (platelet endothelial cell adhesion molecule-1), and Nectin). Pericytes interact with endothelial cells via gap junctions(GJ), adhesion N-cadherin and growth factor signalling. TJ (tight junctions). DHA (docosahexaenoic acid). MFSD2a (Major facilitator domain-containing protein 2A). Astrocytes release apolipoprotein E (ApoE3 and ApoE4). ApoE3 binds to LRP1 (lipoprotein receptor-related protein 1) in pericytes, resulting in the suppression of the CypA (cyclophilin A), which activate the nuclear factor-kB (NFkB) MMP-9 pathway, causing TJ and BM degradation. SSeCKS (Src-suppressed C-kinase substrate) secreted from astrocytes induce the expression of TJ in endothelial cells. Increase the release of $Ca^{2+}$ in response to neural activity. GJs connect the adjacent astrocytic endfeet (Zhao et al., 2015).	36
Figure 13. Astrocytes as mediator connection between endothelium and the neuron (Cardoso et al., 2010).	40
Figure 14. The structure of tight junctions (N. Joan Abbott et al., 2006).	43

Figure 15. Schematic diagram illustrating the BBB function. A- Paracellular barrier, B- Transcellular barrier, C-Enzymatic barrier, D- Efflux transport to protect the brain from neurotoxins and drugs, E- Transport of the nutrition into the brain, F- Remove the metabolites from the brain. Modified from (Wilhelm and Krizbai, 2014). ....	48
Figure 16. The transport of molecules across the blood-brain barrier (Rocha, 2013). ....	51
Figure 17. Diagram summarizes the inflammatory events in Blood brain barrier. Modified from (Weidenfeller and Shusta, 2007). ....	53
Figure 18. Schematic presentation shows the difference between brain edema types which associated with CNS disease, in the brain tumor, the vasogenic edema is always observed (Cherian et al., 2018). ....	70
Figure 19. Schematic demonstration of the tumour regions of solid tumors based on oxygen concentration (Al Tameemi et al., 2019). ....	71
Figure 20. HIF regulation under normoxic and hypoxic conditions (Walsh et al., 2014). ....	73
Figure 21. Metabolic difference between cancer and healthy cells. PPP (Pentose phosphate pathway). K (Krebs cycle). ATP (adenosine triphosphate) (Oronsky et al., 2014). ....	76
Figure 22. Overview of glucose and glutamine catabolism in the cells in normoxia (aerobic condition) and hypoxia (in cancer cells): In normoxia, cells use glucose and glutamine to produce the biomass via the tricarboxylic acid cycle (TCA). In hypoxia, cancer cells mainly convert glucose to lactate. Hypoxic cancer cells use the TCA independently than glucose to produce lipid for their growth by reversing the TCA. a-ketoglutarate generated from glutamine can convert to isocitrate by isocitrate dehydrogenase (IDH) (Reductive carboxylation (Red arrows) (Zaravinos and Deltas, 2014). ....	78
Figure 23. Metabolism in healthy endothelial cells. Glycolysis: the broken-down pathway of glucose to pyruvate, resulting 2 molecules of ATP(adenosine triphosphate). Pyruvate transfer to mitochondria to enter TCA (tricarboxylic acid cycle). Lactate is converted from pyruvate then exported from the cells. PFKFB3 (6-phosphofructo-2-kinase/fructose-2,6-biophosphatase3, activator of glycolysis. G6P (Glucose-6-phosphate), 1,3BPG (1,3-bisphosphoglycerate). PPP (Pentose phosphate pathway), side branch from the glycolysis; R5P (ribose-5-phosphate), Ru5P(ribulose-5-phosphate). PPP produces NADPH (nicotinamide adenine dinucleotide phosphate) used to catalyse the conversion of GSSG (oxidize glutathione) to GSH (glutathione). HPB (Hexosamine biosynthetic pathway), other side branches of glycolysis pathway, DHAP(dihydroxyacetone), HPB produces pro-duces N-acetylglucosaminewhich is important for N-linked and O-linked glycosylation. Glutamine metabolism( glutamine converts to glutamate then to a-ketoglutarate (not shown) in TCA. FA (Fatty acids pathway); FA enter the mitochondria and produces acetyl CoA to enter TCA, CPT1(carnitine palmitoyltransferase1) (de Zeeuw et al., 2015). ....	81

## List of tables

Table 1: Description of Gliomas developed from astrocytes .....	16
Table 2: Summarization of tight junctions at the blood-brain barrier (BBB). ....	43



UNIVERSITY *of the*  
WESTERN CAPE

# List of contents

Abstract.....	I
Keywords.....	III
Declaration.....	IV
Acknowledgements.....	V
Dedication.....	VI
Publications/conferences.....	VII
List of abbreviations.....	VIII
List of figures.....	XI
List of tables.....	XIV
List of contents.....	XV
CHAPTER 1.....	1
Introduction.....	1
1.1. Background .....	1
1.2. Rationale of the study.....	3
1.3. Aim of the study.....	4
1.4. Objective of the study.....	5
1.5. Significance of the study.....	5
1.6. Scope.....	6
1.7. Chapter summary.....	6
CHAPTER 2.....	7
Literature review.....	7
2.1. Overview of cancer.....	7
2.1.1. Overview of cancer types used in this study.....	14

2.1.1.1. Brain tumour.....	14
2.1.1.2. GBM in brain tumour classifications.....	15
2.1.1.3.Types of glioblastoma (GBM).....	17
2.1.1.4. Biology of glioblastoma.....	19
2.1.1.5. Over view of Breast Cancer.....	20
2.1.1.6. Functional anatomy of the breast.....	20
2.1.1.7. Breast Cancer.....	22
2.1.1.8. Breast cancer metastasis to the brain.....	24
2.2. Overview of the Blood-Brain Barrier (BBB).....	29
2.2.1. History of the BBB.....	29
2.2.2. The location of the BBB.....	30
2.2.3. The neurovascular unit (NVU).....	31
2.2.3.1. Brain Endothelial Cells.....	32
2.2.3.2. Supporting component of the BBB.....	34
2.2.3.2.1. Pericytes (PCs).....	34
2.2.3.2.2. Basement membrane (BM).....	37
2.2.3.2.3. Astrocytes (ACs).....	39
2.2.3.3. Brain endothelial cell-cell interaction.....	41
2.2.3.3.1. Junctional proteins complex.....	41
2.2.3.3.1.1. Claudins.....	44
2.2.3.3.1.2. Occludin.....	44
2.2.3.3.1.3. Junctional adhesion molecules (JAMs).....	45
2.2.3.3.1.4. The cytoplasmic plaque proteins.....	45
2.2.3.3.1.5. Adherence junctions(AJs).....	46
2.2.4. The function of the blood-brain barrier.....	46
2.2.5.Transport at the blood-brain barrier.....	49

2.2.6. Factors that modulate the BBB permeability.....	52
2.2.6.1. Inflammation.....	52
2.2.6.2. Reactive Oxygen species (ROS).....	55
2.2.7. Mechanisms that influence the BBB permeability.....	56
2.2.7.1. Mechanisms influence the paracellular permeability.....	56
2.2.7.2. Mechanisms influence the transcellular permeability at the BBB.....	58
2.3. Brain tumour environment.....	59
2.3.1. Blood-brain barrier state in the tumour environment.....	59
2.3.1.1. Brain endothelial cells in the tumour environment.....	60
2.3.1.2. Alterations of Tumour-endothelial cells.....	61
2.3.1.3. Tumor-Endothelial cells interaction ways.....	63
2.3.1.4. Pericytes state in the tumour environment.....	65
2.3.1.5. Basal membrane alteration in the tumour environment.....	66
2.3.1.6. Astrocytes state in the tumour environment.....	67
2.3.2. Features of the BBB disruption in the tumour environment.....	68
2.3.2.1. Oedema formation.....	68
2.3.3. Hypoxic tumour environment.....	70
2.4. Overview of cancer metabolism.....	75
2.4.1. Cancer secretion.....	79
2.5. Endothelial metabolism in the tumour environment.....	80
References.....	84
CHAPTER 3.....	110
PUBLISHED MANUSCRIPT “Differential Effects of Normoxic versus Hypoxic Derived Breast Cancer Paracrine Factors on Brain Endothelial Cells” .....	110
CHAPTER 4.....	130
PUBLISHED MANUSCRIPT “The Effect of Normoxic and Hypoxic U-87 Glioblastoma Paracrine Secretion on the Modulation of Brain Endothelial Cells” .....	130

CHAPTER 5.....	154
PUBLISHED MANUSCRIPT “The paracrine effect of hypoxic and normoxic cancer secretion on the proliferation of brain endothelial cells (bEnd.3)” .....	154
CHAPTER 6.....	169
General conclusions and recommendations.....	169
6.1. General conclusion.....	169
6.2. Recommendations.....	171



UNIVERSITY *of the*  
WESTERN CAPE

# CHAPTER 1

## Introduction

### 1.1. Background

Cancer remains a worldwide public health problem, with an estimated 18 million cases per year, of which 9.5 million cases were in men and 8.5 million in women (World Health Organisation, 2018). Cancer is expected to rank as the leading cause of death and the single most important barrier to increasing life expectancy worldwide in the 21st century. According to estimates from the World Health Organization (WHO) in 2015, cancer is the main cause of death before the age of 70 years (Bray *et al.*, 2018). The most common cancers are lung and breast cancers. They represent 12.3% of all cancer cases worldwide, whereas other types of cancer such as brain cancer, represent 1.7 % (World Health Organisation, 2018).

Cancer can arise and develop in the same site ( non-metastatic cancer) or spread naturally from the site of origin to develop in another location ( metastatic cancer) (Thomas N. Seyfried<sup>1</sup>, 2013). The current study focused on brain and breast cancers. These cancers are well known as highly invasive cancers (Hatoum *et al.*, 2019; Watkins, 2019), The high-grade brain cancer cells (glioblastoma) arise and develop in brain tissue. Breast cancer is the second frequent metastatic cancer in the brain after lung cancer (Leone and Leone, 2015), and 30% of breast cancer patients develop metastatic breast cancer into the brain (Witzel *et al.*, 2016). Despite the technologically and clinically advanced research regarding the diagnosis and treatment, which improved the life expectancy of patients, the effective specific therapy for these types of cancer is yet non-existent, and many issues related with these cancer types still need to be investigated.



Glioblastoma and breast cancer cells were observed to manipulate their environments, and changes were observed in the surrounding tissues of these cancers. In this study, the focus was on the effect of glioblastoma and breast cancer cells on the brain endothelial cells.

Brain endothelial cells form a physical barrier separating the brain tissue and the blood, also called the blood-brain barrier (BBB). The BBB is a specialized, highly selective barrier that controls the movement (of molecules, cells and ions) between the peripheral circulation and the central nervous system (CNS) (Keaney and Campbell, 2015). Other brain cells, including astrocytes and pericytes provide structural and functional support to brain endothelial cells to maintain the BBB function.

The dysfunction of the BBB has been reported in CNS diseases (Profaci *et al.*, 2020; Xiao *et al.*, 2020), including primary and metastatic brain cancer (Arvanitis and Ferraro, 2020). The results of the BBB impairment are manifested in the accumulation of the plasma proteins leading to the formation of cerebral oedema (Stummer, 2016) also the penetration of blood cells in the brain tissue (Guan *et al.*, 2021).

Endothelial cells were reported to be morphologically and functionally altered by cancer (Baluk *et al.*, 2005; Mierke, 2011; Dudley, 2012; Hida and Maishi, 2018), in particularly in brain cancer (Charalambous *et al.*, 2005), which alters the BBB function. The endothelial abnormality during cancer includes a morphological abnormality (Hashizume *et al.*, 2000; Bussolati *et al.*, 2010), changes in the expression of tight junction proteins (Ishihara *et al.*, 2008), and the alteration in the transporter proteins (Demeule *et al.*, 2004). Despite the progress, the mechanisms behind these changes remain unclear.

The cross-talk between cancer cells and endothelial cells regulates these mechanisms. Cancer cells interact with endothelial cells physically or via secreted factors that impact

the physiological aspect of cancer and endothelial cells (Funasaka *et al.*, 2002; Kenig *et al.*, 2010; Krishnan *et al.*, 2015; Lee *et al.*, 2015; Choi and Moon, 2018).

Cancer cells are highly proliferative cells, and that increases the mass of cancer tumours, resulting in reduction in the availability of oxygen (O<sub>2</sub>), therefore, developing a low O<sub>2</sub> area (hypoxia) (Muz *et al.*, 2015; Xie and Simon, 2017). Hypoxia induces genetic and metabolic alteration in cancer cells in order to support their survival (Al Tameemi *et al.*, 2019).

The current study focused on the metabolic changes in the brain endothelial cells under the influence of brain and breast cancer secretions. The mitochondrial activities and other cellular processes related to the mitochondria (such as proliferation and endothelial integrity) were chosen as axis of this study.

Mitochondria is the key metabolic regulator that influences the cells' general health by providing metabolic energy and thus regulating various cellular processes, including ion homeostasis, proliferation, and apoptotic cell death (Tang *et al.*, 2014). Mitochondria also modulate the intracellular calcium (Davidson and Duchon, 2007), and play a role in maintaining the blood-brain barrier integrity (Doll *et al.*, 2015). Thus the disruption of the BBB may be initiated via the mitochondria damage (Dickman *et al.*, 2012).

## **1.2. Rationale of the study**

The crosstalk between the cancer cells and endothelial cells is crucial. It reflects the mechanism of cancer cells to re-programme endothelial cells, inducing their weakness to infiltrate into other tissues (Choi and Moon, 2018). Cancer cells do not grow far from the blood vessels to enable quick access to oxygen and nutrients required for the highly proliferating cells. In addition, they can cross to other tissues that are more suitable for their growth (Pezzella *et al.*, 2015). However, the mechanism by which cancer cells

interact with the components of the blood vessel, in particular the endothelial cells, is still largely unknown.

The endothelial-cancer interaction is initiated via soluble factors secreted from cancer and endothelial cells, attracting cancer cells toward endothelial cells (Lopes-Bastos *et al.*, 2016). To date, many studies have shown various mechanisms of endothelial disruption by factors secreted from cancer cells, which negatively affect the blood vessel homeostasis (Funasaka *et al.*, 2002; Schneider *et al.*, 2004; Dwyer *et al.*, 2012; Giusti *et al.*, 2016; Anchan *et al.*, 2020), but no focus on the paracrine effect of cancer secreted factors on the endothelial metabolism. Therefore, it remains necessary to investigate whether cancer cells target the metabolism of endothelial cells, in particular, the mitochondria, as the vital organ of endothelial cells (Tang *et al.*, 2014).

Mitochondria regulate the cellular metabolic process (proliferation, growth, apoptosis) and cellular signalling responses to the environment (Caja and Enríquez, 2017). Brain endothelial cells have a higher content of mitochondria than the peripheral endothelial cells, reflecting their vital function as an essential component of the BBB (Caja and Enríquez, 2017). The impairment of the mitochondrial function caused dysfunction in endothelial cells (Doll *et al.*, 2015; Haileselassie *et al.*, 2020) and leads to disruption in the BBB integrity (Lee *et al.*, 2020). Thus, it was crucial to investigate whether cancer secreted factors intervene in the mitochondrial activity in brain endothelial cells and whether other cellular processes regulated by mitochondria such as proliferation and the cell-cell endothelial adhesion are affected.

### **1.3. Aim of the study**

The study aimed to determine the *in vitro* effect of normoxic and hypoxic paracrine cancer secretions modulating brain endothelial cells.

## **1.4. Objective of the study**

### ***1.4.1. To investigate the mitochondrial function of bEnd.3 cells:***

- Measure the function of mitochondrial dehydrogenases in bEnd.3 cells exposed to U-87or MCF7 cells and selected concentrations of their normoxic and hypoxic conditioned media.
- Evaluate the mitochondrial potential membrane in bEnd.3 cells chronically exposed to selected concentrations of normoxic and hypoxic U-87 or MCF7 conditioned media.
- Measure the ATP levels in bEnd.3 cells chronically exposed to U-87or MCF7 cells and selected concentrations of their normoxic and hypoxic conditioned media

### ***1.4.2.To investigate changes in bEnd.3 permeability:***

- Measure the transendothelial electrical resistance (TEER) of bEnd.3 monolayer chronically exposed to cancer cells and selected concentrations of their normoxic and hypoxic conditioned media.
- Quantify gene expression of tight junction (Claudin-5 and Occludin) in bEnd.3 cells chronically exposed to selected concentrations of normoxic and hypoxic conditioned media generated from U-87 and MCF7 cells.

### ***1.4.3.To investigate the bEnd.3 proliferation:***

- Measure the relative increase in cell number of bEnd.3 cells after chronic exposure to selected concentrations of U-87 or MCF7 conditioned media.
- Investigate the cell cycles changes of bEnd.3 after chronic exposure to selected concentrations of U-87 or MCF7 conditioned media.

## **1.5. Significance of the study**

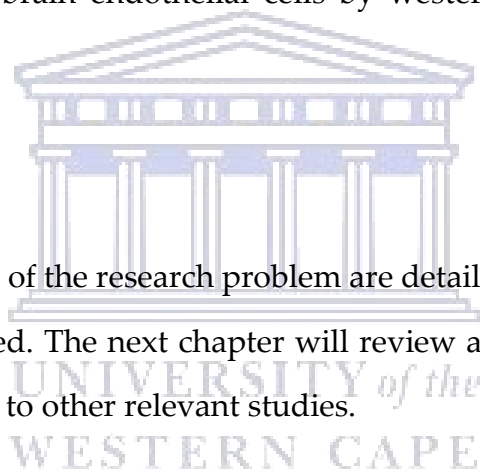
This study provides insights into the mechanism of the cancer cells to induce metabolic changes in brain endothelial cells, as the main motor for BBB integrity.

## 1.6. Scope

The study was designed to use conditioned media generated from glioblastoma (U-87 cells) and breast cancer (MCF7 cells) under low hypoxia (5%O<sub>2</sub>) and normoxia (21% O<sub>2</sub>) to treat brain endothelial cells (bEnd.3). Measurement of mitochondrial activity (dehydrogenase activity, ATP production) were used as an indicator for the cell viability. Moreover, the endothelial integrity, proliferation and cell cycle progression were experimentally monitored. The work did not include an identification of hypoxic or normoxic cancer secretion by liquid chromatograph-mass spectrometry (LC-MC/MC). Additionally, the work does not cover the quantification of tight junction proteins of changes in brain endothelial cells by western blot analysis of protein expression changes.

## 1.7. Chapter summary

In this chapter, the basic of the research problem are detailed. The background of this study is clearly explained. The next chapter will review a discussion of the relevant current work in relation to other relevant studies.



# CHAPTER 2

## Literature review

### 2.1. Overview of cancer

Cancer affects millions of people worldwide and has been a global health problem (Xue *et al.*, 2008). It has been projected that cancer will become the leading cause of mortality in the coming decades all over the world (Bratu *et al.*, 2011). Worldwide, cancer causes more than six million deaths annually, with ten million new cases diagnosed each year (Xue *et al.*, 2008). In normal physiological conditions, cell growth is a well-regulated process where new cells replace the old, senescent, or damaged ones.

Tumour cells, however, are products of dysregulated cell divisions with the subsequent production of abnormal tissues. All types of cancer arise due to changes by either internal factors such as genetic mutations (Pietras and Östman, 2010) or the causative effects of environmental factors such as tobacco, chemicals, radiation, and infectious organisms. These factors work either in sequence or synergy, causing changes in cell behaviour resulting in excessive cell growth and proliferation, which subsequently affects the surrounding normal tissues (Croce, 2008).

Fouad and Aanei (2017) pointed out seven hallmarks of cancer (Figure 1) which include (i) selective growth and proliferative advantage, (ii) altered stress response favouring overall survival, (iii) vascularisation, (iv) invasion and metastasis, (v) metabolic rewiring, (vi) an abetting microenvironment, and (vi) immune modulation. The main characteristic of cancer cells is their ability to stimulate proliferation. In contrast, normal cells control the release of growth factors that influence the regulation of cell growth and division (Fouad and Aanei, 2017). In addition, they can generate proliferative signalling either by producing growth factor ligands themselves, enabling the response via the expression of cognate receptors or stimulate the surrounding normal cells, which

respond by supplying the cancer cells with various growth factors (Hanahan and Weinberg, 2011). Cancer cells alter the extracellular growth signals or transcellular transducers of those signals or the intracellular circuits that translate these signals into action (Houben *et al.*, 2009). These variable signals are generated by growth factors binding to the receptors of the cell surface, which in turn are linked to tyrosine kinase within cells, resulting in an abnormal cell cycle and growth (Lemmon and Schlessinger, 2011). These signals often affect other biological cell properties, such as cell viability (Hanahan and Weinberg, 2011).

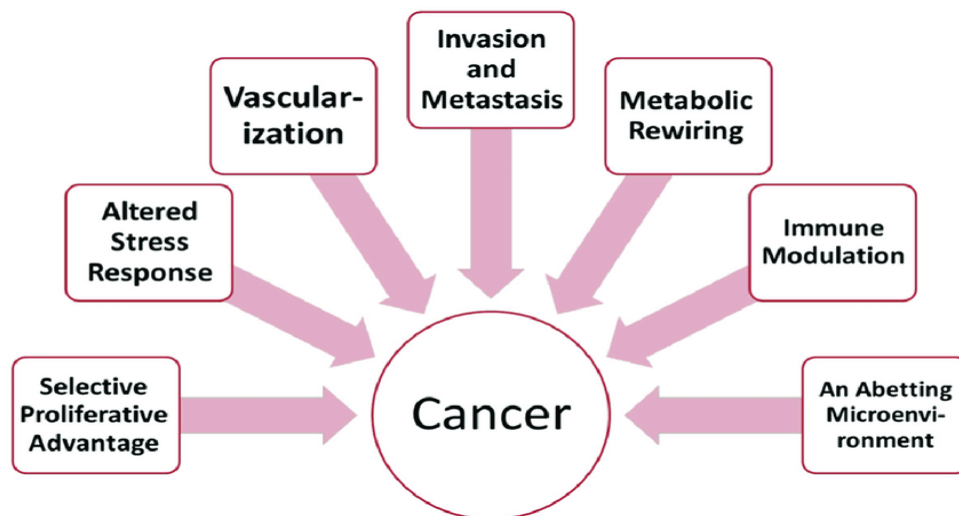


Figure 1. Cancer hallmarks where normal cells transform to cancerous cells (Fouad and Aanei, 2017).

There are three signalling pathways frequently involved in genetic alterations in cancer; Receptor tyrosine kinase (RTK), retinoblastoma (RB) (Figure 2), and tumour protein (p53) pathway signalling pathways (Figure 3) (Duncan and Yan, 2011).

The RTKs are cell-surface receptors; the activation of these receptors by their ligands induce several types of signalling pathways (Ramos *et al.*, 2018; Cheng and Guo, 2019). Mutations in these pathways can contribute to the malignancy of cancer (Cheng

and Guo, 2019). The common alterations in the RTK pathway are the mutation in the growth factor receptor Epidermal Growth Factor Receptor (EGFR), platelet-derived growth factor receptor (PDGFR), mesenchymal-epithelial transition factor (MET), mutation of phosphatidylinositol-3-kinases (PIK3CA and PIK3R1), and mutation or homozygous deletion of the PTEN tumour suppressor gene (Duncan and Yan, 2011; Cruickshanks *et al.*, 2017).

Epidermal Growth Factor Receptor (EGFR) belongs to receptor tyrosine kinases (RTKs); the binding of this receptor with its ligand causes phosphorylation of specific targets, including phosphatidylinositol 4,5- biphosphate 1-kinase (PI3K), tumour suppressor protein (called PTEN) naturally inhibits PI3K, and loss of PTEN leads to overactivity of the PI3K pathway, increasing cell growth and division (Ramos *et al.*, 2018). In high-grade brain cancer, EGFR gene amplification is the most frequent genetic alteration of RTKs and correlates with EGFR overexpression. EGFR gene overexpression and amplification are identified in 70% -90% of GBM cases (Ozawa *et al.*, 2010).

Platelet-derived growth factor receptor (PDGFR) includes PDGFR $\alpha$  and PDGFR $\beta$ ; their ligands are the PDGF family (PDGF-A, PDGF-B, PDGF-C, and PDGF-D). The activation of these proteins induces the signal pathways of MAP kinase, PI3K/AKT, JAK/STAT, and PLC-PKC, promoting oncogenesis (Ozawa *et al.*, 2010; Alentorn *et al.*, 2012; Li *et al.*, 2016).

Mesenchymal-epithelial transition factor (MET) (also known as hepatocyte growth factor receptor (HGFR)) plays a critical role in the multiple cellular processes, including angiogenesis, survival, proliferation, scattering, cell motility, and invasion (Cheng and Guo, 2019). MET is coded by the MET gene located on chromosome 7q31, and its ligand HGF gene is located on chromosome 7q21.1. MET is spontaneously deregulated in approximately 2–3% of cancers (Cheng and Guo, 2019).



MET activation in tumour cells promotes cell growth, angiogenesis, and invasion through various mechanisms, including amplification of MET, elevated levels of its ligand HGF, and mutations within the promoter region of HGF (Cruickshanks *et al.*, 2017). The interaction between MET and its receptor HGF results in autophosphorylation at multiple tyrosine residues, which activate STAT3, Ras/MAPK/ERK, and PI3K/Akt signal pathways. Genetic abnormality in MET includes mutations, overexpression, and amplification in various types of cancer (Cruickshanks *et al.*, 2017; Zhang *et al.*, 2018).

Phosphatidylinositol-3-kinases (PIK3CA & PIK3RI) are the genes coded of lipid kinase (PI3K) (Li Chen *et al.*, 2018). PI3K plays a role in various signalling pathways of many cellular processes, such as cell division, proliferation, and apoptosis (Miller *et al.*, 2018). The activation of PI3K is mediated by the phosphorylation of phosphatidylinositol-4, 5-bisphosphate (PIP2) to phosphatidylinositol-3, 4, 5-triphosphate (PIP3), resulting in the recruitment and activation of other factors such as AKT (Miller *et al.*, 2018), which regulate the cell proliferation, survival, and motility (Huang *et al.*, 2007). Genetic alterations in PIK3CA was found to be altered in 10% of brain cancer patients (Miller *et al.*, 2018) and 36% of breast cancer patients (Li Chen *et al.*, 2018).

The PTEN is a tumour suppressor protein coded by the PTEN gene located on chromosome 10q23.3 (Wang *et al.*, 2015). PTEN gene is one of the most commonly mutated tumour suppressors in human malignancies. It is absent in many cancer (Ramos *et al.*, 2018). The loss of PTEN function occurring through various genetic alterations includes mutations (missense and nonsense mutations), large chromosomal deletions (homozygous, heterozygous deletions), and epigenetic mechanisms such as hypermethylation of the PTEN promoter region (Ciuffreda *et al.*, 2014; Wang *et al.*, 2015). PTEN protein plays a role in regulating cellular growth; however, its function is

dependent on its location, either in the cytoplasmic or in the nucleus. PTEN acts as lipid phosphatase in the cytoplasm that antagonises (PI3K) signalling by PIP3 to PIP2, which negatively regulate the protein kinase B (AKT), phosphatidylinositol dependent kinase-1 (PDK1), and other PIP3-dependent moieties, and that inhibit growth, protein synthesis, cell cycle progression, metabolism, and migration and allow for apoptosis and cell cycle arrest. In the nucleus, PTEN act in a PI3K-independent manner, where it inhibits migration and affects the stability of the genome, gene expression, and the cell cycle (Hopkins *et al.*, 2014).

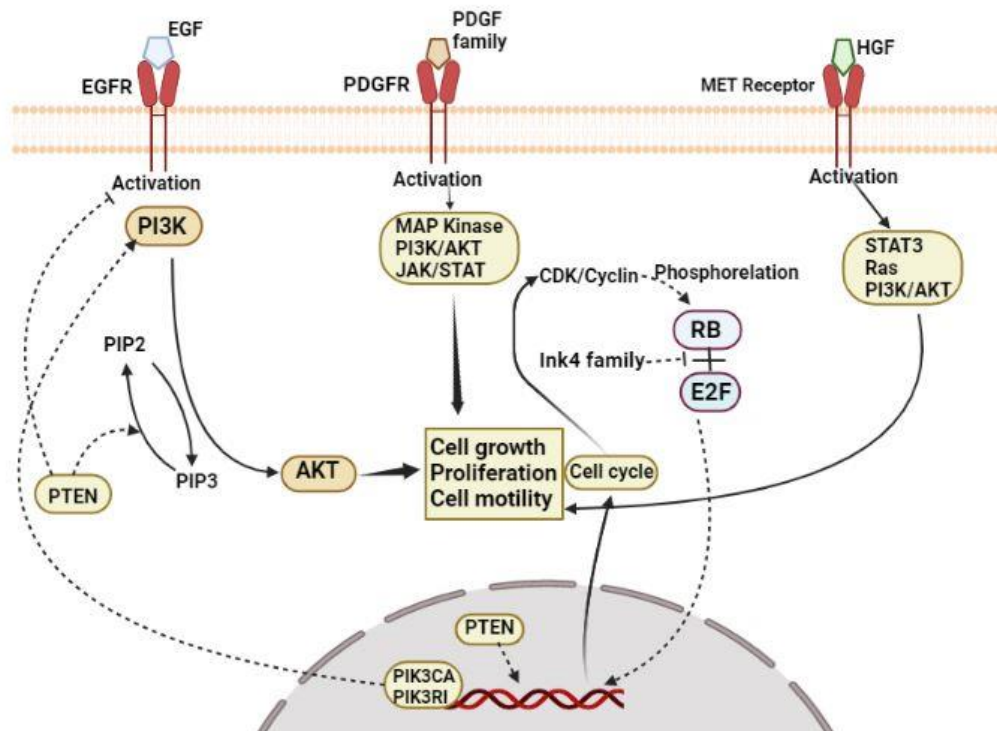


Figure 2. A summarization of Receptor tyrosine kinase (RTK) and retinoblastoma (RB) signalling pathways involved in cancer. The binding of RTK receptors EGFR, PDGFR, and MET with their ligands EGF, PDGF, and HGF activate various signalling pathways of many cellular processes, such as cell growth, proliferation, and motility. These activations are mediated by a series of pathways, including PI3K/AKT, MAP Kinase, STAT3, Ras and JAK/STAT (Ozawa *et al.*, 2010; Cruickshanks *et al.*, 2017). PTEN regulates the AKT activity by inhibiting the phosphorylation of PI3K and controlling the conversion of PIP3 to PIP2. PTEN influences gene expression (Hopkins *et al.*, 2014). PI3K is coded by PIK3CA and PIK3RI genes. Cell cycle portions (CDK/Cyclin)

*induce phosphorylation of RB to bind to the transcription factor E2F, which influences the transcription of growth genes needed for DNA synthesis. Ink4 family proteins negatively regulate the RB activation (Crespo et al., 2015). Created by Biorender.com*

The RB pathway is vital in the regulation of cell proliferation (Figure 2). The RB in the quiescent cell is an active state (hypophosphorylation) bound to E2 transcription factor (E2F), which regulates the cell cycle. This RB-E2F interaction prevents the transcription of genes for mitosis, thus preventing the progression through the cell cycle (G1/S). In the proliferating cells, growth factors activate proteins (cyclin D1 and CDK2/cyclin E) which induce the phosphorylation of RB in the late G1 phase. This phosphorylation enables the release of the E2F, which influences the transcription of other growth genes required for DNA synthesis (Crespo *et al.*, 2015). The negative regulators of the RB signalling pathway include the Ink4 family of proteins (CDKN2A-p16INK4a, CDKN2B-p15INK4b, CDKN2C-p18INK4c, and CDKN2D-p19INK4d) that compete with the D-cyclins for CDK4/6 to prevent the formation of the active kinase complex that phosphorylates RB (Crespo *et al.*, 2015). The mutation of the RB gene or the loss of RB expression, or the inactivation of RB by phosphorylation through CDK/cyclin complexes, inhibits the RB pathway by disrupting the RB-E2F interaction (Duncan and Yan, 2011; Crespo *et al.*, 2015). The mutated RB pathway includes mutations in P16/INK4A amplification of cyclin-dependent kinases 4 and 6 (Ramos *et al.*, 2018); these genetic alterations deregulate the communication pathways of regulatory molecules that control various cellular process, which contributes to malignancy (Sathornsumetee and Rich, 2008).

The TP53 plays a vital role in the negative regulation of the cell cycle. In response to genotoxic stress, the TP53 gene either induce cell cycle arrest, apoptosis, and DNA repair. Mutation or loss in the TP53 gene is associated with abnormal cell division and

neoplastic transformation (Sathornsumetee and Rich, 2008). The mutation of TP53 occurs in 35% of tumours and 87% of GBMs. The alteration of TP53 signalling includes mutation and deletions of p53 and amplification of proteins regulator of TP53 such as murine double minute proteins (MDM2 and MDM4) (Ramos *et al.*, 2018). The TP53 arrest cells in the G1 phase, checking the replication of damaged DNA. The deletion in TP53 leads to rapidly dividing cells with genomic instability. TP53 causes apoptosis to occur in case of irreversible DNA damage. The loss of TP53 function results in the continuous growth of damaged cells. Mutations in p53 were initially observed frequently in low-grade astrocytomas and secondary glioblastomas (Ranjit *et al.*, 2015).

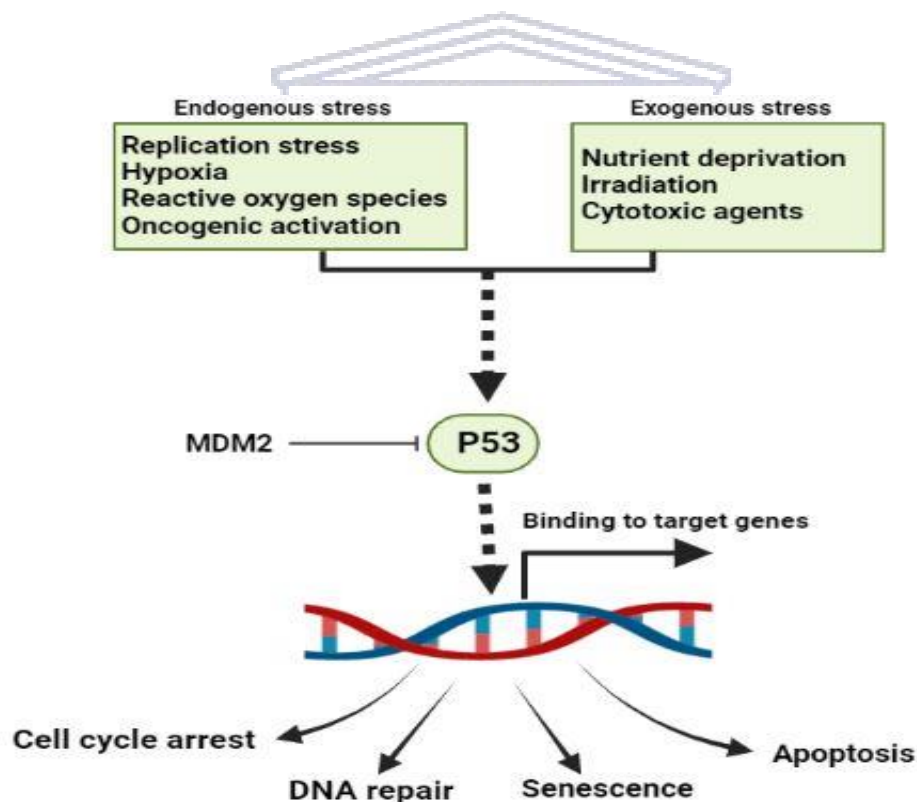


Figure 3. A summarization of P53 pathway: Cells are exposed to different sources of stress, including endogenous and exogenous stresses, that activate P53 via a series of cellular responses that rely on the type and degree of insults. P53 activate the expression of genes responsible for cell cycle arrest, DNA repair.

*MDM2 binding to P53 to inhibit its activity. The P53 pathway is vital to maintaining cellular homeostasis. This pathway is either mutated or lost in cancer cells, thus promoting cancer progression. Modified from (Hu et al., 2021).*

### **2.1.1. Overview of cancer types used in this study**

#### **2.1.1.1. Brain tumour**

Brain tumours result from abnormal cell growth in the brain and are classified as either primary or secondary. The primary brain tumour refers to those arising from tissues in the brain compartment. In contrast, secondary brain tumour arises from tissues in other locations in the body then migrate to the brain. However, the majority of brain tumour cases are primary tumours. The primary brain tumour is divided according to the tissue of phenotypic origin into glioma and non-glioma. Gliomas arise from glial cells, representing 60% of brain tumours, whereas non-glioma tumours arise from other intracranial cells (Moore and Kim, 2010; Timmons, 2012). Glioma includes astrocytic tumours (astrocytoma, anaplastic astrocytoma and glioblastoma multiforme (GBM)), oligodendrogliomas, ependymomas, and mixed glioma (Komori, 2014).

GBM is the most malignant or aggressive brain tumour, accounting for more than 60% of all brain tumours in adults (Hanif *et al.*, 2017). GBM is 1.6 times more frequent in males than females, with a median age of 64 years at diagnosis. The age group between 75-84 years has the greatest rate of GBM, with an estimation of 37.1% survival at one year and only 5.1% survival at five years. Surgery and chemoradiation result in median survival of approximately 14-15 months (Ramos *et al.*, 2018). GBM exhibits specific characteristics that led to their malignancy; some of these are phenotypic features, including self-sustained proliferation, resistance to apoptotic stimuli, evasion of external growth control and immune surveillance, tissue invasion, and the ability to form new

blood vessels. In addition, GBM is genetically heterogeneous between patients and within tumours (Sathornsumetee and Rich, 2008).

#### **2.1.1.2. GBM in brain tumour classifications**

The World Health Organization (WHO) has developed a system to classify brain tumours. In this classification (1979), gliomas are divided into a four-tiered grading system (Joshi, 2015). The grading system is based on the cell type of origin and the morphology of the tumour under the microscope. Grade I & II refer to a benign tumour where the growth is slow, non-infiltrative and can be cured with complete surgical resection. Grade III & IV are the most malignant and aggressive forms where the tumour is high infiltrative, diffuse and cannot be cured with surgical resection only (Moore and Kim, 2010).

The WHO classification of CNS tumours means that gliomas are classified into astrocytoma, oligodendroglioma, and oligoastrocytomas. Astrocytoma types are pilocytic astrocytoma (grade I), diffuse astrocytoma (DA; grade II), anaplastic astrocytoma (AA; grade III), and glioblastoma multiforme (GBM; grade IV) (Table 1). In contrast, Oligodendroglioma types are diffuse oligodendroglioma (DO; grade II) and anaplastic oligodendroglioma (AO; grade III). Pilocytic tumours are the most benign; they are slow-growing, non-infiltrating, and usually cured by surgery. Diffuse astrocytoma is more infiltrative but less aggressive than anaplastic astrocytoma (AA), anaplastic oligodendroglioma (AO) and glioblastoma multiforme (GBM)) which are considered malignant gliomas (Moore and Kim, 2010; Sreekanthreddy *et al.*, 2010).

Table 1: Description of Gliomas developed from astrocytes

Cell types		Astrocytes		
Tumour	Pilocytic astrocytoma (Grade I)	Diffuse astrocytoma (Grade II)	Anaplastic astrocytoma (Grade III)	Glioblastoma multiforme (Grade IV)
Brief description	More frequent in children and young adults  Non-infiltrated and cured by surgery	Common in adults  Slow growing but, It can develop to malignant Glioma	Frequent in adults  Fast-growing, diffused and infiltrated glioma	It arises de novo in old patients, and it is developed from low grade in young patients Fast-growing, high invasive and infiltrated
References	(Louis <i>et al.</i> , 2016; Park <i>et al.</i> , 2019)	(Lind-Landström <i>et al.</i> , 2012; Picca <i>et al.</i> , 2018)	(Sarica <i>et al.</i> , 2012; Wahner <i>et al.</i> , 2020)	(Alifieris and Trafalis, 2015; Hanif <i>et al.</i> , 2017)

In 2016, the WHO updated the classification of a brain tumour. The new version of classification was mostly based on the genotypic parameters of the brain tumour. Mutations such as isocitrate dehydrogenase (IDH) is implicated in the development of glioma in this classification (Louis *et al.*, 2016). IDH plays a critical role in cell metabolism, it catalyses the oxidative decarboxylation of isocitrate to alpha-ketoglutarate ( $\alpha$ -KG). It also plays a role in reducing NADP<sup>+</sup> to nicotinamide adenine dinucleotide phosphate (NADPH) (Al-Khallaf, 2017). The IDH mutation induces the formation of the tumour environment by upregulating the level of vascular endothelial growth factor (VEGF) and inducing high levels of hypoxia-inducible factor-1 $\alpha$  (HIF-1 $\alpha$ ) (Huang *et al.*, 2019). In the 2016 CNS WHO classification, glioblastoma is divided into IDH-wild-type, present in



about 90% of cases, and IDH-mutant glioblastoma, representing approximately 10% of patients (Louis *et al.*, 2016).

Additionally, the Cancer Genome Atlas (TCGA) divided GBM into molecular subclasses based on different gene expression patterns and expression profiles, especially PDGFRA, EGFR, IDH1 (Verhaak *et al.*, 2010). The molecular genetic classification of GBM is divided into four distinct subgroups, i.e. proneural, classical, mesenchymal, and neural. These subclasses reflect the common signalling abnormalities in GBM. The classical subtype is defined by amplification of chromosome 7 with loss of chromosome 10, epidermal growth factor receptor (EGFR) amplification, homozygous deletion of focal 9p21.3 with resultant loss of cyclin-dependent kinase inhibitor 2A gene (CDKN2A) (Ranjit *et al.*, 2015; Hanif *et al.*, 2017; Cai and Sughrue, 2018).

The mesenchymal subtype showed loss of tumour protein p53, CDKN2A, and an increase of neurofibromin 1(NF1) mutation or deletion of its expression (Hanif *et al.*, 2017; Cai and Sughrue, 2018). This subtype also showed a high expression of genes for the tumour Necrosis Factor (TNF) superfamily pathway and NF-kB (Nuclear Factor kappa-light chain enhancer of activated B cells) pathway (Ranjit *et al.*, 2015). The proneural subtype exhibited amplifications in PDGFRA, mutations in IDH1, mutations in TP53, and loss of heterozygosity. The neural subtype has a normal brain gene expression profile (Alifieris and Trafalis, 2015), and expressed markers such as inhibitory neurotransmitter receptor GABRA1 (Gamma-Amino Butyric Acid A Receptor), synaptic neurotransmitter release trigger synaptotagmin 1 (SYT1) and neuronal chloride homeostasis maintaining solute carrier family 12 members 5 (SLC12A5) (Ranjit *et al.*, 2015).

#### **2.1.1.3. Types of glioblastoma (GBM)**

Clinically, GBM classification into two subgroups includes primary and secondary. The primary GBM arises *de novo* from native glial tissue, whereas the



secondary progresses from pre-existing low-grade GBM. Statistics shows that 90% of GBM cases are primary, and this type of GBM affects the elderly, with a mean age of 62 years. By contrast, secondary GBM affects the younger population with a mean age of 45 years at diagnosis. This type of GBM is less common and represents less than 10% of total GBM cases (Joshi, 2015).

Primary and secondary GBMs are not histologically distinguishable. However, they share some genetic abnormalities such as loss of phosphatase and tensin homolog, PTEN, deletion or mutation of cyclin-dependent kinase inhibitors p16INK4A on chromosome 9 and amplification of HDM2 or CDK4 (Sathornsumetee and Rich, 2008). GBM subgroups have different genetic alterations (Figure 4) and genomic profiles (Hottinger *et al.*, 2016). The loss of heterozygosity (LOH) at 10q, the amplification of epidermal growth factor receptor (EGFR), P16/INK4A deletion, PTEN mutations on chromosome 10, deletion of P16 are common in primary GBMs (Hanif *et al.*, 2017). The loss in TP53 is frequently shown in secondary GBMs and low-grade astrocytoma (Sathornsumetee and Rich, 2008; Joshi, 2015; Ramos *et al.*, 2018). The overexpression of platelet-derived growth factor A (PDGFA), platelet-derived growth factor receptor alpha (PDGFRa), retinoblastoma (RB), loss of heterozygosity (LOH) of 19q, and mutations of isocitrate dehydrogenase (IDH) are implicated in secondary GBM (Hanif *et al.*, 2017). These are common mutations in the pathways that control cellular survival and proliferation (Alifieris and Trafalis, 2015; Joshi, 2015).

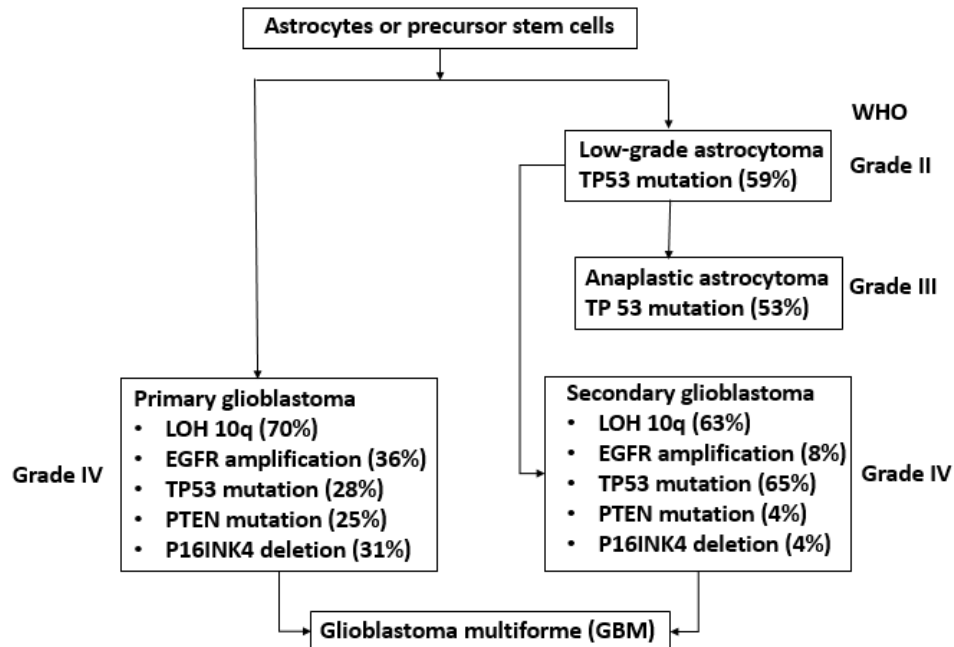


Figure 4. Genetic alterations involved in glioblastoma (GBM). Modified from (Joshi, 2015).

#### 2.1.1.4. Biology of glioblastoma

Glioblastoma is often called Glioblastoma multiforme (GBM). The term multiform refers to the heterogeneity of this type of tumour. They are very heterogenic in their biological and morphological features. Under the microscope, GBM cells have polygonal spindle shapes with acidophilic cytoplasm and indistinct cellular borders. The nuclei are oval or elongated and have coarsely clumped hyperchromatic chromatin with multiply distinct nucleoli centrally or peri-centrally (Urbanska *et al.*, 2014).

GBM vascularisation is very high, and the developed vessels are morphologically similar to renal glomeruli. The pathological features common in GBM include pronounced hypercellularity, pleomorphism, numerous mitoses, foci of necrosis and palisading, and excessive vascularisation (D'Alessio *et al.*, 2019). Furthermore, necrotic foci are one of the common characteristic features of GBM. Two types of necrosis are

typically presented in GBM, depending on the localisation and size of the necrotic area. Large necrosis area located in the central area of the tumour, resulting from insufficient blood supply in all tumours. The other areas of necrosis are small with irregular shapes; they are surrounded by pseudopalisading areas (Rong *et al.*, 2006; Urbanska *et al.*, 2014). Pseudopalisades areas have varied sizes, between 30 to 1500  $\mu\text{m}$  in width and 50 to 3500  $\mu\text{m}$  in length. Pseudopalisades which are  $<100\text{ }\mu\text{m}$  wide, show hypercellular zones encompassing internal fibrillarity without central necrosis area. The pseudopalisades (200–400  $\mu\text{m}$ ) are characterised by central necrosis, central vacuolisation, individual dying cells, and a peripheral zone of fibrillarity. The pseudopalisades with  $>500\text{ }\mu\text{m}$  show extensive necrotic zones and always have central vessels (Urbanska *et al.*, 2014).

The difficulty of treating GBM due to the high ability to invade the surrounding tissue and integrate into the normal brain tissue (Zhang *et al.*, 2012). In general, GBM affects the brain by three mechanisms: first by direct effect where the brain tissue is destroyed as a result of necrosis, second, a secondary effect resulting from the increase of intracranial pressure, which is a consequence of the increase in the tumour size and the increase of oedema surrounding the tumour, third, effect depending on the tumour location (Hanif *et al.*, 2017).

#### **2.1.1.5. Overview of Breast Cancer**

#### **2.1.1.6. Functional anatomy of the breast**

Anatomically, female breasts are composed of lobes. The lobes consist of smaller lobules comprised of clusters of alveoli (glands) containing lactocytes that produce breast milk. The alveoli are connected through milk ducts (Figure 5) (Burrell *et al.*, 2013). The breast ducts have a plasma membrane layer of luminal epithelial and myoepithelial cells. These cells composing the stroma include leucocytes, fibroblast, myofibroblast and endothelial cells (Polyak, 2007).

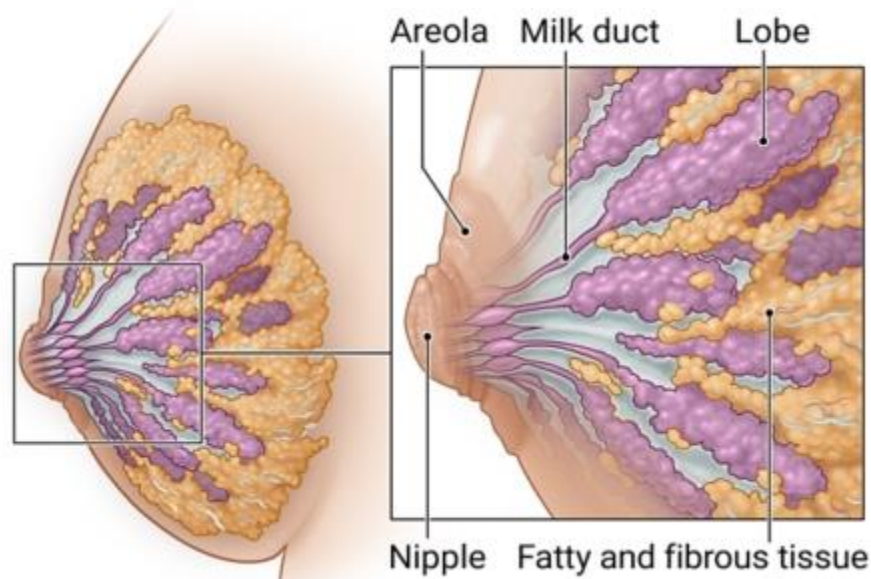


Figure 5. The anatomy of the female breast, the areola, lobules, and ducts are indicated.

<https://myhealth.alberta.ca/Health/pages/conditions.aspx?hwid=hw139826>. Date: 09/12/2021

The development of breasts occurs during the foetal growth period, infancy (prepuberty), puberty, and pregnancy. Mammary differentiation is enhanced during the pregnancy and lactation cycle (PLC) when the mammary glands are transformed into functional milk-secreting organs. The PLC cycle can recur in multiparous females, and therefore childbearing and breastfeeding offer some protection against the development of breast cancer (Hassiotou and Geddes, 2013).

In humans, crosstalk occurs between the signalling pathways that drive normal mammary morphogenesis during the PLC and those oncogenic (aberrantly activated or suppressed) signals that are associated with breast cancer initiation, progression and metastasis (Key *et al.*, 2001; Kobayashi *et al.*, 2012; Hassiotou and Geddes, 2013; Javed and Lteif, 2013).

#### 2.1.1.7. Breast Cancer

Breast cancer originates within the breast tissue. It is a heterogeneous malignant disease commonly arising from the epithelial cells lining the milk ducts or the lobules (Polyak, 2011). Breast tumour heterogeneity is observed between patients (intratumoral heterogeneity) and within the same individual (intratumoral heterogeneity). Intratumour heterogeneity occurs at the morphologic, genomic, transcriptomic, and proteomic levels, which creates a challenge in the diagnosis and the treatment (Badve, 2016).

Breast cancer is a heterogeneous disease with an increase in the biological subtypes that are being recognised. Based on the high heterogeneity of breast cancer, it becomes difficult to establish a perfect cancer classification. Breast cancer is classified primarily by the histological appearance of cancer cells and histological examinations of tumours, which are primarily inaccurate, which remain the classification method of choice. According to this classification, there are two types of breast cancer: carcinoma *in situ* (CIS) and invasive (infiltrating) carcinoma (IDS). CIS is non-invasive cancer classified based on its cytological features into either ductal (DCIS) or lobular (LCIS). In this type, DCIS is more common than the LCIS, where cancer cells are present within the ducts but have not yet spread and infiltrate the surrounding breast tissues (Malhotra *et al.*, 2010; Bravaccini *et al.*, 2013).

Carcinoma IDS is classified into invasive ductal carcinomas (IDCs) or invasive lobular carcinoma (ILC). IDCs arise from the milk ducts, whereas ILCs arise from the lobules. Both are invasive cancer that can spread to the surrounding breast tissues. IDC is the most common invasive type of breast cancer and is divided into five categories: tubular, ductal lobular, infiltrating ductal, mucinous, and medullary subtypes (Figure 6) (Watkins, 2019). ILC is characterised by a general thickening of an area of the breast,

usually the section above the nipple and toward the arm (Cao *et al.*, 2012). This type of breast cancer spreads to different parts of the body, such as the brain, bones, lungs, and liver, within three months when medical intervention is lacking (Switzer *et al.*, 2015).

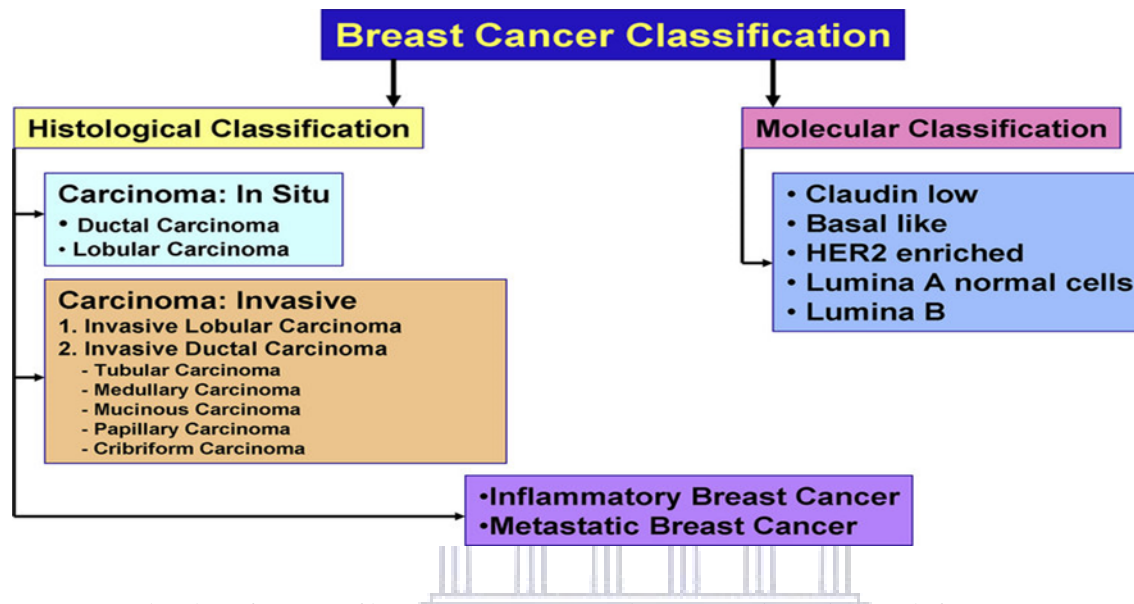


Figure 6. The classification of breast cancer. HER2: human epidermal growth factor receptor 2 (Sharma *et al.*, 2019).

UNIVERSITY of the  
WESTERN CAPE

Histologic classification is based on the pathologic growth pattern. Twenty different histologic types have been recognised in invasive breast cancers. The most common belongs to IDCs, which account for 70% to 80% of all invasive cancers, followed by invasive lobular carcinomas (ILC) (around 10% of all invasive cancers). In contrast, other histologic types of breast tumour are less common, namely mucinous, cribriform, micropapillary, papillary, tubular, medullary, metaplastic, and apocrine carcinomas (Feng *et al.*, 2018).

The classification into histologic types is dependent on a wide range of criteria, including tumour cell type (e.g., carcinoma with apocrine features), extracellular

secretion (e.g., mucinous carcinoma), architectural features (e.g., papillary carcinoma), and immunohistochemical profile (e.g., carcinoma with neuroendocrine differentiation). IDCs do not exhibit specific morphologic characteristics of any other specific histologic types; thus, most breast cancers fall into a single category. This classification is fully reflected in the biological heterogeneity of breast cancers (Tsang and Tse, 2019).

In the new century, genomic methods were used to understand the molecular heterogeneity of breast cancer. Thus a molecular classification has been developed. This classification is based on gene expression analysis using a real-time reverse transcription-polymerase chain reaction (qRT-PCR). Further, this classification was able to identify the majority of types of breast cancer (Viale, 2012). According to this classification, breast cancer is classified into several molecular sub-type: basal-like breast cancers (BLBC), HER2-overexpressing breast cancer, normal breast-like tumour, Claudin-low, luminal subtype A and luminal subtype B (Malhotra *et al.*, 2010; Prat and Perou, 2011; Viale, 2012).

The molecular classification shows the relevance of the immunophenotypic type by hormone estrogen receptors (ER) status. Thus breast cancer is divided into two distinct clusters: ER<sup>+</sup> and ER<sup>-</sup>. Luminal A and B subtypes are ER-positive cancers (ER<sup>+</sup>), whereas HER2-overexpressing, BLBC, and normal-like tumours are ER<sup>-</sup>. These subtypes showed differences in the expression of genes that related to proliferation and HER2 amplicon. Thus, that explains the differences in the clinical and pathological features observed in breast cancer (Sharma *et al.*, 2019; Tsang and Tse, 2019).

#### **2.1.1.8. Breast cancer metastasis to the brain**

The brain is the fourth destination for breast cancer metastatic after the bone, lung and liver (Riggio *et al.*, 2021). Breast cancer represents 20% of brain metastasis (Medress and Hayden Gephart, 2015). 30-40% of women with breast cancer develop secondary breast cancer metastatic in the brain (Hosonaga *et al.*, 2020). The ability of cancer to



metastasis is the main reason for the high rate of mortality related to breast cancer (Tayyeb and Parvin, 2016). Within breast cancer sub-types, the highest ability to spread to the brain is Triple-negative breast cancer (TNBC), then breast cancer HRE2 with a rate of 30% to 20%, respectively (Hosonaga *et al.*, 2020; Lv *et al.*, 2021).

The metastatic process of cancer cells occurs in sequential series of stages called metastatic cascade (Figure 7) (Tayyeb and Parvin, 2016), starting with the detachment from the primary site and penetrating the surrounding tissue, then the intravasation in the bloodstream; at this point, cancer cells try to survive with their anoikis resistance, following by arrestation at the capillary bed, before migration to the secondary site (Fidler, 2003). Metastatic cancer cells (also called circulating cancer cells) are significantly modulated by their environment, the interaction between the circulating cancer cells and the surrounded cells and tissues is crucial for their survival in this metastatic phase. Factors secreted from metastatic cancer cells and non-cancerous stromal cells are the mediators for a successful metastatic process (Maishi and Hida, 2017).



UNIVERSITY of the  
WESTERN CAPE



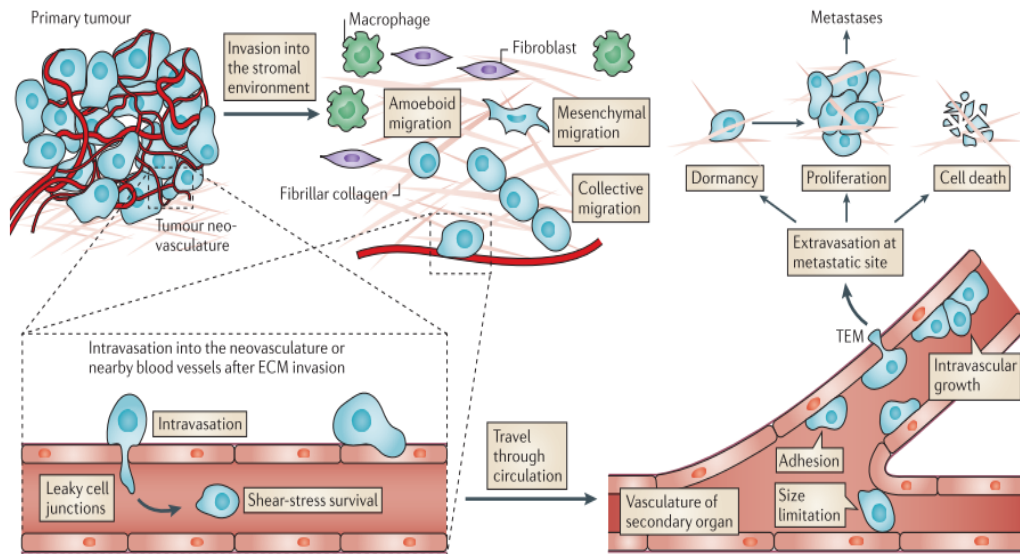


Figure 7. Metastatic cascade through the blood capillary: At the primary tumour site, cancer cells are highly proliferated, and have the ability to detach from the tumour and invade into the surrounded tissues. Some of the cancer cells successfully invade the extracellular matrix and reach the blood vessel. Cancer cells enter the blood vessel through the endothelial cell-cell connection (via the endothelial tight junction). Cancer cells use the blood vessel to spread into new locations. Cancer cells are arrested at the endothelial surface and preparing to extravasate into the new place; at this step, a cross-talk occurs between cancer cells and endothelial cells via soluble factors and the physical endothelial-cancer cells adhesion to facilitate the extravasation between the endothelial cells (also called transendothelial migration (TEM)). After the extravasation, a few cancer cells adapt to the new place and proliferate to arise the secondary tumour tissue. However, some metastatic cancer cells enter into the dormancy, but the majority of metastatic cancer cells dead after the extraversion (Reymond *et al.*, 2013).

At the initial location of cancer, cancer cells interact with the surrounding components such as extracellular matrix and stromal cells (including fibroblasts, macrophages, endothelial cells and other inflammatory cells). The cross-talk between cancer cells and stromal cells enhance cancer cells metastasis. Cancer cells release substances such as TGF- $\beta$ , PDGF, and FGF which activate fibroblasts secrete MMP, promoting cancer invasion by degrading the basement membrane and extracellular matrix (Tao *et al.*, 2017). Cancer cells also secrete chemokine such as colony stimulating

factor 1 (CSF1), which attract macrophages (also called tumour associated macrophages TAM)(Goswami *et al.*, 2005), TAM in turn secrete interleukins (IL-8), the activator of protein kinase C in cancer cells, inducing the secretion of CSF1 (Ge and Ding, 2020). The crosstalk between cancer cells and endothelial cells has a critical role in the metastasis process (Choi and Moon, 2018), metastasis cancer cells were found to grow close to the blood vessel (Carbonell *et al.*, 2009), endothelial cells induce activation of Akt and NF- $\kappa$ B pathways in cancer cells promoting their invasion and metastasis (Wang *et al.*, 2013), endothelial cells promote the metastasis of breast cancer by inducing the secretion of MMPs (Lee *et al.*, 2011). Cancer cells secrete variety of cytokines and chemokines after the interaction with endothelial cells inducing the expression of endothelial adhesion proteins such as VCAM and vascular adhesion protein 1 (VAP1) (Reymond *et al.*, 2013).

In the blood vessel, circulating metastatic cancer cells are exposed to the blood flow, and that induce their death due to the shear stress, the immune cells action (e.g natural killer cells), or a result of their loss of the adhesion with the extracellular matrix via integrins which is required for tumour cells survival (Strilic and Offermanns, 2017). However, cancer cells can escape from the immuno-surveillance factors by activating the coagulation and formation of platelet-rich thrombi around them (Labelle and Hynes, 2013). Metastatic cancer cells arrest at the bed of the blood capillary before crossing the endothelial barrier to the new location (Perea Paizal *et al.*, 2021); in brain capillary, this step was found to be fundamental in the metastatic process cross the brain endothelium (Kienast *et al.*, 2010).

Genes coded for cyclooxygenase COX2, epidermal growth factor receptor (EGFR), and  $\alpha$ 2,6-sialyltransferase ST6GALNAC5 were reported to mediate the breast cancer cells infiltration through the brain endothelium (Bos *et al.*, 2009). The recurrence of metastatic breast cancer can occur in a month to a year after the surgical compared to the metastatic

lung cancer cells which reoccur in weeks (Riggio *et al.*, 2021). That suggests that metastatic breast cancer cells develop the ability of metastasis by adapting to the selective environment in the targeted organ (Bos *et al.*, 2009). The interaction between cancer cells and endothelial cells induces activation of endothelial and cancer cells. Factors such as cytokines, growth factors are the mediators for this activation; such factors induce the expression of endothelial adhesion molecules selectins, and integrins, the mediator of the physical interaction between cancer and endothelial cells (Choi and Moon, 2018).



## 2.2. Overview of the Blood-Brain Barrier (BBB).

BBB plays a critical role in protecting the CNS against toxic and infectious agents while maintaining ionic and volumetric environments (Daneman and Prat, 2015). It is represented at the endothelium level in the brain capillaries and separates the brain parenchyma from the blood and the peripheral compartment (Daneman and Prat, 2015).

The BBB components include the EC layer and its basement membrane, adjoined by tight cell-to-cell junction proteins with specific transport mechanisms and pinocytic vesicles. The endothelium is surrounded by cellular elements, including pericytes and astroglial foot processes, forming an additional continuous stratum separating blood vessels from the brain tissue (Serlin *et al.*, 2015).

### 2.2.1. History of the BBB

Paul Ehrlich discovered a physical interface between the CNS and peripheral circulation in 1885 (Wolburg *et al.*, 2008). Paul Ehrlich (1885) saw that dye injection into the blood circulation stained the peripheral organs but not the CNS (spinal cord and the brain) (Serlin *et al.*, 2015). Thirty years later, a student of Ehrlich, Goldman, showed that the injection of Trypan blue directly to the CSF stained all CNS but not the peripheral organs, thus suggesting a barrier between the CNS and the circulation system. The term blood-brain barrier was first introduced by Lewandowsky in 1900, after studying the limited penetration of potassium into the brain (Cardoso *et al.*, 2010). The existence of the transmembrane protein (tight junction) was confirmed later in 1967 by using horseradish peroxidase (HP), the injection of which showed the diffusion of HP between endothelial cells lining skeletal and cardiac but not between cerebral endothelial cells (Wolff *et al.*, 2015; Banks, 2016).

### 2.2.2. The location of the BBB

BBB is located at the microvascular capillary of the CNS. This barrier has unique properties different from other capillaries in the body. These properties allow the BBB to strictly regulate the movement of molecules, ions, and cells between the blood and the brain. The regulation of these movements maintains the CNS homeostasis, which is required for the proper function of the brain. The dysregulation of BBB may contribute to brain disease (Obermeier *et al.*, 2016).

Paradoxically, the restrictive nature of the BBB represents the main obstacle to drug delivery into the CNS (Daneman and Prat, 2015). The brain needs a balanced microenvironment for normal function. The BBB, therefore, provides a different type of protection to maintain brain homeostasis. It essentially regulates the influx and efflux of ions, oxygen, and nutrients between the blood and brain compartments. It also restricts the invasion of cells, toxins, and pathogens from the blood into the brain (Keaney and Campbell, 2015).

Anatomically, CNS capillaries are formed by a single layer of endothelial cells. The luminal plasma membrane represents this physical barrier. It extends through the cytoplasm of the endothelial cell, the basolateral plasma membrane, and a specialised basal lamina produced by both endothelial cells and surrounding cells (Stock *et al.*, 2017). BBB acts as an enzymatic barrier; it expresses a high level of enzymes that metabolise drugs. These enzymes include  $\gamma$ -glutamyl transpeptidase ( $\gamma$ -GTP), aromatic acid decarboxylase, and alkaline phosphatase (AP) expressed at the luminal surface of endothelial cells, whereas  $\text{Na}^+$ - $\text{K}^+$  ATPase and sodium-dependent neutral transporters are expressed at the abluminal side. The polarity between luminal and abluminal endothelial sides participates in the barrier function (Persidsky *et al.*, 2006).

### 2.2.3. The neurovascular unit (NVU)

The BBB is made from multiple cell types, including endothelial cells, which form the walls of the blood capillaries, and pericytes (PCs) which incompletely cover the endothelial cells. ECs and PCs are based on a basement membrane (BM) and surrounded by the endfeet of astrocytes. These cells with the neurons and the basement membrane form the neurovascular unit (NVU) (Figure 8) (Weiss *et al.*, 2009; Manton, 2015).

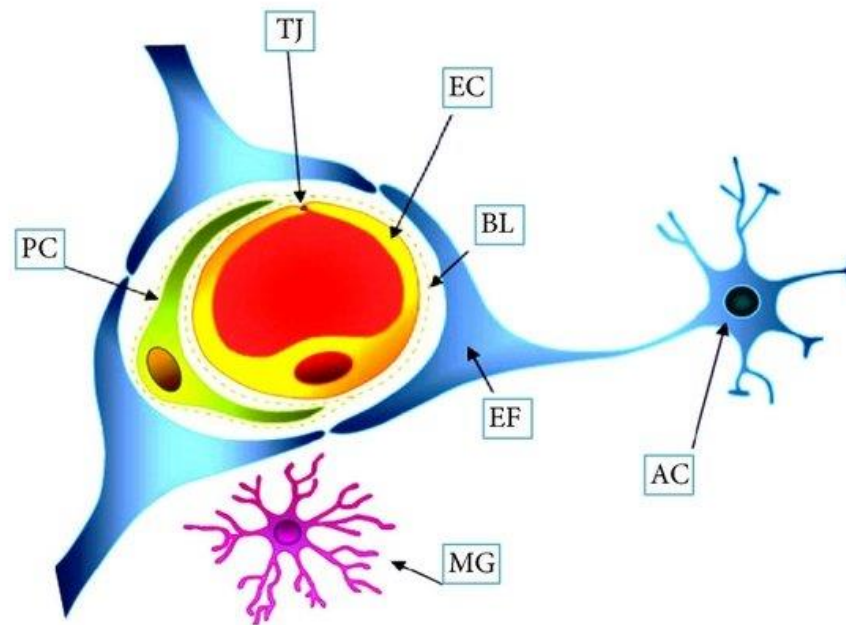


Figure 8. Schematic diagram representing the neurovascular unit (NVU): (EC) endothelial cell is lined at the luminal side of the capillary and connected by the tight junction. On the abluminal side, pericytes (PC) incompletely covers the endothelial cell separating (BL) basal lamina of the basement membrane. Astrocytes (AC) endfeet envelop the capillary and are connected to the basement membrane (MG) macroglia cells, the immune defence agent in the brain (Islam and Mohamed, 2015).

The high coordination activities between cells result in this barrier's regulated function. This function is manifested within the ECs. However, interaction with the other cellular

components of NVU is required to maintain the BBB properties (Figure 9) (Daneman and Prat, 2015).

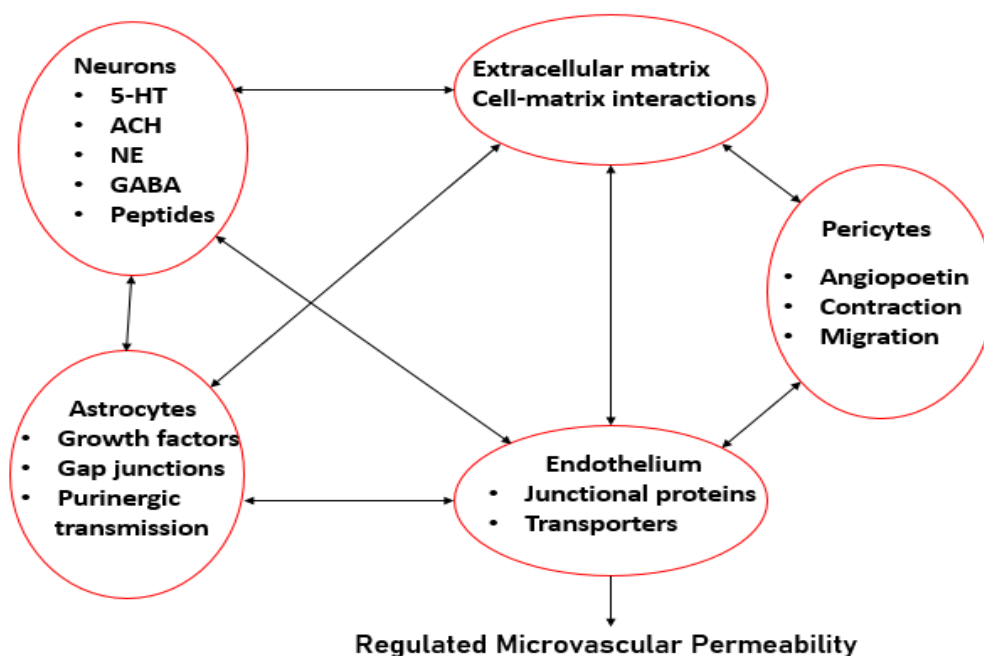


Figure 9. The above scheme shows examples of the correlation between NVU components which result in the BBB function. 5-HT:5-hydroxytryptamine, Ach: Acetylcholine, NE: norepinephrine. GABA: neurotransmitter  $\gamma$ -aminobutyric acid. Modified from (Arshad *et al.*, 2010).

### 2.2.3.1. Brain Endothelial Cells.

The ECs are situated at the interface between the brain and the blood (Persidsky *et al.*, 2006). The cerebral ECs are the functional site of the BBB, having specific properties which distinguish them from endothelial cells in other tissues; the most prominent feature of which is the presence of continuous structural proteins called tight junctions (TJs) (Review and Design, 2010). These proteins link the ECs together, thus, significantly limiting the paracellular flux of solutes and the passage of cells. The tight junctions at the cerebral endothelium have been more complex in the brain endothelium than at the peripheral endothelium (N. Joan Abbott *et al.*, 2006). A particular transport system

(transporter and receptor proteins) at the cerebral ECs regulates the passage of metabolites through the cell allowing specific nutrients to enter the brain and remove specific wastes from the brain into the blood. Low transcytotic vesicles and fenestration levels also characterise cerebral ECs compared to peripheral endothelial cells (Keaney and Campbell, 2015).

The cerebral ECs are different from ECs in the rest of the body; the major peculiarities are highlighted thus: (1) ECs in the BBB are held together by various types of proteins (tight junction, adherent junction), these structures allow ECs to tightly and strictly regulate the paracellular movement of ions, molecules, and cells between the blood and CNS tissue. (2) The absence of fenestration and transcytosis characterises brain ECs compared with peripheral ECs, thus regulating molecules' intracellular movements. (3) A high number of mitochondria also depicts brain ECs compared with other ECs. The high content of mitochondria generates a high amount of ATP needed to maintain ionic fluxes and homeostasis. (4) The polarised expression of receptors and transporters allows the active transport of nutrients into the brain and exclude potentially toxic substances out of the brain (Weiss *et al.*, 2009)(5). The brain ECs express a low level of leucocyte adhesion molecules (LAMs), which limit the penetration of immune cells into the brain (Figure 10) (Daneman and Prat, 2015).



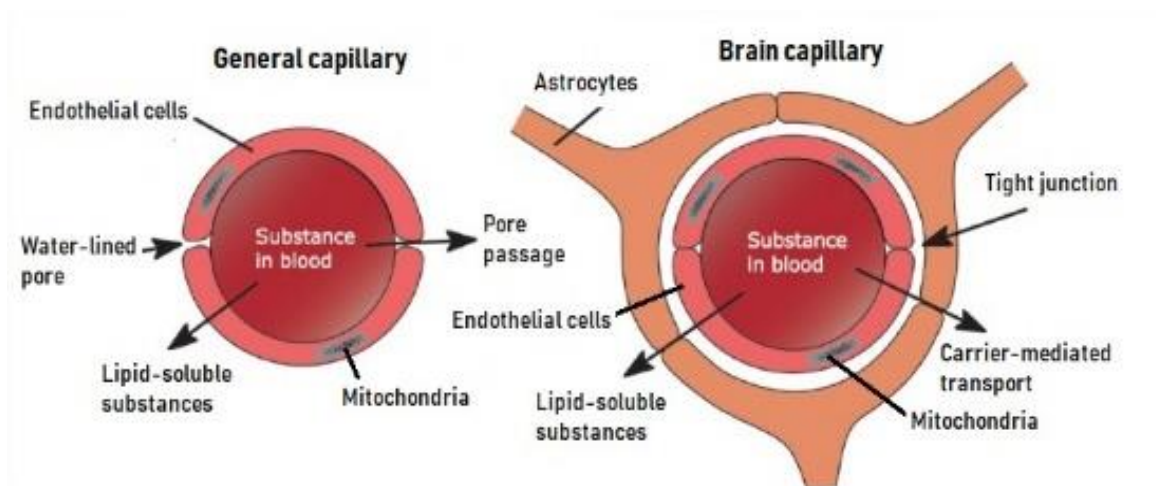


Figure 10. Comparison between the brain and systemic capillary. Endothelial cells are tightly connected by tight junctions in the brain capillary and entirely covered by astrocytes endfeet. In the peripheral capillary, tight junctions also hold endothelial cells; however, they are less tighter and permeable for large types of substances, and astrocytes cover is absent (Boonstra *et al.*, 2015).

### 2.2.3.2. Supporting component of the BBB

#### 2.2.3.2.1. Pericytes (PCs)

Pericytes are mural cells found throughout the body and sit along the abluminal surface of the endothelium in the brain and non-brain microvasculature (Weiss *et al.*, 2009). In the brain vasculature, PCs are separated from the endothelium by the basement membrane, and they are embedded in it (Figure 11) (Daneman and Prat, 2015).

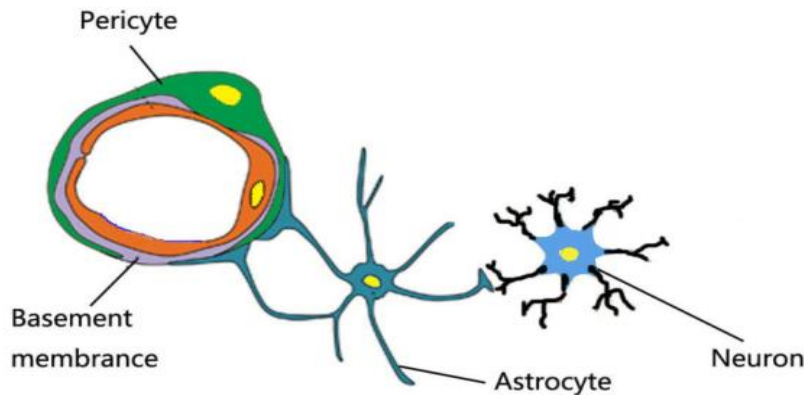


Figure 11. Location of pericyte in the NVU, Pericyte is embedded in the basal membrane. It is the cellular mediator between endothelial cells and astrocytes (Yang *et al.*, 2017).

Pericytes-endothelial cells interact in three ways, as shown in (Figure 12). This involves growth factor-mediated signalling (unidirectional and bidirectional), the N-cadherin and gap junctions (GJs) (Zhao *et al.*, 2015). Pericytes are essential for maintaining BBB integrity and regulating angiogenesis and microvascular stability. Pericytes have contractile proteins, controlling the capillary diameter and the cerebral blood flow, which is essential for the brain's normal function (Kisler *et al.*, 2017). Pericytes have a phagocytosing toxic effect of cleaning tissue debris and foreign metabolites. Pericytes have multiple stem cell activities and differentiate into the neurovascular components (Nakagomi *et al.*, 2015). Pericyte controls the BBB permeability by regulating gene expression in the endothelial cells, leading to the upregulation of TJ proteins and the inhibition of bulk flow transcytosis across the BBB (Zhao *et al.*, 2015). PCs have been found to regulate the immune cells adhesion and infiltration into the CNS (Sweeney *et al.*, 2016).

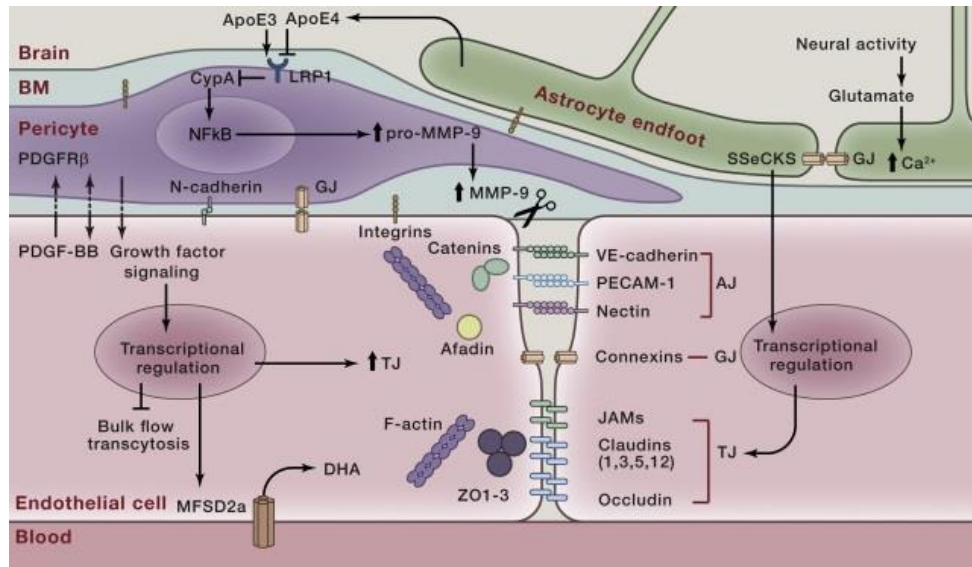


Figure 12. Interaction between cellular components in the neurovascular unit (NVU). Endothelial cells link each other by tight junctions (Claudins, Occludin and JAMs (junctional adhesion molecules), the adherent junction (VE-cadherin (bind to F-actin by catenins), and gap junction, PECAM-1 (platelet endothelial cell adhesion molecule-1), and Nectin). Pericytes interact with endothelial cells via gap junctions (GJ), adhesion N-cadherin and growth factor signalling. TJ (tight junctions). DHA (docosahexaenoic acid). MFSD2a (Major facilitator domain-containing protein 2A). Astrocytes release apolipoprotein E (ApoE3 and ApoE4). ApoE3 binds to LRP1 (lipoprotein receptor-related protein 1) in pericytes, resulting in the suppression of the CypA (cyclophilin A), which activates the nuclear factor- $\kappa$ B (NF $\kappa$ B) MMP-9 pathway, causing TJ and BM degradation. SSeCKS (Src-suppressed C-kinase substrate) secreted from astrocytes induces the expression of TJ in endothelial cells. Increase the release of  $\text{Ca}^{2+}$  in response to neural activity. GJs connect the adjacent astrocytic endfeet (Zhao *et al.*, 2015).

The PCs play a role in regulating the BBB formation, thus maintaining its function. A study using mice with mutations in platelet-derived growth factor-b (PDGFR-b) has shown the vital role of PCs in regulating BBB. Endothelial cells secrete PDGFR-b into the basement membrane. On the other side, pericytes have PDGFR-b receptors. The interaction of PDGF-b with its receptors attracts the pericytes to the endothelial cells. The analysis of mice with PDGFR-b-null that die at birth showed a complete lack of pericytes and an impaired BBB (high rate of transcytosis and the expression of leukocyte adhesion molecules (LAMs) (Daneman and Prat, 2015; Lyle *et al.*, 2016).

Studies have also reported that the number of pericytes cells are essential for normal BBB permeability. The ratio of pericytes to endothelial cells is approximately 1:3 (Serlin *et al.*, 2015). The increase or decrease of PCs number and secreted factors from them, such as transforming growth factor-beta (TGF- $\beta$ ), could influence the vascular integrity (Serlin *et al.*, 2015) and result in the BBB dysfunction (Siegenthaler *et al.*, 2013; Blanchette and Daneman, 2015). Pericytes contribute to glioblastoma progression and metastasis in systemic models. The brain has the highest pericyte coverage, whereas abnormal pericyte coverage and function are responsible for CNS diseases, including diabetic retinopathy, stroke, and neurodegeneration (Lyle *et al.*, 2016).

#### **2.2.3.2.2. Basement membrane (BM)**

The BM is a complex structure surrounding the endothelial and epithelial tissue; it provides these tissues with essential functions by supporting the cell structure and offering a signalling transduction area (Jayadev and Sherwood, 2017). In the NVU, BM is presented in two areas: between endothelial and pericytes (endothelial BM) and between pericytes and the other NVU components (parenchymal BM) (Xu *et al.*, 2019).

At the structural level, BM is composed of three layers. ECs and PCs secrete the first inner vascular basement composed of laminins  $\alpha 4$  and  $\alpha 5$ . In contrast, the second is the outer parenchymal basement secreted by astrocytes and is composed of laminins  $\alpha 1$ ,  $\alpha 2$ . The third layer is in the middle and made up of collagen IV and is released by both cell types (Blanchette and Daneman, 2015). The BM represents support for the signalling process at the vascular tube and represents an additional barrier for molecules and cells before reaching the neural tissue (S. Stamatovic *et al.*, 2008).

Laminin is a trimeric protein composed of  $\alpha$ ,  $\beta$ , and  $\gamma$  chains. Laminin  $\alpha 5$ ,  $\beta 4$ , and  $\gamma 3$  are the most known (Jayadev and Sherwood, 2017). Laminin  $\alpha 5$  has been shown to inhibit lymphocyte infiltration (Wu *et al.*, 2009). Collagen IV (known as COL4A). It is an

exclusive member of the basement membrane (Khoshnoodi *et al.*, 2008), composed of six genetically distinct  $\alpha$ -chains;  $\alpha 1(\text{IV})$  (COL4A1) to  $\alpha 6(\text{IV})$  (COL4A6), the specific interaction and assembly of the chains form three distinct heterotrimers of  $\alpha 1\alpha 1\alpha 2$ ,  $\alpha 3\alpha 4\alpha 5$ , and  $\alpha 5\alpha 5\alpha 6$  (Khoshnoodi *et al.*, 2008).  $\alpha 1(\text{IV})$  COL4A1 and  $\alpha 2(\text{IV})$  COL4A2 are present in the majority of BM of all tissues, whereas COL4A3-6 are spatially and temporally presented (Xu *et al.*, 2019). The  $\alpha 3(\text{IV})$  COL4A3,  $\alpha 4(\text{IV})$  COL4A4, and  $\alpha 5(\text{IV})$  COL4A5 chains are present in the glomerular basement membrane (GBM) of the kidney, lung, testis, and eye, whereas the  $\alpha 5(\text{IV})$  COL4A5 and  $\alpha 6(\text{IV})$  COL4A6 chains are present in the BM of skin, smooth muscle, and the kidney (Khoshnoodi *et al.*, 2008).

The  $\alpha 1(\text{IV})$  COL4A1 and  $\alpha 2(\text{IV})$  COL4A2 are required for the BM maintenance; thus, the BBB integrity, their genetic deletion result in an abnormal BM structure. In addition, mice with a mutation lacking exon 41 of COL4A1 in both alleles, die during embryogenesis. In contrast, those with such mutation in one allele show cerebrovascular defects and intracerebral haemorrhage (Xu *et al.*, 2019).

In addition to the Laminins and collagen, other proteins such as nidogens and heparan sulfate proteoglycans belonging to the glycoprotein family are also part of BM components. These proteins link the BM components and ECs (Luissint *et al.*, 2012). Two types of nidogens have been identified in the BM; nidogen-1 and nidogen-2. The genetic mutation for nidogen-1 shows a mild alteration in the BM at the brain capillary (Xu *et al.*, 2019).

BM contributes to maintaining BBB stability through agrins. Agrins are involved in the development of the BBB by contributing to astrocytes polarity (Wolburg *et al.*, 2009). Agrins interact with their transmembrane receptors (integrins) of the ECs, resulting in the adhesion of ECs to the BM.  $\beta 1$ -integrin links ECs to BM and plays a role in the stability of localisation of claudin-5 at the TJs (Osada *et al.*, 2011). It has been reported

that, in brain tumours, ECs seems detached from the BM, and the absence of the agrains is observed, which correlate with the lack of claudin5 and occludin (Luissint *et al.*, 2012). The disruption of the BM is one of the features of BBB dysfunction (Thomsen *et al.*, 2017).

BM support the endothelial proliferation; the attachment of ECs to the BM occurred through the interaction between the cell surface integrins with the BM agrins; this interaction is necessary to activate the p44/p42 (Erk1/Erk2) mitogen-activated protein kinase (MAPK) signalling pathway in ECs by cytokines, this activation is critical for ECs proliferation. The adhesion of ECs with the BM also induced activation of cyclin-dependent kinases necessary for the cell cycle progression (Davis and Senger, 2005).

#### **2.2.3.2.3. Astrocytes (ACs)**

ACs are the principal glial cells represented in the brain. Their end feet are almost ensheathed in the vascular tube, where they envelop >99% of the BBB (Persidsky *et al.*, 2006). They offer contact between neural activity and blood vessels, and this position allows astrocytes to transfer the signals that regulate blood flow in response to neuronal activity (Figure 13). Astrocytes and endothelial cells interact indirectly. This interaction induces the BBB development and provides unique brain endothelial phenotypes, such as the formation of tight junctions (Abbott, 2002). On the other hand, Astrocytes density is enriched by interacting with endothelial cells (Persidsky *et al.*, 2006; Sofroniew and Vinters, 2010). Moreover, astrocytes present structural support for the NVU, providing variety of cell adhesion and extracellular matrix molecules that are necessary for proper synaptic function (Oksanen *et al.*, 2019)

Astrocytes have been reported to play an essential role in maintaining the brain microenvironment (Haseloff *et al.*, 2005). Some substances secreted by astrocytes, such as glial-derived neurotrophic factor (GDNF), angiopoietin-1, and angiotensin II have been suggested to participate in BBB integrity (Michinaga and Koyama, 2019). Astrocytic



angiopoietin 1 (ANG-1) is transferred through the endfeet to bind to its specific receptor TIE2 on endothelial cells, increasing the endothelial stability and resistance (Alvarez *et al.*, 2013). Similarly, the endothelial-derived factor LIF has a role in inducing astrocytic differentiation (Dyrna *et al.*, 2013). Astrocytic endfeet expresses the potassium channel Kir4.1, water channel aquaporin-4 (AQP4), which controls the water balance and ion homeostasis (Michinaga and Koyama, 2019). As neuronal activity leads to the release of potassium, an increase of intercellular  $K^+$  is transferred into the astrocytic endfeet via the  $K^+$  channel Kir4.1. The movement of the  $K^+$  into astrocytes results in osmotic water uptake, which causes cellular swelling. Thus, aquaporin 4 (AQP4) redistributes the water through the channels on the astrocytic endfeet (Dyrna *et al.*, 2013).

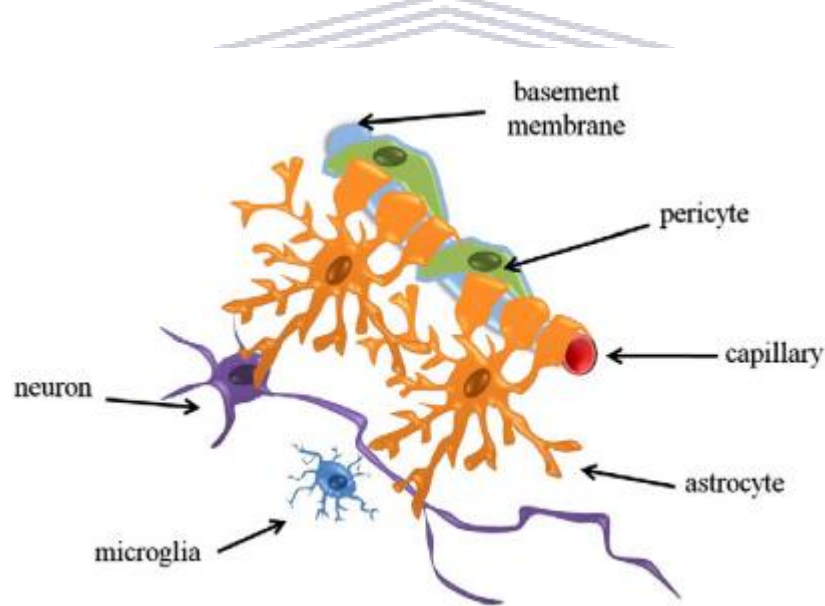


Figure 13. Astrocytes as mediator connection between endothelium and the neuron (Cardoso *et al.*, 2010).

In addition to the neurotransmitter uptake, ACs endfeet contain dystroglycan and dystrophin proteins. Dystroglycan- dystrophin complex binds the endfeet cytoskeleton to the BM by agrin (Noell *et al.*, 2011). ACs also support neuronal metabolism and

regulate the ion concentration in the extracellular space and CNS repair after injury (Michinaga and Koyama, 2019).

In certain CNS diseases such as AD, PD, and ALS, astrocytes contribute to BBB disruption through their release of proinflammatory cytokines, including IL-6, IL-1 $\beta$ , and TNF- $\alpha$ , which influence the expression of endothelial TJs and an increase in the expression of AQP4 and reduced Kir4.1 which disrupt the water/potassium homeostasis in the brain (Oksanen *et al.*, 2019).

#### **2.2.3.3. Brain endothelial cell-cell interaction**

Brain endothelial cells contact each other by junctional proteins and gap junction (Stamatovic *et al.*, 2016; Johnson *et al.*, 2018). The junctional proteins promote the adhesion of opposing endothelial cells, therefore maintaining the correlation of the endothelial barrier (S. M. Stamatovic *et al.*, 2008). In contrast, gap junctions form channels between neighbouring cells allowing the movement of water, ions, and other small molecules and are designed to transmit signals between cells (Thuringer *et al.*, 2017).

##### **2.2.3.3.1. Junctional proteins complex**

The endothelial junction proteins can be divided into two main groups, the integral proteins and connector proteins (Dyrna *et al.*, 2013) (Table 2). The integral group includes the occludin and claudin families, which were discovered first. The other two proteins belong to Ig-superfamily known as junctional adhesion molecules (JAM) and endothelial cells-selective molecules ESAM (Stamatovic *et al.*, 2016). The connector proteins also are divided into two subgroups based on their connection with the integral protein into ZO proteins (ZO-1,2 and 3) (which directly interact with claudin and occludin) and others that are indirect connection with the integral proteins, include cingulin, paracingulin, and junction-associated coiled-coil protein (JACOP) (Luissint *et*



*al.*, 2012). Catenins and desmoplakin, p120 and ZO-1 link adhesion junction and cytoskeleton (Figure 14) (N. Joan Abbott *et al.*, 2006).

Table 2: Summarization of tight junctions at the blood-brain barrier (BBB).

<b>Type of proteins</b>		<b>Brief description</b>	
<b>Tight junction proteins</b>	<i>Integral proteins (Located at the apical side of the plasma membrane)</i>	<i>Occludins</i>	<i>They are composed of two extracellular domains and three intracytoplasmic domains. They bind to the cytoplasmic ZO-1 via its C-terminus intracellular domain.</i>
		<i>Claudins</i>	<i>Claudins are composed of four domains, two extracellular and two cytoplasmic intracellular. They bind to the cytoplasmic proteins via their PDZ domain claudins interact heterotypically and homotypical, forming the backbone of TJs.</i>
		<i>Junctional adhesion molecules (JAM)</i>	<i>They are composed of JAM-A/B/C and endothelial cell adhesion molecules (ESAMs). They are required for BBB stability; they bind to the PDZ domain of cytoplasmic proteins.</i>  <i>(Liu et al., 2012; Luissint et al., 2012; Tajés et al., 2014; Greene and Campbell, 2016).</i>
	<i>Connector proteins</i>	<i>Cytoplasmic proteins</i>	<i>They consist of zonula occludens family (ZO-1/2/3), they have a specific PDZ domain (a specific sequences of 80–90 amino acids in the carboxyl terminal side), by which they connect to the integral proteins (Luissint et al., 2012; Tajés et al., 2014).</i>
	<i>Adherens junctions (AJs)</i>	<i>Cadherin proteins, platelet endothelial cell adhesion molecule-1</i>	<i>They bind to the cytoskeleton through <math>\alpha</math>-catenin forming adhesive cell-cell contact. The extracellular domains of cadherin on the surface of neighbouring cells contact</i>

	(They are close to the basolateral side of the plasma membrane)	(PECAM-1), and $\alpha, \beta$ -catenin	homophilically in a calcium-dependent way to form the adhesive connection between the cells (Luissint <i>et al.</i> , 2012; Kadry <i>et al.</i> , 2020; Xiao <i>et al.</i> , 2020)
--	---	---	--

The function of the tight junctions between brain endothelial cells is to create a high electrical resistance and low paracellular diffusion. The electrical resistance of the brain endothelium is in the range of 1500-2000  $\Omega \cdot \text{cm}^2$  (pial vessels) compared to 3-33  $\Omega \cdot \text{cm}^2$  of the endothelium in other tissues (S. Stamatovic *et al.*, 2008).

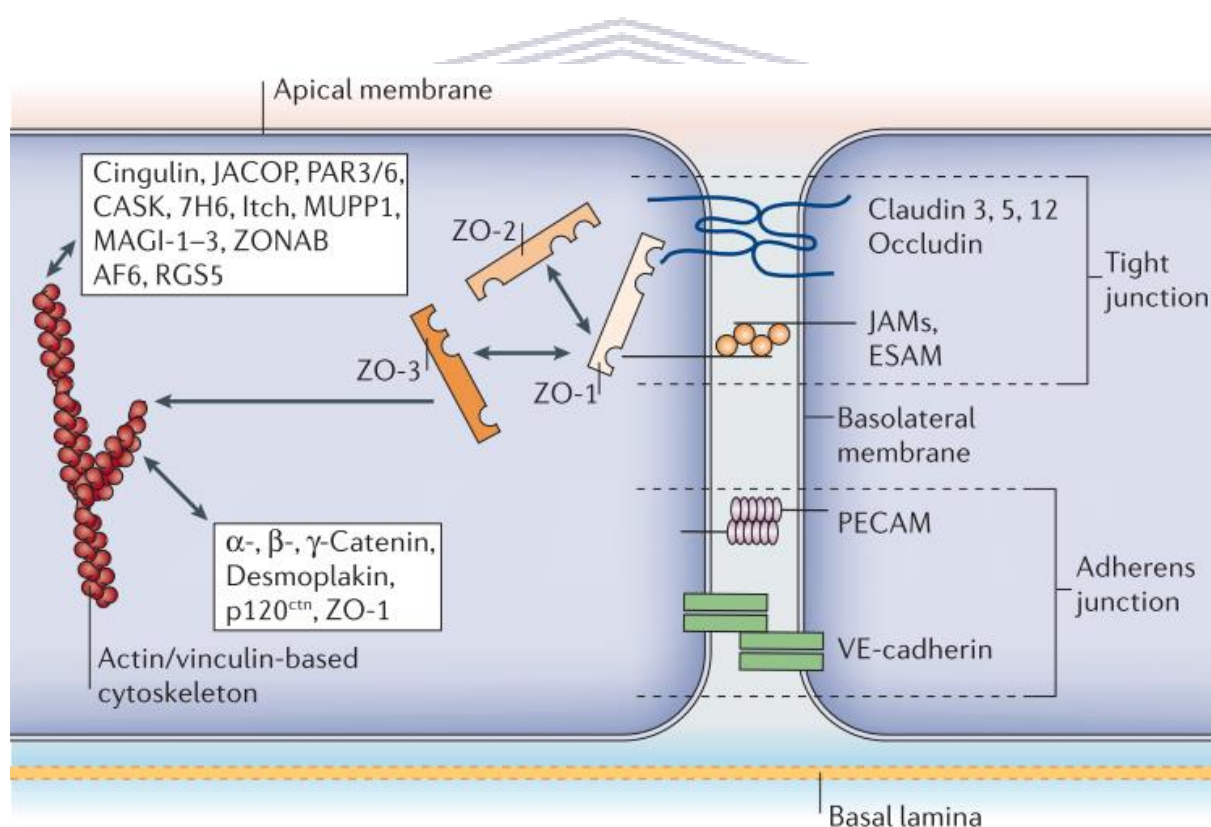


Figure 14. The structure of tight junctions (N. Joan Abbott *et al.*, 2006).

#### 2.2.3.3.1.1. Claudins

Claudin is composed of 24 proteins (20 to 24 KDa) exclusively localised at TJs and represents TJs' major components (Liu *et al.*, 2012). Four transmembrane domains, two extracellular loops, and a short C-terminus tail characterize claudins. Claudins connect to cytoplasmic zona proteins via the PDZ domain and bind homotopically to other claudin molecules in the neighbouring endothelial cell via intracellular loops with C-terminus (Liu *et al.*, 2012). Occludin and claudin extracellular domains between neighbouring cells form TJ's paracellular barrier (Gonzalezmariscal, 2003)

The claudin family consists of various members (Claudin 1, 2, 3, 5, 11, and 12) (Stamatovic *et al.*, 2016). In the cerebral ECs, claudin 3, 12 and 5 are present. However, claudin 5 contains the dominant claudins (Greene and Campbell, 2016). Claudins in the brain ECs form pores of variable size ( $\sim 10\text{\AA}$ ); these pores might be implicated in the water movement (Greene and Campbell, 2016; Stamatovic *et al.*, 2016; Fisher and Mentor, 2020). Claudin-5 is expressed explicitly at the brain ECs and forms E-face associated with the exocyttoplasmic fracture face (E-face) of tight junctions (Liebner, Fischmann, *et al.*, 2000). It is also essential to develop a stable TJs network and the BBB. Knockout mice of claudin-5 showed an impaired BBB with increased permeability of molecules up to 800 Da in size (Greene and Campbell, 2016).

#### 2.2.3.3.1.2. Occludin

Occludin ( $\sim 65$  kDa) was the first membrane protein identified at tight junctions (Cummins, 2012). It has four transmembrane domains, two extracellular domains, and two cytoplasmic domains (Bhowmik *et al.*, 2015). The N and C-terminus are located in the intracellular space, the C-terminus binds to F-actin, and the GK domain of ZO-proteins, which in turn links to the cytoskeleton (Feldman *et al.*, 2005; Liu *et al.*, 2012; Greene and Campbell, 2016).

#### 2.2.3.3.1.3. *Junctional adhesion molecules (JAMs)*

JAMs belong to the immunoglobulin superfamily; they structurally consist of an extracellular N terminus domain with two loops (IgG-like domains), a short intracellular C-terminus tail containing the PDZ domain, and a single transmembrane domain. JAMs bind to the PDZ domain of AF-6, ASIP/Par3, cingulin, and ZO-1 with its C-terminus in intracellular loops. The JAMs can form heterophilic interactions with different JAM family members and also form homophilic interactions with molecules in the adjacent cells (Greene and Campbell, 2016).

#### 2.2.3.3.1.4. *The cytoplasmic plaque proteins*

Cytoplasmic proteins link the adhesive transmembrane proteins (occludin, claudins, and JAM) to actin, a primary cytoskeleton protein. These proteins have sequence similarities with each other, and they are divided based on whether they have a PDZ motif or not. The PDZ motif is a sequence with 80-90 amino acids on the carboxyl-terminal. PDZ motifs allow the interaction of cytoplasmic proteins with transmembrane proteins or with PDZ motifs on other cytoplasmic proteins (Ballabh *et al.*, 2004).

Cytoplasmic proteins containing PDZ motifs belong to the family of MAGUKs (membrane-associated guanylate kinase-like proteins). These cytoplasmic proteins have three PDZ domains (PDZ1, PDZ2, and PDZ3), one SH3 domain, and one guanylate kinase-like (GUK) domain (Ballabh *et al.*, 2004). The cytoplasmic proteins in the TJs complex are divided into cytoplasmic proteins contained PDZ, such as zonula occludins proteins (Huber *et al.*, 2001); partitioning defective proteins (Par)3, (Par)6, afidin/Af-6, and cytoplasmic proteins lacking PDZ which include cingulin, 7H6, Rab13, ZONAB, AP-1, PKC, PKC and heterotrimeric G protein (S. Stamatovic *et al.*, 2008)

Zonula occludins proteins include ZO1, ZO2, and ZO3 and, they interact directly with TJs proteins (Huber *et al.*, 2001). ZO-1 is a 220 kDa phosphoprotein; it was the first

cytoplasmic protein found in TJs. It binds to other transmembrane proteins with its PDZs to the C-terminus of claudins by PDZ-1, JAMs by PDZ- 2 and -3, and occludin GUK domain. ZO-1 also binds to the actin cytoskeleton via its C-terminus. This interaction is vital to the stability and function of the TJs complex. The dissociation of ZO-1 from the junctional complex often leads to increased permeability of the BBB (Liu *et al.*, 2012).

Cingulin is a 140 kDa protein that links TJs cytoplasmic proteins and the actin-myosin cytoskeleton. It maintains the tight barrier in brain endothelium *in vivo* and *in vitro* (Schossleitner *et al.*, 2016). The 7H6 is a 155 kDa protein that plays a role in TJ maturation. ZONAB is a transcription factor that regulates paracellular permeability, Rab13 plays a role in the fusion of transport vesicles at TJs finally. PKC regulates the polarisation and TJs assembly. G proteins act with the ZO-1 to accelerate the TJ assembly and maintain the transendothelial electrical resistance (Liu *et al.*, 2012).

#### **2.2.3.3.1.5. Adherence junctions(AJs)**

AJs composed of membrane proteins cadherin and other proteins known as catenin ( $\alpha$ ,  $\gamma$ ,  $\beta$ -catenin). These intermediary proteins bind cadherin to the cytoskeleton. Cadherin has two domains, i.e. the extracellular domain and a cytoplasmic domain. The extracellular domain, which is calcium-dependent, interacts homophilically with the extracellular domain of cadherin in the adjacent cell. In contrast, the cytoplasmic domain binds to the cytoplasmic proteins ( $\alpha$  or  $\gamma$ -catenin) that link with  $\beta$ -catenin, which joins the cytoskeleton (Ballabh *et al.*, 2004).

#### **2.2.4. The function of the blood-brain barrier**

The primary function of the BBB comprises the brain homeostasis and providing the brain with nutrition (Figure 15). BBB selectively transports various substances to the brain. Most of these substances are essential nutrients for the brain. BBB also mediates the removal of waste products from the brain and can respond to changes in the local

environment. This physical barrier function is supported by the continuous presence of the transmembrane proteins between ECs (Cardoso *et al.*, 2010). The BBB is also a metabolic barrier expressing enzymes such as acetylcholinesterase, alkaline phosphatase,  $\gamma$ -glutamyl transpeptidase, monoamine oxidases, and drug-metabolising enzymes (Wilhelm and Krizbai, 2014). These enzymes are expressed in elevated concentrations in the brain endothelial cells compared to non-brain endothelial cells. These enzymes are often polarised between the luminal and abluminal membrane surface of brain endothelial cells (S. Stamatovic *et al.*, 2008).

BBB controls ionic homeostasis in the brain by regulating ionic and fluid movements between the blood and the brain. The protection of the brain from changes in ionic composition can happen in various conditions, such as after a meal or exercise. Anionic distribution would disturb synaptic and axonal signalling, therefore, affect brain function (Hladky and Barrand, 2016). It is essential to have a homeostatic mechanism to maintain the ionic composition of the fluid around the neurons to protect them from fluctuations in the blood's ionic composition, thus protecting the brain (Abbott, 2013). BBB, through the TJs, strictly regulate the entry of ions to the brain via the transcellular pathways. For example, ions such as  $\text{Na}^+$ ,  $\text{K}^+$ , and  $\text{Ca}^{2+}$  must be maintained within a very narrow range of concentrations. The brain endothelial cells express transporters involved in the ion homeostasis, including  $\text{Na}^+\text{-K}^+\text{-ATPase}$ , and many of these transporters have a polarised distribution at the cerebral endothelium. They are associated with the abluminal portion of the endothelium (Hladky and Barrand, 2016).

The BBB helps separate the pools of neurotransmitters and neuroactive agents that act centrally (in the CNS) and peripherally (in the peripheral tissues and blood). The BBB also protects the brain from harmful substances and microorganisms from the peripheral environment (Abbott and Friedman, 2012). The BBB protects the brain by allowing the

needed substances to cross and blocking the harmful ones. The plasma contains high concentrations of the excitatory amino acid glutamate, which may cause neuroexcitatory damage. In addition, the BBB also prevents non-meaningful crosstalk as the peripheral and central nervous systems often use the same neurotransmitters (N Joan Abbott *et al.*, 2006; Bernacki *et al.*, 2008; Abbott and Friedman, 2012). Furthermore, the BBB protects the CNS against neurotoxin substances such as proteins, xenobiotics, and endogenous metabolites. The ECs have various ATP-binding cassette transporters that actively pump respective agents out of the brain (Dyrna *et al.*, 2013).

Providing the brain with the required nutrition is an essential function of BBB (Campos-Bedolla *et al.*, 2014). The presence of high level of TJs between brain endothelial cells forces the nutrition to cross the endothelial cells transcellularly to get to the brain. For this, the brain endothelial cells process specific transporters to facilitate transport the of glucose and amino acids. In addition, BBB has other transporters, such as P-glycoprotein and organic anion transporters, to remove the waste products from the brain or prevent the entry of potentially neurotoxic compounds from the blood to the brain (S. Stamatovic *et al.*, 2008).

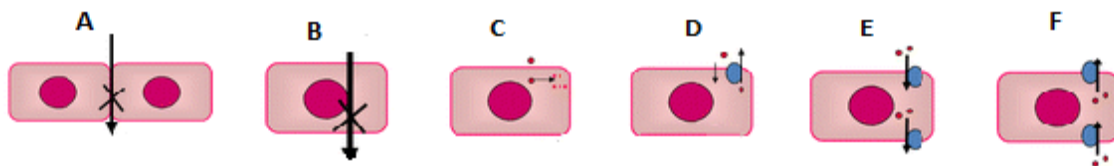


Figure 15. Schematic diagram illustrating the BBB function. A- Paracellular barrier, B-Transcellular barrier, C-Enzymatic barrier, D- Efflux transport to protect the brain from neurotoxins and drugs, E- Transport of the nutrition into the brain, F- Remove the metabolites from the brain. Modified from (Wilhelm and Krizbai, 2014).



### 2.2.5. Transport at the blood-brain barrier

In normal physiological conditions, BBB is a highly selective semipermeable barrier which strictly controls the transport of molecules and cells to the brain. Hence, it prevents most drugs from reaching the brain (Keaney and Campbell, 2015). There are various molecules that are important for brain function and homeostasis, and also other molecules need to be removed from the brain; therefore, the brain endothelial cells are provided with a transport system to control the influx and efflux between the brain and the blood (Abbott *et al.*, 2009). The main way by which molecules, solutes, and fluid are transported across the BBB is by the movement across the ECs (transcellular way) (Komarova and Malik, 2010). The presence of TJs between endothelial cells prevents the transport of substances through the paracellular way. The transfer by the transcellular way mostly depends on the properties of the molecules, such as the size and the lipophilic and hydrophilic ability. Lipophilic soluble molecules freely diffuse through the endothelial membrane into the brain. However, hydrophilic molecules need specific transporters to cross the BBB. Although lipophilic molecules are diffused through the BBB, they are actively returned to the blood, even against their concentration by the efflux transporters such as ATP-binding cassette (ABC) proteins, which are expressed at the luminal side of ECs; thus, they transport lipophilic molecules diffused via the EC membrane into the blood (Persidsky *et al.*, 2006). The efflux transporters include P-gp (P-glycoprotein), MDR (multidrug resistance proteins), and BCRP (breast cancer resistance protein). These transporters belong to the superfamily of ATP-binding cassette (ABC) proteins and are expressed at the luminal side of ECs; thus, they transport lipophilic molecules diffused via the EC membrane into the blood (Weiss *et al.*, 2009).

The transcellular transport acrosses the BBB can occur in different ways by passive and active diffusion (Figure 16). Passive movement occurs via the cell membrane by direct diffusion to the lipid plasma membrane of ECs, where the small substances with



lipophilic solubility can freely penetrate the ECs (Wong *et al.*, 2013). Active transfer of molecules occurs via active transporters; this transport is ATP-dependent, which occurs against the molecules concentration gradient. Active transport includes active efflux transporters (such as P-glycoprotein, which transfer drugs out of the brain) and Carrier-mediated transporters (CMTs). CMTs are classified into two groups; carrier proteins (they carry specific proteins through the BEC) and channel proteins (form pores for ions to pass); channel proteins are also mediators for the passive transport to facilitate the spontaneous transfer of ions down their gradients (Fong, 2015).

In endocytic transport, the substances are engulfed by the cell membrane, which forms a vesicle. The vesicle passes through the cell to be released on the other side. The number of vesicles is very limited in the brain endothelial cells, compared with the endothelial cells of permeable vessels (Strazielle and Gherzi-Egea, 2013).

Some large essential molecules like hormones, growth factors, and enzymes use membrane proteins expressed at the luminal side of ECs as a receptor to facilitate the endocytotic transport to the other side (Wong *et al.*, 2013). In the absorptive mediated endocytosis, the difference of charge of molecules is essential to cross the cell. The electrostatic interaction between positive and negative charge leads to the uptake of these molecules into vesicles in the cell being released on the other side (Jouyban and Soltani, 2012).

Water, O<sub>2</sub>, CO<sub>2</sub>, and glucose are the most common substances transferred across the BBB. The cerebral blood flow that goes to the choroid plexuses is less than ~1%, which is not enough to supply the brain with the needed amount of water, O<sub>2</sub>, CO<sub>2</sub>, and glucose; thus, these essential substances easily diffuse past the membranes of brain endothelial cells (Hladky and Barrand, 2016), O<sub>2</sub> and CO<sub>2</sub> can be transferred through the cell membrane by their concentrations (Wong *et al.*, 2013). However, glucose is transferred

passively via saturable glucose transporter (GLUT1), which is expressed on the luminal and abluminal membranes of the brain ECs (Hladky and Barrand, 2016).

The transport between endothelial cells (paracellular way) is effectively limited by the endothelial TJs (Komarova and Malik, 2010); however, in particular brain pathological conditions, blood cells cross the BBB via the paracellular way. Although the microglia is the surveillance agent against infections in the brain, the circulating leucocytes cross the BBB in inflammatory conditions. Such conditions are the pathogenic features found in brain diseases like cerebral infection, stroke, trauma, and multiple sclerosis (Profaci *et al.*, 2020). In a previous *in vitro* study, Winger and his colleagues (2014) demonstrated that leucocytes mostly migrate across the brain endothelium via the paracellular pathway, and molecules expressed on endothelial cells PECAM-1 and CD99 are mediators for this process. In addition, they showed that TJ proteins, including claudin-5, are dynamic and undergo rapid remodelling during this process (Winger *et al.*, 2014).

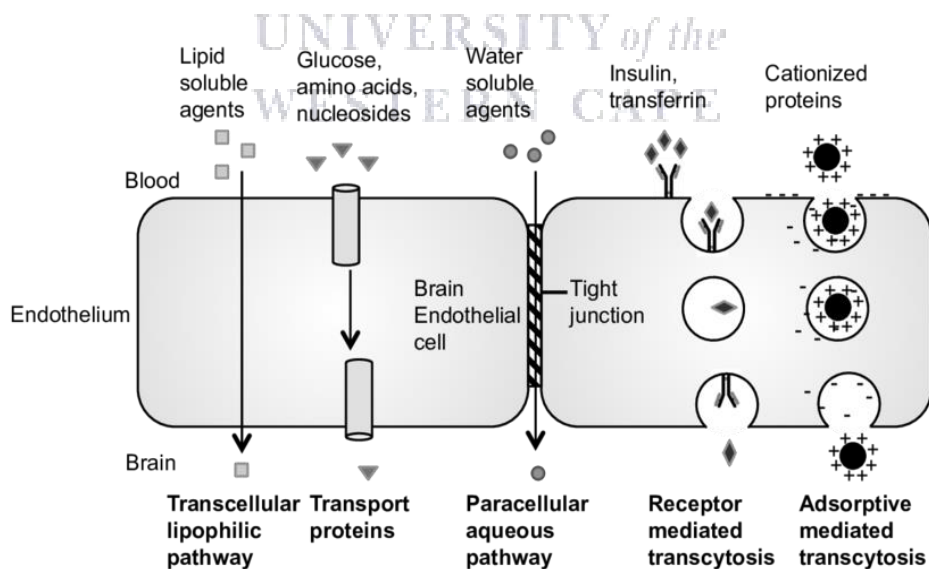


Figure 16. The transport of molecules across the blood-brain barrier (Rocha, 2013).

## **2.2.6. Factors that modulate the BBB permeability**

### **2.2.6.1. Inflammation**

The inflammation has a deleterious effect on the BBB function (Stolp and Dziegielewska, 2009). The central role of the BBB in maintaining the homeostasis of the brain for a normal function is changed transiently or permanently (Elwood *et al.*, 2017). The alteration in the BBB due to the inflammation could be disruptive or non-disruptive. The disruptive effect is more related to the histological level of the BBB, including an alteration in the TJs complex, damage in the ECs, and a breakdown in the communication of ECs with the other cells in NVU, which support the BBB properties (Varatharaj and Galea, 2017). On the other hand, the nondisruptive effect on the BBB is more in transcellular ways through the specific receptors and transporters (Varatharaj and Galea, 2017).

In general, inflammation on the BBB permeability is defined as the disassociation in the endothelial TJs assembly, followed by extravasation of the leukocytes and an increase in the diffusion of solutes across ECs, prompting pathogens and toxins into CNS (Figure 17) (Dyken and Lacoste, 2018; Linlin Chen *et al.*, 2018).

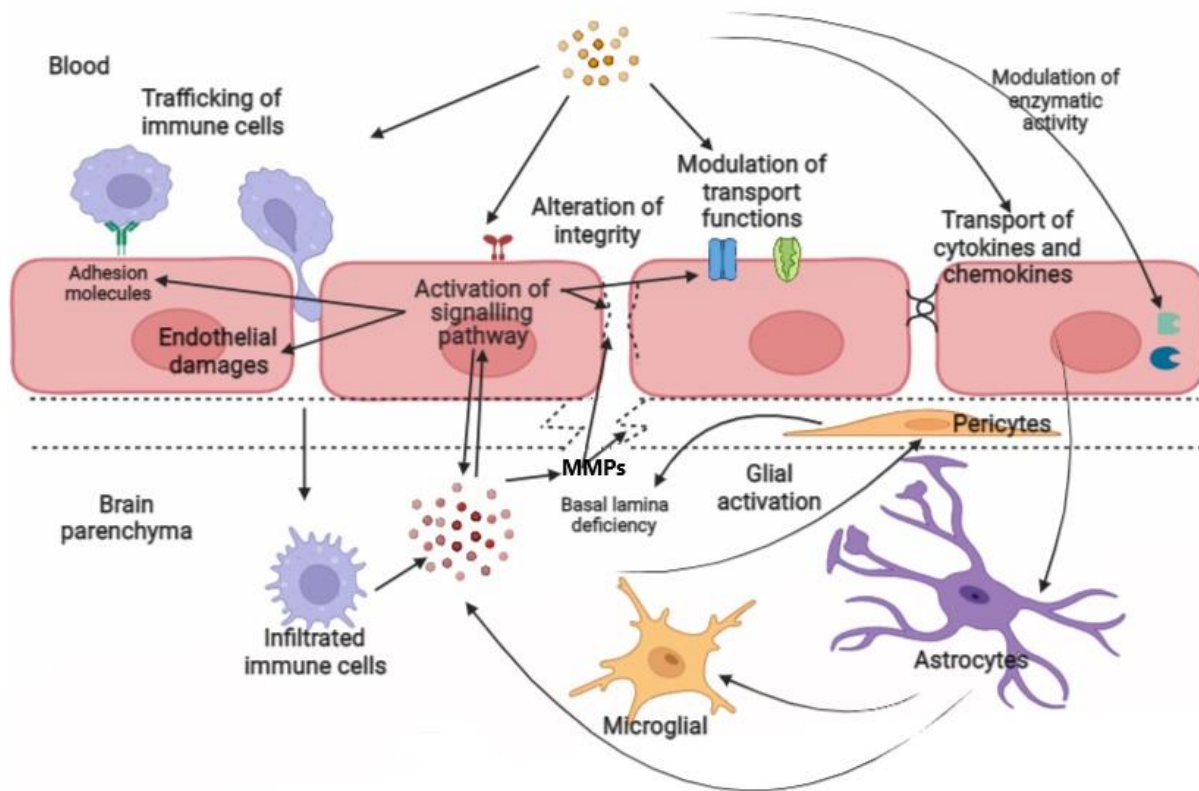


Figure 17. Diagram summarizes the inflammatory events in Blood-brain barrier. Modified from (Weidenfeller and Shusta, 2007).

Cytokines remain an essential inflammatory factor produced during the inflammation stimulating the cells for further inflammation. BECs express several cytokine receptors such as IL-1b, IL-6, and TNF- $\alpha$ ; therefore, these cytokines can transport across the endothelium to the CNS and play an essential role in the inflammatory response (Pan *et al.*, 2014). Pro-inflammatory cytokines can disrupt the BBB. Some cytokines exclusively affect paracellular barriers through the tight junction proteins, and others affect the transcellular processes mediated by caveolae (Wardill *et al.*, 2016).

Pro-inflammatory cytokines increase the paracellular permeability and reduce the expression of the cytoplasmic ZO proteins *in vitro* model of the BBB (Wardill *et al.*, 2016).

In human endothelial cells, pro-inflammatory cytokines TNF- $\alpha$  and interleukin-6 (IL-6) significantly affect the expression of the inter-endothelial junction proteins VE-cadherin (AJ), occludin (TJ) and claudin-5 (TJ) in a dose and time-dependent manner (Rochfort *et al.*, 2014).

Transcytosis permeability is also altered by the pro-inflammatory cytokines, multifunctional efflux transporter P-glycoprotein, and other transporters such as receptors for organic anions, monocarboxylates, amino acids,  $\beta$ -amyloid, leptin through downregulation (Varatharaj and Galea, 2017).

ECs, astrocytes and pericytes under the stimulation of different pro-inflammatory cytokines can release a varied range of cytokines. Activated astrocyte release cytokines including interleukin-1 $\beta$  (IL-1 $\beta$ ), interleukin-6 (IL-6), tumour necrosis factor- $\alpha$  (TNF- $\alpha$ ), and prostaglandins while TNF- $\alpha$  induces activation of NF- $\kappa$ B to lead to further inflammatory responses resulting in extravasation of macrophages (-Galvan *et al.*, 2016). These inflammatory mediators induce a chemoattracts process of the neutrophils, then facilitate their transmigration across the BBB (Liu *et al.*, 2018).

Activated pericytes express a high level of proinflammatory cytokines, such as histocompatibility complexes (MHC II), and increase the neutrophils' phagocyte activity. IL-1 $\beta$  stimulates pericytes activation releases other molecules IL-6 and CXCL8. These inflammatory mediators induce a chemoattraction of the neutrophils to the pericytes, facilitating their transmigration across the BBB (Hurtado-Alvarado *et al.*, 2014).

Vascular endothelial growth factor (VEGF) is a homodimeric 45-kDa glycoprotein secreted by different endothelial cells involving in proliferation and angiogenesis (Azimi-Nezhad, 2014). VEGF interacts with its receptors on the endothelial cell surface, resulting in downstream signalling mediators by stimulating endothelial growth and increasing

the permeability (Carmeliet, 2005). *In vitro* and *in vivo*, VEGF alters tight junction assembly and increases permeability by reducing occludin expression, disrupting ZO-1 and cludin-5 organization, inducing BBB breakdown (Petty and Lo, 2002; Wardill *et al.*, 2016).

The distribution in the BBB associated with the increase in its permeability was observed in diverse brain diseases and accompanying inflammatory responses. The inflammation promotes changes in the TJs complex resulting in enhanced paracellular transport and transcellular transport (Wu *et al.*, 2017; Villaseñor *et al.*, 2019).

Brain diseases like Alzheimer's Disease (AD), stroke, and multiple sclerosis (MS) were characterized by a high level of inflammation and changes in the transcellular transport pathway at the BBB. In AD, the transcytosis across the BECs is responsible for both clearances of  $\beta$ -amyloid ( $A\beta$ ) from the brain and delivery of therapeutic antibodies to the brain (Villaseñor *et al.*, 2019). In stroke, caveolin-1, and caveolin-2, are the mediators of the transcytosis via up-regulation in the BECs (Villaseñor *et al.*, 2019). In MS, the increase in the number of intracellular vesicles within BECs depicts disease severity. Caveolin-1 and caveolin-2 levels are upregulated because the pro-inflammatory transcription factor NF- $\kappa$ B regulation, which determine the expression of caveolin-1. In addition, inflammatory cytokines likely present in MS lesions is also known to stimulate fluid-phase endocytosis (Curley, 2019).

#### **2.2.6.2. Reactive Oxygen species (ROS)**

Regulation of ROS level is an essential key in cell homeostasis. ROS induces various signalling pathways that are crucial to maintaining normal cell function. Uncontrolled cellular ROS production causes oxidative stress resulting in cell dysfunction (Carvalho and Moreira, 2018). Different sources of ROS in the cell include the mitochondrial electron-transport chain, cyclooxygenases (COXs), lipoxygenases,

cytochrome P450 reductases, xanthine oxidase, and nitric oxide synthase (NOS (Miller *et al.*, 2010; Forrester *et al.*, 2018). The NVU cells have a powerful antioxidant defence system; glutathione (GSH), glutathione peroxidase, glutathione reductase, superoxide dismutase, and catalase to combat ROS generated from ECs and other cell types astrocytes, pericytes microglia, and neurons. The imbalance between ROS and antioxidants results in the disruption of the NVU (Wevers and de Vries, 2016).

Although ROS are produced naturally in cells and more in the mitochondria, the oxidative activity of ROS activate various signalling pathways, including NF- $\kappa$ B, JNK, and JAK/STAT, resulting upregulation of inflammatory cytokines, such as IL-1, IL-6, IL-18, TGF- $\beta$ , and TNF- $\alpha$ , these inflammatory factors target the TJs and induce more inflammation leading to promote the BBB permeability and leukocyte infiltration (Rochfort *et al.*, 2014; Forrester *et al.*, 2018).



### **2.2.7. Mechanisms that influence the BBB permeability**

#### **2.2.7.1. Mechanisms influence the paracellular permeability**

The BBB represents a physical barrier due to junction complex proteins (TJs and AJ) between endothelial cells. These proteins are the key points that control paracellular permeability (Cardoso, Brites and Brito, 2010). The physical open and close between endothelial cells are controlled by the dynamic interaction in the TJs and AJs. The change in the TJs and AJs properties and the reorganisation of the cytoskeleton form an intercellular gap at BBB (S. Stamatovic *et al.*, 2008; Keaney and Campbell, 2015).

Mechanisms that affect the paracellular pathways, including phosphorylation status of TJs, and intracellular and extracellular  $\text{Ca}^{2+}$  levels. TJ proteins have many phosphorylation sites; the phosphorylation status of these sites regulates the protein-



protein interaction between TJs proteins which controls the BBB permeability. The phosphorylation or dephosphorylation changes the localisation of the transmembrane protein. It induces their redistribution, causing the dissociation of the junction complex from its cytoskeleton anchor with increased permeability of the BBB (Chen and Liu, 2012). In brain endothelial cells, phosphorylation or dephosphorylation of tight junction occurs on claudin-5, occludin, and ZO-1. Tyrosine phosphorylation of occludin causes BBB dysfunction and hyperpermeability in ischemia (Takenaga *et al.*, 2009). Claudin-5 phosphorylation by Rho-kinase is related to the BBB disruption (Yamamoto *et al.*, 2008). Phosphorylation of ZO-1 on Tyr, Thr, and Ser residues causes its dissociation from TJs during inflammatory conditions (Rochfort and Cummins, 2015). The phosphorylation of Ser/Thr and Tyr residues in AJ proteins (VE-cadherin and  $\beta$ -catenin) is related to BBB impairment (Stamatovic *et al.*, 2016).

$\text{Ca}^{2+}$  level is critical for TJ integrity (Ma *et al.*, 2000). Both extra and intracellular  $\text{Ca}^{2+}$  levels are essential for endothelial integrity. Low levels of extracellular calcium disrupt AJ within cadherin-cadherin interaction. Cadherin has a calcium-binding site in its extracellular domain, whereas the intracellular domain binds to actin with  $\alpha$ - and  $\beta$ -catenin. The lack of calcium on the binding sites on the cadherin interrupts the cadherin-cadherin linkage and the loss of cell-cell adhesion TJ (Brown and Davis, 2002).

Increased intracellular calcium affects the integrity of TJ. Actin cytoskeleton interacts with myosin II, situated close to the plasma membrane. Myosin light chain (MLC) is a regulator of myosin II. Myosin II is phosphorylated by MLC kinase (MLCK), which ultimately increases the contractility of the cytoskeleton and the formation of stress fibres. The activation of MLCK is associated with increasing the  $\text{Ca}^{2+}$  level (De Bock *et al.*, 2013; Rakkar and Bayraktutan, 2016). The depletion of intracellular calcium affects the



interaction between ZO-1 and actin and alters occludin expression (Brown and Davis, 2002).

#### ***2.2.7.2. Mechanisms influence the transcellular permeability at the BBB***

The movement across the BBB occurs mainly through the transcellular way. A complex transcellular transport system that includes transcellular lipophilic pathway, carrier-mediated transport, adsorptive transcytosis, and receptor-mediated transcytosis (RMT) accompany BECs. Transcellular transports across the BECs occur in endocytic vesicles form and can distinguish these processes, initiated by internalization, sorting, and exocytosis (Villaseñor *et al.*, 2019).

The internalization occurs via caveolae, clathrin-dependent, or independent endocytosis (Villaseñor *et al.*, 2019). In comparison, ligand and its receptor on the apical membrane of the ECs (blood side) result in internalization of the ligand-receptor complex to form an endosome. The endosome is transported through the cytosol and releases its cargo on the basolateral of the ECs (brain side) (Curley, 2019). Clathrin-coated vesicles involvement in most of the RMT, and caveola participate in adsorptive-mediated endocytosis of extracellular molecules and receptor trafficking and pinocytotic vesicles (Preston *et al.*, 2014). Once a vesicle is internalised, the common intracellular pathway begins with the initial sorting station (Pulgar, 2019).

The increase in the BBB permeability was observed in diverse brain diseases such as Alzheimer's Disease (AD), stroke, and multiple sclerosis (MS) (Kadry *et al.*, 2020). That is often accompanied by inflammatory responses. The inflammation induces changes in the TJs complex resulting in promoting paracellular and transcellular transport (Galea, 2021). The transcytosis across the BECs was found responsible for clearances of  $\beta$ -amyloid ( $A\beta$ ) from the brain (Villaseñor *et al.*, 2019). Caveolin-1 and caveolin-2, the mediators of the transcytosis, were up-regulated in stroke (Curley, 2019).

### **2.3. Brain tumour environment**

Primary brain cancer arises from brain tissues, whereas secondary brain cancer initiated from metastatic cancer cells derived from primary cancer arised outside the brain (Lorger, 2012). The brain cancer environment includes cancer cells and non-cancerous stromal cells, and the extracellular matrix. The mechanism of cancer development is highly dependent on the interaction between tumour cells and stromal cells via factors secreted by all tumour microenvironment components (Choi and Moon, 2018). Major stromal cells presented in the tumour environment include endothelial cells, Astrocytes, pericytes, and infiltrated immune cells; these cells play a vital role in cancer progression (Charles *et al.*, 2011).

#### **2.3.1. Blood-brain barrier state in the tumour environment**

The BBB refers to an interface between the brain parenchyma and the systemic circulation, while the blood-tumour barrier (BTB) refers to the endothelial interface between the blood circulation system and the brain tumour tissue. The alteration in the BBB produces the BTB. BTB is characterized by non-continuous endothelial cells, high levels of VEGF, overactivated astrocytes and microglia cells, low expression of the endothelial ZO-1 protein, and altered AQP4 water channel in astrocyte end-feet (Blecharz *et al.*, 2015; Arvanitis and Ferraro, 2020).

The BTB are exceptionally variable in size, shape, and branching pattern without the conventional hierarchy organisation of arterioles, capillaries, and veins. Tumour vasculature is varied by region. They are significant in the periphery areas but absent in the areas of necrosis (Baluk *et al.*, 2005). The abnormality in the BTB significantly promotes the abnormal microenvironment in cancer. The dysfunctional vessels in the tumour area deprive the nearby tissue of nutrition and removal of the waste product. The

accumulation of the waste-like lactate increases the acidity, and the lack of O<sub>2</sub> induce hypoxia (Siemann and Horsman, 2015). The high expression of VEGF-A at tumour vessels induces abnormal branching morphogenesis and small gaps in the vasculature, promoting fluid leakage (Claesson-Welsh and Welsh, 2013). The chronic stimulation of endothelial cells by VEGF induces an excessive branching of tip cells (Mühleder *et al.*, 2021), forming irregular and dysfunctional TEC monolayers (Padera *et al.*, 2004). In a tumour environment, all components of NVU directly or non-directly contact (by soluble factors) with endothelial cells induce changes in the properties and function (Dudley, 2012).

#### **2.3.1.1. Brain endothelial cells in the tumour environment**

Endothelial cells are a vital element in the tumour environment. Tumour cannot grow away from endothelial cells; endothelial cells from the blood vessels provide the nutrition and oxygen for the tumour and removal the metabolic wastes. Unhealthy endothelial cells could be the metastatic site of the circulatory system (Cheng *et al.*, 2017; Hida and Maishi, 2018).

Blood vessels in the tumour area differ in many ways from normal blood vessels (Baluk *et al.*, 2005). The tumour blood vessels lose the integrity of the endothelium monolayer (Baluk *et al.*, 2005) and show an increase in gap and fenestrae formation resulting in haemorrhage leakiness of plasma proteins. However, brain endothelial cells are uniform with a low level of fenestration (Hida *et al.*, 2008).

Tumour vessels lack the tight endothelial monolayer, which is essential for normal barrier function to prevent the cross of circulating cells and molecules into the brain; this abnormality leads to its leakiness. In contrast, ECs in normal tissue form a continuous and tight monolayer (Baluk *et al.*, 2005).

### ***2.3.1.2. Alterations of Tumour-endothelial cells***

Endothelial cells, the direct component of blood vessels, have attracted more significant research interests, especially in tumour progression. The ability of cancer cells to penetrate the endothelium barrier to relocate in other areas indicate the inefficiency of endothelial cells. At the molecular and functional levels, a phenotypic difference was observed in the endothelial cells isolated from tumour tissue (Hida and Maishi, 2018).

Endothelial cells in the tumour area demonstrate a morphological irregular shape and size; they have ruffled margins and long, fragile cytoplasmic projections extending outward and across the vessel lumen. The tips of some branched TECs may penetrate the lumen creating openings or small intercellular gaps in the vessel wall. These openings allow extravasated erythrocytes to pool at the periphery of tumour blood vessels, forming "blood lakes" which are not anastomosed with the vasculature. The scanning electron microscopy reveals larger openings (~1.5 mm) in the walls of tumour blood vessels and holes with (~ 0.5 mm) fenestrations in tumour endothelial cells. These endothelial gaps and large openings contribute to the plasma leakage observed in most tumours (Dudley, 2012).

Tumour-endothelial cell abnormalities denote differences in their response to growth factors, such as EGF, adrenomedullin, and VEGF, contributing to the proangiogenic phenotype of endothelial cells. Cytogenetic abnormalities in the tumour-endothelial cell include aneuploidy and abnormal centrosomes, implicated as genetic instability promoting resistance to chemotherapeutic agents (Hida and Maishi, 2018).

Metastatic tumour cells have been suggested to induce changes in the endothelial cells, including reorganizing the cytoskeleton and upregulation of adhesion molecule receptor expression. In addition, metastatic cells through factors such as ROS cascade of signalling pathways in endothelial cells causing disassociation in the endothelial TJs,

activation of Src protein tyrosine kinases disrupt the endothelial-cadherin-b-catenin cell-cell adhesions resulting in the formation of holes between endothelial cells (Hu *et al.*, 2008; Mierke, 2008). The presence of metastatic tumour cells close to endothelial cells causes an increase in the expression of CXC2 and Il-8 gens in endothelial cells and their receptors on tumour cells. The binding of CXC2 and Il-8 with their receptors causes dynamic remodelling of the cytoskeleton (Mierke *et al.*, 2008).

Proposed mechanisms implicated in causing abnormality in tumour endothelial cells include the interaction between tumour cells and stromal cells and the hypoxic conditions of the tumour microenvironment (Hida *et al.*, 2018). Consequently, the endothelial cells cultured with tumour conditioned medium showed upregulation of proangiogenic gene expression with changes similar to tumour endothelial cells (Ohga *et al.*, 2012). The lack of oxygen in the tumour environment is one of the most vital mechanisms proposed to cause abnormalities in endothelial cells. Hypoxia is closely related to tumours and their genetic instability and malignancy. Hypoxia enhances tumour growth (Kondoh *et al.*, 2013) by stimulating the excessive secretion of angiogenic factors such as VEGF, which also plays a role in ROS production; ROS is directly involved in the proliferation, migration, and increased leakage in the blood vessels. Immature and leaking blood vessels cause increased pressure within the tumour, leading to the collapse of blood vessels and, therefore, increases in hypoxia and lack of nutrients. In addition, induction of secretion of other factors such as cytokine is also known to affect endothelial cells. VEGF expression is also upregulated in TECs, contributing to their high viability through an autocrine mechanism. The activation of VEGF signalling in TECs under hypoxic conditions cause chromosomal aberrations in TECs through ROS accumulation. The hypoxic conditions and the secretion of cytokines such as VEGF promote tumour revascularization by inducing the mobilization of bone

marrow-derived endothelial progenitor cells towards cancer (Kondoh *et al.*, 2013; Hida *et al.*, 2018).

The tumour microenvironment (TME) influences tissue function as well as the development of malignancies. The alterations in endothelial cells are essential for cancer cells to grow and metastasize; such changes target the endothelial cell-cell interaction at the site of TJs. Alteration in the expression levels of TJs leads to an increase in the intercellular permeability, reduces the cellular polarity, and increases in the genes coded to growth (Martin and Jiang, 2009; Salvador *et al.*, 2016).

In the brain, microvascular endothelial cells are characteristic of a highly complex network of strands predominantly localized on the P-face of the junctional membrane. However, in tumour endothelial cells, a tight junction strand is associated with the outer leaflet (E-face). At the P-face ridges, particles were only sparsely distributed (Liebner, Kniesel, *et al.*, 2000). The expression of occludin, claudin-1 and claudin-5 using immunofluorescence and confocal laser scanning microscopy denote the identical distribution of their expression in mature brain microvessels. The BBB in tumour presence is molecularly altered as revealed by changes in the expression of junction proteins (Liebner, Fischmann, *et al.*, 2000). *In vitro* study has demonstrated that TJs proteins' expression includes occludin, claudin 1, and claudin 5 in endothelial cells belonging to anaplastic astrocytoma and glioblastoma samples were significantly reduced in comparison with normal endothelial cells (Ishihara *et al.*, 2008).

### ***2.3.1.3. Tumour-Endothelial cells interaction ways***

Cancer cells cannot grow away from endothelial cells, which support the formation of new vessels needed to supply nutrition and oxygen. The communication of cancer cells with endothelial cells induces changes in endothelial cells. Cancer cells communicate with endothelial cells via soluble factors, adhesion receptors, gap junctions,

and vesicles (Lopes-Bastos *et al.*, 2016; Choi and Moon, 2018). Cancer cells secrete various factors such as different cytokines, growth factors, scatter factor/hepatocyte growth factor (SF/HGF), proteases, including matrix metalloproteinase (MMP)-2 and MMP-9, plasminogen activators and cathepsin B into the extracellular space, which targets the endothelial cells (Schneider *et al.*, 2004).

Growth factors secreted by cancer cells are the vital stimulator of endothelial angiogenesis. Five types of VEGFs have been identified in mammals, VEGF A, -B, -C, and -D and placental growth factor. The secreted VEGFA binds to its receptors on the surface of vascular endothelial cells, therefore, inducing an intracellular response that modulates cellular processes such as proliferation, migration, and permeability (Nishida *et al.*, 2006). VEGFA is the most important antigenic factor expressed from almost all types of tumours. It increases the intracellular level of calcium, leading to an increase in endothelial permeability (Lopes-Bastos *et al.*, 2016). VEGFs are produced at higher levels by malignant gliomas than by low-grade gliomas, which often show an impairment of BBB and oedema formation (Schneider *et al.*, 2004).

Tumour cells release cytokines like IL-6, IL-8, and chemokines like CCL2, CCL5; these molecules induce inflammatory stimuli of endothelial cells, inducing the expression of adhesion molecules such as VCAM 1 and vascular adhesion protein 1 (VAP1))(Choi and Moon, 2018). These molecules mediate cancer cells attached to the endothelium and play a role in the metastatic process (Ferjančič *et al.*, 2013).

In addition, cancer cells directly communicate with endothelial cells through gap junctions. Gap junctions are a cell-cell channel formed by a protein family called connexin, with expression in both cancer and endothelial cells (Totland *et al.*, 2020). In humans, the connexin family contains 21 members, the physical interaction between cancer cells and endothelial cells in the tumour environment allow these proteins to form

channels between cells where they can exchange ions and small metabolites, providing a connection between the cytoplasm of the two cells (Aasen *et al.*, 2019). In this aspect, connexins provide an intercellular communication between cancer cells and endothelial cells and permit the adhesion of cancer cells to vessels, therefore, the intravasation of cancer cells and tumour progression (Lopes-Bastos *et al.*, 2016; Aasen *et al.*, 2019). The adhesion of cancer cells to the endothelial cells and astrocytes by connexion was observed both *in vitro* and *in vivo*, such that interaction induces endothelial tube formation, and enhance the metastatic ability of cancer cells and cause phenotype changes in astrocytes (Ito *et al.*, 2000; City, 2003; Pollmann-mudryj *et al.*, 2005).

Furthermore, tumour cells also communicate with the endothelial cells through vesicles. Vesicles are released from tumour cells into the extracellular space, which then integrates with the plasma membranes of the endothelial cells. Several types of vesicles have been identified: microvesicles, exosomes, membrane particles, and exosomes (Chin and Wang, 2016; Lopes-Bastos *et al.*, 2016). For example, breast cancer and glioblastoma secrete exosomes and microvesicles; these vesicles contain vascular growth factors, IL-6, IL-8, and microRNAs (Chin and Wang, 2016; Giusti *et al.*, 2016).

#### **2.3.1.4. Pericytes state in the tumour environment**

Pericytes in tumour vessels have abnormal shapes and are loosely attached to endothelial cells (Barlow *et al.*, 2013). Impaired electrotonic coupling of pericytes to one another or endothelial cells could affect the metabolic activity and functional state over a stipulated time. Pericytes' abnormalities in tumours are consistent with alterations in PDGF signalling pathways. The gain- or loss of function mutations to PDGF and its receptors has established a vital role for PDGF-B in endothelial cell signalling through PDGFR- $\beta$  receptors on pericytes of growing vessels. Mice genetically deficient in PDGF-B or its receptors have been shown to have blood vessels with loose pericytes attachment,



irregular vessel calibre, luminal projections of endothelial cells, and haemorrhage (Baluk *et al.*, 2005). In brain metastasis, pericytes PDGFR- $\beta$  expression decreased, and the pericytes subpopulations were altered (Lyle *et al.*, 2016).

#### **2.3.1.5. Basal membrane alteration in the tumour environment**

The vascular basement membrane is a complex of proteins, glycoproteins, and proteoglycans. The basement membrane is an anchor for signalling processes in the brain capillaries due to its intermediate position between NVU cells. It provides an additional barrier against the movement of transit molecules to the neural parenchyma. BM is tightly associated with endothelial cells and pericytes in normal conditions, while endothelial cells are also based on the BM where the pericytes are surrounded by it. Pericytes coverage of vasculature may be discontinuous due to BM interaction between astrocytes and ECs.

The BM is essential to proper NVU functioning as it directly mediates the receptor activation on the cellular components of this unit (McConnell *et al.*, 2017; Hida and Maishi, 2018).

In tumour vessels, the BM is presented but shows structural abnormalities consistent with the dynamic nature of the endothelial cells and pericytes. First, it has a loose association with endothelial cells. Second, the basement membrane consists of multiple redundant layers with irregular thickness, focal holes and broad extensions into the tumour. In addition, basement membrane in tumours can contain distinctive forms of fibronectin containing the ED-B domain and type IV collagen with exposed cryptic sites (Baluk *et al.*, 2003).

The basement membrane in tumours is a source of antigenic and a site of growth factor binding and a participant in angiogenesis. These features highlight the potential of

the basement membrane as a target in cancer therapy (Baluk *et al.*, 2005). BM is degraded by matrix-degrading enzymes such as MMPs produced by tumour cells or immune cells that accumulate around tumour cells during tumour angiogenesis. BM degradation includes the liberation of endothelial cells to migrate and proliferate, the liberation of growth factors (VEGF and bFGF), and the detachment of pericytes (Neve *et al.*, 2014).

#### **2.3.1.6. Astrocytes state in the tumour environment**

Under physiological conditions, astrocytes maintain the homeostatic balance of the CNS. However, under pathological inflammatory states, they produce neurotoxic factors resulting in an amplification of the disease state. Activated astrocytes increase the level of glial fibrillary acidic protein (GFAP) and pro-inflammatory cytokines such as INF- $\gamma$ , IL-1 $\beta$ , IL-6, and TNF $\alpha$ . The neurotoxic factors are mediators that increase activation of NF- $\kappa$ B pathway, production of ROS and NO, and further release of IL-1 $\beta$ , IL-6, and TNF $\alpha$  (Zhang *et al.*, 2017; Oksanen *et al.*, 2019).

Astrocytes have a heterogeneous effect on the maintenance and distribution of BBB, providing support to endothelial TJs (Alvarez *et al.*, 2013). Astrocytes release factors that affect the expression of TJs, such as Sonic hedgehog (Shh) (Xing *et al.*, 2020), angiotensin-1, FGF, TGF- $\beta$ , glia-derived neurotrophic factor (GDNF), and retinoic acid (RA) (Lécuyer *et al.*, 2016). Astrocytes secreted proteins increase the gene expression of the TJs, such as ZO-1, Claudin-5, and Occludin (Xing *et al.*, 2020). Astrocytes have been demonstrated to promote tumour progression (Gong *et al.*, 2019) and increase resistance to therapy (Pustchi *et al.*, 2020).

During the extravasation of metastatic tumour cells, astrocytes become activated and associate around the vasculature in the penetration point, and this behaviour was also observed even before the extravasation (Cekanaviciute and Buckwalter, 2016; Gronseth *et al.*, 2018). Astrocytes and their secretome have been shown to increase the

tumour cell infiltration through the BBB by inducing alteration in the tumour cell morphology to become a more elongated phenotype and promote actin stress fiber organization (Shumakovich *et al.*, 2017). Astrocytes can interact with the tumour cells through the gap junctions directly; this contact has been found to induce astrocyte activation. Activated astrocytes increase their secretion of various types of proinflammatory cytokines, growth factors, GFAP, nestin, and matrix metalloproteinase 9 (MMP-9); these factors promote tumour growth and facilitate the movement of tumour cells across the BBB (Gronseth *et al.*, 2018). Astrocytes have also been found to be implicated in the development of hypoxia in the tumour regions; this was confirmed by the high expression of astrocytes activation marker glial fibrillary acid protein (GFAP) (Lin *et al.*, 2019).

### **2.3.2. Features of the BBB disruption in the tumour environment**

The endothelial permeability at the BBB regulation is vital to control the distribution and the disassociation of the TJs assembly; this indicates BBB dysfunction. The BBB leakage is the most important result of the uncontrolled paracellular and transcellular ways. Such phenomenon is often associated with the tumour (Steeg, 2021), where plasma proteins and water accumulate in the brain parenchyma, resulting in oedema (Stummer, 2016).

#### **2.3.2.1. Oedema formation**

Cerebral oedema is an abnormal accumulation of water and plasma proteins inside the brain tissue. It can accumulate in volume up to 90 ml per day in severe cases. It is the leading cause of death in glioma patients. Cerebral oedema is common in GBM patients and leads to brain herniation in up to 60% of patients (Michinaga and Koyama, 2015). Vasogenic and cytotoxic oedema are types of oedema formation in the brain (Stokum *et al.*, 2016).

Brain tumour oedema is associated with vasogenic oedema, and it is due to the BBB distribution (Michinaga and Koyama, 2015). The disruption of the BBB, which allows leakage of fluids from the blood into the brain parenchyma, is the main cause of vasogenic oedema. Tumour vessels have defective TJs, and the absence of normal astrocytes might be the reason behind that. Astrocytes are the vital support of the normal function of the TJs, and their absence causes a lack in their secretion of angiogenic factors needed for BBB. In addition, Tumor cells secrete a mixture of vascular permeability factors such as VEGF and scatter factor/hepatocyte growth factor (SF/HGF)(Papadopoulos *et al.*, 2004), which increase the endothelial permeability (Abounader and Laterra, 2005; Ishihara *et al.*, 2008).

In contrast, cytotoxic oedema is implicated in the pathophysiology of peri-tumoral swelling. It may result from cellular swelling after the breakdown of transmembrane ion gradients due to energy depletion (Figure 18) (Stummer, 2007). The cytotoxic oedema is characterized by intracellular accumulation of fluid and Na<sup>+</sup> resulting in cell swelling. After cytotoxic oedema formation, extravasation of fluid is evoked by disruption of the osmotic pressure gradient resulting from decreased extracellular Na<sup>+</sup> without BBB disruption (ionic oedema) (Michinaga and Koyama, 2015). Cytotoxic oedema is related to glioma-induced neuronal cell death and neurodegeneration, leading to further brain swelling and neurological deficit (Dubois *et al.*, 2014) from reduced ATP generation that disrupts plasma membrane ions pump (Wang *et al.*, 2018).

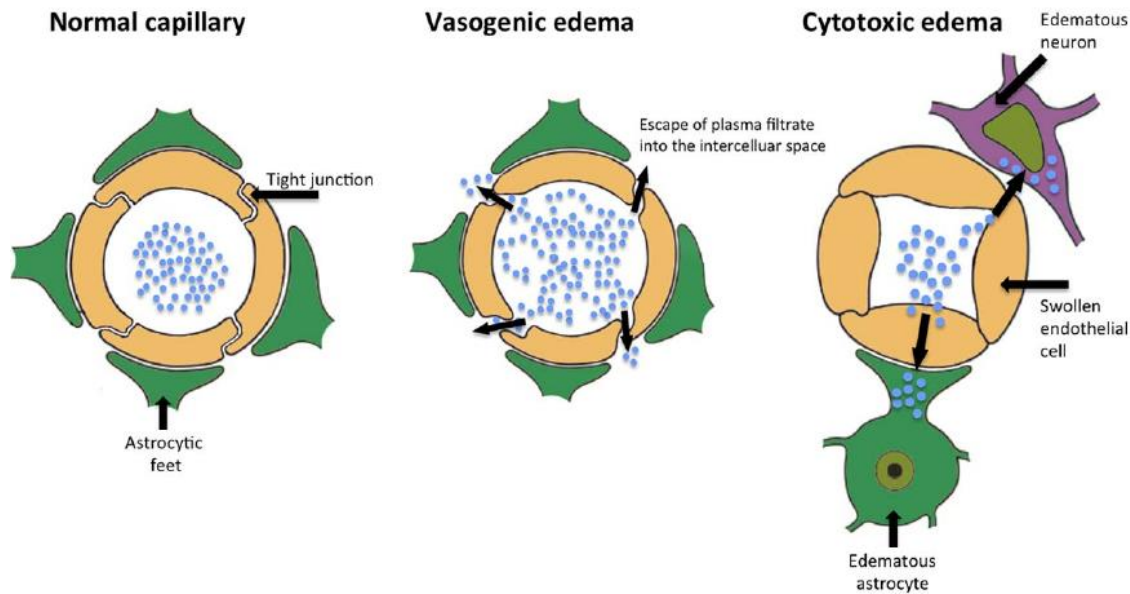


Figure 18. Schematic presentation shows the difference between brain oedema types which associated with CNS disease, in the brain tumour, the vasogenic oedema is always observed (Cherian et al., 2018).

### 2.3.3. Hypoxic tumour environment

The low level of  $O_2$  availability (hypoxia) is a hallmark of the tumour environment, which arises from an imbalance between increased oxygen consumption and inadequate oxygen supply. In normal tissues, the adequate distribution of vasculature contributes to the delivery of oxygenated blood. However, in the tumour, the irregular distribution of blood vessels increases the distance between the capillaries, exceeding the capacity of oxygen to diffuse, the permanent non-diffusion of  $O_2$  causes the necrosis of tumour cells (Jing et al., 2019).

Solid tumours are distinguished into several regions depending on oxygen concentration (Figure 19), thus closeness to blood vessels. Cancer cells near the blood vessels are in the normal level of  $O_2$  (normoxia), whereas those distant from the blood vessels are at lower  $O_2$  levels (hypoxia region). Furthermore, necrotic areas are typically

hypoxic. In normal tissues, oxygen tension exceeds 40 mmHg, whereas, in the tumour area, it is between 0 – 20 mmHg (Al Tameemi *et al.*, 2019).

The blood vessels in tumour areas are abnormal; therefore, they fail to deliver sufficient oxygen and nutrition to the rapidly proliferative tumour cells, which results in the development of the hypoxic tumour region (Al Tameemi *et al.*, 2019). Under such hypoxic conditions, genomic instability can lead to tumour cell variants where cells can adapt to survive in an oxygen-depleted environment leading to tumour progression, metastasis, acquired resistance to chemotherapy, and treatment failure (Tannock, 2001; Ramachandran *et al.*, 2015).

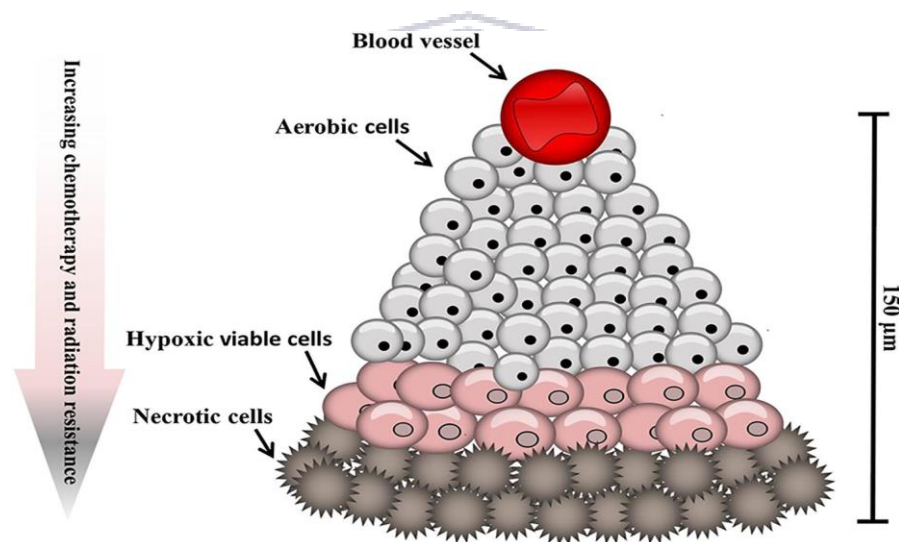


Figure 19. Schematic demonstration of the tumour regions of solid tumours based on oxygen concentration (Al Tameemi *et al.*, 2019).

Cellular proliferation rate in the hypoxia region is heterogeneous; it decreases with increasing distance from the blood vessels, the limited diffusion of functional blood vessels, and the interruptions in blood flow, resulting in low O<sub>2</sub> and nutrition needed for cell proliferation leads to inhibition of cell proliferation. Fluctuations in blood flow lead to disruption in delivering drugs through the same blood vessels (Tannock, 2001).

Tumour cells in the hypoxic regions can acclimate and survive in a nutrient-deprived environment (Al Tameemi et al., 2019). The hypoxic effect in the tumour environment belongs to hypoxia-inducible factors (HIFs) (Figure 20) (Petrova *et al.*, 2018). In humans, three HIF family members have been identified, HIF-1, HIF-2, and HIF-3; these heterodimers comprise  $\alpha$ - and  $\beta$ -subunit. HIF-1 is frequently overexpressed in all tumour cells; subsets of tumour-associated macrophages strongly express HIF-2 and HIF-3 expressed in pulmonary alveolar epithelial cells and human kidney (Al Tameemi *et al.*, 2019; Jing *et al.*, 2019).

The HIF proteins contain an oxygen-sensitive HIF- $\alpha$  subunit (HIF1- $\alpha$ , HIF2- $\alpha$  or HIF3- $\alpha$ ). HIF1- $\alpha$  and HIF2- $\alpha$  contain two proline residues (HIF1- $\alpha$ : P402/P564 and HIF2- $\alpha$ : P405/P531). Under normoxic conditions, these subunits are hydroxylated by enzymes called HIF prolyl hydroxylase domain family proteins (PHDs) in the presence of oxygen, resulting HIF- $\alpha$  to bind to von Hippel-Lindau tumour suppressor (pVHL), which lead to HIF- $\alpha$  degradation (Petrova *et al.*, 2018; Jing *et al.*, 2019). Under hypoxic conditions, the absence of oxygen inhibits PHDs and FIH, causing a cessation of the hydroxylation process. Genetic mutations cause a loss of tumour-suppressor functions (ING4, p53, PTEN, VHL), cytokines, lipopolysaccharides, growth factors, mediated by PI3K/AKT/mTOR, MAPK, mitochondrial ROS, nitric oxide (NO), and NF $\kappa$ B pathways regulate HIF activity (Ogunshola and Al-Ahmad, 2012; Muz *et al.*, 2015).



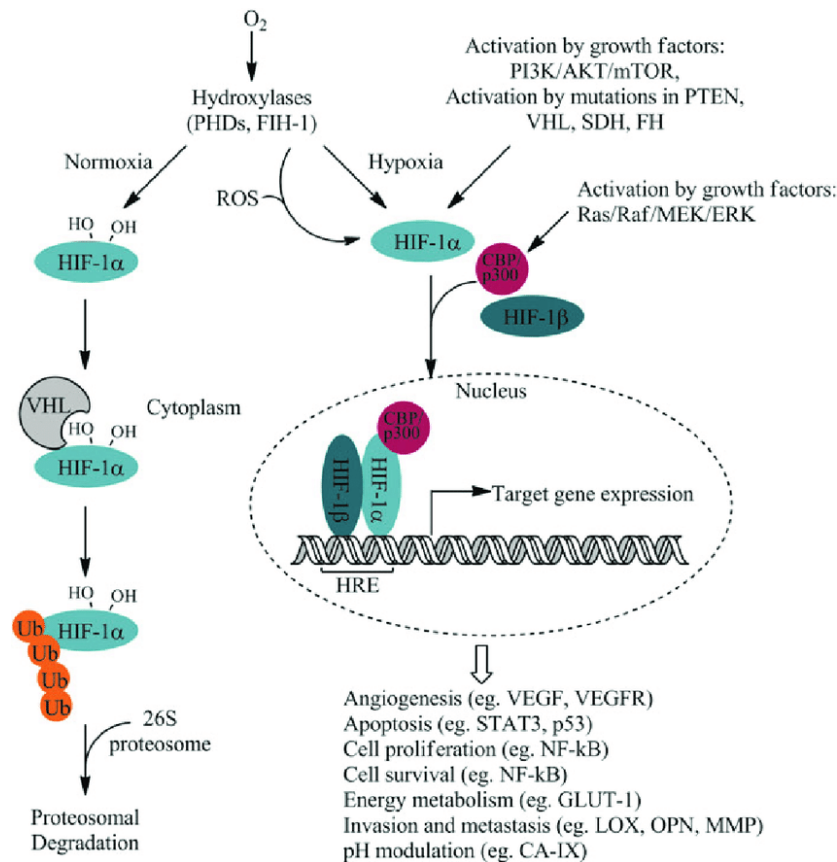


Figure 20. HIF regulation under normoxic and hypoxic conditions (Walsh *et al.*, 2014).

UNIVERSITY of the  
WESTERN CAPE

Hypoxia is a potent regulator of angiogenesis via activation of HIF. HIF regulates the genes that encode proteins involved in angiogenesis. HIF stimulates the generation of angiogenic factors such as VEGF and other factors supporting endothelium vessels like thrombin, endothelin-1 (ET-1), and heme oxygenase-1 (HO-1). Hypoxia inhibits the production of anti-angiogenic factors such as thrombospondins (TSPs) (Luo *et al.*, 2012). The BBB function is severely disturbed in the hypoxic condition causing physiological alteration, including disturbed energy balance and water/ion homeostasis, inflammatory events, and leakage of blood proteins into the brain (Engelhardt *et al.*, 2015).



An *in vivo* study on the endothelial response to hypoxia showed that the short exposure (less than eight hours) of brain endothelial cells to hypoxia did not affect their morphology; however, pro-and anti-angiogenic proteins are revealed after two hours exposure. In addition, hypoxia causes a decrease in nitric oxide synthase and thrombospondin-2 levels. Although hypoxia induces angiogenesis factors, brain endothelial cell exposures to hypoxia also reduce tube length, indicating the reduction of proliferation (Luo *et al.*, 2012).

HIF activity alters the cellular metabolism towards the glycolytic mode and increases the use of glucose and pyruvate, lactate production (Petrova *et al.*, 2018). Oxygen is required for the efficient generation of adenosine triphosphate (ATP). Therefore alterations in oxygen tension have a sensitive effect on cellular metabolism. The reductions in ATP production by oxidative phosphorylation, which required oxygen, lead to an increased rate of ATP production by glycolysis. Due to the insufficient ATP generated from the glycolysis (2 mol ATP/mol glucose, compared to 36 mol ATP/mol glucose produced from oxidative phosphorylation), cells under hypoxia increase their consumption of glucose (Eales *et al.*, 2016).

Hypoxia directly increases lactate production due to the changes in mitochondrial redox status elicited by reduced oxygen availability. Pyruvate generated from glycolysis is used to oxidize the NADH and is consequently reduced to lactate. Lactate is transferred from the cell, resulting in extracellular acidification that contributes to the malignant phenotype of cancer (Eales *et al.*, 2016). Hypoxia through HIF factor regulates BBB permeability through the disruption of TJ complexes (Luo *et al.*, 2018).

In an *in-vitro* study using rat brain endothelial cells, Engelhardt *et al.*, 2014 showed a significant stabilization of HIF-1 after two hours of exposure to hypoxia. The stable state of HIF is the key point that induces the activation of the HIF-1 pathway. Engelhardt and

colleagues (2014) showed that an opening followed the HIF-1 stabilization in the endothelial barrier. The treatment with HIF-1 inhibitor resulted in decreased hypoxic barrier disruption. HIF-1a stabilization caused a rearrangement of the TJs proteins, where ZO-1 and claudin-5 delocalized from the plasma membrane. Also, VE-cadherin was disturbed (Engelhardt *et al.*, 2014).

In tumours, blood vessels are often abnormal, immature, and leaky. Tumours promote the proliferation of blood vessels through their secretion of growth factors. New blood vessels provide the tumour with nutrients and oxygen; however, the rapid proliferation of tumour cells causes more hypoxia. Hypoxia, in turn, stimulates angiogenesis to ameliorate the hypoxic condition in which tumour tissue suffers from highly hypoxic with immature excessive and dysfunctional vasculature (Muz *et al.*, 2015).

#### **2.4. Overview of cancer metabolism**

In the mammalian cell, glucose and glutamine are the primary nutrients that cells use in biosynthesis. The catabolism of these molecules provides the cell with carbon intermediates to build various macromolecules, including the formation of NADH, NADPH, and FADH<sub>2</sub> to generate ATP for the biosynthetic reactions (Pavlova and Thompson, 2016).

The difference in the metabolism between cancer cells and normal cells was first reported in the 1920s (Al Tameemi *et al.*, 2019). In the normal oxygen condition, the cell breaks the glucose into pyruvate (glycolysis), which is subsequently catalyzed via TCA and oxidative phosphorylation in the mitochondria (Kalyanaraman, 2017). In contrast, cancer cells also break the glucose into pyruvate, but the pyruvate is mainly catalyzed into lactate. According to of Warburg effect (1930), cancer cells mostly rely on glycolysis to generate the needed energy more than oxidative phosphorylation (Figure 21) (Potter *et al.*, 2016)

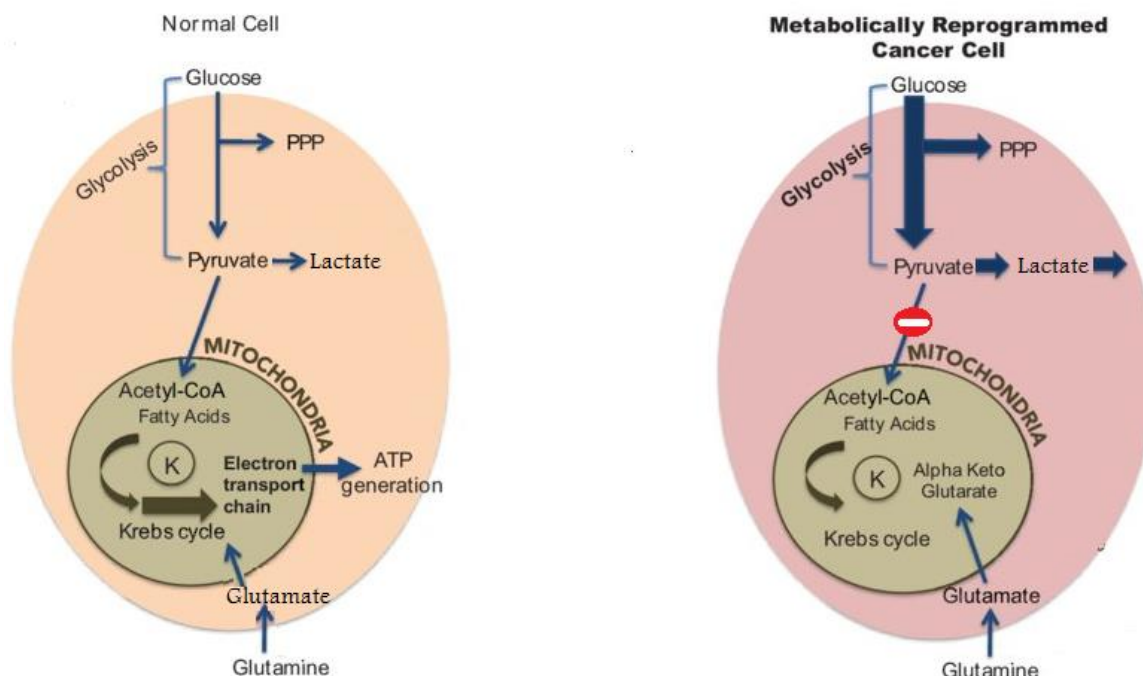


Figure 21. Metabolic difference between cancer and healthy cells. PPP (Pentose phosphate pathway). K (Krebs cycle). ATP (adenosine triphosphate) (Oronsky et al., 2014).

In normal conditions, pyruvate, the end product of the glucose catabolism, is converted to acetyl-CoA to enter into the tricarboxylic acid (TCA) cycle. Citrate is formed from acetyl-CoA and oxaloacetate; since the citrate began, a new TCA cycle started again, generating ATP, CO<sub>2</sub>, and carbon skeletons biosynthesis. Citrate is also converted in the cytosol into acetyl-CoA by ATP citrate lyase (ACLY) for fatty acid synthesis and generation of bio-membranes. Through the pentose phosphate pathway (PPP), glucose from ribose forms nucleic acid synthesis and NADPH reductive biosynthesis (Goda and Kanai, 2012).

In hypoxia, pyruvate is converted to lactate; this process is regulated by hypoxia factor HIF-1 (Goda and Kanai, 2012). HIF-1 activates pyruvate dehydrogenase kinase (PDK1). The PDK1 inhibits the pyruvate dehydrogenase (PDH), promoting pyruvate conversion

to acetyl-CoA (Kim *et al.*, 2006). Normal cells use monocarboxylate transporter-1 to remove the extracellular lactate from the extracellular fluid and convert it back to pyruvate for further oxidation by using the lactate dehydrogenase B (LDHB) isoform. However, this process is not observed in hypoxic cancer cells, where lactate is exported out of the cells, creating an acidic tumour environment (Marie and Shinjo, 2011). In addition to glucose catabolism, cancer cells also use glutamine to fuel their energy needs (De Berardinis and Chandel, 2016). Glutamine is an essential source of energy in the cells (Daye and Wellen, 2012). Catabolism of glutamine (glutaminolysis) is the source of other amino acids required by rapidly proliferating cells (Amoêdo *et al.*, 2013). Glutamine serves as an essential carbon source to replenish the TCA cycle, produce glutathione, and serve as a precursor to nucleotides and lipid synthesis via reductive carboxylation (Cluntun *et al.*, 2017). Glutamine convert to glutamate and then to  $\alpha$ -ketoglutarate ( $\alpha$ KG), which is a mediator in TCA. In hypoxic conditions, pyruvate, the end product of the glucose catabolism, is converted mainly to lactate; therefore cell does not catalyse glutamine through the TCA cycle (Dang, 2012).

Glutamine participates in the citrate and lipid metabolism through the reversal of the TCA cycle or reductive carboxylation of  $\alpha$ KG by isocitrate dehydrogenase (IDH) to form citrate or through forwarding cycling of glutamine carbons (Figure 22) (Amoêdo *et al.*, 2013). Reductive carboxylation is a way for hypoxic cancer cells to synthesize lipids from glutamine to grow. Under glucose limitation, the TCA cycle could also be reprogrammed and driven solely by glutamine, generating citrate that consists of only glutamine carbons. As such, hypoxic proliferating cell reprograms the TCA cycle to maximize the use of glutamine for lipid synthesis (Dang, 2012).

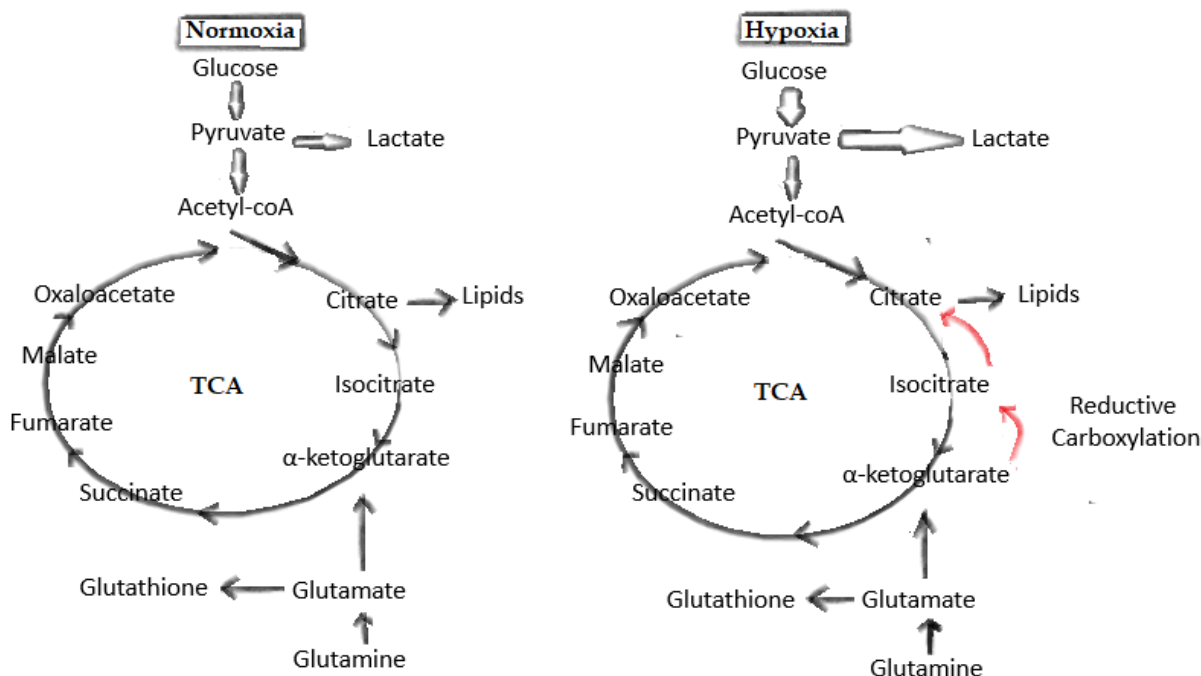


Figure 22. Overview of glucose and glutamine catabolism in the cells in normoxia (aerobic condition) and hypoxia (in cancer cells): In normoxia, cells use glucose and glutamine to produce the biomass via the tricarboxylic acid cycle (TCA). In hypoxia, cancer cells mainly convert glucose to lactate. Hypoxic cancer cells use the TCA independently than glucose to produce lipid for their growth by reversing the TCA.  $\alpha$ -ketoglutarate generated from glutamine can convert to isocitrate by isocitrate dehydrogenase (IDH) (Reductive carboxylation (Red arrows)) (Zaravinos and Deltas, 2014).

Pavlova and Thompson (2016) have identified six hallmarks of the metabolic changes in cancer: (1) deregulation in the uptake of glucose, and amino acids, (2) use of opportunistic modes of nutrient acquisition, (3) Glycolysis/TCA cycle intermediates are used for the biosynthesis and NADPH production, (4) increased demand for nitrogen, (5) alterations in metabolite-driven gene regulation, and (6) metabolic interactions with the microenvironment (Pavlova and Thompson, 2016).

In the tumour, cells have different metabolic phenotypes, depending on their anatomical location within the tumour. Cells situated close to the blood vessels have access to oxygen and nutrients; therefore, glycolysis and oxidative phosphorylation help

get energy, whereas those located in the core of the tumour in the hypoxic environment use aerobic glycolysis to obtain energy (Amoêdo *et al.*, 2013).

Another regulated factor of cancer metabolism is the multifaceted oncogene Myc. Myc regulates the expression of many genes that support anabolic growth, including transporters and enzymes involved in glycolysis, fatty acid synthesis, glutaminolysis, serine metabolism, and mitochondrial metabolism (Miller *et al.*, 2012). Tumour suppressor genes can also regulate cancer metabolism. TP53 is the most well-known tumour suppressor gene. TP53 is found to be inactivated in more than 50 different types of cancer. P53 controls metabolic genes that code for proteins responsible for glucose uptakes, such as glucose transporters such as GLUT1, GLUT3, and GLUT4 (Marie and Shinjo, 2011).

#### **2.4.1. Cancer secretion**

Cancer secretion refers to all the molecules released from cancer cells (including; soluble factors and exosome-microvesicles) (Karagiannis *et al.*, 2010). Cancer cells communicate with other cells in their environment by these secreting factors (Urooj *et al.*, 2019). In *vivo*, cancer secretion represents all the proteins secreted in the interstitial fluid of the tumour mass, whereas *in-vitro*, this term refers to the secretion of the cancer cell line in their medium or supernatant (Karagiannis *et al.*, 2010).

Using technics such as mass spectrometry and LC-MS/MS, various proteins have been identified in cancer secretion, including Growth factors, chemokines and cytokines, enzymes like protease. These factors act as autocrine or paracrine stimulators, promoting cancer malignancy. Secreted factors from cancer cells mediate cancer cells' invasive and metastatic events from the initial site to their new location (Cacho-Díaz *et al.*, 2020).

Metastatic breast cells secrete various factors cytokines (such as IL-1 $\beta$ , TNF- $\alpha$ , IFN- $\gamma$ ) and chemokines (like CCL2, CXCL8) to facilitate their passage between endothelial cells. After penetrating, cancer cells secrete protease (e.g. MMP) to degrade the basement membrane (Fidler, 2015). Breast cancer cells release factors such as interleukin-1 beta (IL-1 $\beta$ ) and tumour necrosis factor-alpha (TNF- $\alpha$ ), which activate astrocytes to produce growth factor-beta 2 (TGF- $\beta$ 2), promoting the metastasis of cancer cells (Xing *et al.*, 2013; Gong *et al.*, 2019).

Glioblastoma cells interact with astrocytes through extracellular vesicles, which carry molecules such as miRNAs and cytokines, activating astrocytes to produce other molecules such as IL-6, inducing the secretion of MMPs from glioblastoma cells facilitating their invasion. Glioblastoma also secretes interleukins (such as IL10, IL4, and IL13), activating microglial cells to release TGF- $\beta$  that enhance glioblastoma growth (Matias *et al.*, 2018).

Physiological conditions of cancer cells; affect their secretion; for example, hypoxia induces upregulating of growth factors secreted from Human malignant glioma U373MG cells (Yoon *et al.*, 2014).

## **2.5. Endothelial metabolism in the tumour environment**

Endothelial metabolism plays a crucial role in supporting particular functions of the endothelial cells. ECs rely on different metabolic pathways to support their activities. Metabolic pathways, including glycolysis, fatty acid oxidation, and amino acid metabolism, secure the production of energy and biomass and the maintenance of redox homeostasis of endothelial cells (Figure 23) (Bierhansl *et al.*, 2017).



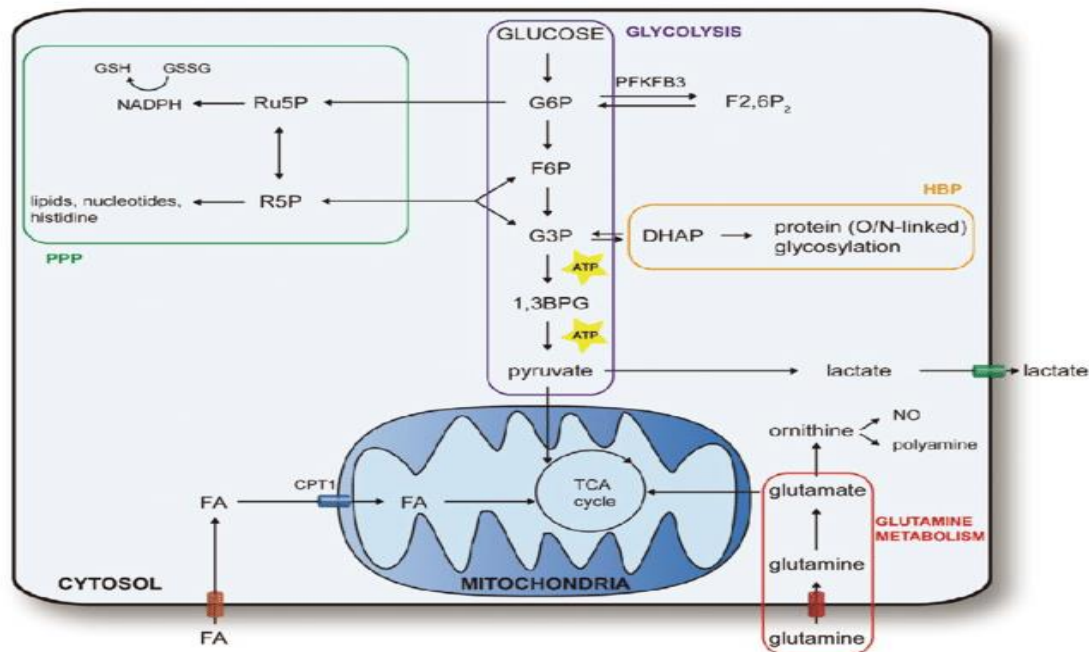


Figure 23. Metabolism in healthy endothelial cells. Glycolysis: the broken-down pathway of glucose to pyruvate, resulting 2 molecules of ATP(adenosine triphosphate). Pyruvate transfer to mitochondria to enter TCA (tricarboxylic acid cycle). Lactate is converted from pyruvate then exported from the cells. PFKFB3 (6-phosphofructo-2-kinase/fructose-2,6-biophosphatase3, activator of glycolysis. G6P (Glucose-6-phosphate), 1,3BPG (1,3-bisphosphoglycerate). PPP (Pentose phosphate pathway), side branch from the glycolysis; R5P (ribose-5-phosphate), Ru5P(ribulose-5-phosphate). PPP produces NADPH (nicotinamide adenine dinucleotide phosphate) used to catalyse the conversion of GSSG (oxidize glutathione) to GSH (glutathione). HPB (Hexosamine biosynthetic pathway), other side branches of glycolysis pathway, DHAP(dihydroxyacetone), HPB produces pro-duces N-acetylglucosaminewhich is important for N-linked and O-linked glycosylation. Glutamine metabolism( glutamine converts to glutamate then to  $\alpha$ -ketoglutarate (not shown) in TCA. FA (Fatty acids pathway); FA enter the mitochondria and produces acetyl CoA to enter TCA, CPT1(carnitine palmitoyltransferase1) (de Zeeuw et al., 2015).

Recently ECs were classified into three different subtypes to form a new vessel; ECs in the subtypes have modified metabolism based on functions. These endothelial subtypes have different proliferative and biosynthetic requirements based on different metabolic states. The first subtype is migratory tip cells located at the leading edge in vessel sprouting during angiogenesis. The second is highly proliferative stalk cells that



follow the tip cells, and they are responsible for sprout elongation. The third subtype is quiescent phalanx cells that line the newly established perfused vessels (Norton and Popel, 2016; Zecchin *et al.*, 2017).

Migratory tip cells are the leader of the sprouting process, and they are rich in cell-surface receptors and molecules involved in extracellular matrix degradation. Although this type of cell faces blood, therefore, they are in an environment with a high level of oxygen; however, the rate of oxygen consumption in these cells is lower than other endothelial subtypes, and that 85% of cellular ATP is generated by glycolysis (Zecchin *et al.*, 2017).

Although the ATP resulting from glycolysis is much less than the energy produced from the Krebs cycle, the unlimited availability of glucose and high glycolytic flux induces more ATP production within a short time to support the migratory cells in the blood vessel tissues to restore physiological oxygen levels. In addition, relying on anaerobic metabolism to produce ATP lead the ECs to spare oxygen to the perivascular cells. On the other hand, reducing mitochondrial respiration reduces ROS generated. Migratory cells also use different pathways such as PPP and the serine synthesis pathway to generate the energy needed to produce biomass. Quiescent phalanx endothelial cells line the new vessels. Although they are exposed to higher oxygen concentrations in the circulation, these cells have lower glycolytic flux than proliferating endothelial cells to reduce ROS production to lower oxidative damage (Zecchin *et al.*, 2017).

In the tumour environment, endothelial growth and metabolism are affected by tumour metabolism. Tumour cells release high amounts of lactate, which augment the acidic pH in the tumour tissue (acidosis). Due to the tumour environment conditions (lack of nutrients, an increased accumulation of metabolic waste products, and efficient blood perfusion), cellular secretions are changed. Metabolic substances secreted can be

used from endothelial such as succinate, a mediator in the TCA cycle (Rohlenova *et al.*, 2018).

Cancer cells can also affect the endothelial metabolism; cancer cells stimulate endothelial cells to increase their glucose uptake for proliferation. For example, conditioned media from hypoxic glioma cells induced endothelial cells to upregulate the expression of the glucose transporter GLUT1 (Allison N. Lau<sup>1</sup> and Matthew G. Vander Heiden<sup>1</sup>, 2020).

As a result of the Warburg effect, cancer cells release a massive amount of Lactate. Lactate is released from tumour cells via monocarboxylate transporter 4 (MCT4), whose expression is increased in hypoxic tumour regions (Lyssiotis and Kimmelman, 2017). In hypoxia, lactate largely contributes to angiogenesis by activating HIF1a. Activation of HIF1a increases the production of interleukin- 8/CXCL8, which drives the autocrine stimulation of endothelial cell proliferation and increases VEGFA levels (Harjes *et al.*, 2012; Polet and Feron, 2013). In addition, the extracellular accumulation of lactate augments the acidity, which induces an endothelial inflammatory response (Rohlenova *et al.*, 2018).

## References

- Galvan, R., F., Barranco, V., Galvan, J.C., Batlle, Sebastian FeliuFajardo, S. and García (2016) 'Astrocytes: Initiators of and Responders to Inflammation', *Intech, i(tourism)*, p. 13. doi:http://dx.doi.org/10.5772/57353.
- Aasen, T., Leithe, E., Graham, S. V., Kameritsch, P., Mayán, M.D., Mesnil, M., Pogoda, K. and Tabernero, A. (2019) 'Connexins in cancer : bridging the gap to the clinic', *Oncogene*, pp. 4429–4451. doi:10.1038/s41388-019-0741-6.
- Abbott, N.J. (2002) 'Astrocyte-endothelial interactions and blood-brain barrier permeability', *Journal of Anatomy*, pp. 629–638. doi:10.1046/j.1469-7580.2002.00064.x.
- Abbott, N.J., Patabendige, A.A.K., Dolman, D.E.M., Yusof, S.R. and Begley, D.J. (2009) 'Structure and function of the blood–brain barrier', *Neurobiology of Disease*, 37, pp. 13–25. doi:10.1016/j.nbd.2009.07.030.
- Abbott, N.J. (2013) 'Blood-brain barrier structure and function and the challenges for CNS drug delivery', *Journal of Inherited Metabolic Disease* [Preprint]. doi:10.1007/s10545-013-9608-0.
- Abbott, N.J. and Friedman, A. (2012) 'Overview and introduction: the blood-brain barrier in health and disease.', *Epilepsia*, 53 Suppl 6, pp. 1–6. doi:10.1111/j.1528-1167.2012.03696.x.
- Abbott, N. Joan, Rönnbäck, L. and Hansson, E. (2006) 'Astrocyte-endothelial interactions at the blood-brain barrier', *Nature Reviews Neuroscience*, pp. 41–53. doi:10.1038/nrn1824.
- Abbott, N Joan, Rönnbäck, L. and Hansson, E. (2006) 'Astrocyte–endothelial interactions at the blood–brain barrier', *Nature Reviews Neuroscience*, 7(1), pp. 41–53. doi:10.1038/nrn1824.
- Abounader, R. and Laterra, J. (2005) 'Scatter factor/hepatocyte growth factor in brain tumor growth and angiogenesis', *Neuro-Oncology*, 7(4), pp. 436–451. doi:10.1215/s1152851705000050.
- Al-Khallaf, H. (2017) 'Isocitrate dehydrogenases in physiology and cancer: Biochemical and molecular insight', *Cell and Bioscience*, 7(1), pp. 1–18. doi:10.1186/s13578-017-0165-3.
- Alentorn, A., Marie, Y., Carpentier, C., Boisselier, B., Giry, M., Labussière, M., Mokhtari, K., Hoang-Xuan, K., Sanson, M., Delattre, J.Y. and Idhah, A. (2012) 'Prevalence, clinico-pathological value, and co-occurrence of PDGFRA abnormalities in diffuse gliomas', *Neuro-Oncology*, 14(11), pp. 1393–1403. doi:10.1093/neuonc/nos217.
- Alifieris, C. and Trafalis, D.T. (2015) 'Glioblastoma multiforme: Pathogenesis and treatment', *Pharmacology and Therapeutics*, 152, pp. 63–82. doi:10.1016/j.pharmthera.2015.05.005.
- Allison N. Lau<sup>1</sup> and Matthew G. Vander Heiden<sup>1, 2</sup> (2020) 'Metabolism in the Tumor Microenvironment', *OncoImmunology*, 9(1). doi:10.1146/annurev-cancerbio-030419-033333 Copyright.
- Alvarez, J.I., Katayama, T. and Prat, A. (2013) 'Glial influence on the blood brain barrier', *GLIA*,

pp. 1939–1958. doi:10.1002/glia.22575.

Amoêdo, N.D., Valencia, J.P., Rodrigues, M.F., Galina, A. and Rumjanek, F.D. (2013) 'How does the metabolism of tumour cells differ from that of normal cells', *Bioscience Reports*, 33(6), pp. 865–873. doi:10.1042/BSR20130066.

Anchan, A., Martin, O., Hucklesby, J.J.W., Finlay, G., Johnson, R.H., Robilliard, L.D., O'carroll, S.J., Angel, C.E. and Graham, E.S. (2020) 'Analysis of melanoma secretome for factors that directly disrupt the barrier integrity of brain endothelial cells', *International Journal of Molecular Sciences*, 21(21), pp. 1–22. doi:10.3390/ijms21218193.

Arshad, F., Wang, L., Sy, C., Avraham, S. and Avraham, H.K. (2010) 'Blood-brain barrier integrity and breast cancer metastasis to the brain.', *Pathology research international*, 2011, p. 920509. doi:10.4061/2011/920509.

Arvanitis, C.D. and Ferraro, G.B. (2020) 'The blood – brain barrier and blood – tumour barrier in brain tumours and metastases', *Nature Reviews Cancer*, 20(January). doi:10.1038/s41568-019-0205-x.

Azimi-Nezhad, M. (2014) 'Vascular endothelial growth factor from embryonic status to cardiovascular pathology.', *Reports of biochemistry & molecular biology*, 2(2), pp. 59–69.

Badve, S. (2016) 'Tumor heterogeneity in breast cancer', *Molecular Pathology of Breast Cancer*, 4(December), pp. 121–132. doi:10.1007/978-3-319-41761-5\_9.

Ballabh, P., Braun, A. and Nedergaard, M. (2004) 'The blood-brain barrier: An overview: Structure, regulation, and clinical implications', *Neurobiology of Disease*, pp. 1–13. doi:10.1016/j.nbd.2003.12.016.

Baluk, P., Morikawa, S., Haskell, A., Mancuso, M. and McDonald, D.M. (2003) 'Abnormalities of Basement Membrane on Blood Vessels and Endothelial Sprouts in Tumors', *American Journal of Pathology*, 163(1), pp. 1801–1813. doi:10.1016/S0002-9440(10)65006-7.

Baluk, P., Hashizume, H. and M, D.M. (2005) 'Cellular abnormalities of blood vessels as targets in cancer', *Current Opinion in Genetics and Development*, 15(1), pp. 102–111. doi:10.1016/j.gde.2004.12.005.

Banks, W.A. (2016) 'From blood-brain barrier to blood-brain interface: new opportunities for CNS drug delivery.', *Nature reviews. Drug discovery*, 15(4), pp. 275–292. doi:10.1038/nrd.2015.21.

Barlow, K.D., Sanders, A.M., Soker, S., Ergun, S. and Metheny-Barlow, L.J. (2013) 'Pericytes on the tumor vasculature: Jekyll or hyde?', *Cancer Microenvironment*, 6(1), pp. 1–17. doi:10.1007/s12307-012-0102-2.

De Berardinis, R.J. and Chandel, N.S. (2016) 'Fundamentals of cancer metabolism', *Science Advances*, 2(5). doi:10.1126/sciadv.1600200.

Bernacki, J., Dobrowolska, A., Nerwińska, K. and Małecki, A. (2008) 'Physiology and

pharmacological role of the blood-brain barrier', *Pharmacological Reports*, pp. 600–622.

Bhowmik, A., Khan, R. and Ghosh, M.K. (2015) 'Blood Brain Barrier : A Challenge for Effectual Therapy of Brain Tumors', 2015.

Bierhansl, L., Conradi, L.-C., Treps, L., Dewerchin, M. and Carmeliet, P. (2017) 'Central Role of Metabolism in Endothelial Cell Function and Vascular Disease', *Physiology*, 32(2), pp. 126–140. doi:10.1152/physiol.00031.2016.

Blanchette, M. and Daneman, R. (2015) 'Formation and maintenance of the BBB', *Mechanisms of Development*, 138, pp. 8–16. doi:10.1016/j.mod.2015.07.007.

Blecharz, K.G., Colla, R., Rohde, V. and Vajkoczy, P. (2015) 'Control of the blood-brain barrier function in cancer cell metastasis', *Biology of the Cell*, 107(10), pp. 342–371. doi:10.1111/boc.201500011.

De Bock, M., Wang, N., Decrock, E., Bol, M., Gadicherla, A.K., Culot, M., Cecchelli, R., Bultynck, G. and Leybaert, L. (2013) 'Endothelial calcium dynamics, connexin channels and blood-brain barrier function', *Progress in Neurobiology*, 108, pp. 1–20. doi:10.1016/j.pneurobio.2013.06.001.

Boonstra, E., de Kleijn, R., Colzato, L.S., Alkemade, A., Forstmann, B.U. and Nieuwenhuis, S. (2015) 'Neurotransmitters as food supplements: The effects of GABA on brain and behavior', *Frontiers in Psychology*, 6(OCT). doi:10.3389/fpsyg.2015.01520.

Bos, P.D., Zhang, X.H.F., Nadal, C., Shu, W., Gomis, R.R., Nguyen, D.X., Minn, A.J., Van De Vijver, M.J., Gerald, W.L., Foekens, J.A. and Massagué, J. (2009) 'Genes that mediate breast cancer metastasis to the brain', *Nature*, 459(7249), pp. 1005–1009. doi:10.1038/nature08021.

Bratu, D.P., Catrina, I.E. and Marras, S.A.E. (2011) 'Tiny molecular beacons for in vivo mRNA detection.', *Methods in molecular biology (Clifton, N.J.)* [Preprint]. doi:10.1007/978-1-61779-005-8\_9.

Bravaccini, S., Granato, A.M., Medri, L., Foca, F., Falcini, F., Zoli, W., Ricci, M., Lanzaova, G., Masalu, N., Serra, L., Buggi, F., Folli, S., Silvestrini, R. and Amadori, D. (2013) 'Biofunctional characteristics of in situ and invasive breast carcinoma', *Cellular Oncology* [Preprint]. doi:10.1007/s13402-013-0135-7.

Bray, F., Ferlay, J., Soerjomataram, I., Siegel, R.L., Torre, L.A. and Jemal, A. (2018) 'Global cancer statistics 2018: GLOBOCAN estimates of incidence and mortality worldwide for 36 cancers in 185 countries', *CA: A Cancer Journal for Clinicians*, 68(6), pp. 394–424. doi:10.3322/caac.21492.

Brown, R.C. and Davis, T.P. (2002) 'Calcium Modulation of Adherens and Tight Junction Function', *Stroke*, 33(6), pp. 1706–1711. doi:10.1161/01.str.0000016405.06729.83.

Burrell, R.A., McGranahan, N., Bartek, J. and Swanton, C. (2013) 'The causes and consequences of genetic heterogeneity in cancer evolution', *Nature*, 501(7467), pp. 338–345. doi:10.1038/nature12625.

Bussolati, B., Deregibus, M.C. and Camussi, G. (2010) 'Characterization of molecular and

functional alterations of tumor endothelial cells to design anti-angiogenic strategies.', *Current vascular pharmacology*, 8(2), pp. 220–32. Available at: <http://www.ncbi.nlm.nih.gov/pubmed/19485921>.

Cacho-Díaz, B., García-Botello, D.R., Wegman-Ostrosky, T., Reyes-Soto, G., Ortiz-Sánchez, E. and Herrera-Montalvo, L.A. (2020) 'Tumor microenvironment differences between primary tumor and brain metastases', *Journal of Translational Medicine*, 18(1), pp. 1–12. doi:10.1186/s12967-019-02189-8.

Cai, X. and Sughrue, M.E. (2018) 'Glioblastoma: New therapeutic strategies to address cellular and genomic complexity', *Oncotarget*, 9(10), pp. 9540–9554. doi:10.18632/oncotarget.23476.

Caja, S. and Enríquez, J.A. (2017) 'Mitochondria in endothelial cells: Sensors and integrators of environmental cues', *Redox Biology*, 12(April), pp. 821–827. doi:10.1016/j.redox.2017.04.021.

Campos-Bedolla, P., Walter, F.R., Veszeka, S. and Deli, M.A. (2014) 'Role of the Blood-Brain Barrier in the Nutrition of the Central Nervous System', *Archives of Medical Research*, 45(8), pp. 610–638. doi:10.1016/j.arcmed.2014.11.018.

Cao, A.Y., Huang, L., Wu, J., Lu, J.S., Liu, G.Y., Shen, Z.Z., Shao, Z.M. and Di, G.H. (2012) 'Tumor characteristics and the clinical outcome of invasive lobular carcinoma compared to infiltrating ductal carcinoma in a Chinese population', *World Journal of Surgical Oncology*, 10, pp. 1–10. doi:10.1186/1477-7819-10-152.

Carbonell, W.S., Ansorga, O., Sibson, N. and Muschel, R. (2009) 'The vascular basement membrane as "soil" in brain metastasis', *PLoS ONE*, 4(6). doi:10.1371/journal.pone.0005857.

Cardoso, F.L., Brites, D. and Brito, M.A. (2010) 'Looking at the blood-brain barrier: Molecular anatomy and possible investigation approaches', *Brain Research Reviews*, 64(2), pp. 328–363. doi:10.1016/j.brainresrev.2010.05.003.

Carmeliet, P. (2005) 'VEGF as a key mediator of angiogenesis in cancer', *Oncology*, 69(SUPPL. 3), pp. 4–10. doi:10.1159/000088478.

Carvalho, C. and Moreira, P.I. (2018) 'Oxidative stress: A major player in cerebrovascular alterations associated to neurodegenerative events', *Frontiers in Physiology*, 9(JUL), pp. 1–14. doi:10.3389/fphys.2018.00806.

Cekanaviciute, E. and Buckwalter, M.S. (2016) 'Astrocytes: Integrative Regulators of Neuroinflammation in Stroke and Other Neurological Diseases', *Neurotherapeutics* [Preprint]. doi:10.1007/s13311-016-0477-8.

Charalambous, C., Hofman, F.M. and Chen, T.C. (2005) 'Functional and phenotypic differences between glioblastoma multiforme—derived and normal human brain endothelial cells', *Journal of Neurosurgery*, 102(4), pp. 699–705. doi:10.3171/jns.2005.102.4.0699.

Charles, N.A., Holland, E.C., Gilbertson, R., Glass, R. and Kettenmann, H. (2011) 'The brain tumor microenvironment', *Glia*, 59(8), pp. 1169–1180. doi:10.1002/glia.21136.



- Chen, Li, Yang, L., Yao, L., Kuang, X.Y., Zuo, W.J., Li, S., Qiao, F., Liu, Y.R., Cao, Z.G., Zhou, S.L., Zhou, X.Y., Yang, W.T., Shi, J.X., Huang, W., Hu, X. and Shao, Z.M. (2018) 'Characterization of PIK3CA and PIK3R1 somatic mutations in Chinese breast cancer patients', *Nature Communications*, 9(1), pp. 1–17. doi:10.1038/s41467-018-03867-9.
- Chen, Linlin, Deng, H., Cui, H., Fang, J., Zuo, Z., Deng, J., Li, Y., Wang, X. and Zhao, L. (2018) 'Inflammatory responses and inflammation-associated diseases in organs', *Oncotarget* [Preprint]. doi:10.18632/oncotarget.23208.
- Chen, Y. and Liu, L. (2012) 'Modern methods for delivery of drugs across the blood-brain barrier', *Advanced Drug Delivery Reviews*, 64(7), pp. 640–665. doi:10.1016/j.addr.2011.11.010.
- Cheng, F. and Guo, D. (2019) 'MET in glioma: Signaling pathways and targeted therapies', *Journal of Experimental and Clinical Cancer Research*, 38(1), pp. 1–13. doi:10.1186/s13046-019-1269-x.
- Cheng, H.-W., Chen, Y.-F., Wong, J.-M., Weng, C.-W., Chen, H.-Y., Yu, S.-L., Chen, H.-W., Yuan, A. and Chen, J.J.W. (2017) 'Cancer cells increase endothelial cell tube formation and survival by activating the PI3K/Akt signalling pathway', *Journal of Experimental & Clinical Cancer Research*, 36(1), p. 27. doi:10.1186/s13046-017-0495-3.
- Cherian, I., Beltran, M., Landi, A., Alafaci, C., Torregrossa, F. and Grasso, G. (2018) 'Introducing the concept of "CSF-shift edema" in traumatic brain injury', *Journal of Neuroscience Research*, 96(4), pp. 744–752. doi:10.1002/jnr.24145.
- Chin, A.R. and Wang, S.E. (2016) 'Cancer-derived extracellular vesicles: the "soil conditioner" in breast cancer metastasis?', *Cancer and Metastasis Reviews*, 35(4), pp. 669–676. doi:10.1007/s10555-016-9639-8.
- Choi, H. and Moon, A. (2018) 'Crosstalk between cancer cells and endothelial cells: implications for tumor progression and intervention', *Archives of Pharmacal Research*, 41(7), pp. 711–724. doi:10.1007/s12272-018-1051-1.
- City, S.L. (2003) 'Communication between malignant glioma cells and vascular endothelial cells through gap junctions', 98, pp. 846–853.
- Ciuffreda, L., Falcone, I., Cesta Incani, U., Del Curatolo, A., Conciatori, F., Matteoni, S., Vari, S., Vaccaro, V., Cognetti, F. and Milella, M. (2014) 'PTEN expression and function in adult cancer stem cells and prospects for therapeutic targeting', *Advances in Biological Regulation*, 56, pp. 66–80. doi:10.1016/j.jbior.2014.07.002.
- Claesson-Welsh, L. and Welsh, M. (2013) 'VEGFA and tumour angiogenesis', *Journal of Internal Medicine*, 273(2), pp. 114–127. doi:10.1111/joim.12019.
- Cluntun, A.A., Lukey, M.J., Cerione, R.A. and Locasale, J.W. (2017) 'Glutamine Metabolism in Cancer: Understanding the Heterogeneity', *Trends in Cancer* [Preprint]. doi:10.1016/j.trecan.2017.01.005.
- Crespo, I., Vital, A.L., Gonzalez-Tablas, M., Patino, M.D.C., Otero, A., Lopes, M.C., De Oliveira,

- C., Domingues, P., Orfao, A. and Tabernero, M.D. (2015) 'Molecular and Genomic Alterations in Glioblastoma Multiforme', *American Journal of Pathology*, 185(7), pp. 1820–1833. doi:10.1016/j.ajpath.2015.02.023.
- Croce, C.M. (2008) 'Oncogenes and cancer', *New England Journal of Medicine*, 358(5), pp. 502–511. doi:10.1056/NEJMra072367.
- Cruikshanks, N., Zhang, Y., Yuan, F., Pahuski, M., Gibert, M. and Abounader, R. (2017) 'Role and therapeutic targeting of the HGF/MET pathway in glioblastoma', *Cancers*, 9(7), pp. 1–16. doi:10.3390/cancers9070087.
- Cummins, P.M. (2012) 'Occludin: One Protein, Many Forms', *Molecular and Cellular Biology*, 32(2), pp. 242–250. doi:10.1128/mcb.06029-11.
- Curley, S.M. (2019) 'Biologically-Derived Nanomaterials for Targeted Therapeutic Delivery to the Biologically-derived nanomaterials therapeutic delivery to the brain for targeted', (July). doi:10.3184/003685018X15306123582346.
- D'Alessio, A., Proietti, G., Sica, G. and Scicchitano, B.M. (2019) 'Pathological and molecular features of glioblastoma and its peritumoral tissue', *Cancers*, 11(4). doi:10.3390/cancers11040469.
- Daneman, R. and Prat, A. (2015) 'The Blood-Brain barrier', *Cold Spring Harbor Perspectives in Biology*, 7(1). doi:10.1101/cshperspect.a020412.
- Dang, C. V. (2012) 'Links between metabolism and cancer', *Genes and Development*, 26(9), pp. 877–890. doi:10.1101/gad.189365.112.
- Davidson, S.M. and Duchon, M.R. (2007) 'Endothelial mitochondria: Contributing to vascular function and disease', *Circulation Research*, 100(8), pp. 1128–1141. doi:10.1161/01.RES.0000261970.18328.1d.
- Davis, G.E. and Senger, D.R. (2005) 'Endothelial extracellular matrix: Biosynthesis, remodeling, and functions during vascular morphogenesis and neovessel stabilization', *Circulation Research*, 97(11), pp. 1093–1107. doi:10.1161/01.RES.0000191547.64391.e3.
- Daye, D. and Wellen, K.E. (2012) 'Metabolic reprogramming in cancer: Unraveling the role of glutamine in tumorigenesis', *Seminars in Cell and Developmental Biology*, 23(4), pp. 362–369. doi:10.1016/j.semcdb.2012.02.002.
- Demeule, M., Regina, A., Annabi, B., Bertrand, Y., Bojanowski, M.W. and Beliveau, R. (2004) 'Brain endothelial cells as pharmacological targets in brain tumors', *Mol Neurobiol*, 30(2), pp. 157–183. doi:10.1385/mn:30:2:157.
- Dickman, K.G., Hempson, S.J., Anderson, J., Lippe, S., Burakoff, R., Shaw, R.D., Andris, F., Denanglaire, S., Baus, E., Rongvaux, A., Steuve, J., Flavell, R.A., Leo, O., Zhao, L. and Kathleen, G. (2012) 'Rotavirus alters paracellular permeability and energy metabolism in Caco-2 cells', *Cultures* [Preprint].



- Doll, D.N., Hu, H., Sun, J., Lewis, S.E., Simpkins, J.W. and Ren, X. (2015) 'Mitochondrial Crisis in Cerebrovascular Endothelial Cells Opens the Blood-Brain Barrier', *Stroke*, 46(6), pp. 1681–1689. doi:10.1161/STROKEAHA.115.009099.
- Dubois, L.G., Campanati, L., Righy, C. and Andrea-meira, I.D. (2014) 'Gliomas and the vascular fragility of the blood brain barrier', (December). doi:10.3389/fncel.2014.00418.
- Dudley, A.C. (2012) 'Tumor endothelial cells.', *Cold Spring Harbor perspectives in medicine*, 2(3), pp. 1–18. doi:10.1101/cshperspect.a006536.
- Duncan, C.G. and Yan, H. (2011) 'Genomic alterations and the pathogenesis of glioblastoma', *Cell Cycle*, 10(8), pp. 1174–1175. doi:10.4161/cc.10.8.15225.
- Dwyer, J., Hebda, J.K., Le Guelte, A., Galan-Moya, E.M., Smith, S.S., Azzi, S., Bidere, N. and Gavard, J. (2012) 'Glioblastoma Cell-Secreted Interleukin-8 Induces Brain Endothelial Cell Permeability via CXCR2', *PLoS ONE*, 7(9). doi:10.1371/journal.pone.0045562.
- Dyken, P. Van and Lacoste, B. (2018) 'Impact of Metabolic Syndrome on Neuroinflammation and the', 12(December), pp. 1–19. doi:10.3389/fmins.2018.00930.
- Dyrna, F., Hanske, S., Krueger, M. and Bechmann, I. (2013) 'The blood-brain barrier.', *Journal of neuroimmune pharmacology : the official journal of the Society on NeuroImmune Pharmacology*, 8(4), pp. 763–773. doi:10.1007/s11481-013-9473-5.
- Eales, K.L., Hollinshead, K.E.R. and Tennant, D.A. (2016) 'Hypoxia and metabolic adaptation of cancer cells', *Oncogenesis*, 5(1), pp. e190–e190. doi:10.1038/oncsis.2015.50.
- Elwood, E., Lim, Z., Naveed, H. and Galea, I. (2017) 'The effect of systemic inflammation on human brain barrier function', *Brain, Behavior, and Immunity*, 62, pp. 35–40. doi:10.1016/j.bbi.2016.10.020.
- Engelhardt, S., Al-Ahmad, A.J., Gassmann, M. and Ogunshola, O.O. (2014) 'Hypoxia selectively disrupts brain microvascular endothelial tight junction complexes through a hypoxia-inducible factor-1 (HIF-1) dependent mechanism', *Journal of Cellular Physiology*, 229(8), pp. 1096–1105. doi:10.1002/jcp.24544.
- Engelhardt, S., Huang, S., Patkar, S., Gassmann, M. and Ogunshola, O.O. (2015) 'Differential responses of blood-brain barrier associated cells to hypoxia and ischemia: a comparative study', pp. 1–16.
- Feldman, G.J., Mullin, J.M. and Ryan, M.P. (2005) 'Occludin: Structure, function and regulation', *Advanced Drug Delivery Reviews*, 57(6), pp. 883–917. doi:10.1016/j.addr.2005.01.009.
- Feng, Y., Spezia, M., Huang, S., Yuan, C., Zeng, Z., Zhang, L., Ji, X., Liu, W., Huang, B., Luo, W., Liu, B., Lei, Y., Du, S., Vuppapapati, A., Luu, H.H., Haydon, R.C., He, T.C. and Ren, G. (2018) 'Breast cancer development and progression: Risk factors, cancer stem cells, signaling pathways, genomics, and molecular pathogenesis', *Genes and Diseases*, 5(2), pp. 77–106. doi:10.1016/j.gendis.2018.05.001.

- Ferjančič, Š., Gil-Bernabé, A.M., Hill, S.A., Allen, P.D., Richardson, P., Sparey, T., Savory, E., McGuffog, J. and Muschel, R.J. (2013) 'VCAM-1 and VAP-1 recruit myeloid cells that promote pulmonary metastasis in mice', *Blood* [Preprint]. doi:10.1182/blood-2012-08-449819.
- Fidler, I.J. (2003) 'The pathogenesis of cancer metastasis: the "seed and soil" hypothesis revisited', *Nature Publishing Group*, 3(1), pp. 46–56. doi:doi: 10.1038/nrc1098.
- Fidler, I.J. (2015) 'The Biology of Brain Metastasis', *Cancer Journal (United States)*, 21(4), pp. 284–293. doi:10.1097/PPO.0000000000000126.
- Fisher, D. and Mentor, S. (2020) 'Are claudin-5 tight-junction proteins in the blood-brain barrier porous?', *Neural Regeneration Research*, 15(10), pp. 1838–1839. doi:10.4103/1673-5374.280308.
- Fong, C.W. (2015) 'Permeability of the Blood–Brain Barrier: Molecular Mechanism of Transport of Drugs and Physiologically Important Compounds', *Journal of Membrane Biology*, 248(4), pp. 651–669. doi:10.1007/s00232-015-9778-9.
- Forrester, S.J., Kikuchi, D.S., Hernandez, M.S., Xu, Q. and Griendling, K.K. (2018) 'Reactive oxygen species in metabolic and inflammatory signaling', *Circulation Research*, 122(6), pp. 877–902. doi:10.1161/CIRCRESAHA.117.311401.
- Fouad, Y.A. and Aanei, C. (2017) 'Revisiting the hallmarks of cancer', *American Journal of Cancer Research* [Preprint].
- Funasaka, T., Haga, A., Raz, A. and Nagase, H. (2002) 'Autocrine motility factor secreted by tumor cells upregulates vascular endothelial growth factor receptor (Flt-1) expression in endothelial cells', *International Journal of Cancer*, 101(3), pp. 217–223. doi:10.1002/ijc.10617.
- Galea, I. (2021) 'The blood–brain barrier in systemic infection and inflammation', *Cellular and Molecular Immunology*, 18(11), pp. 2489–2501. doi:10.1038/s41423-021-00757-x.
- Ge, Z. and Ding, S. (2020) 'The Crosstalk Between Tumor-Associated Macrophages (TAMs) and Tumor Cells and the Corresponding Targeted Therapy', *Frontiers in Oncology*, 10(November), pp. 1–23. doi:10.3389/fonc.2020.590941.
- Giusti, I., Monache, D.S., Di Francesco, M., Sanit, P., D'Ascenzo, S., Gravina, G.L., Festuccia, C. and Dolo, V. (2016) 'From glioblastoma to endothelial cells through extracellular vesicles: messages for angiogenesis', *Tumor Biology*, 37(9), pp. 12743–12753. doi:10.1007/s13277-016-5165-0.
- Goda, N. and Kanai, M. (2012) 'Hypoxia-inducible factors and their roles in energy metabolism', *International Journal of Hematology*, 95(5), pp. 457–463. doi:10.1007/s12185-012-1069-y.
- Gong, X., Hou, Z., Endsley, M.P., Gronseth, E.I., Rarick, K.R., Jorns, J.M., Yang, Q., Du, Z., Yan, K., Bordas, M.L., Gershan, J., Deepak, P., Geethadevi, A., Chaluvally-Raghavan, P., Fan, Y., Harder, D.R., Ramchandran, R. and Wang, L. (2019) 'Interaction of tumor cells and astrocytes promotes breast cancer brain metastases through TGF- $\beta$ 2/ANGPTL4 axes', *npj Precision Oncology*, 3(1). doi:10.1038/s41698-019-0094-1.

- Gonzalezmariscal, L. (2003) 'Tight junction proteins', *Progress in Biophysics and Molecular Biology*, 81(1), pp. 1–44. doi:10.1016/S0079-6107(02)00037-8.
- Goswami, S., Sahai, E., Wyckoff, J.B., Cammer, M., Cox, D., Pixley, F.J., Stanley, E.R., Segall, J.E. and Condeelis, J.S. (2005) 'Erratum: Macrophages promote the invasion of breast carcinoma cells via a colony-stimulating factor-1/epidermal growth factor paracrine loop (Cancer Research (June 15, 2005) 65 (5278-5283))', *Cancer Research*, 65(15), p. 7031. doi:10.1158/0008-5472.CAN-65-15-COR.
- Greene, C. and Campbell, M. (2016) 'Tight junction modulation of the blood brain barrier: CNS delivery of small molecules', *Tissue Barriers* [Preprint]. doi:10.1080/21688370.2015.1138017.
- Gronseth, E., Wang, L., Harder, D.R. and Ramchandran, R. (2018) 'The Role of Astrocytes in Tumor Growth and Progression', *Astrocyte - Physiology and Pathology* [Preprint]. doi:10.5772/intechopen.72720.
- Guan, Z., Lan, H., Cai, X., Zhang, Y., Liang, A. and Li, J. (2021) 'Blood–Brain Barrier, Cell Junctions, and Tumor Microenvironment in Brain Metastases, the Biological Prospects and Dilemma in Therapies', *Frontiers in Cell and Developmental Biology*, 9(August). doi:10.3389/fcell.2021.722917.
- Haileselassie, B., Joshi, A.U., Minhas, P.S., Mukherjee, R., Andreasson, K.I. and Mochly-Rosen, D. (2020) 'Mitochondrial dysfunction mediated through dynamin-related protein 1 (Drp1) propagates impairment in blood brain barrier in septic encephalopathy', *Journal of Neuroinflammation*, 17(1), pp. 1–11. doi:10.1186/s12974-019-1689-8.
- Hanahan, D. and Weinberg, R.A. (2011) 'Hallmarks of cancer: The next generation', *Cell*, 144(5), pp. 646–674. doi:10.1016/j.cell.2011.02.013.
- Hanif, F., Muzaffar, K., Perveen, K., Malhi, S.M. and Simjee, S.U. (2017) 'Glioblastoma Multiforme: A Review of its Epidemiology and Pathogenesis through Clinical Presentation and Treatment', *Asian Pacific journal of cancer prevention: APJCP*, 18(1), pp. 3–9. doi:10.22034/APJCP.2017.18.1.3.
- Harjes, U., Bensaad, K. and Harris, A.L. (2012) 'Endothelial cell metabolism and implications for cancer therapy', *British Journal of Cancer*, 107(8), pp. 1207–1212. doi:10.1038/bjc.2012.398.
- Haseloff, R.F., Blasig, I.E., Bauer, H.C. and Bauer, H. (2005) 'In search of the astrocytic factor(s) modulating blood-brain barrier functions in brain capillary endothelial cells in vitro', *Cellular and Molecular Neurobiology*, pp. 25–39. doi:10.1007/s10571-004-1375-x.
- Hashizume, H., Baluk, P., Morikawa, S., McLean, J.W., Thurston, G., Roberge, S., Jain, R.K. and McDonald, D.M. (2000) 'Openings between defective endothelial cells explain tumor vessel leakiness', *American Journal of Pathology*, 156(4), pp. 1363–1380. doi:10.1016/S0002-9440(10)65006-7.
- Hassiotou, F. and Geddes, D. (2013) 'Anatomy of the human mammary gland: Current status of knowledge', *Clinical Anatomy* [Preprint]. doi:10.1002/ca.22165.

Hatoum, A., Mohammed, R. and Zakieh, O. (2019) 'The unique invasiveness of glioblastoma and possible drug targets on extracellular matrix', *Cancer Management and Research*, 11, pp. 1843–1855. doi:10.2147/CMAR.S186142.

Hida, K., Maishi, N., Annan, D.A. and Hida, Y. (2018) 'Contribution of tumor endothelial cells in cancer progression', *International Journal of Molecular Sciences*, 19(5), pp. 1–12. doi:10.3390/ijms19051272.

Hida, K., Hida, Y. and Shindoh, M. (2008) 'Understanding tumor endothelial cell abnormalities to develop ideal anti-angiogenic therapies', *Cancer Science*, 29(3), pp. 459–466. doi:10.1111/j.1349-7006.2007.00704.x.

Hida, K. and Maishi, N. (2018) 'Abnormalities of tumor endothelial cells and cancer progression', *Oral Science International*, 15(1), pp. 1–6. doi:10.1016/S1348-8643(17)30041-1.

Hladky, S.B. and Barrand, M.A. (2016) *Fluid and ion transfer across the blood-brain and blood-cerebrospinal fluid barriers; a comparative account of mechanisms and roles.*, *Fluids and barriers of the CNS*. BioMed Central. doi:10.1186/s12987-016-0040-3.

Hopkins, B.D., Hodakoski, C., Barrows, D., Mense, S.M. and Parsons, R.E. (2014) 'PTEN function: The long and the short of it', *Trends in Biochemical Sciences* [Preprint]. doi:10.1016/j.tibs.2014.02.006.

Hosonaga, M., Saya, H. and Arima, Y. (2020) 'Molecular and cellular mechanisms underlying brain metastasis of breast cancer', *Cancer and Metastasis Reviews*, 39(3), pp. 711–720. doi:10.1007/s10555-020-09881-y.

Hottinger, A.F., Abdullah, K.G. and Stupp, R. (2016) *Current Standards of Care in Glioblastoma Therapy*, *Glioblastoma*. doi:10.1016/B978-0-323-47660-7.00006-9.

Houben, R., Schrama, D. and Becker, J.C. (2009) 'Molecular pathogenesis of Merkel cell carcinoma', *Experimental Dermatology* [Preprint]. doi:10.1111/j.1600-0625.2009.00853.x.

Hu, G., Place, A.T. and Minshall, R.D. (2008) 'Regulation of Endothelial Permeability by Src Kinase Signaling', *Chemistry & Biology*, 17(2), pp. 177–189. doi:10.1016/j.cbi.2007.08.006.Regulation.

Hu, J., Cao, J., Topatana, W., Juengpanich, S., Li, S., Zhang, B., Shen, J., Cai, L., Cai, X. and Chen, M. (2021) 'Targeting mutant p53 for cancer therapy: direct and indirect strategies', *Journal of Hematology and Oncology*, 14(1), pp. 1–19. doi:10.1186/s13045-021-01169-0.

Huang, C.H., Mandelker, D., Schmidt-Kittler, O., Samuels, Y., Velculescu, V.E., Kinzler, K.W., Vogelstein, B., Gabelli, S.B. and Amzel, L.M. (2007) 'The structure of a human p110 $\alpha$ /p85 $\alpha$  complex elucidates the effects of oncogenic PI3K $\alpha$  mutations', *Science*, 318(5857), pp. 1744–1748. doi:10.1126/science.1150799.

Huang, J., Yu, J., Tu, L., Huang, N., Li, H. and Luo, Y. (2019) 'Isocitrate dehydrogenase mutations in glioma: From basic discovery to therapeutics development', *Frontiers in Oncology*.

doi:10.3389/fonc.2019.00506.

Huber, J.D., Egleton, R.D. and Davis, T.P. (2001) 'Molecular physiology and pathophysiology of tight junctions in the blood-brain barrier.', *Trends in neurosciences*, 24(12), pp. 719–725. doi:10.1016/S0166-2236(00)02004-X.

Hurtado-Alvarado, G., Cabañas-Morales, A.M. and Gómez-González, B. (2014) 'Pericytes: Brain-immune interface modulators', *Frontiers in Integrative Neuroscience*, 7(JAN), pp. 1–10. doi:10.3389/fnint.2013.00080.

Ishihara, H., Kubota, H., Lindberg, R.L.P., Leppert, D., Gloor, S.M., Errede, M., Virgintino, D., Fontana, A., Yonekawa, Y. and Frei, K. (2008) 'Endothelial cell barrier impairment induced by glioblastomas and transforming growth factor beta2 involves matrix metalloproteinases and tight junction proteins.', *Journal of neuropathology and experimental neurology*, 67(5), pp. 435–48. doi:10.1097/NEN.0b013e31816fd622.

Islam, M.M. and Mohamed, Z. (2015) 'Computational and Pharmacological Target of Neurovascular Unit for Drug Design and Delivery', *BioMed Research International*, 2015(October). doi:10.1155/2015/731292.

Ito, A., Katoh, F., Kataoka, T.R., Okada, M., Tsubota, N., Asada, H., Yoshikawa, K., Maeda, S., Kitamura, Y., Yamasaki, H. and Nojima, H. (2000) 'A role for heterologous gap junctions between melanoma and endothelial cells in metastasis', 105(9), pp. 1189–1197.

Javed, A. and Lteif, A. (2013) 'Development of the human breast', *Seminars in Plastic Surgery* [Preprint]. doi:10.1055/s-0033-1343989.

Jayadev, R. and Sherwood, D.R. (2017) 'Basement membranes', *Current Biology*, 27(6), pp. R207–R211. doi:10.1016/j.cub.2017.02.006.

Jing, X., Yang, F., Shao, C., Wei, K., Xie, M., Shen, H. and Shu, Y. (2019) 'Role of hypoxia in cancer therapy by regulating the tumor microenvironment', *Molecular Cancer*, 18(1), pp. 1–15. doi:10.1186/s12943-019-1089-9.

Johnson, A.M., Roach, J.P., Hu, A., Stamatovic, S.M., Zochowski, M.R., Keep, R.F. and Andjelkovic, A. V. (2018) 'Connexin 43 gap junctions contribute to brain endothelial barrier hyperpermeability in familial cerebral cavernous malformations type III by modulating tight junction structure', *FASEB Journal*, 32(5), pp. 2615–2629. doi:10.1096/fj.201700699R.

Joshi, S.K. (2015) 'Molecular pathogenesis of glioblastoma multiforme: Nuances, obstacles, and implications for treatment', *World Journal of Neurology*, 5(3), p. 88. doi:10.5316/wjn.v5.i3.88.

Jouyban, A. and Soltani, S. (2012) 'Blood Brain Barrier Permeation', *Toxicity and Drug Testing*, pp. 3–24. doi:10.5772/20360.

Kadry, H., Noorani, B. and Cucullo, L. (2020) 'A blood–brain barrier overview on structure, function, impairment, and biomarkers of integrity', *Fluids and Barriers of the CNS*, 17(1), pp. 1–24. doi:10.1186/s12987-020-00230-3.



- Kalyanaraman, B. (2017) 'Teaching the basics of cancer metabolism: Developing antitumor strategies by exploiting the differences between normal and cancer cell metabolism', *Redox Biology*, 12(February), pp. 833–842. doi:10.1016/j.redox.2017.04.018.
- Karagiannis, G.S., Pavlou, M.P. and Diamandis, E.P. (2010) 'Cancer secretomics reveal pathophysiological pathways in cancer molecular oncology', *Molecular Oncology*, 4(6), pp. 496–510. doi:10.1016/j.molonc.2010.09.001.
- Keaney, J. and Campbell, M. (2015) 'The dynamic blood-brain barrier', *FEBS Journal*, 282(21), pp. 4067–4079. doi:10.1111/febs.13412.
- Kenig, S., Alonso, M.B.D., Mueller, M.M. and Lah, T.T. (2010) 'Glioblastoma and endothelial cells cross-talk, mediated by SDF-1, enhances tumour invasion and endothelial proliferation by increasing expression of cathepsins B, S, and MMP-9', *Cancer Letters*, 289(1), pp. 53–61. doi:10.1016/j.canlet.2009.07.014.
- Key, T.J., Verkasalo, P.K. and Banks, E. (2001) 'Epidemiology of breast cancer', *Lancet Oncology* [Preprint]. doi:10.1016/S1470-2045(00)00254-0.
- Khoshnoodi, J., Pedchenko, V. and Hudson, B.G. (2008) 'Mammalian collagen IV', *Microscopy Research and Technique* [Preprint]. doi:10.1002/jemt.20564.
- Kienast, Y., Von Baumgarten, L., Fuhrmann, M., Klinkert, W.E.F., Goldbrunner, R., Herms, J. and Winkler, F. (2010) 'Real-time imaging reveals the single steps of brain metastasis formation', *Nature Medicine*, 16(1), pp. 116–122. doi:10.1038/nm.2072.
- Kim, J.W., Tchernyshyov, I., Semenza, G.L. and Dang, C. V. (2006) 'HIF-1-mediated expression of pyruvate dehydrogenase kinase: A metabolic switch required for cellular adaptation to hypoxia', *Cell Metabolism*, 3(3), pp. 177–185. doi:10.1016/j.cmet.2006.02.002.
- Kisler, K., Nelson, A.R., Montagne, A. and Zlokovic, B. V. (2017) 'Cerebral blood flow regulation and neurovascular dysfunction in Alzheimer's disease', *Nat Rev Neurosci*, 176(18), pp. 419–434. doi:https://doi.org/10.1038/nrn.2017.48.
- Kobayashi, S., Sugiura, H., Ando, Y., Shiraki, N., Yanagi, T., Yamashita, H. and Toyama, T. (2012) 'Reproductive history and breast cancer risk', *Breast Cancer* [Preprint]. doi:10.1007/s12282-012-0384-8.
- Komarova, Y. and Malik, A.B. (2010) *Regulation of endothelial permeability via paracellular and transcellular transport pathways.*, *Annual review of physiology*. doi:10.1146/annurev-physiol-021909-135833.
- Komori, T. (2014) 'Pathology and genetics of diffuse gliomas in adults', *Neurologia Medico-Chirurgica*, 55(1), pp. 28–37. doi:10.2176/nmc.ra.2014-0229.
- Kondoh, M., Ohga, N., Akiyama, K., Hida, Y., Maishi, N., Towfik, A.M., Inoue, N., Shindoh, M. and Hida, K. (2013) 'Hypoxia-induced reactive oxygen species cause chromosomal abnormalities in endothelial cells in the tumor microenvironment', *PLoS ONE*, 8(11), pp. 1–14.

doi:10.1371/journal.pone.0080349.

Krishnan, S., Szabo, E., Burghardt, I., Frei, K., Tabatabai, G. and Weller, M. (2015) 'Modulation of cerebral endothelial cell function by TGF- $\beta$  in glioblastoma: VEGF-dependent angiogenesis versus endothelial mesenchymal transition.', *Oncotarget*, 6(26), pp. 22480–95. doi:10.18632/oncotarget.4310.

Labelle, M. and Hynes, R.O. (2013) 'The initial hours of metastasis: the importance of cooperative host-tumor cell interactions during hematogenous dissemination', 2(12), pp. 1091–1099. doi:10.1158/2159-8290.CD-12-0329.The.

Lécuyer, M.A., Kebir, H. and Prat, A. (2016) 'Glial influences on BBB functions and molecular players in immune cell trafficking', *Biochimica et Biophysica Acta - Molecular Basis of Disease*, 1862(3), pp. 472–482. doi:10.1016/j.bbadis.2015.10.004.

Lee, E., Pandey, N.B. and Popel, A.S. (2015) 'Crosstalk between cancer cells and blood endothelial and lymphatic endothelial cells in tumour and organ microenvironment', *Expert Reviews in Molecular Medicine*, 17. doi:10.1017/erm.2015.2.

Lee, K.Y., Kim, Y.J., Yoo, H., Lee, S.H., Park, J.B. and Kim, H.J. (2011) 'Human brain endothelial cell-derived COX-2 facilitates extravasation of breast cancer cells across the blood-brain barrier', *Anticancer Research*, 31(12), pp. 4307–4313.

Lee, M.J., Jang, Y., Han, J., Kim, S.J., Ju, X., Lee, Y.L., Cui, J., Zhu, J., Ryu, M.J., Choi, S.Y., Chung, W., Heo, C., Yi, H.S., Kim, H.J., Huh, Y.H., Chung, S.K., Shong, M., Kweon, G.R. and Heo, J.Y. (2020) 'Endothelial-specific Crif1 deletion induces BBB maturation and disruption via the alteration of actin dynamics by impaired mitochondrial respiration', *Journal of Cerebral Blood Flow and Metabolism*, 40(7), pp. 1546–1561. doi:10.1177/0271678X19900030.

Lemmon, M.A. and Schlessinger, J. (2011) '( ALL STRUCTURES) NIH Public Access', 141(7), pp. 1117–1134. doi:10.1016/j.cell.2010.06.011.Cell.

Leone, J.P. and Leone, B.A. (2015) 'Breast cancer brain metastases: The last frontier', *Experimental Hematology and Oncology*, 4(1), pp. 1–10. doi:10.1186/s40164-015-0028-8.

Li, Q.J., Cai, J.Q. and Liu, C.Y. (2016) 'Evolving molecular genetics of glioblastoma', *Chinese Medical Journal*, 129(4), pp. 464–471. doi:10.4103/0366-6999.176065.

Liebner, S., Fischmann, A., Rascher, G., Duffner, F., Grote, E.H., Kalbacher, H. and Wolburg, H. (2000) 'Claudin-1 and claudin-5 expression and tight junction morphology are altered in blood vessels of human glioblastoma multiforme.', *Acta neuropathologica*, 100(3), pp. 323–331. doi:10.1007/s004010000180.

Liebner, S., Kniessel, U., Kalbacher, H. and Wolburg, H. (2000) 'Correlation of tight junction morphology with the expression of tight junction proteins in blood-brain barrier endothelial cells', *European Journal of Cell Biology*, 79(10), pp. 707–717. doi:10.1078/0171-9335-00101.

Lin, C.M., Yu, C.F., Huang, H.Y., Chen, F.H., Hong, J.H. and Chiang, C.S. (2019) 'Distinct tumor

microenvironment at tumor edge as a result of astrocyte activation is associated with therapeutic resistance for brain tumor', *Frontiers in Oncology*, 9(APR), pp. 1–12. doi:10.3389/fonc.2019.00307.

Lind-Landström, T., Habberstad, A.H., Sundström, S. and Torp, S.H. (2012) 'Prognostic value of histological features in diffuse astrocytomas WHO grade II', *International Journal of Clinical and Experimental Pathology*, 5(2), pp. 152–158.

Liu, W.Y., Wang, Z. Bin, Zhang, L.C., Wei, X. and Li, L. (2012) 'Tight junction in blood-brain barrier: An overview of structure, regulation, and regulator substances', *CNS Neuroscience and Therapeutics*, 18(8), pp. 609–615. doi:10.1111/j.1755-5949.2012.00340.x.

Liu, Y.W., Li, S. and Dai, S.S. (2018) 'Neutrophils in traumatic brain injury (TBI): Friend or foe?', *Journal of Neuroinflammation*, 15(1), pp. 1–18. doi:10.1186/s12974-018-1173-x.

Lopes-Bastos, B.M., Jiang, W.G. and Cai, J. (2016) 'Tumour-Endothelial Cell Communications: Important and Indispensable Mediators of Tumour Angiogenesis.', *Anticancer research*, 36(3), pp. 1119–26. Available at: <http://www.ncbi.nlm.nih.gov/pubmed/26977007>.

Lorger, M. (2012) 'Tumor microenvironment in the brain', *Cancers*, 4(1), pp. 218–243. doi:10.3390/cancers4010218.

Louis, D.N., Perry, A., Reifenberger, G., von Deimling, A., Figarella-Branger, D., Cavenee, W.K., Ohgaki, H., Wiestler, O.D., Kleihues, P. and Ellison, D.W. (2016) 'The 2016 World Health Organization Classification of Tumors of the Central Nervous System: a summary', *Acta Neuropathologica*, 131(6), pp. 803–820. doi:10.1007/s00401-016-1545-1.

Luissint, A.-C., Artus, C., Glacial, F., Ganeshamoorthy, K. and Couraud, P.-O. (2012) 'Tight junctions at the blood brain barrier: physiological architecture and disease-associated dysregulation.', *Fluids and barriers of the CNS*, 9(1), p. 23. doi:10.1186/2045-8118-9-23.

Luo, J., Martinez, J., Yin, X., Sanchez, A., Tripathy, D. and Grammas, P. (2012) 'Hypoxia induces angiogenic factors in brain microvascular endothelial cells', *Microvascular Research*, 83(2), pp. 138–145. doi:10.1016/j.mvr.2011.11.004.

Luo, P.L., Wang, Y.J., Yang, Y.Y. and Yang, J.J. (2018) 'Hypoxia-induced hyperpermeability of rat glomerular endothelial cells involves HIF-2 $\alpha$  mediated changes in the expression of occludin and ZO-1', *Brazilian Journal of Medical and Biological Research*, 51(7), pp. 1–7. doi:10.1590/1414-431x20186201.

Lv, Y., Ma, X., Du, Y. and Feng, J. (2021) 'Understanding patterns of brain metastasis in triple-negative breast cancer and exploring potential therapeutic targets', *OncoTargets and Therapy*, 14, pp. 589–607. doi:10.2147/OTT.S293685.

Lyle, L.T., Lockman, P.R., Adkins, C.E., Mohammad, A.S., Sechrest, E., Hua, E., Palmieri, D., Liewehr, D.J., Steinberg, S.M., Kloc, W., Izycka-swieszewska, E., Duchnowska, R., Nayyar, N., Brastianos, P.K., Steeg, P.S. and Gril, B. (2016) 'Alterations in Pericyte Subpopulations Are Associated with Elevated Blood – Tumor Barrier Permeability in Experimental Brain Metastasis



of Breast Cancer', pp. 5287–5300. doi:10.1158/1078-0432.CCR-15-1836.

Lyssiotis, C.A. and Kimmelman, A.C. (2017) 'Metabolic Interactions in the Tumor Microenvironment.', *Trends in cell biology*, 27(11), pp. 863–875. doi:10.1016/j.tcb.2017.06.003.

Ma, T.Y., Hoa, N.T., Tran, D., Merryfield, M., Nguyen, D. and Tarnawski, A. (2000) 'Mechanism of extracellular calcium regulation of intestinal epithelial tight junction barrier: Role of cytoskeletal involvement', *Gastroenterology*, 118(4), p. A1268. doi:10.1016/s0016-5085(00)80919-1.

Maishi, N. and Hida, K. (2017) 'Tumor endothelial cells accelerate tumor metastasis', *Cancer Science*. Blackwell Publishing Ltd, pp. 1921–1926. doi:10.1111/cas.13336.

Malhotra, G.K., Zhao, X., Band, H. and Band, V. (2010) 'Histological, molecular and functional subtypes of breast cancers', *Cancer Biology and Therapy*, 10(10), pp. 955–960. doi:10.4161/cbt.10.10.13879.

Manton, C.A. (2015) 'Induction of caspase-dependent death by proteasome targeted therapy in glioblastoma'.

Marie, S.K.N. and Shinjo, S.M.O. (2011) 'Metabolism and brain cancer', *Clinics*, 66(SUPPL.1), pp. 33–43. doi:10.1590/S1807-59322011001300005.

Martin, T.A. and Jiang, W.G. (2009) 'Loss of tight junction barrier function and its role in cancer metastasis', *Biochimica et Biophysica Acta - Biomembranes*, 1788(4), pp. 872–891. doi:10.1016/j.bbamem.2008.11.005.

Matias, D., Balça-Silva, J., da Graça, G.C., Wanjiru, C.M., Macharia, L.W., Nascimento, C.P., Roque, N.R., Coelho-Aguiar, J.M., Pereira, C.M., Dos Santos, M.F., Pessoa, L.S., Lima, F.R.S., Schanaider, A., Ferrer, V.P., e Spohr, T.C.L. de S. and Moura-Neto, V. (2018) 'Microglia/astrocytes–glioblastoma crosstalk: Crucial molecular mechanisms and microenvironmental factors', *Frontiers in Cellular Neuroscience*, 12(August), pp. 1–22. doi:10.3389/fncel.2018.00235.

McConnell, H.L., Kersch, C.N., Woltjer, R.L. and Neuwelt, E.A. (2017) 'The translational significance of the neurovascular unit', *Journal of Biological Chemistry* [Preprint]. doi:10.1074/jbc.R116.760215.

Medress, Z. and Hayden Gephart, M. (2015) 'Molecular and Genetic Predictors of Breast-to-Brain Metastasis: Review and Case Presentation', *Cureus*, 7(1), pp. 1–9. doi:10.7759/cureus.246.

Michinaga, S. and Koyama, Y. (2015) 'Pathogenesis of brain edema and investigation into anti-edema drugs', *International Journal of Molecular Sciences* [Preprint]. doi:10.3390/ijms16059949.

Michinaga, S. and Koyama, Y. (2019) 'Dual roles of astrocyte-derived factors in regulation of blood-brain barrier function after brain damage', *International Journal of Molecular Sciences*, 20(3), pp. 1–22. doi:10.3390/ijms20030571.

Mierke, C.T., Zitterbart, D.P., Kollmannsberger, P., Raupach, C., Schlötzer-Schrehardt, U.,

Goecke, T.W., Behrens, J. and Fabry, B. (2008) 'Breakdown of the endothelial barrier function in tumor cell transmigration.', *Biophysical journal*, 94(7), pp. 2832–46. doi:10.1529/biophysj.107.113613.

Mierke, C.T. (2008) 'Role of the Endothelium during Tumor Cell Metastasis: Is the Endothelium a Barrier or a Promoter for Cell Invasion and Metastasis?', *Journal of Biophysics*, 2008, pp. 1–13. doi:10.1155/2008/183516.

Mierke, C.T. (2011) 'Cancer cells regulate biomechanical properties of human microvascular endothelial cells.', *The Journal of biological chemistry*, 286(46), pp. 40025–37. doi:10.1074/jbc.M111.256172.

Miller, A.A., Budzyn, K. and Sobey, C.G. (2010) 'Vascular dysfunction in cerebrovascular disease: Mechanisms and therapeutic intervention', *Clinical Science* [Preprint]. doi:10.1042/CS20090649.

Miller, C.R., Stroobant, E.E., Shelton, A.K., Bash, R.E., Schmid, R.S. and Holland, E. (2018) 'PIK3CA missense mutations promote glioblastoma pathogenesis, but do not enhance targeted PI3K inhibition', *PLoS ONE*, pp. 1–21.

Miller, D.M., Thomas, S.D., Islam, A., Muench, D. and Sedoris, K. (2012) 'c-Myc and cancer metabolism', *Clinical Cancer Research* [Preprint]. doi:10.1158/1078-0432.CCR-12-0977.

Moore, K. and Kim, L. (2010) 'Primary Brain Tumors: Characteristics, Practical Diagnostic and Treatment Approaches', in, pp. 43–76. doi:10.1007/978-1-4419-0410-2.

Mühleder, S., Fernández-Chacón, M., Garcia-Gonzalez, I. and Benedito, R. (2021) 'Endothelial sprouting, proliferation, or senescence: tipping the balance from physiology to pathology', *Cellular and Molecular Life Sciences*, 78(4), pp. 1329–1354. doi:10.1007/s00018-020-03664-y.

Muz, B., de la Puente, P., Azab, F. and Azab, A.K. (2015) 'The role of hypoxia in cancer progression, angiogenesis, metastasis, and resistance to therapy', *Hypoxia*, p. 83. doi:10.2147/hp.s93413.

Nakagomi, T., Kubo, S., Nakano-Doi, A., Sakuma, R., Lu, S., Narita, A., Kawahara, M., Taguchi, A. and Matsuyama, T. (2015) 'Brain vascular pericytes following ischemia have multipotential stem cell activity to differentiate into neural and vascular lineage cells', *Stem Cells*, 33(6), pp. 1962–1974. doi:10.1002/stem.1977.

Neve, A., Cantatore, F.P., Maruotti, N., Corrado, A. and Ribatti, D. (2014) 'Extracellular matrix modulates angiogenesis in physiological and pathological conditions', *BioMed Research International*, 2014. doi:10.1155/2014/756078.

Nishida, N., Yano, H., Nishida, T., Kamura, T. and Kojiro, M. (2006) 'Angiogenesis in cancer', *Vascular Health and Risk Management*, 2(3), pp. 213–219. doi:10.2147/vhrm.2006.2.3.213.

Noell, S., Wolburg-Buchholz, K., Mack, A.F., Beedle, A.M., Satz, J.S., Campbell, K.P., Wolburg, H. and Fallier-Becker, P. (2011) 'Evidence for a role of dystroglycan regulating the membrane architecture of astroglial endfeet', *European Journal of Neuroscience*, 33(12), pp. 2179–2186.

doi:10.1111/j.1460-9568.2011.07688.x.

Norton, K.A. and Popel, A.S. (2016) 'Effects of endothelial cell proliferation and migration rates in a computational model of sprouting angiogenesis', *Scientific Reports* [Preprint]. doi:10.1038/srep36992.

Obermeier, B., Verma, A. and Ransohoff, R.M. (2016) *The blood-brain barrier*. 1st edn, *Handbook of Clinical Neurology*. 1st edn. Elsevier B.V. doi:10.1016/B978-0-444-63432-0.00003-7.

Ogunshola, O.O. and Al-Ahmad, A. (2012) 'HIF-1 at the blood-brain barrier: A mediator of permeability?', *High Altitude Medicine and Biology*, 13(3), pp. 153–161. doi:10.1089/ham.2012.1052.

Ohga, N., Ishikawa, S., Maishi, N., Akiyama, K., Hida, Y., Kawamoto, T., Sadamoto, Y., Osawa, T., Yamamoto, K., Kondoh, M., Ohmura, H., Shinohara, N., Nonomura, K., Shindoh, M. and Hida, K. (2012) 'Heterogeneity of tumor endothelial cells: Comparison between tumor endothelial cells isolated from high- and low-metastatic tumors', *American Journal of Pathology* [Preprint]. doi:10.1016/j.ajpath.2011.11.035.

Oksanen, M., Lehtonen, S., Jaronen, M., Goldsteins, G., Hämäläinen, R.H. and Koistinaho, J. (2019) 'Astrocyte alterations in neurodegenerative pathologies and their modeling in human induced pluripotent stem cell platforms', *Cellular and Molecular Life Sciences*, 76(14), pp. 2739–2760. doi:10.1007/s00018-019-03111-7.

Oronsky, B., Oronsky, N., Fanger, G., Parker, C., Caroen, S., Lybeck, M. and Scicinski, J. (2014) 'Follow the ATP: Tumor Energy Production: A Perspective', *Anti-Cancer Agents in Medicinal Chemistry* [Preprint]. doi:10.2174/1871520614666140804224637.

Osada, T., Gu, Y.H., Kanazawa, M., Tsubota, Y., Hawkins, B.T., Spatz, M., Milner, R. and Del Zoppo, G.J. (2011) 'Interendothelial claudin-5 expression depends on cerebral endothelial cell-matrix adhesion by B 1-integrins', *Journal of Cerebral Blood Flow and Metabolism*, 31(10), pp. 1972–1985. doi:10.1038/jcbfm.2011.99.

Ozawa, T., Brennan, C.W., Wang, L., Squatrito, M., Sasayama, T., Nakada, M., Huse, J.T., Pedraza, A., Utsuki, S., Yasui, Y., Tandon, A., Fomchenko, E.I., Oka, H., Levine, R.L., Fujii, K., Ladanyi, M. and Holland, E.C. (2010) 'PDGFRA gene rearrangements are frequent genetic events in PDGFRA-amplified glioblastomas', *Genes and Development*, 24(19), pp. 2205–2218. doi:10.1101/gad.1972310.

Padera, T.P., Stoll, B.R., Tooredman, J.B., Capen, D., Di Tomaso, E. and Jain, R.K. (2004) 'Cancer cells compress intratumour vessels', *Nature*, 427(6976), p. 695. doi:10.1038/427695a.

Pan, W., Stone, K.P., Hsuehou, H., Manda, V.K., Zhang, Y. and Kastin, A.J. (2014) 'Cytokine Signaling Modulates BBB Function', 17(33), pp. 3729–3740.

Papadopoulos, M.C., Saadoun, S., Binder, D.K., Manley, G.T., Krishna, S. and Verkman, A.S. (2004) 'Molecular mechanisms of brain tumor edema', *Neuroscience*, 129(4), pp. 1011–1020. doi:10.1016/j.neuroscience.2004.05.044.

Park, J.H., Jung, N., Kang, S.J., Kim, H.S., Kim, E., Lee, H.J., Jung, H.R., Choe, M. and Shim, Y.J.

- (2019) 'Survival and Prognosis of Patients with Pilocytic Astrocytoma: A Single-Center Study', *Brain Tumor Research and Treatment*, 7(2), p. 92. doi:10.14791/btrt.2019.7.e36.
- Pavlova, N.N. and Thompson, C.B. (2016) 'THE EMERGING HALLMARKS OF CANCER METABOLISM', *Cell Metab*, 176(1), pp. 139–148. doi:10.1016/j.cmet.2015.12.006.
- Perea Paizal, J., Au, S.H. and Bakal, C. (2021) 'Squeezing through the microcirculation: survival adaptations of circulating tumour cells to seed metastasis', *British Journal of Cancer*, 124(1), pp. 58–65. doi:10.1038/s41416-020-01176-x.
- Persidsky, Y., Ramirez, S.H., Haorah, J. and Kanmogne, G.D. (2006) 'Blood-brain barrier: Structural components and function under physiologic and pathologic conditions', *Journal of Neuroimmune Pharmacology*, 1(3), pp. 223–236. doi:10.1007/s11481-006-9025-3.
- Petrova, V., Annicchiarico-Petruzzelli, M., Melino, G. and Amelio, I. (2018) 'The hypoxic tumour microenvironment', *Oncogenesis*, 7(1). doi:10.1038/s41389-017-0011-9.
- Petty, M.A. and Lo, E.H. (2002) 'Junctional complexes of the blood-brain barrier: Permeability changes in neuroinflammation', *Progress in Neurobiology*, pp. 311–323. doi:10.1016/S0301-0082(02)00128-4.
- Pezzella, F., Harris, A.L., Tavassoli, M. and Gatter, K.C. (2015) 'Blood vessels and cancer much more than just angiogenesis', *Cell Death Discovery*, 1(1), pp. 1–2. doi:10.1038/cddiscovery.2015.64.
- Picca, A., Berzero, G. and Sanson, M. (2018) 'Current therapeutic approaches to diffuse grade II and III gliomas', *Therapeutic Advances in Neurological Disorders*, 11(6), pp. 1–13. doi:https://doi.org/10.1177/1756285617752039.
- Pietras, K. and Östman, A. (2010) 'Hallmarks of cancer: Interactions with the tumor stroma', *Experimental Cell Research*, 316(8), pp. 1324–1331. doi:10.1016/j.yexcr.2010.02.045.
- Polet, F. and Feron, O. (2013) 'Endothelial cell metabolism and tumour angiogenesis: Glucose and glutamine as essential fuels and lactate as the driving force', *Journal of Internal Medicine*, 273(2), pp. 156–165. doi:10.1111/joim.12016.
- Pollmann-mudryj, M.A., Pollmann, M., Shao, Q., Laird, D.W. and Sandig, M. (2005) 'Connexin 43 mediated gap junctional communication enhances breast tumor cell diapedesis in culture Research article Connexin 43 mediated gap junctional communication enhances breast tumor cell diapedesis in culture', (June 2014). doi:10.1186/bcr1042.
- Polyak, K. (2007) 'Science in medicine Breast cancer : origins and evolution', *The journal of clinical investigation*, 117(11), pp. 3155–3163. doi:10.1172/JCI33295.group.
- Polyak, K. (2011) 'Heterogeneity in breast cancer Review series introduction Heterogeneity in breast cancer', *The Journal of Clinical Investigation*, 121(10), p. 3786. doi:10.1172/JCI60534.
- Potter, M., Newport, E. and Morten, K.J. (2016) 'The Warburg effect: 80 years on', *Biochemical Society Transactions*, 44(5), pp. 1499–1505. doi:10.1042/BST20160094.

- Prat, A. and Perou, C.M. (2011) 'Deconstructing the molecular portraits of breast cancer', *Molecular Oncology*, 5(1), pp. 5–23. doi:10.1016/j.molonc.2010.11.003.
- Preston, J.E., Abbott, N.J. and Begley, D.J. (2014) 'Transcytosis of macromolecules at the blood-brain barrier', *Advances in Pharmacology*, 71, pp. 147–163. doi:10.1016/bs.apha.2014.06.001.
- Profaci, C.P., Munji, R.N., Pulido, R.S. and Daneman, R. (2020) 'The blood–brain barrier in health and disease: Important unanswered questions', *Journal of Experimental Medicine*, 217(4), pp. 1–16. doi:10.1084/jem.20190062.
- Pulgar, V.M. (2019) 'Transcytosis to cross the blood brain barrier, new advancements and challenges', *Frontiers in Neuroscience*, 13(JAN), pp. 1–9. doi:10.3389/fnins.2018.01019.
- Pustchi, S.E., Avci, N.G., Akay, Y.M. and Akay, M. (2020) 'Astrocytes decreased the sensitivity of glioblastoma cells to temozolomide and bay 11-7082', *International Journal of Molecular Sciences*, 21(19), pp. 1–18. doi:10.3390/ijms21197154.
- Rakkar, K. and Bayraktutan, U. (2016) 'Increases in intracellular calcium perturb blood-brain barrier via protein kinase C-alpha and apoptosis', *Biochimica et Biophysica Acta - Molecular Basis of Disease*, 1862(1), pp. 56–71. doi:10.1016/j.bbadis.2015.10.016.
- Ramachandran, S., Ient, J., Göttgen, E.L., Krieg, A.J. and Hammond, E.M. (2015) 'Epigenetic therapy for solid tumors: Highlighting the impact of tumor hypoxia', *Genes*, 6(4), pp. 935–956. doi:10.3390/genes6040935.
- Ramos, A.D., Magge, R.S. and Ramakrishna, R. (2018) 'Molecular Pathogenesis and Emerging Treatment for Glioblastoma', *World Neurosurgery*, 116, pp. 495–504. doi:10.1016/j.wneu.2018.04.021.
- Ranjit, M., Motomura, K., Ohka, F., Wakabayashi, T. and Natsume, A. (2015) 'Applicable advances in the molecular pathology of glioblastoma', *Brain Tumor Pathology*, 32(3), pp. 153–162. doi:10.1007/s10014-015-0224-6.
- Review, S. and Design, S. (2010) 'Article in Press Article in Press', *GEF Bulletin of Biosciences*, 1(1), pp. 1–6.
- Reymond, N., D'Água, B.B. and Ridley, A.J. (2013) 'Crossing the endothelial barrier during metastasis', *Nature Reviews Cancer*, 13(12), pp. 858–870. doi:10.1038/nrc3628.
- Riggio, A.I., Varley, K.E. and Welm, A.L. (2021) 'The lingering mysteries of metastatic recurrence in breast cancer', *British Journal of Cancer*, 124(1), pp. 13–26. doi:10.1038/s41416-020-01161-4.
- Rocha, S. (2013) 'Targeted Drug Delivery Across the Blood Brain Barrier in Alzheimer's Disease', *Current Pharmaceutical Design*, 19(37), pp. 6635–6646. doi:10.2174/13816128113199990613.
- Rochfort, K.D., Collins, L.E., Murphy, R.P. and Cummins, P.M. (2014) 'Downregulation of blood-brain barrier phenotype by proinflammatory cytokines involves NADPH oxidase-dependent ROS generation: Consequences for interendothelial adherens and tight junctions', *PLoS ONE*,



9(7). doi:10.1371/journal.pone.0101815.

Rochfort, K.D. and Cummins, P.M. (2015) 'Cytokine-mediated dysregulation of zonula occludens-1 properties in human brain microvascular endothelium', *Microvascular Research* [Preprint]. doi:10.1016/j.mvr.2015.04.010.

Rohlenova, K., Veys, K., Miranda-Santos, I., De Bock, K. and Carmeliet, P. (2018) 'Endothelial Cell Metabolism in Health and Disease', *Trends in Cell Biology*, 28(3), pp. 224–236. doi:10.1016/j.tcb.2017.10.010.

Rong, Y., Durden, D.L., Van Meir, E.G. and Brat, D.J. (2006) "'Pseudopalisading" necrosis in glioblastoma: A familiar morphologic feature that links vascular pathology, hypoxia, and angiogenesis', *Journal of Neuropathology and Experimental Neurology*, 65(6), pp. 529–539. doi:10.1097/00005072-200606000-00001.

Salvador, E., Burek, M. and Förster, C.Y. (2016) 'Tight Junctions and the Tumor Microenvironment', *Current Pathobiology Reports*, 4(3), pp. 135–145. doi:10.1007/s40139-016-0106-6.

Sarica, F., Cekinmez, M., Sen, O., Onal, H., Mertsoylu, H., Pehlivan, B., Erdogan, B., Altinors, M., Tufan, K. and Topkan, E. (2012) 'Five-year follow-up results for patients diagnosed with anaplastic astrocytoma and effectiveness of concomitant therapy with temozolomide for recurrent anaplastic astrocytoma', *Asian Journal of Neurosurgery*, 7(4), p. 181. doi:10.4103/1793-5482.106650.

Sathornsumetee, S. and Rich, J.N. (2008) 'Designer therapies for glioblastoma multiforme', *Annals of the New York Academy of Sciences*, 1142, pp. 108–132. doi:10.1196/annals.1444.009.

Schneider, S.W., Ludwig, T., Tatenhorst, L., Braune, S., Oberleithner, H., Senner, V. and Paulus, W. (2004) 'Glioblastoma cells release factors that disrupt blood-brain barrier features', *Acta Neuropathologica*, 107(3), pp. 272–276. doi:10.1007/s00401-003-0810-2.

Schossleitner, K., Rauscher, S., Gröger, M., Friedl, H.P., Finsterwalder, R., Habermeyer, A., Sibilia, M., Brostjan, C., Födinger, D., Citi, S. and Petzelbauer, P. (2016) 'Evidence That Cingulin Regulates Endothelial Barrier Function in Vitro and in Vivo', *Arteriosclerosis, Thrombosis, and Vascular Biology*, 36(4), pp. 647–654. doi:10.1161/ATVBAHA.115.307032.

Serlin, Y., Shelef, I., Knyazer, B. and Friedman, A. (2015) 'Anatomy and Physiology of the Blood-Brain Barrier', *Seminars in cell & developmental biology*, 38, pp. 2–6. doi:10.1016/j.semcdb.2015.01.002.

Sharma, V.R., Sharma, A.K., Punj, V. and Priya, P. (2019) 'Recent nanotechnological interventions targeting PI3K/Akt/mTOR pathway: A focus on breast cancer', *Seminars in Cancer Biology* [Preprint], (September). doi:10.1016/j.semcancer.2019.08.005.

Shumakovich, M.A., Mencia, C.P., Siglin, J.S., Moriarty, R.A., Geller, H.M. and Stroka, K.M. (2017) 'Astrocytes from the brain microenvironment alter migration and morphology of metastatic

breast cancer cells', *FASEB Journal*, 31(11), pp. 5049–5067. doi:10.1096/fj.201700254R.

Siegenthaler, J.A., Sohet, F. and Daneman, R. (2013) "'Sealing off the CNS": Cellular and molecular regulation of blood-brain barrierogenesis', *Current Opinion in Neurobiology* [Preprint]. doi:10.1016/j.conb.2013.06.006.

Siemann, D. and Horsman, M. (2015) 'Modulation of the Tumor Vasculature and Oxygenation to Improve Therapy', *Pharmacol Ther*, 153(12), pp. 107–124. doi:10.1016/j.pharmthera.2015.06.006.

Sofroniew, M. V and Vinters, H. V (2010) 'Astrocytes: Biology and pathology', *Acta Neuropathologica*, 119(1), pp. 7–35. doi:10.1007/s00401-009-0619-8.

Sreekanthreddy, P., Srinivasan, H., Kumar, D.M., Nijaguna, M.B., Sridevi, S., Vrinda, M., Arivazhagan, A., Balasubramaniam, A., Hegde, A.S., Chandramouli, B.A., Santosh, V., Rao, M.R.S., Kondaiah, P. and Somasundaram, K. (2010) 'Identification of potential serum biomarkers of glioblastoma: Serum osteopontin levels correlate with poor prognosis', *Cancer Epidemiology Biomarkers and Prevention*, 19(6), pp. 1409–1422. doi:10.1158/1055-9965.EPI-09-1077.

Stamatovic, S., Keep, R. and Andjelkovic, A. (2008) 'Brain Endothelial Cell-Cell Junctions: How to "Open" the Blood Brain Barrier', *Current Neuropharmacology*, 6(3), pp. 179–192. doi:10.2174/157015908785777210.

Stamatovic, S.M., Johnson, A.M., Keep, R.F. and Andjelkovic, A. V. (2016) 'Junctional proteins of the blood-brain barrier: New insights into function and dysfunction', *Tissue Barriers*, 4(1). doi:10.1080/21688370.2016.1154641.

Stamatovic, S.M., Keep, R.F. and Andjelkovic, A. V (2008) 'Brain endothelial cell-cell junctions: how to "open" the blood brain barrier.', *Current neuropharmacology*, 6(3), pp. 179–92. doi:10.2174/157015908785777210.

Steeg, P.S. (2021) 'The blood–tumour barrier in cancer biology and therapy', *Nature Reviews Clinical Oncology*, 18(11), pp. 696–714. doi:10.1038/s41571-021-00529-6.

Stock, A.D., Gelb, S., Pasternak, O., Ben-Zvi, A. and Putterman, C. (2017) 'The blood brain barrier and neuropsychiatric lupus: new perspectives in light of advances in understanding the neuroimmune interface', *Autoimmunity Reviews*, 16(6), pp. 612–619. doi:10.1016/j.autrev.2017.04.008.

Stokum, J.A., Gerzanich, V. and Simard, J.M. (2016) 'Molecular pathophysiology of cerebral edema', *Journal of Cerebral Blood Flow and Metabolism* [Preprint]. doi:10.1177/0271678X15617172.

Stolp, H.B. and Dziegielewska, K.M. (2009) 'Review: Role of developmental inflammation and blood-brain barrier dysfunction in neurodevelopmental and neurodegenerative diseases', *Neuropathology and Applied Neurobiology*, 35(2), pp. 132–146. doi:10.1111/j.1365-2990.2008.01005.x.

Strazielle, N. and Gherzi-Egea, J.F. (2013) 'Physiology of blood-brain interfaces in relation to brain disposition of small compounds and macromolecules', *Molecular Pharmaceutics*, 10(5), pp. 1473–

1491. doi:10.1021/mp300518e.

Strilic, B. and Offermanns, S. (2017) 'Intravascular Survival and Extravasation of Tumor Cells', *Cancer Cell*, 32(3), pp. 282–293. doi:10.1016/j.ccell.2017.07.001.

Stummer, W. (2007) 'Mechanisms of tumor-related brain edema.', *Neurosurgical focus*, 22(5), p. E8. doi:10.3171/foc.2007.22.5.9.

Stummer, W. (2016) 'Mechanisms of Tumor - related Brain Edema', 22(5), pp. 1–11.

Sweeney, M.D., Ayyadurai, S. and Zlokovic, B. V. (2016) 'Pericytes of the neurovascular unit: Key functions and signaling pathways', *Nature Neuroscience*, 19(6), pp. 771–783. doi:10.1038/nn.4288.

Switzer, N., Lim, A., Du, L., Al-Sairafi, R., Tonkin, K. and Schiller, D. (2015) 'Case series of 21 patients with extrahepatic metastatic lobular breast carcinoma to the gastrointestinal tract', *Cancer Treatment Communications*, 3, pp. 37–43. doi:10.1016/j.ctrc.2014.11.006.

Tajes, M., Ramos-Fernández, E., Weng-Jiang, X., Bosch-Morató, M., Guivernau, B., Eraso-Pichot, A., Salvador, B., Fernández-Busquets, X., Roquer, J. and Muñoz, F.J. (2014) 'The blood-brain barrier: Structure, function and therapeutic approaches to cross it', *Molecular Membrane Biology*, 31(5), pp. 152–167. doi:10.3109/09687688.2014.937468.

Takenaga, Y., Takagi, N., Murotomi, K., Tanonaka, K. and Takeo, S. (2009) 'Inhibition of Src activity decreases tyrosine phosphorylation of occludin in brain capillaries and attenuates increase in permeability of the blood-brain barrier after transient focal cerebral ischemia', *Journal of Cerebral Blood Flow and Metabolism* [Preprint]. doi:10.1038/jcbfm.2009.30.

Al Tameemi, W., Dale, T.P., Al-Jumaily, R.M.K. and Forsyth, N.R. (2019) 'Hypoxia-Modified Cancer Cell Metabolism', *Frontiers in Cell and Developmental Biology*, 7(January), pp. 1–15. doi:10.3389/fcell.2019.00004.

Tang, X., Luo, Y.X., Chen, H.Z. and Liu, D.P. (2014) 'Mitochondria, endothelial cell function, and vascular diseases', *Frontiers in Physiology*, 5 MAY(May), pp. 1–17. doi:10.3389/fphys.2014.00175.

Tannock, I.F. (2001) 'Tumor physiology and drug resistance', *Cancer and Metastasis Reviews*, 20(1–2), pp. 123–132. doi:10.1023/A:1013125027697.

Tao, L., Huang, G., Song, H., Chen, Y. and Chen, L. (2017) 'Cancer associated fibroblasts: An essential role in the tumor microenvironment (review)', *Oncology Letters*, 14(3), pp. 2611–2620. doi:10.3892/ol.2017.6497.

Tayyeb, B. and Parvin, M. (2016) 'Pathogenesis of Breast Cancer Metastasis to Brain: a Comprehensive Approach to the Signaling Network', *Molecular Neurobiology*, 53(1), pp. 446–454. doi:10.1007/s12035-014-9023-z.

Thomas N. Seyfried<sup>1</sup>, and L.C.H. (2013) 'On the Origin of Cancer Metastasis Thomas', *Medical Hypotheses*, 46(6), pp. 581–583. doi:10.1016/S0306-9877(96)90136-X.

Thomsen, M.S., Routhe, L.J. and Moos, T. (2017) 'The vascular basement membrane in the healthy



and pathological brain', *Journal of Cerebral Blood Flow and Metabolism*, 37(10), pp. 3300–3317. doi:10.1177/0271678X17722436.

Thuringer, D., Solary, E. and Garrido, C. (2017) 'The microvascular gap junction channel: A route to deliver microRNAs for neurological disease treatment', *Frontiers in Molecular Neuroscience*, 10(August), pp. 1–8. doi:10.3389/fnmol.2017.00246.

Timmons, J. (2012) 'Primary Brain Tumours – Everything a Medical Student Needs to Know', *Medical Journal*, 1(1), pp. 31–37.

Totland, M.Z., Rasmussen, N.L., Knudsen, L.M. and Leithe, E. (2020) 'Regulation of gap junction intercellular communication by connexin ubiquitination: physiological and pathophysiological implications', *Cellular and Molecular Life Sciences* [Preprint]. doi:10.1007/s00018-019-03285-0.

Tsang, J.Y.S. and Tse, G.M. (2019) 'Molecular Classification of Breast Cancer', *Advances in Anatomic Pathology*, 27(1). doi:10.1097/PAP.0000000000000232.

Urbanska, K., Sokolowska, J., Szmidi, M. and Sysa, P. (2014) 'Glioblastoma multiforme - An overview', *Wspolczesna Onkologia*, 18(5), pp. 307–312. doi:10.5114/wo.2014.40559.

Urooj, T., Wasim, B., Mushtaq, S., Shah, S.N.N. and Shah, M. (2019) 'Cancer Cell-derived Secretory Factors in Breast Cancer-associated Lung Metastasis: Their Mechanism and Future Prospects', *Current Cancer Drug Targets*, 20(3), pp. 168–186. doi:10.2174/1568009620666191220151856.

Varatharaj, A. and Galea, I. (2017) 'The blood-brain barrier in systemic inflammation', *Brain, Behavior, and Immunity*, 60, pp. 1–12. doi:10.1016/j.bbi.2016.03.010.

Verhaak, R.G.W., Hoadley, K.A., Purdom, E., Wang, V., Qi, Y., Wilkerson, M.D., Miller, C.R., Ding, L., Golub, T., Mesirov, J.P., Alexe, G., Lawrence, M., O'Kelly, M., Tamayo, P., Weir, B.A., Gabriel, S., Winckler, W., Gupta, S., Jakkula, L., Feiler, H.S., Hodgson, J.G., James, C.D., Sarkaria, J.N., Brennan, C., Kahn, A., Spellman, P.T., Wilson, R.K., Speed, T.P., Gray, J.W., Meyerson, M., Getz, G., Perou, C.M. and Hayes, D.N. (2010) 'Integrated Genomic Analysis Identifies Clinically Relevant Subtypes of Glioblastoma Characterized by Abnormalities in PDGFRA, IDH1, EGFR, and NF1', *Cancer Cell* [Preprint]. doi:10.1016/j.ccr.2009.12.020.

Viale, G. (2012) 'The current state of breast cancer classification', *Annals of Oncology*, 23(SUPPL. 10). doi:10.1093/annonc/mds326.

Villaseñor, R., Lampe, J., Schwaninger, M. and Collin, L. (2019) 'Intracellular transport and regulation of transcytosis across the blood–brain barrier', *Cellular and Molecular Life Sciences* [Preprint]. doi:10.1007/s00018-018-2982-x.

Wahner, H.C.W., Träger, M., Bender, K., Schweizer, L., Onken, J., Senger, C., Ehret, F., Budach, V. and Kaul, D. (2020) 'Predicting survival in anaplastic astrocytoma patients in a single-center cohort of 108 patients', *Radiation Oncology*, 15(1), pp. 1–9. doi:10.1186/s13014-020-01728-8.

Walsh, J.C., Lebedev, A., Aten, E., Madsen, K., Marciano, L. and Kolb, H.C. (2014) 'The clinical

- importance of assessing tumor hypoxia: Relationship of tumor hypoxia to prognosis and therapeutic opportunities', *Antioxidants and Redox Signaling* [Preprint]. doi:10.1089/ars.2013.5378.
- Wang, F., Cao, Y., Ma, L., Pei, H., Rausch, W.D. and Li, H. (2018) 'Dysfunction of Cerebrovascular Endothelial Cells: Prelude to Vascular Dementia', *Frontiers in Aging Neuroscience*, 10(November), pp. 1–23. doi:10.3389/fnagi.2018.00376.
- Wang, X., Huang, H. and Young, K.H. (2015) 'The PTEN tumor suppressor gene and its role in lymphoma pathogenesis', *Aging*, 7(12), pp. 1032–1049. doi:10.18632/aging.100855.
- Wang, Y.H., Dong, Y.Y., Wang, W.M., Xie, X.Y., Wang, Z.M., Chen, R.X., Chen, J., Gao, D.M., Cui, J.F. and Ren, Z.G. (2013) 'Vascular endothelial cells facilitated HCC invasion and metastasis through the Akt and NF- $\kappa$ B pathways induced by paracrine cytokines', *Journal of Experimental and Clinical Cancer Research*, 32(1), p. 1. doi:10.1186/1756-9966-32-51.
- Wardill, H.R., Mander, K.A., Van Seville, Y.Z.A., Gibson, R.J., Logan, R.M., Bowen, J.M. and Sonis, S.T. (2016) 'Cytokine-mediated blood brain barrier disruption as a conduit for cancer/chemotherapy-associated neurotoxicity and cognitive dysfunction', *International Journal of Cancer*, 139(12), pp. 2635–2645. doi:10.1002/ijc.30252.
- Watkins, E.J. (2019) 'Overview of breast cancer', *Journal of the American Academy of Physician Assistants*, 32(10), pp. 13–17. doi:10.1097/01.JAA.0000580524.95733.3d.
- Weidenfeller, C. and Shusta, E. V. (2007) 'Blood–brain barrier', *Endothelial Biomedicine*, pp. 1124–1139. doi:10.1017/CBO9780511546198.124.
- Weiss, N., Miller, F., Cazaubon, S. and Couraud, P.O. (2009) 'The blood-brain barrier in brain homeostasis and neurological diseases', *Biochimica et Biophysica Acta - Biomembranes*, 1788(4), pp. 842–857. doi:10.1016/j.bbamem.2008.10.022.
- Wevers, N.R. and de Vries, H.E. (2016) 'Morphogens and blood-brain barrier function in health and disease', *Tissue Barriers* [Preprint]. doi:10.1080/21688370.2015.1090524.
- Wilhelm, I. and Krizbai, I.A. (2014) 'In vitro models of the blood-brain barrier for the study of drug delivery to the brain', *Molecular Pharmaceutics*, 11(7), pp. 1949–1963. doi:10.1021/mp500046f.
- Winger, R.C., Kobinski, J.E., Kanda, T., Ransohoff, R.M. and Muller, W.A. (2014) 'Rapid Remodeling of Tight Junctions during Paracellular Diapedesis in a Human Model of the Blood–Brain Barrier', *The Journal of Immunology* [Preprint]. doi:10.4049/jimmunol.1400700.
- Witzel, I., Oliveira-Ferrer, L., Pantel, K., Müller, V. and Wikman, H. (2016) 'Breast cancer brain metastases: Biology and new clinical perspectives', *Breast Cancer Research*, 18(1), pp. 1–9. doi:10.1186/s13058-015-0665-1.
- Wolburg, H., Noell, S., Mack, A., Wolburg-Buchholz, K. and Fallier-Becker, P. (2008) 'Brain endothelial cells and the glio-vascular complex', *Cell and Tissue Research*, 335(1), pp. 75–96. doi:10.1007/s00441-008-0658-9.

Wolburg, H., Noell, S., Wolburg-Buchholz, K., MacK, A. and Fallier-Becker, P. (2009) 'Agrin, aquaporin-4, and astrocyte polarity as an important feature of the blood-brain barrier', *Neuroscientist* [Preprint]. doi:10.1177/1073858408329509.

Wolff, A., Antfolk, M., Brodin, B. and Tenje, M. (2015) 'In Vitro Blood-Brain Barrier Models - An Overview of Established Models and New Microfluidic Approaches', *Journal of Pharmaceutical Sciences*, 104(9), pp. 2727–2746. doi:10.1002/jps.24329.

Wong, A.D., Ye, M., Levy, A.F., Rothstein, J.D., Bergles, D.E. and Searson, P.C. (2013) 'The blood-brain barrier: an engineering perspective', *Frontiers in Neuroengineering*, 6(August), p. 7. doi:10.3389/fneng.2013.00007.

World Health Organisation (2018) 'Latest global cancer data', *International Agency for Research on cancer*, (September), pp. 13–15. Available at: <http://gco.iarc.fr/>.

Wu, C., Ivars, F., Anderson, P., Hallmann, R., Vestweber, D., Nilsson, P., Robenek, H., Tryggvason, K., Song, J., Korpos, E., Loser, K., Beissert, S., Georges-Labouesse, E. and Sorokin, L.M. (2009) 'Endothelial basement membrane laminin  $\alpha 5$  selectively inhibits T lymphocyte extravasation into the brain', *Nature Medicine* [Preprint]. doi:10.1038/nm.1957.

Wu, F., Liu, L. and Zhou, H. (2017) 'Endothelial cell activation in central nervous system inflammation', *Journal of Leukocyte Biology*, pp. 1119–1132. doi:10.1189/jlb.3ru0816-352rr.

Xiao, M., Xiao, Z.J., Yang, B., Lan, Z. and Fang, F. (2020) 'Blood-Brain Barrier: More Contributor to Disruption of Central Nervous System Homeostasis Than Victim in Neurological Disorders', *Frontiers in Neuroscience*, 14(August), pp. 1–17. doi:10.3389/fnins.2020.00764.

Xie, H. and Simon, M.C. (2017) 'Oxygen availability and metabolic reprogramming in cancer', *Journal of Biological Chemistry*, 292(41), pp. 16825–16832. doi:10.1074/jbc.R117.799973.

Xing, F., Kobayashi, A., Okuda, H., Watabe, M., Pai, S.K., Pandey, P.R., Hirota, S., Wilber, A., Mo, Y.Y., Moore, B.E., Liu, W., Fukuda, K., Iizumi, M., Sharma, S., Liu, Y., Wu, K., Peralta, E. and Watabe, K. (2013) 'Reactive astrocytes promote the metastatic growth of breast cancer stem-like cells by activating Notch signalling in brain', *EMBO Molecular Medicine*, 5(3), pp. 384–396. doi:10.1002/emmm.201201623.

Xing, G., Zhao, T., Zhang, X., Li, H., Li, X., Cui, P., Li, M., Li, D., Zhang, N. and Jiang, W. (2020) 'Astrocytic Sonic Hedgehog Alleviates Intracerebral Hemorrhagic Brain Injury via Modulation of Blood-Brain Barrier Integrity', *Frontiers in Cellular Neuroscience*, 14(December), pp. 1–15. doi:10.3389/fncel.2020.575690.

Xu, L., Nirwane, A. and Yao, Y. (2019) 'Basement membrane and blood-brain barrier', *Stroke and Vascular Neurology*, 4(2), pp. 78–82. doi:10.1136/svn-2018-000198.

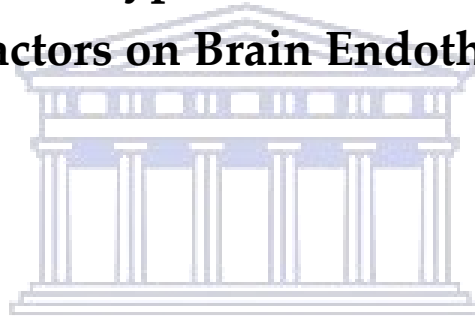
Xue, H., Lu, B. and Lai, M. (2008) 'The cancer secretome: A reservoir of biomarkers', *Journal of Translational Medicine* [Preprint]. doi:10.1186/1479-5876-6-52.

Yamamoto, M., Ramirez, S.H., Sato, S., Kiyota, T., Cerny, R.L., Kaibuchi, K., Persidsky, Y. and

- Ikezu, T. (2008) 'Phosphorylation of claudin-5 and occludin by Rho kinase in brain endothelial cells', *American Journal of Pathology* [Preprint]. doi:10.2353/ajpath.2008.070076.
- Yang, S., Jin, H., Zhu, Y., Wan, Y., Opoku, E.N., Zhu, L. and Hu, B. (2017) 'Diverse Functions and Mechanisms of Pericytes in Ischemic Stroke', *Current Neuropharmacology*, 15(6), pp. 892–905. doi:10.2174/1570159x15666170112170226.
- Yoon, J.H., Kim, J., Kim, K.L., Kim, D.H., Jung, S.J., Lee, H., Ghim, J., Kim, D., Park, J.B., Ryu, S.H. and Lee, T.G. (2014) 'Proteomic analysis of hypoxia-induced U373MG glioma secretome reveals novel hypoxia-dependent migration factors', *Proteomics*, 14(12), pp. 1494–1502. doi:10.1002/pmic.201300554.
- Zaravinos, A. and Deltas, C. (2014) 'ccRCC is fundamentally a metabolic disorder', *Cell Cycle*, 13(16), pp. 2481–2482. doi:10.4161/15384101.2014.947225.
- Zecchin, A., Kalucka, J., Dubois, C. and Carmeliet, P. (2017) 'How endothelial cells adapt their metabolism to form vessels in tumors', *Frontiers in Immunology*, 8(DEC). doi:10.3389/fimmu.2017.01750.
- de Zeeuw, P., Wong, B.W. and Carmeliet, P. (2015) 'Metabolic adaptations in diabetic endothelial cells', *Circulation Journal*, 79(5), pp. 934–941. doi:10.1253/circj.CJ-15-0230.
- Zhang, S., Wu, M., Peng, C., Zhao, G. and Gu, R. (2017) 'GFAP expression in injured astrocytes in rats', *Experimental and Therapeutic Medicine* [Preprint]. doi:10.3892/etm.2017.4760.
- Zhang, X., Zhang, W., Cao, W.-D., Cheng, G. and Zhang, Y.-Q. (2012) 'Glioblastoma multiforme: Molecular characterization and current treatment strategy (Review)', *Experimental and Therapeutic Medicine*, 3(1), pp. 9–14. doi:10.3892/etm.2011.367.
- Zhang, Y., Xia, M., Jin, K., Wang, S., Wei, H., Fan, C., Wu, Y., Li, Xiaoling, Li, Xiayu, Li, G., Zeng, Z. and Xiong, W. (2018) 'Function of the c-Met receptor tyrosine kinase in carcinogenesis and associated therapeutic opportunities', *Molecular Cancer*, 17(1), pp. 1–14. doi:10.1186/s12943-018-0796-y.
- Zhao, Z., Nelson, A.R., Betsholtz, C. and Zlokovic, B. V. (2015) 'Establishment and Dysfunction of the Blood-Brain Barrier', *Cell*, 163(5), pp. 1064–1078. doi:10.1016/j.cell.2015.10.067.

## CHAPTER 3

### **PUBLISHED MANUSCRIPT “Differential Effects of Normoxic versus Hypoxic Derived Breast Cancer Paracrine Factors on Brain Endothelial Cells”**



UNIVERSITY *of the*  
WESTERN CAPE

Article

# Differential Effects of Normoxic versus Hypoxic Derived Breast Cancer Paracrine Factors on Brain Endothelial Cells

Mariam Rado <sup>1</sup>, Brian Flepisi <sup>2</sup> and David Fisher <sup>1,\*</sup>

<sup>1</sup> Medical Bioscience Department, Faculty of Natural Sciences, University of the Western Cape, Robert Sobukwe Road, Bellville 7535, South Africa; 3580480@myuwc.ac.za

<sup>2</sup> Department of Pharmacology, Faculty of Health Sciences, University of Pretoria, 9 Bophelo Road, Pretoria 0002, South Africa; brian.flepisi@up.ac.za

\* Correspondence: dfisher@uwc.ac.za; Tel.: +27-21-959-2185

**Simple Summary:** The potential of breast cancer to spread to the brain increases the clinical complications of the disease; breast cancer is considered to have the second-highest capacity to spread to the brain after lung cancer. The brain is protected by highly specialized endothelial cells, forming a barrier against the entry of circulating molecules and cells. The ability of breast cancer cells to penetrate the protective endothelial barrier is still not completely understood. Here, we aimed to investigate the effect of breast cancer cells on the brain's endothelial cells. We showed that breast cancer cells induce changes in endothelial cells by releasing factors that target the mitochondria, affecting the endothelial cells and their attachment to each other and, therefore, their function as a protective barrier of the brain. Understanding the mechanism that breast cancer cells utilize to affect endothelial cells under normoxic and hypoxic conditions contributes to the development of treatments to prevent the metastasis of cancer cells to the brain.



**Citation:** Rado, M.; Flepisi, B.; Fisher, D. Differential Effects of Normoxic versus Hypoxic Derived Breast Cancer Paracrine Factors on Brain Endothelial Cells. *Biology* **2021**, *10*, 1238. <https://doi.org/10.3390/biology10121238>

Received: 28 September 2021

Accepted: 18 October 2021

Published: 27 November 2021

**Publisher's Note:** MDPI stays neutral with regard to jurisdictional claims in published maps and institutional affiliations.



**Copyright:** © 2021 by the authors. Licensee MDPI, Basel, Switzerland. This article is an open access article distributed under the terms and conditions of the Creative Commons Attribution (CC BY) license (<https://creativecommons.org/licenses/by/4.0/>).

**Abstract: Background:** The blood-brain barrier (BBB) is a central nervous system protective barrier formed primarily of endothelial cells that regulate the entry of substances and cells from entering the brain. However, the BBB integrity is disrupted in disease, including cancer, allowing toxic substances, molecules, and circulating cells to enter the brain. This study aimed to determine the mitochondrial changes in brain endothelial cells co-cultured with cancer cells. **Method:** Brain endothelial cells (bEnd.3) were co-cultivated with various concentrations of breast cancer (MCF7) conditioned media (CM) generated under normoxic (21% O<sub>2</sub>) and hypoxic conditions (5% O<sub>2</sub>). The mitochondrial activities (including; dehydrogenases activity, mitochondrial membrane potential ( $\Delta\Psi_m$ ), and ATP generation) were measured using Polarstar Omega B.M.G-Plate reader. Trans-endothelial electrical resistance (TEER) was evaluated using the EVOM system, followed by quantifying gene expression of the endothelial tight junction (ETJs) using qPCR. **Results:** bEnd.3 cells had reduced cell viability after 72 h and 96 h exposure to MCF7CM under hypoxic and normoxic conditions. The  $\Delta\Psi_m$  in bEnd.3 cells were hyperpolarized after exposure to the hypoxic MCF7CM ( $p < 0.0001$ ). However, the normoxic MCF7CM did not significantly affect the state of  $\Delta\Psi_m$  in bEnd.3 cells. ATP levels in bEnd.3 co-cultured with hypoxic and normoxic MCF7CM was significantly reduced ( $p < 0.05$ ). The changes in brain endothelial mitochondrial activity were associated with a decrease in TEER of bEnd.3 monolayer co-cultured with MCF7CM under hypoxia ( $p = 0.001$ ) and normoxia ( $p < 0.05$ ). The bEnd.3 cells exposed to MCF7CM significantly increased the gene expression level of ETJs ( $p < 0.05$ ). **Conclusions:** MCF7CM modulate mitochondrial activity in brain endothelial cells, affecting the brain endothelial barrier function.

**Keywords:** breast cancer; cancer secretome; brain endothelial cells; mitochondrial activity; blood-brain barrier



## 1. Introduction

The Blood-brain barrier (BBB) is a multicellular barrier located between the blood and the brain tissues. It is composed of brain endothelial cells (BECs), followed by pericytes, basement membrane, and astrocytes [1]. BECs are characterized by the presence of continuous structural proteins called tight junctions (TJs). The TJs link the BECs together, thus, significantly limiting the paracellular flux of solutes and the passage of cells [2]. Moreover, TJs at the cerebral endothelium are only encountered in the brain capillaries and not at the systemic capillaries [1]. It has been hypothesized that the BBB may be disrupted by metastatic cancers such as breast cancer [3]. Breast cancer is the most prevalent malignant tumor in women and the second-leading cause of brain metastases following lung cancer [4]. Approximately 30% of women with metastatic breast cancer acquire brain metastases [5]. The initial step of cancer cells to metastasis is to separate from the primary tissue and enter the circulatory system. Then, the cancer cells are arrested at the capillary bed before the extravasation, which is followed by cancer cell proliferation at the new location [6]. For metastasis into the brain, breast cancer cells must cross the BBB [7]. Cancer cells commonly penetrate the endothelial barriers either by the transcellular or paracellular route. The transcellular route includes cancer cells moving in large vacuoles through endothelial cells [4,8], while the paracellular route requires a breakdown of the endothelial cell-cell junction to allow cancer cells to enter the brain [5]. Cancer cells manage to survive despite the exposure to the high stress of being in circulation [6,9]. At the point that the cancer cells are arrested at the BEC's apical surface, and before penetrating the endothelial barrier [8], potential interactions occur between cancer cells and endothelial cells. These interactions are characterized by either physical adhesion to the BECs or via secretory paracrine factors [10,11], which induces disruption of the brain endothelial cells and facilitates the migration of cancer cells into the brain. The mechanism proposed for this interaction, in general, suggest that physiological changes occur in endothelial cells under the stimulation of cancer cells, resulting in the activation of adhesion molecules such as E-selectin in endothelial cells. Once these BEC plasma membrane proteins interact with their ligand on the metastatic cancer cell, a series of signaling pathways affect the opening of the cell-cell junctions allowing cancer cells to cross the endothelial barrier [12,13].

Interaction between endothelial cells and metastatic cancer cells induces genetic modification in the endothelial cells [14,15]. The physical interaction between metastatic cancer cells and endothelial cells occurs as an endothelial response to cancer stimulation [13]. The mediators of this stimulation are thought to be paracrine factors secreted from cancer cells [16]. Therefore it is not surprising that cancer cells release a variety of molecules such as growth factors, enzymes, and cytokines and that these molecules may modulate the endothelial properties [17,18]. Stimulated cancer cells secrete enzymes such as matrix-metalloproteinases, MMP2, and MMP9, which degrade the basement membrane components and tight junction proteins of BECs [19–21]. Cytokines can activate BECs by inducing the adhesion proteins such as E-selectin and P-selectin, followed by the presentation of vascular cell adhesion molecule-1 and intercellular adhesion molecule-1 at the surfaces of endothelial cells. These proteins are the mediators of the diapedesis of cancer cells [6]. Cancer cells induce changes in the endothelial cell by upregulating the expression of adhesion molecules receptors, remodelling the cytoskeleton fibres, and disrupting the endothelial cell-cell junctions [17]. The present study aimed to investigate the paracrine effect of breast cancer cells on the mitochondrial activity and viability of brain endothelial cells under both normoxic and hypoxic conditions.

## 2. Materials and Methods

### 2.1. Cell Culture & Condition Media Collection

Murine brain microvascular endothelial cells (bEnd.3 ATCC<sup>®</sup> CRL-2299, Gaithersburg, MD, USA) and invasive breast cancer cells (MCF7(ATCC HTB-22)) were cultured in Dulbecco's Modified Eagle Medium (DMEM, Gibco, No. 22320022, 8717 Grovemont Cir, Gaithersburg, MD, USA) supplemented with 10% Fetal Bovine Serum (FBS, Biowest, No. 10493-106,

2 Rue du Vieux Bourg, Nuaillé, France) and 100 U/mL penicillin/streptomycin (Gibco. No. 15070063) (Complete DMEM media). TrypleE (ThermoFisher Scientific, No. A1285901, 168 Third Avenue, Waltham, MA, USA) was used for harvesting the cells.

To collect the MCF7 conditioned medium (MCF7CM),  $1 \times 10^5$  of cancer cells were grown in 75-cm<sup>2</sup> culture flasks in normal humidity 5% CO<sub>2</sub> incubator at 37 °C, when they reached 50% confluence, the spent growth media was replaced with a fresh growth media and further incubated under normoxic conditions (21% O<sub>2</sub>) or hypoxic conditions (5% O<sub>2</sub>) for 48 h (The incubation under hypoxic conditions was performed by placing the TC flasks in a sterilized Modular Incubator Chamber (Hypoxia chamber—MIC 101)—Billups-Rothenberg, Inc., Sorrento Valley Blvd, San Diego, CA, USA). The hypoxia chamber is provided with a Greisinger Oxygen meter with a sensor (GOX 100-0-CO. No. 600437), which allowed for the measurement of O<sub>2</sub> during the incubation). After 48 h incubation in either normoxic or hypoxic conditions, the supernatant was collected in ice-cooled centrifuge tubes, centrifuged at 3500 rpm for 5 min at 4 °C, then filtered with a GVS filter (0.20 µm). The liquated supernatants were collected in 2–5 mL tubes and stored at –80 °C until required.

### 2.2. bEnd.3 Treatments with MCF7CM

The collected supernatants were thawed at 21 °C and added to fresh complete DMEM to concentrations 20%, 40%, and 75%, called MCF7 conditioned media (MCF7CM). The bEnd.3 monoculture cells were seeded at the seeding densities required by the assay and incubated at normal humidity 5% CO<sub>2</sub> incubator at 37 °C for 24 h to allow for cell attachment. Following 24 h incubation, the spent growth media were removed, then cells were exposed daily to either 20%, 40%, or 75% MCF7CM for 24, 48, 72, and 96 h.

Metastatic breast cancer cells, gain access to the CNS by crossing the endothelium of brain capillaries. These breast cancer cells firstly have to adhere to the apical/luminal side of the BEC, and then secondly, modulate/compromise the BECs via paracrine factors to cross the BBB. To therefore understand how paracrine factors from the luminal side of the capillary could affect the mitochondrial aspects of BEC function, bEnd.3 cells in Transwell inserts (Transwell® insert (pore size of 0.45 µm, filtration diameter of 12 mm, and an effective surface area of 0.6 cm<sup>2</sup>) (Merck-Millipore. PIHA01250, 6 Hatters Ln, Watford, UK) were treated by adding MCF7CM to the apical insert chamber on a daily basis. However, in bEnd.3 cell and MCF7 cell coculture experiments, the Transwell three-legged insert was used as the basis of our bicameral chamber experimental system, where MCF7 cells were seeded in the abluminal side (in the wells) while bEnd.3 cells were seeded in the inserts (apical chamber) to ensure that we could measure TEER across bEnd.3 cell monolayers. These experiments were carried out in triplicate.

### 2.3. Research Design

The study is designed to study the physiological changes in brain endothelial cells bEnd.3 under the influence of MCF7 cells. All experiments were carried out in triplicate as a minimum ( $n = 3$ ) and duplicated to ensure repeatability. The effect of normoxic and hypoxic paracrine factors secreted from MCF7 was compared. The diagram below in Figure 1 summarizes the research design of this study.

For the in vitro model of the BBB, we utilized the bicameral chamber system, where the well assumes the abluminal side of the capillary endothelium, while the apical chamber (the insert) assumes the luminal side of the capillary. This allowed for MCF7 cells to be cocultured in wells while a three-legged insert (Merck-Millipore, PIHA01250, 6 Hatters Ln, Watford, UK) was used for growing the endothelial BEC monolayers. These three-legged inserts also facilitated the movement of inserts between varying treatment conditions (e.g., normoxic versus hypoxic conditions).



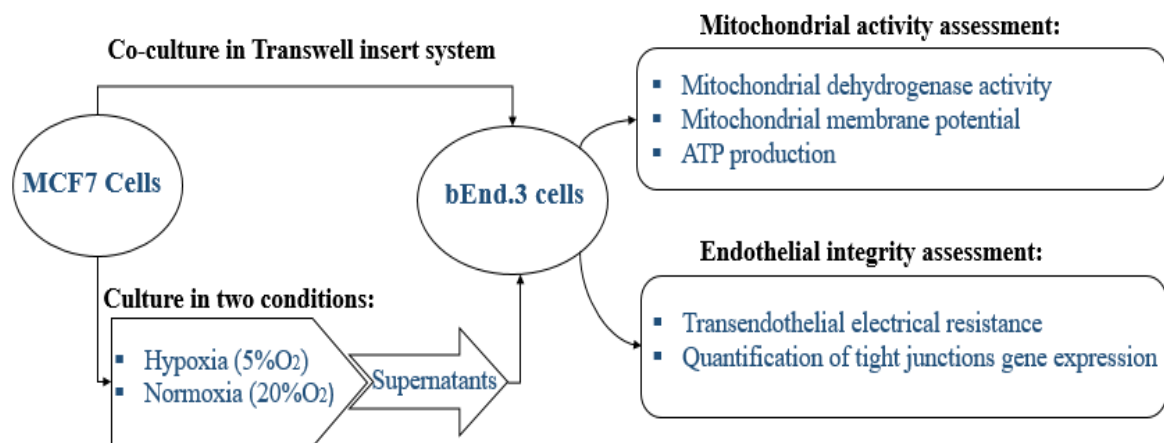


**Figure 1.** Schematic diagram of the research design to study the effect of the paracrine factors secreted by MCF7 cells on bEnd.3 cells.

In order to ensure that our MCF7CM always had sufficient metabolic constituents, a minimum of 25% fresh growth media (DMEM) was always added to the MCF7CM to make up the selected treatment concentrations (20%, 40%, and 75%). Furthermore, MCF7 cell cultures were grown to 50% confluency and exposed for maximally 48 h, before supernatants were removed and prepared for experimentation. Lastly, media for treating cells were replaced daily to ensure continuity in our treatment process.

In addition, we had to avoid using an O<sub>2</sub> level that would compromise the viability bEnd.3 cells when cocultured under hypoxic conditions. We show in our study that bEnd.3 cell monolayers are indeed sensitive to 5% O<sub>2</sub> but can recover within 24 h to control levels of permeability (TEER) (Figures 6 and 7).

#### 2.4. Endothelial Cells Viability Assay

For the determination of cell viability, bEnd.3 cells were seeded on Transwell® insert (pore size of 0.45 µm, internal insert diameter of 12 mm, and an effective surface area of 0.6 cm<sup>2</sup>) (Merck-Millipore, PIHA01250, 6 Hatters Ln, Watford, UK) a density of 2000 cells/insert; the inserts were placed in 24 well plates (Bio-Smart Scientific, No. 30024, Park Edge Mews, Edgemoor, Link Way, Edgemoor, Cape Town, South Africa). Growth media (completed DMEM) was added to both luminal (300 µL) and basolateral side (800 µL), and cells were incubated at 37 °C and 5% CO<sub>2</sub> overnight, allowing them to attach to the surface of the filter membrane. MCF7 cells were separately seeded at a density of 1000 cells/well on the same day in 12 well plates (Bio-Smart Scientific, No. 30012, Park Edge Mews, Edgemoor, Link Way, Edgemoor, Cape Town, South Africa).

Following 24 h of incubation, bEnd.3 cells were co-cultured with MCF7 cells by placing the inserts with bEnd.3 cells in the 12 well plates containing MCF7 cells. Plates were incubated at 37 °C with 5% CO<sub>2</sub> for 96 h. Then, the inserts were removed from the 12 well plates and placed in new 24 well plates. This ensured that only bEnd.3 cells were assayed for viability. 100 µL of XTT solution was added to each insert, and the cells were incubated for an additional 4 h at 37 °C and 5% CO<sub>2</sub>. Then the medium from the inserts was transferred into 96 well plates (SPL-Life Sciences, No. 30096, 26, Geumgang-ro 2047 beon-gil, Naechon-myeon Pocheon-si, Gyeonggi-do, Korea). The absorbance was measured at 450 nm by using a microplate reader.

In addition, the bEnd.3 cells were seeded in 96-well plates (SPL-Life Sciences, No. 30096) at a density of  $4 \times 10^3$  cells/well, each experimental group was seeded in 5 replicate wells, the cells were incubated for 24 h and treated with MCF7CM as previously described (i.e., MCF7CM was added in the luminal compartment). Following the treatment, the viability of bEnd.3 cells were determined using an XTT assay kit (Roche, No. 11465015001) in 24 h intervals up to 96 h. At each 24 h interval, 50 µL of XTT solution was added to each well, the cells were then incubated for 4 h at 37 °C in a 5% CO<sub>2</sub> incubator. The absorbance

was then measured at 450 nm using a (Polarstar Omega B.M.G. Labtech, Allmendgrün 8, Ortenberg, Germany) microplate reader.

## 2.5. Mitochondrial Membrane Potential ( $\Delta\psi_m$ )

Changes in  $\Delta\psi_m$  in bEnd.3 cells after exposure to MCF7CM were analyzed using Tetramethylrhodamine Ethylesterperchlorate (TMRE) (ThermoFisher. No. T669) assay. TMRE is a permeable cationic, lipophilic dye, emitting red-orange fluorescent. It is actively taken up by active mitochondria into the negatively charged mitochondrial matrix. The intensity of the fluorescent signal obtained is indicative of the  $\Delta\psi_m$ . The higher membrane potential (more polarized) indicates more TMRE accumulation in the mitochondrial matrix [17]. Therefore, the higher red-orange fluorescence would indicate a higher membrane potential (hyperpolarization). In this assay, the bEnd.3 cells were seeded in flasks at a density of  $3 \times 10^4$  per flask and treated as previously described. In addition, bEnd.3 were also treated with carbonylcyanide-3-chlorophenylhydrazone (CCCP) (Sigma, Eschenstr. 5, Taufkirchen, Germany) as a control. The CCCP is well known as an uncoupling agent of the  $\Delta\psi_m$ . CCCP was used to confirm that the uptake of the TMRE is related to the mitochondrial membrane potential. At 24 h intervals, 100  $\mu$ M of CCCP was added and incubated for 10 min before staining with Tetramethylrhodamine Ethylesterperchlorate (TMRE) (ThermoFisher Scientific, No. T669, 168 Third Avenue, Waltham, MA, USA) at 300 nM for 20 min. The solution stain was then removed, and cells were washed twice with PBS. Cells were then scraped and lysed in a lysis buffer composed of SDS (0.1% v/v) in 0.1M Tris-HCl buffer. The 150  $\mu$ L of the lysates were loaded in 96 well plates. The fluorescence of TMRE was measured with a multi-well fluorescence plate reader with excitation and emission set at  $508 \pm 20$  nm and  $589 \pm 40$  nm, respectively. A total protein concentration was then determined in the remaining lysate samples corresponding in their lysates using Bicinchoninic acid (BCA) kit (ThermoFisher Scientific, No. 232225, address: 168 Third Avenue, Waltham, MA, USA). The fluorescence in each well was normalized for the protein concentration of its corresponding lysate.

## 2.6. ATP Production

The bEnd.3 were seeded on Transwell® insert (pore size of 0.45  $\mu$ m, filtration diameter of 12 mm, and an effective surface area of 0.6 cm<sup>2</sup>) at a density of  $2 \times 10^3$  cells/insert; the inserts were placed in 24 well plates. Growth media (completed DMEM) was added to both luminal (300  $\mu$ L) and basolateral side (800  $\mu$ L), cells were incubated at 37 °C and 5% CO<sub>2</sub> overnight. MCF7 cells were separately seeded at a density of  $1 \times 10^3$  cells/well on the same day in 12 well plates. After 24 h, the growth medium was replaced with fresh completed DMEM (1 mL). Following 24 h incubation, bEnd.3 were placed in the 12 well plates which had MCF7 cancer cells growing in the well bottom. The co-culture cells were incubated at 37 °C under 5% CO<sub>2</sub> for 96 h (During the co-culture incubation time, the medium in the inserts (for bEnd.3 cells) were changed daily). The inserts were then removed from 12 well plates and placed in new 24 well plates (this ensured that ATP detection solution will only apply on bEnd.3 cells). Then, 100  $\mu$ L of ATP detection solution was added to each insert. Cells were then incubated for an additional 5 min at room temperature in a plate shaker. The mixture from the inserts was transferred into 96 white well plates (SPL-Life Sciences. No. 31396, address: 26, Geumgang-ro 2047 beon-gil, Naechon-myeon Pocheon-si, Gyeonggi-do, Korea). The luminescence was measured using a microplate reader (B.M.G Labtech, address: Allmendgrün 8, Ortenberg, Germany).

In addition, bEnd.3 cells were seeded ( $1 \times 10^3$  cells/well) in 96 white well plates (SPL-Life Sciences. No. 31396) and were exposed daily to the MCF7CM as previously described. At 24 h intervals, relative intracellular ATP levels were determined using the Mitochondrial ToxGlo™ kit (Promega (G8000), address: 2800 Woods Hollow Road, Madison, WI, USA). The Mitochondrial ToxGlo™ assay was conducted according to the supplier's protocol. An ATP detection solution was prepared by mixing 10 mL of ATP buffer with an ATP detection substrate. The components were homogenized by vortex,

forming an ATP detection solution. At 24 h intervals, 100 µL of ATP detection solution was added to each well. Then the plates were incubated for 5 min at room temperature in a plate shaker. ATP content was measured using a luminescent plate reader (B.M.G Labtech, Allmendgrün 8, Ortenberg, Germany).

## 2.7. Transendothelial Electrical Resistance (TEER)

The endothelial monolayer integrity was tested by determining the transendothelial electrical resistance (TEER) using the EVOM TEER measurement system. The bEnd.3 cells were grown on insert membrane (Transwell® Inserts with 0.45 µm pore size) (Merck-Millipore, PIHA01250, 6 Hatters Ln, Watford, UK) at a density of  $5 \times 10^4$  cells/insert. MCF7 cells were seeded in the 12 well plates. Both cell lines were first grown separately for 96 h, then the inserts with bEnd.3 cells were placed in the 12 well plates where MCF7 cells were grown. The co-cultured cells were incubated in normoxic conditions, TEER was measured daily starting from day two.

In addition, bEnd.3 cells and MCF7 cells were grown separately in similar conditions for 72 h, then the two cell lines were co-cultured by placing the bEnd.3 inserts in the MCF7 well plates. The co-cultured cells were incubated in normoxic conditions (21% O<sub>2</sub>) for 24 h, then incubated in hypoxic conditions (5% O<sub>2</sub>) for the rest of the experimental time frame. TEER was measured daily starting from day three.

To determine the effect of MCF7CM on bEnd.3 monolayer transendothelial electrical resistance (TEER), bEnd.3 cells were seeded on inserts (Merck-Millipore, PIHA01250) at a density of  $5 \times 10^4$  cells/well in 12 well plates for 72 h and incubated with hypoxic and/or normoxic MCF7CM at 20%, 40%, and 75% concentrations. Cells were then incubated at 37 °C and 5% CO<sub>2</sub>. The TEER measurement started by day three. In control groups, bEnd.3 cells were grown in inserts and placed in wells with fresh media. The measurement was performed by connecting the electrodes to either side of the cell monolayer and measuring the resistance. The resistance of the blank (inserts without cells) was subtracted from the resistance value of the cell monolayer (inserts with cells), and the resultant value was multiplied by the surface area of the inserts to standardize the TEER value. The measurement was performed as described by Srinivasan et al., 2015 [22].

## 2.8. Quantitative PCR (q-PCR) Gene Expression Assay

To determine whether the reduction in the endothelial resistance of bEnd.3 cells exposed to MCF7CM was associated with the expression of tight junction proteins, a qPCR was performed to quantify the gene expression of tight junction proteins (Occludin and Claudin-5). The bEnd.3 cells were grown in T75 flasks and chronically exposed to normoxic or/and hypoxic MCF7CM as previously mentioned. Following the exposure, a total RNA was extracted using Tripure isolation reagent (Roche, Ref:11667157001, Ground Floor Liesbeeck House River Park, River Lane, Mowbray, Cape Town, South Africa). The first strand of cDNA was synthesized from total RNA using Transcriptor first-strand cDNA synthesis kit (Roche, No. 04379012001). The resultant cDNA served as a template for real-time PCR amplification using SYBR Luna universal qPCR master mix kit (New England bio labs), and Real-Time PCR System (Applied bio-system real-time-PCR instrument (ThermoFisher Scientific, REF 4484643). To amplify a fragment of claudin-5, occludin, and GAPDH (as house-keeping gene), the primer pairs detailed were used (Table 1). The amplification was conducted at 95 °C for 1 s, followed by 44 cycles of 95 °C for 15 s, 63 °C for 30 s and 95 °C for 15 s. Results were analyzed using the Pfaffl method as described by Pfaffl et al., 2002 [23].

## 2.9. Statistical Analysis

Statistical analysis was performed by Graph Pad Prism software (version 6), Data was expressed as mean ± SEM, and the differences between groups were analyzed by unpaired Students' *t*-test or one-way ANOVA followed by Dunnett's multiple comparison test. The significant level was accepted at  $p < 0.05$  for a 95% confidence interval.

**Table 1.** Primer sequences for quantitative PCR (qPCR) amplification of complementary DNA (cDNA). GAPDH: Glyceraldehyde phosphate dehydrogenase.

N	Primers	Primer Pairs (Sequence (5' > 3'))	Product Length	°C
1	GAPDH	Forward: AGGAGAGTGTTCCTCGTCCC Reverse: TGCCGTTGAATTTGCCGTGA	199	63
2	Claudin-5	Forward: CCCAGTTAAGGCACGGGTAG Reverse: GGCACCGTCGGATCATAGAA	126	53–63
3	Occludin	Forward: TTTCAGGTGAATGGGTCACCG Reverse: ACTTTCAAAAGGCCTCACGGA	242	63

### 3. Results

#### 3.1. The Effect of MCF7 Cells and Their Conditioned Media on bEnd.3 Cell Viability

To evaluate how MCF7 cells modulate brain endothelial physiological functions, the viability of bEnd.3 cells co-cultured with MCF7 cells was evaluated using a XTT assay. As shown in Figure 2A, the viability of bEnd.3 cells co-cultured with MCF7 cells was significantly reduced ( $p < 0.01$ ). Similar results were obtained after bEnd.3 cells were exposed to selected concentrations of MCF7 conditioned media (MCF7CM). Figure 2B shows that bEnd.3 cells, exposed to selected concentrations of MCF7CM under normoxic conditions for 24 h and 48 h, were not significantly different in their viability compared to the control. However, following 48 h of exposure to MCF7CM, the bEnd.3 cell viability was reduced after exposure to 75% for 72 h ( $p < 0.02$ ), whereas at 96 h, MCF7CM exposure significantly reduced bEnd.3 cell viability in a dose-response manner ( $* p < 0.05$ ,  $** p < 0.01$ ). The viability of bEnd.3 cells were significantly reduced after 24 h exposure to the media composed of 75% of hypoxic MCF7CM ( $* p = 0.0450$ ). At 24 h, no significant difference was observed in the viability of bEnd.3 cells were exposed to 20% or 40% of hypoxic MCF7CM for the same point of time (Figure 2C). Although there was a decrease in the means of all concentrations of hypoxic MCF7CM, these were not statistically different to controls. However, the viability of bEnd.3 cells was significantly decreased at all concentrations of hypoxic MCF7CM following 72 h and 96 h exposure ( $* p < 0.05$ ,  $** p < 0.01$ ,  $*** p = 0.0002$ ,  $**** p < 0.0001$ ).

#### 3.2. The Effect of MCF7 CM on the Mitochondrial Membrane Potential ( $\Delta\Psi_m$ )

The changes to mitochondrial membrane potential were investigated as a further measure of bEnd.3 endothelial function after MCF7CM exposure, using Tetramethylrhodamine Ethylesterperchlorate (TMRE) as a measure the  $\Delta\Psi_m$ . The functionality of the TMRE assay on bEnd.3 cells were carried out using carbonylcyanide-3-chlorophenylhydrazine (CCCP), a known inhibitor of  $\Delta\Psi_m$  (negative control). Treatment with CCCP decreased  $\Delta\Psi_m$  consistently throughout the study. Figure 3 illustrates that daily exposure of normoxic MCF7CM did not statistically affect the  $\Delta\Psi_m$  in bEnd.3 cells over 96 h.

Interestingly, bEnd.3 cells exposed to hypoxic MCF7CM show an increase in the  $\Delta\Psi_m$  at all concentrations compared with the control (Figure 4) ( $* p < 0.05$ ,  $**** p < 0.0001$ ). Exceptions to the statistical increase of  $\Delta\Psi_m$  occurred at 24 h at 75% and 72 h at 20% of bEnd.3 cells treated with hypoxic MCF7CM media.

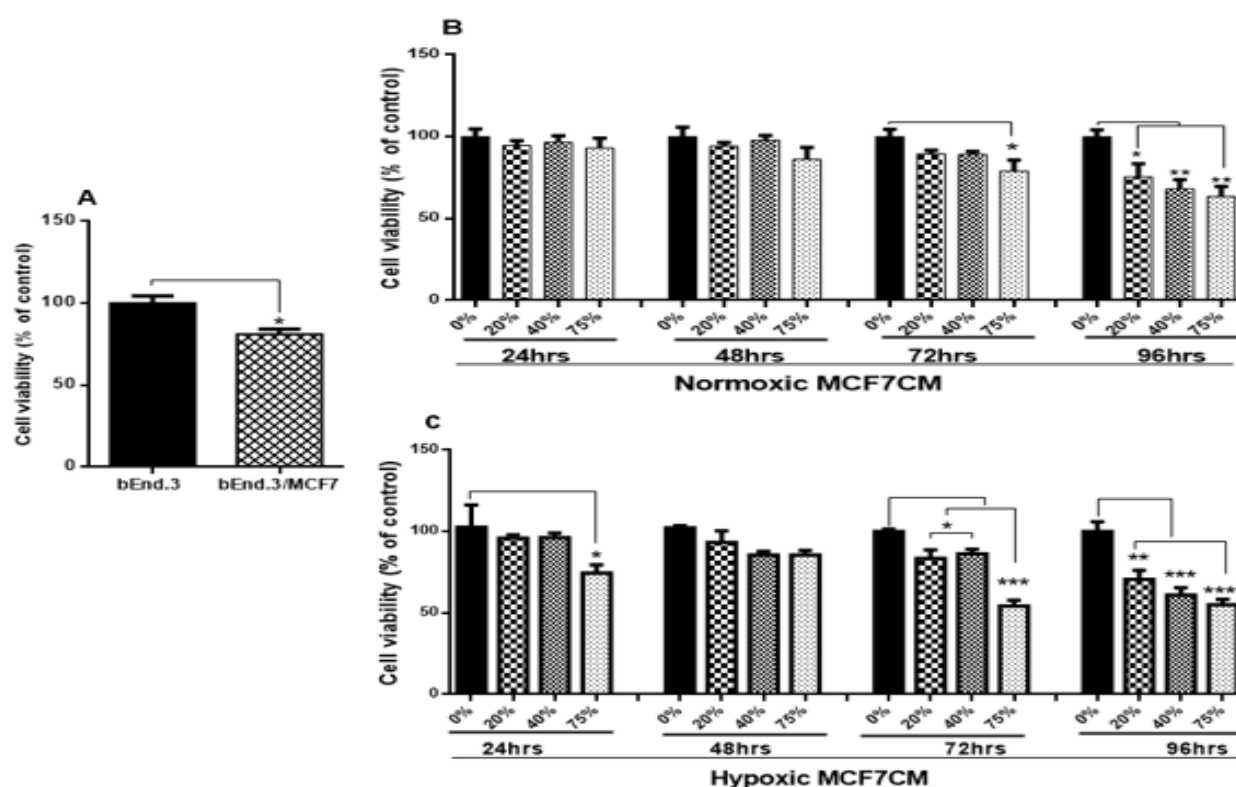


**Figure 2.** The viability of bEnd.3 cells under the chronic influence of MCF7 cells: (A) shows the effects of co-culture with MCF7 cells on bEnd.3 cell viability; (B) represents the viability of bEnd.3 cells after being treated daily with selected concentrations of MCF7CM produced from MCF7 cells under normoxic incubation (21% O<sub>2</sub>); and (C) shows the viability of bEnd.3 cells after exposure to selected concentrations of MCF7CM obtained from MCF7 cells under hypoxic conditions (5% O<sub>2</sub>). ( $n = 5$ ), (\*  $p < 0.05$ , \*\*  $p < 0.01$ , \*\*\*  $p < 0.001$ , \*\*\*\*  $p < 0.0001$ ).

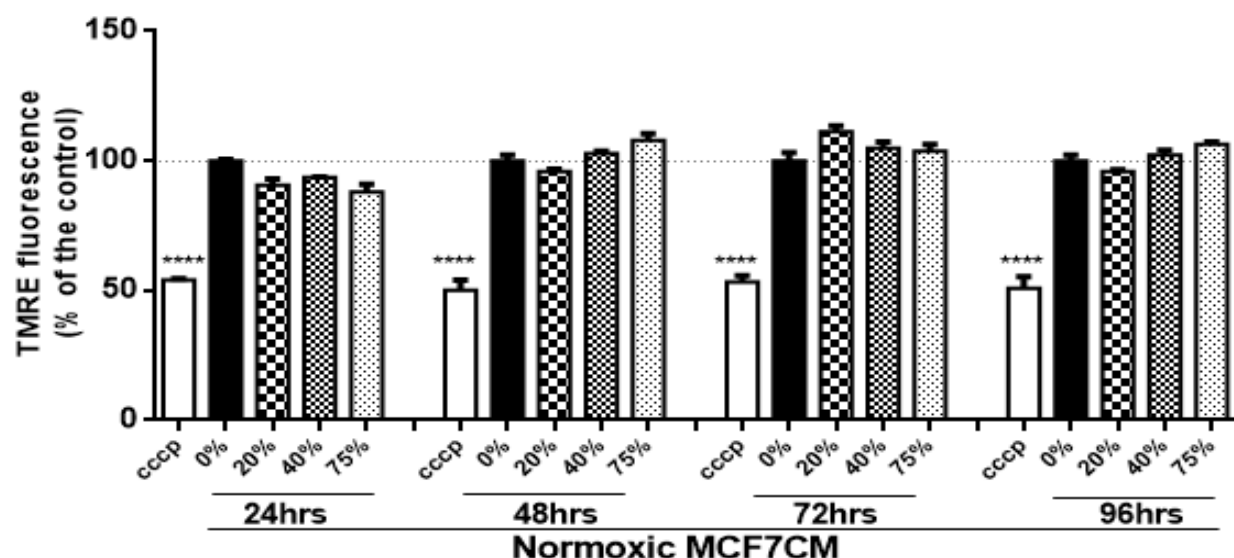


**Figure 3.** Shows the changes in mitochondrial membrane potential ( $\Delta\Psi_m$ ) in bEnd.3 cells after daily exposure to MCF7CM cultured under normoxic conditions (20% O<sub>2</sub>). (CCCP: carbonylcyanide-3-chlorophenylhydrazone (negative control)). ( $n = 4$ ) (\*\*\*\*  $p < 0.0001$ ).



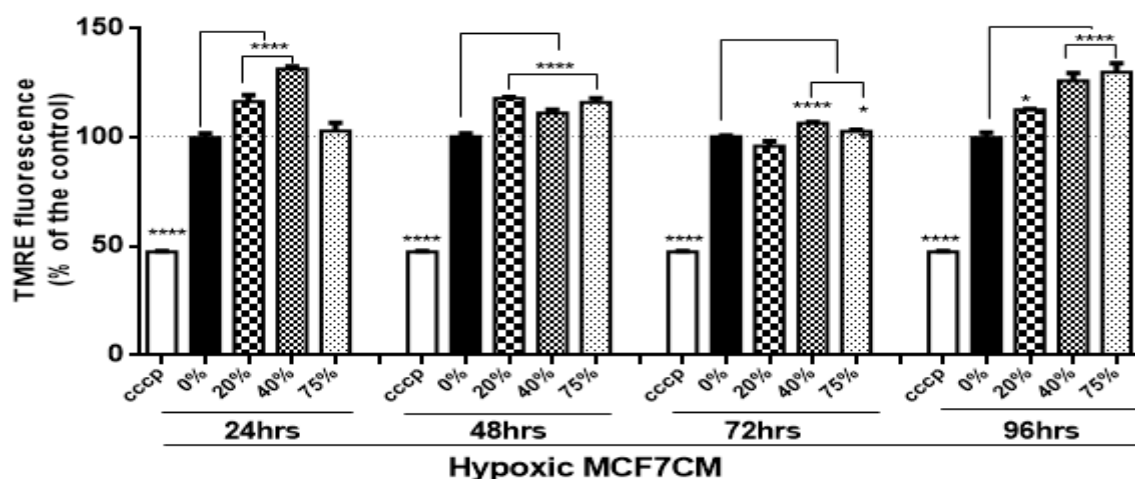


**Figure 4.** Shows the changes in mitochondrial membrane potential ( $\Delta\Psi_m$ ) in bEnd.3 cells after chronic exposure to selected concentrations of MCF7CM derived from MCF7 cells cultured under hypoxic conditions (5%  $O_2$ ). (CCCP: carbonylcyanide-3-chlorophenylhydrazone (negative control)). ( $n = 4$ ) (\*  $p < 0.05$ , \*\*\*\*  $p < 0.0001$ ).

### 3.3. ATP Level in bEnd.3 Cells under the Influence of MCF7 Cells

The classic function of mitochondria is to generate ATP through oxidative phosphorylation. Here, bEnd.3 cells co-cultured with MCF7 cells exhibited low levels of ATP production compared with the control (Figure 5A) ( $p < 0.001$ ). Similar results were observed when bEnd.3 cells were subjected to both normoxic and hypoxic derived MCF7CM (Figure 5B,C). Exposure to normoxic MCF7CM (Figure 5B) caused a depression of ATP production. At 24 h and partly at 48 h, although the means of ATP produced were depressed, no statistical difference was obtained between the exposed cells and the control, except at 48 h exposure to 75% concentration, where ATP levels were significantly reduced ( $p < 0.0001$ ). After 72 h exposure, only bEnd.3 cells exposed to 40% and 75% demonstrated a decrease in ATP level relative to the control ( $p < 0.01$ , and  $p < 0.001$  respectively). At 96 h exposure, the ATP productivity of bEnd.3 cells were significantly reduced at all concentrations compared to controls (see Figure 5B: \*  $p < 0.05$ , \*\*  $p = 0.003$ , \*\*\*  $p < 0.001$ ).

Although bEnd.3 cells exposed to hypoxic MCF7CM showed similar effects to bEnd.3 cells exposed to normoxic MCF7CM, they were more pronounced. At 24 h exposure all means were depressed and there were no statistical differences between hypoxic MCF7CM treatment and controls. At 48 h and 72 h, only cells exposed to 40% and 75% concentration show a significant decrease in ATP level. However, at 96 h exposure, ATP concentrations were decreased for all treatments (Figure 5C).

### 3.4. The Effect of MCF7 Co-Culture on Transendothelial Electrical Resistance (TEER) of Confluent bEnd.3 Cell Monolayers under Normoxic Conditions

The permeability across monolayers of bEnd.3 cells cultured as a monoculture (control) or co-culture (with MCF7 cells) used the Transwell bicameral system to measure TEER. As shown in Figure 6A the TEER across bEnd.3 cell confluent monolayers were measured in control groups and experimental groups daily for eight days. For days two to four, both groups were grown as a mono-culture, and no difference was observed in TEER. By the end of day four, mono-cultures of confluent bEnd.3 monolayers were introduced to co-cultured of MCF7 cells. TEER of mono-cultured confluent bEnd.3 monolayers compared to co-cultured confluent bEnd.3 monolayers were significantly reduced ( $p < 0.01$ ) after the co-cultures of MCF7 cancer cells (see Figure 6B). Interestingly, the reduction of TEER was not constant, as bEnd.3 cells co-culture with MCF7 cells recovered their TEER by day six, although the increase in TEER remained non-statistically lower than the control.

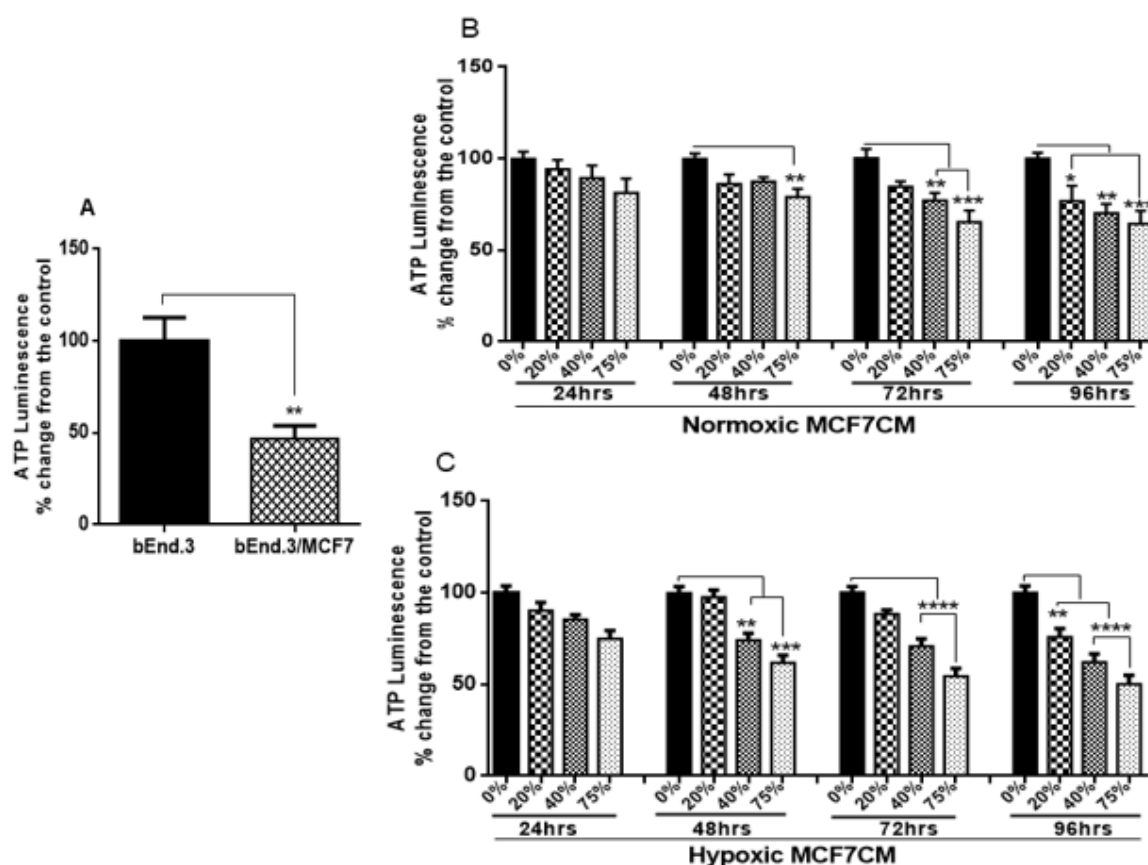


**Figure 5.** Shows the changes in cellular ATP level in bEnd.3 cells under the influence of MCF7 cells: (A) represents ATP levels in bEnd.3 cells co-cultured with MCF7 cells; (B) represents ATP levels in bEnd.3 cells exposed to selected concentrations of MCF7CM produced from MCF7 cells cultured under normoxic conditions (21% O<sub>2</sub>); and (C) represents cellular ATP levels in bEnd.3 cells exposed to selected concentrations of MCF7CM derived from MCF7 cells cultured under hypoxic conditions (5% O<sub>2</sub>). ( $n = 4$ ), (\*\*  $p < 0.01$ , \*\*\*  $p < 0.001$ , \*\*\*\*  $p < 0.0001$ ).

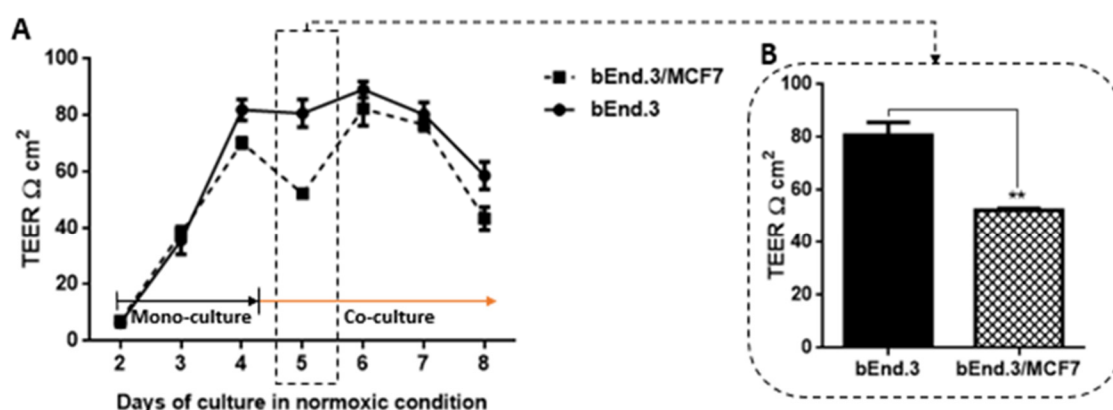


**Figure 6.** Transendothelial electrical resistance (TEER) of bEnd.3 monolayers cocultured with MCF7 cells under normoxia (21% O<sub>2</sub>): (A) shows the changes in TEER across confluent monocultured bEnd.3 cells after co-culture with MCF7 cells under normoxic conditions; (B) TEER of bEnd.3 monolayers after 24 h co-culture with MCF7 cells. Day five was the only day that showed a significant difference from controls. ( $n = 3$ ), (\*\*  $p = 0.002$ ).

### 3.5. The Effect of MCF7 Co-Culture on Transendothelial Electrical Resistance (TEER) of Confluent bEnd.3 Cell Monolayers under Hypoxic Conditions

In addition, TEER was measured for bEnd.3 cell confluent monolayers cultured as a monoculture under normoxic conditions and then introduced co-cultured MCF7 cells



under hypoxic conditions (Figure 7). Similar to the normoxic condition, bEnd.3 cells in both groups were cultured as a monoculture until day three.

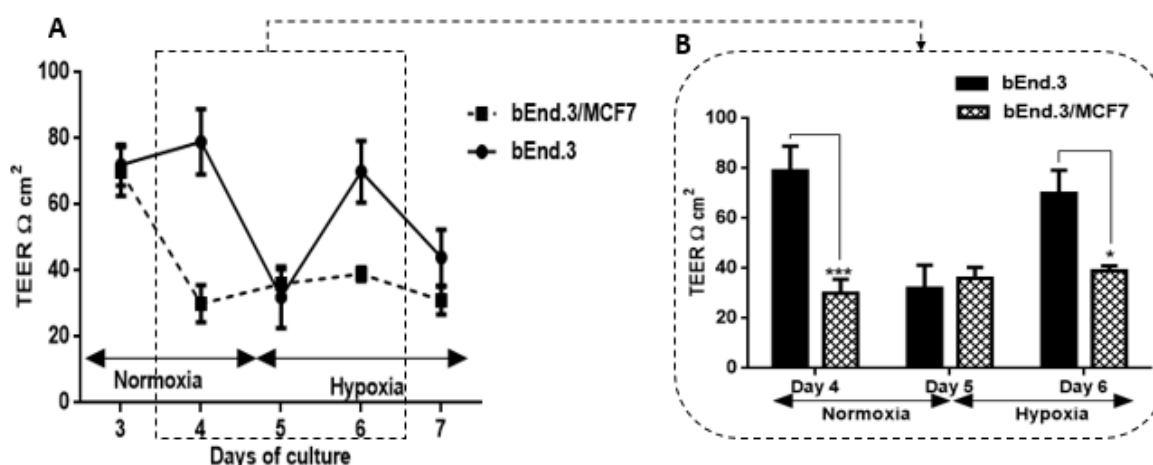


**Figure 7.** Transendothelial electrical resistance (TEER) of bEnd.3 monolayers cocultured with MCF7 cells under hypoxia (5% O<sub>2</sub>): (A) shows changes in TEER across bEnd.3 monolayers co-cultured with MCF7 cells in normoxia and hypoxia. Note that mono-cultures of bEnd.3 monolayers are transiently affected by hypoxic conditions, but recover to control levels within 24 h; (B) show changes in the TEER across bEnd.3 cells monolayers co-cultured with MCF7 cells under normoxic and hypoxic incubation. (\*  $p < 0.05$ , \*\*\*  $p < 0.001$ ), ( $n = 3$ ).

TEER measurement was monitored from day three and before the co-culture of bEnd.3 monolayers with MCF7 cells. Until day four, cells were incubated under normoxic conditions (Figure 7A). By the end of day four, both bEnd.3 monolayers monocultured and co-cultured with MCF7 were incubated under hypoxic conditions until day seven. As shown in Figure 7A, under normoxia, the co-culture with MCF7 cells significantly decreased the endothelial resistance (see Figure 7B on day four (\*\*\*  $p < 0.001$ )). The reduction in TEER of co-cultured bEnd.3 monolayers were not changed by placing the cells in hypoxia. Interestingly, the resistance of monocultured bEnd.3 monolayers (control) also decreased under hypoxic conditions (see Figure 7A on day five). However, the TEER of the control recovered to normal levels by day six (see Figure 7A,B on day six) before declining again on day seven. In contrast, TEER of bEnd.3 co-cultured with MCF7 under hypoxic conditions remained suppressed from day four until the end of the experiment and was always statistically lower than the monocultured bEnd.3 monolayers.

### 3.6. The Effect of MCF7CM on the TEER across Confluent bEnd.3 Monolayers

In addition, the exposure to MCF7CM increased the permeability of the bEnd.3 monolayers (Figure 8A,B). Confluent bEnd.3 monolayers exposed to normoxic MCF7CM demonstrated lower resistance compared to controls (Figure 8A). The exposure to normoxic MCF7CM started by the end of day four of cell culture, and by day five TEER decreased non-statistically compared to the control TEER (0%) (Figure 8B in day five). Following 48 h of MCF7CM exposure, both “peak” TEER (in Figure 8B block) and subsequent TEER were significantly decreased at all concentrations (see Figure 8B on day six). However, the exposure to hypoxic derived MCF7CM significantly reduced TEER of bEnd.3 monolayers after 24 h exposure (Figure 8C), particularly at 40% and 75% (see Figure 8D: day five). On day six, both “peak” TEER and subsequent TEER was significantly suppressed compared to the control (Figure 8D day six).

### 3.7. qPCR-Gene Expression Analysis

The level of mRNA expression for Occludin and Claudin-5 was analyzed from bEnd.3 cells exposed to selected concentrations of MCF7CM media. cDNA was transcribed from mRNA and processed using qPCR. Results demonstrated that Occludin gene expression in

confluent layers of bEnd.3 cells exposed to normoxic MCF7CM media increased compared to the control (Figure 9A), particularly after exposure to 20% of normoxic MCF7CM. However, gene expression levels of Occludin were not changed in the bEnd.3 cells after exposure to hypoxic MCF7CM (Figure 9B).

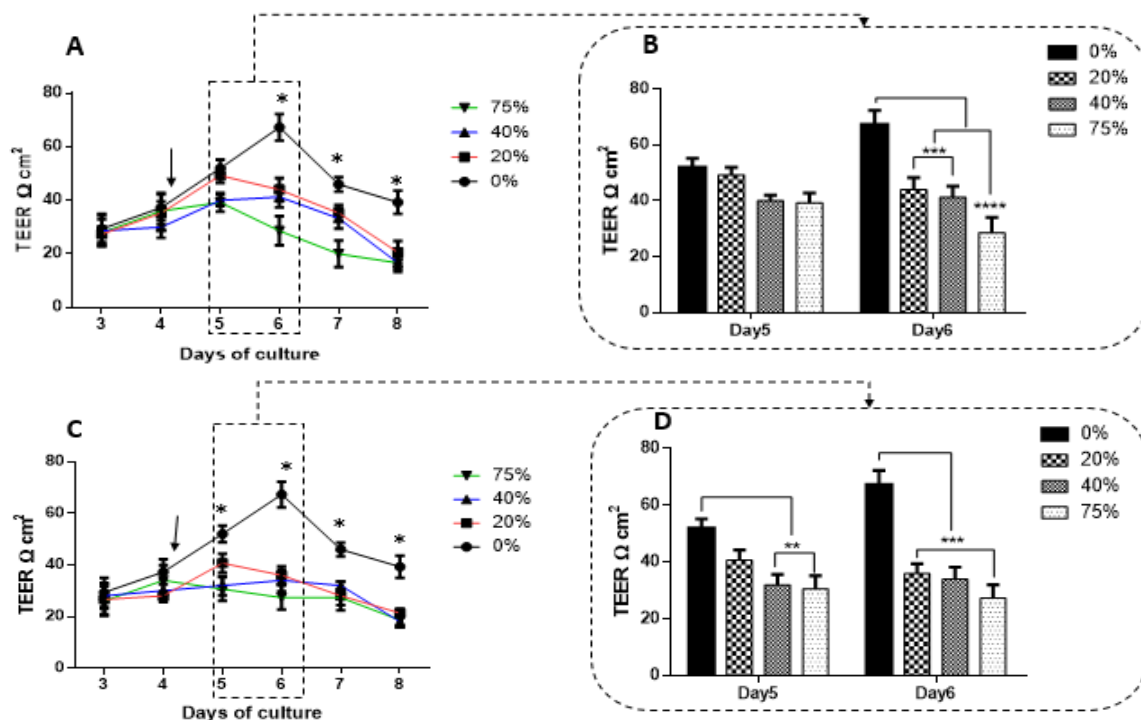


**Figure 8.** TEER of bEnd.3 cells exposed to selected concentrations of MCF7CM: (A) represents TEER across bEnd.3 monolayers exposed to selected concentrations of MCF7CM media harvested from MCF7 cells cultured under normoxic conditions (21% O<sub>2</sub>); the arrow indicates the start of the exposure to normoxic MCF7CM media. The asterisks (\*) refers to the significant difference between controls (0%) and cells exposed to selected concentration of normoxic MCF7CM (\*\*  $p < 0.01$ , \*\*\*  $p < 0.001$ , \*\*\*\*  $p < 0.0001$ ); (B) shows the peak effect of normoxic MCF7CM media on TEER across treated bEnd.3 monolayers after 24 h (day five) and 48 h (day six) treatment (\*\*\*  $p < 0.001$ , \*\*\*\*  $p < 0.0001$ ); (C) shows TEER of bEnd.3 monolayer exposed to selected concentrations of hypoxically derived MCF7CM media. The arrow in Figure 8C indicates the start of the exposure to hypoxically derived MCF7CM media. The asterisks (\*) refers to a significant difference between controls (0%) and cells exposed to normoxic MCF7CM (\*  $p < 0.05$ ); and (D) shows the peak effects of TEER between control (0%) and the exposed cells after 24 h (day five) and 48 h (day six) exposure to hypoxically derived MCF7CM media (\*\*  $p < 0.01$ , \*\*\*  $p < 0.001$ ), ( $n = 3$ ).

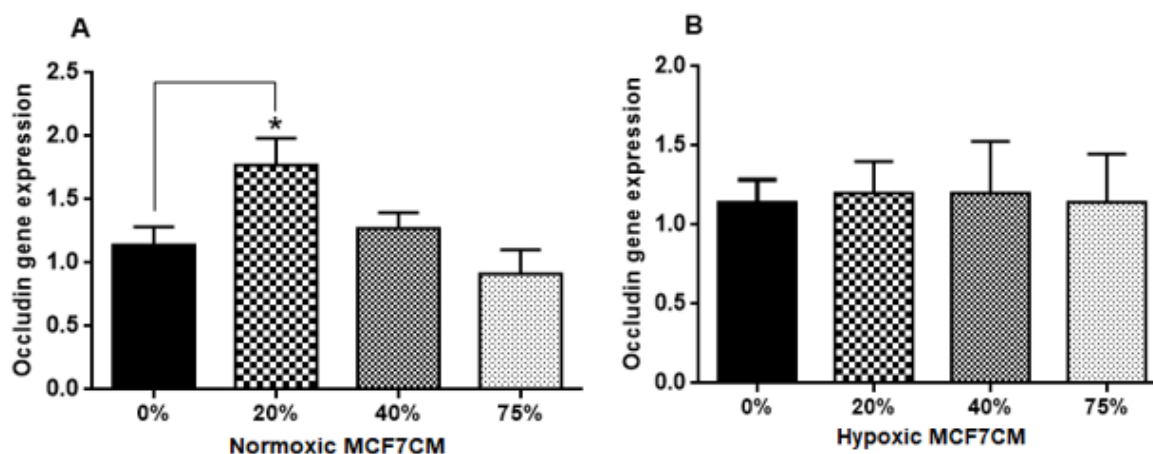


**Figure 9.** Gene expression level of Occludin in bEnd.3 cells after the exposure to selected concentrations of MCF7CM produced under normoxia (A) and hypoxia (B). (\*  $p = 0.0123$ ), ( $n = 4$ ).

Claudin-5 gene expression increased after exposure to both normoxic and hypoxic derived MCF7CM media (Figure 10A, B). The treatment with 75% normoxic MCF7CM media did not produce a statistical difference in Claudin-5 gene expression compared with the control (Figure 10A), whereas, 20% and 40% of normoxic MCF7CM significantly elevated Claudin-5 gene expression (\*\*  $p < 0.01$ , \*  $p < 0.05$  respectively). It was interesting to note that the treatment profile of both Occludin and Claudin-5 to normoxic MCF7CM, were similar. bEnd.3 cells exposed to the higher concentrations of hypoxic derived MCF7CM (40% & 75%) showed significantly higher levels of Claudin-5 gene expression than the control (Figure 10B)) (\*  $p < 0.05$ ).

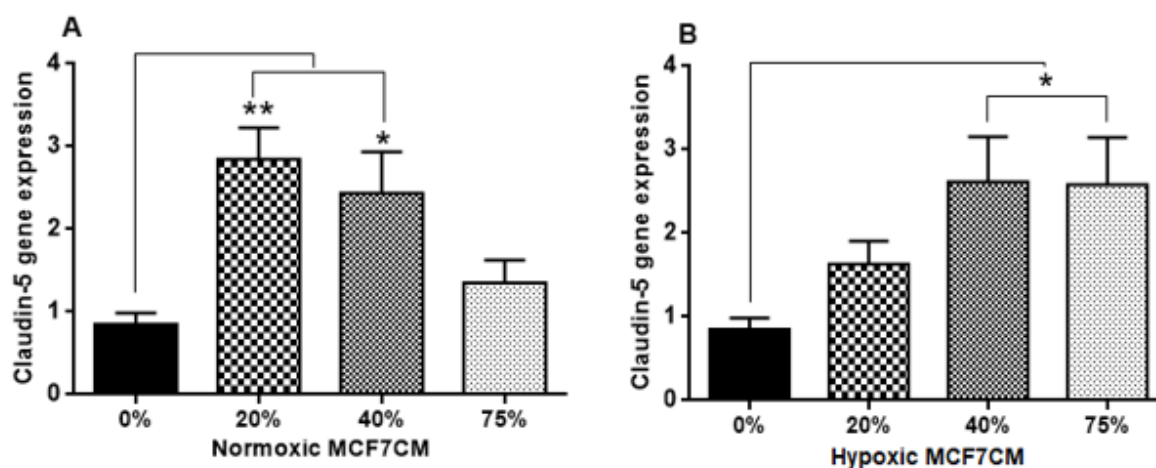


**Figure 10.** Gene expression level for Claudin-5 in bEnd.3 cells after the exposure to selected concentrations of MCF7CM media derived under normoxic (A) and hypoxic (B) conditions. (\*  $p < 0.05$ . \*\*  $p = 0.002$ ), ( $n = 4$ ).

#### 4. Discussion

Metastatic breast cancer often relocates across the notoriously protective BBB to bring about its pathological effects in the neural tissue of the central nervous system (CNS) [3]. We used the established in vitro brain endothelial model of BBB, using the BEC-line (bEnd.3), to further investigate some of the underlying mechanisms used by breast cancer cells (MCF7) to induce the physiological compromise of the endothelial cells of brain capillaries. Furthermore, the phenomenal rate at which metastatic cancer tumors develop most times leads to zones of hypoxia within the tumor itself, as there is often a lag time to angiogenesis within the tumor. We wanted to further understand whether tumor cells act differently under conditions of normoxia (21%  $O_2$ ) and under conditions of low  $O_2$  (5%  $O_2$ ), or hypoxic conditions, and if the level of paracrine cross-talk between cancer cells BECs of brain capillaries are affected.

To facilitate these experiments, we used the established bicameral experimental setup to measure the paracrine effects of MCF7 cells grown as a co-culture with bEnd.3 cells. Secondly, to study whether these paracrine secretions had a dose-related effect on the BECs, we collected the supernatant of MCF7 cells grown under normoxic and hypoxic conditions (MCF7CM media) and treated BECs by exposing them on a daily basis.

##### 4.1. bEnd.3 Cell Viability after MCF7 Exposure

Cell viability is a measure of the proportion of live, healthy cells within a cultured-cell population, and it is essentially used to evaluate the response of a population to a treatment or an agent [24]. Cell viability is dependent on various cellular functions such as enzyme activity, cell membrane permeability, mitochondrial activity, and ATP generation [24,25]. In the present study, cell viability was determined by measuring the activity of mitochondrial dehydrogenases in response to treatment with various concentrations of supernatant derived from breast cancer cells (MCF7 cells) using the XTT cell viability assay. Mitochondrial dehydrogenases catalyze the reactions of transferring the protons in the

electron transfer chain, which in turn drives ATP synthesis [26]. We wanted to evaluate if the viability of BECs exposed to paracrine factors from these MCF7 cells would be affected. Our results showed a marked reduction in cell viability after prolonged exposure of bEnd.3 cells to cocultured MCF7 cells (Figure 2A), and MCF7CM generated under normoxic (Figure 2B), and hypoxic (Figure 2C) conditions. The effects of bEnd.3 exposed to hypoxic MCF7CM was much more pronounced than bEnd.3 cells exposed to normoxic MCF7CM. Furthermore, our data indicate that cell viability was not affected within the 48 h, and whereas only the highest concentration (75%) of normoxic MCF7CM depressed viability at 72 h, all concentrations suppressed BEC viability by treatment with hypoxic MCF7CM. The delayed response in viability to MCF7CM treatment also indicated that the process whereby endothelial cells are affected is manifested after several iterations of cell division. Furthermore, although there is a similar profile between normoxic and hypoxic derived MCF-7CM, the more pronounced effects under hypoxic conditions suggests that breast cancer cells accelerate and increase their paracrine secretory effects on endothelial viability.

A study by Strilic et al. (2016) showed that cancer cells induced endothelial necroptosis in vitro and in vivo, which appears to be essential for the process of extravasation and metastasis of cancer cells [27]. Previous studies have shown that cancer cells under hypoxic conditions demonstrated both genetic and metabolic alteration [28–30], which promote their malignancy [31,32]. In view of the fact that cancer paracrine factor secretion has been reported to be different in normoxia and hypoxia [33], this might explain the difference in endothelial response against the stimulation with hypoxic and normoxic MCF7CM. Constant viability reduction of bEnd.3 cells exposed to MCF7 cells and the derived MCF7CM is an indicator that MCF7 paracrine exposure has the ability to impact mitochondrial function in a dose-related manner and that these effects are more pronounced when exposed to hypoxic-derived MCF7CM, indicates that under hypoxic conditions MCF7 cells scale-up their secretion of paracrine factors to induce long-term suppression of capillary brain endothelial cell viability.

#### 4.2. Mitochondrial Activity of bEnd.3 Cells after MCF7 Exposure

##### 4.2.1. Mitochondrial Membrane Potential ( $\Delta\Psi_m$ )

The suppressive effects of MCF7CM on the levels of mitochondrial dehydrogenase (viability) of bEnd.3 cells, motivated us to investigate the changes in the mitochondrial membrane potential ( $\Delta\Psi_m$ ). Physiologically, during oxidative phosphorylation, the proton pumps (Complexes I, III, and IV) transport hydrogen ions (positive charges) across the mitochondrial inner membrane, resulting in the mitochondrial membrane potential ( $\Delta\Psi_m$ ). This process is essential for generating a proton gradient which in turn drives the production of ATP [34]. In this process, an accumulation of  $H^+$  in the outer membrane space subsequently flows down an  $H^+$  -proton gradient back into the mitochondria via the ATP-producing F1/F0 ATP-synthase to complete the electron transport chain and drive the generation of ATP.

In the present study, bEnd.3 cells exposed to a selected concentration of MCF7CM show an increase in the mitochondrial membrane potential in comparison to the control. At the mitochondrial level, an accumulation of TMRE (positive charge) in the mitochondrial matrix yields high fluorescent intensity proportional to the  $\Delta\Psi_m$  polarization potential. The hyperpolarized state is a result of the transfer and accumulation of  $H^+$  in the outer mitochondrial intermembrane space. Mitochondrial hyperpolarization was more evident in bEnd.3 treated with hypoxic MCF7CM, presenting mitochondrial hyperpolarization after 24 h exposure to hypoxic MCF7CM (Figure 4), whereas bEnd.3 cells exposed to normoxic MCF7CM did not show a significant difference in TMRE fluorescent relative to the control (Figure 3). Mitochondrial hyperpolarization can occur as a result of the inhibition of ATPase activity. ATPase inhibition reduces the electrochemical gradient utilization, which results in less ATP generation and  $\Delta\Psi_m$  hyperpolarization [35,36]. Given the scope of the study, we only investigated the state of  $\Delta\Psi_m$  as an indicator for mitochondrial activity. However,



further study is suggested to determine the mechanism of mitochondrial hyperpolarization in brain endothelial cells in response to exposure of cancer cells.

#### 4.2.2. ATP Generation

Given the hyperpolarization of the BEC mitochondria exposed to hypoxically derived MCF7CM, we investigated the levels of ATP in treated BECs. The main function of mitochondria is ATP synthesis. Therefore, ATP generation is an accurate indicator of mitochondrial activity and cell viability [37]. Mitochondria are the major source of ATP generation (through oxidative phosphorylation) [38], with mitochondria yielding 36 ATP, compared to glycolysis (yielding only 2 ATP per glucose molecule) [39]. Cerebral endothelial cells possess more mitochondria than systemic endothelial cells, indicating the vital role of ATP in the regulatory processes across the BBB [40]. Dysfunction in endothelial mitochondria induces BBB disruption in vitro and in vivo [41]. In the present study, the investigation of ATP generation in brain endothelial cells under the influence of cancer was necessary. Therefore, bEnd.3 cells, chronically exposed to both MCF7 cells and their MCF7CM, were monitored for their ATP production using a luminescence assay. Results show a marked reduction of ATP generation in bEnd.3 cells co-cultured with MCF7 cells (Figure 5A) or exposed to normoxic (Figure 5B) or hypoxic MCF7CM (Figure 5C). The decrease in ATP level was observed after 48 h of exposure to 75% of MCF7CM. Taken together with the hyperpolarization of the  $\Delta\Psi_m$  after exposed to hypoxic MCF7CM, suppressed ATP levels confirm that MCF7 cells induce changes in the mitochondria activity in brain endothelial cells which might contribute in the BBB dysfunction. The hyperpolarization of the outer intermembrane space of the mitochondria suggests that one of the MCF7 derived paracrine affectively decouples  $H^+$  gradient into the matrix of the mitochondria and thereby suppresses the production of ATP.

#### 4.3. Transendothelial Electrical Resistance (TEER) of bEnd.3 Monolayers after Exposure to MCF7 Co-Culture

Endothelial cells are the functional site of the BBB [42]. They are connected by tight junctions, forming a barrier against the paracellular diffusion of molecules and ions into the brain [43]. Occludin and Claudin-5 are the most prominent proteins which form the brain endothelial tight junctions [44,45]. The expression of these proteins is critical for brain capillary (endothelial) integrity, and downregulation of these proteins decreases the brain endothelial resistance [46]. The present study demonstrated that TEER across monolayers of brain endothelial cells (bEnd.3) transiently decreased over a period of 36 h (Figure 7) after exposure to cocultured breast cancer cells (MCF7). This finding is supported by observations that showed that brain endothelial cells were induced in the presence of MCF7 cells to enhance the transmigration of breast cancer through the endothelium instead of providing a secure barrier against breast cancer cells [47]. Interestingly, although the decrease in the endothelial resistance under the treatment of normoxic MCF7CM was not constant, endothelial cells recovered after 24 h to control levels of transendothelial resistance (Figure 6A). This window of transient decreased TEER may indeed assist the breast cancer cells by providing a window for migration across the BBB. We also investigated whether co-culturing MCF7 cells with bEnd3 cells under hypoxic conditions (5%  $O_2$ ) would exacerbate the increased transient permeability (decreased TEER) observed during co-culture under normoxic conditions. Hypoxic conditions transiently decreased our control bEnd3 monolayers for 24 h, but these monolayers adapted within 24 h to normal control levels (Figure 7A). Under normoxic conditions, TEER decreased transiently and recovered to control levels (Figure 6A). However, in hypoxia cocultured bEnd.3 cells, this recovery was nullified by hypoxic conditions (Figure 7). The recovery of TEER of the control bEnd.3 cell monolayer within 24 h was in contrast to the bEnd.3 cell monolayer co-cultured with MCF7 cells, where continued hypoxia-induced long-term suppression of TEER over next 48 h (Figure 7: days six and seven). It is, therefore, indicative that hypoxia causes paracrine induced continued suppression of TEER (increased transendothelial permeability). It is well known that cancer cells modulate their metabolism to adapt to hypoxic

conditions, and thus the mechanism to disrupt the endothelial barrier may differ under hypoxic and normoxic conditions. Moreover, metastatic breast cancer secretes enzymes including matrix metalloproteinases [48], which are involved in the degradation of tight junction proteins [20]. The transient low TEER after exposure to hypoxia (Figure 7B) by bEnd.3 cells not co-cultured with MCF7 cells (control), which recovered to normal levels of TEER the next day, endorses recent reports that hypoxia can induce increase permeability (low TEER) in brain endothelial cells [49]. These conditions for hypoxia may be induced in the capillary by the arrest of circulating cancer cells to the apical membranes of brain capillary endothelia, thereby decreasing lumen effective diameter and reducing blood flow (which induces local hypoxic conditions for endothelial cells).

#### 4.4. Transendothelial Electrical Resistance of bEnd.3 Monolayers after Exposure to MCF7CM

The recording of TEER across most monolayers typically follows a biphasic response where TEER initially increases to a peak, plateaus and then gradually decreases. We compared peak TEER responses on days five and six after exposing bEnd3 monolayers with selected concentrations of MCF7CM under normoxic (21% O<sub>2</sub>) and hypoxic conditions (5% O<sub>2</sub>) (Figure 8). Under both normoxic and hypoxic MCF7CM treatment, peak TEER was suppressed. However, the suppression under normoxic derived MCF7CM was not statistically different from controls on day five, whereas already on day five hypoxic derived MCF7CM suppressed TEER significantly. It is clear that both normoxic and hypoxically derived MCF7CM induces a dose-response effect on TEER and that hypoxic conditions for cancer cells aggressively upscales this effect, producing effects on target capillary endothelia at a much faster rate and also more pronounced effect. However, the similar profiles of these effects suggest that mechanism whereby MCF7 cells deploy to affect changes on TEER occur via a similar molecular mechanism, and thus demands further investigation.

Although there is a clear dichotomy between treating bEnd.3 monolayers apically (luminal perspective) and coculturing MCF7 cells with bEnd3 cells from an abluminal perspective, a number of significant aspects must be noted: Firstly, our data indicate that these paracrine factors can produce similar effects on BECs, whether they are applied from the luminal or abluminal side of endothelial monolayers; and secondly, it speaks to the permeability of these paracrine factors with regards to the ease at which they cross the plasma membrane of the cells.

#### 4.5. The Effect of MCF7CM Exposure on the Tight Junctions (TJs) Expression

In this study, the TEER data (Figures 6–8) did not correlate with the gene expression of the tight junctions, Occludin and Claudin-5 (Figures 9 and 10, respectively). Normoxically derived MCF7CM had similar effects on both Occludin and Claudin-5 expression with increasing concentration of MCF7CM resulting in dose-related suppression in gene expression relative to treated samples. Relative to controls, only the lowest concentration of normoxically derived MCF7CM produced an elevated expression of Occludin. Surprisingly, hypoxically derived MCF7CM had no statistical effect relative to controls. However, bEnd.3 cells which were exposed to hypoxically derived MCF7CM, significantly produced an elevated expression of Claudin-5. Increased levels of Claudin-5 is usually correlated with increased TJs proteins at the apico-lateral membrane of endothelial cells, with the concomitant increase in TEER. However, our data always produced a decrease in TEER after exposure to MCF7CM. Thus, MCF7CM based paracrine factors may be involved in the prevention of the incorporation of TJ proteins at the apico-lateral membranes or the mechanism by which cancer secretions decrease the endothelial resistance is not mediated by the tight junction at the paracellular route, but via increased transcellular permeability resulting in the decrease in TEER. In view of reports that activated cancer cells release various types of metalloproteinase enzymes, which depredate the tight junction proteins [21], suggest that cancer cells would prefer to compromise paracellular spaces and in so doing provide a passage for metastatic cancer cells into the brain parenchyma. PCR reflects the

early protein expression components in the process of mRNA translation to a primary protein. However, before this primary protein is inserted into the membrane, the protein undergoes numerous post-translational modification steps before it is finally inserted into the membrane along with being attached to ZO molecules which connects the TJ protein to actin scaffolding proteins in the cytoplasm of the cell. We suspect that the paracrine factors secreted by the MCF-7 cells compromise one or several of these post-translational aspects compromising the insertion and/or the functional aspects of the TJ-proteins. We have seen in our lab that bEnd.3 cell confluent monolayers produce immunofluorescence to both Occludin and Claudin-5 (unpublished data), so we were surprised that our results did not show clear effects on mRNA transcription/translational processes for Occludin and Claudin-5. A limitation to the PCR data is that we do not have collaborating western blot data and immunofluorescent data, which may produce clues as to where MCF-7 paracrine factors are producing their effects on TJ proteins. Nevertheless, this requires additional investigation.

Furthermore, the less pronounced effects of MCF7CM on Occludin compared to Claudin-5 mRNA expression suggest that breast cancer cells target the Claudin-5 TJs pathways rather than Occludin. This postulate is supported by the fact that the tightness of paracellular spaces is dependent on Claudin-5 rather than Occludin [45].

## 5. Conclusions

Our study showed that breast cancer cells can affect brain capillary endothelial cells by modulating the function of mitochondria, leading to the decrease of generation of ATP with the concomitant effects of causing decrease cell viability, increase paracellular permeability by modulating especially Claudin-5 TJ expression. These induced effects on the brain endothelial capillary cell function show how breast cancer cells use paracrine factors to induce access into brain tissue. Our data show that hypoxic conditions produce exacerbated and accelerated effects on brain capillary endothelial cells. The dose-related responses of MCF7CM indicate that if the secretion of paracrine factors can be minimized, it could also decrease the ability of breast cancer cells to cross the BBB and metastasize CNS tissue. A low level of O<sub>2</sub> is considered as normoxia in some literature [31], and our results show that just by reducing O<sub>2</sub> concentration, breast cancer cells can trigger a more aggressive state. Since the research scope of this study was in vitro, and due to the limitation of the in vitro experiments (particularly in co-culture studies), the repeatability of the study in an in vivo system is recommended. One of the important outcomes of this study is the responsiveness of this brain endothelial cell line (bEnd3) to MCF7 co-culture and the treatment of MCF-7CM conditioned media. This supports our construct of an in vitro BBB model on which we can extensively study the effects of cancer cells on various physiological variables. These findings may help to develop new therapeutic targets to prevent cancer metastasis to the brain.

**Author Contributions:** Conceptualization, D.F. and M.R.; methodology, M.R.; software, D.F.; validation, D.F., B.F. and M.R.; formal analysis, M.R. and D.F.; investigation, M.R.; resources, D.F.; data curation, M.R. and D.F.; writing—original draft preparation, M.R.; writing—review and editing, D.F.; visualization, D.F.; supervision, D.F. and B.F.; project administration, D.F.; funding acquisition, D.F. All authors have read and agreed to the published version of the manuscript.

**Funding:** University of the Western Cape Senate grant.

**Institutional Review Board Statement:** The study was conducted according to the guidelines of the Declaration of Helsinki, and approved by the Institutional Review Board of the Research Office of the University of the Western Cape (Project registration no.: 20/5/9; January 2020).

**Informed Consent Statement:** Not applicable.

**Data Availability Statement:** All experimental data collected is archived within the University of the Western Cape (UWC) archives and is available as per UWC data and intellectual property policy guidelines and its associated copyright protection.



**Acknowledgments:** We acknowledge the SA-MRC (Cape Town) for their assistance and use of their laboratory infrastructure. In this regard, we especially want to thank Bianca Sansom for her insightful suggestions regarding our PCR experiments.

**Conflicts of Interest:** The authors declare no conflict of interest.

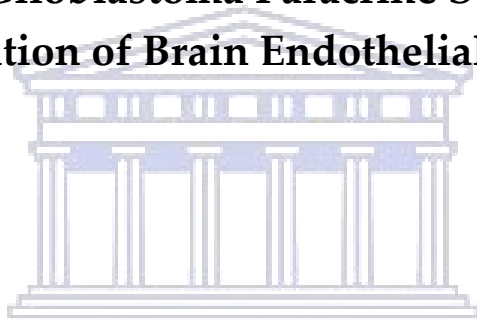
## References

- Serlin, Y.; Shelef, I.; Knyazer, B.; Friedman, A. Anatomy and physiology of the blood–brain barrier. *Semin. Cell Dev. Biol.* **2015**, *38*, 2–6. [\[CrossRef\]](#)
- Kadry, H.; Noorani, B.; Cucullo, L. A blood–brain barrier overview on structure, function, impairment, and biomarkers of integrity. *Fluids Barriers CNS* **2020**, *17*, 69. [\[CrossRef\]](#)
- Witzel, I.; Oliveira-Ferrer, L.; Pantel, K.; Müller, V.; Wikman, H. Breast cancer brain metastases: Biology and new clinical perspectives. *Breast Cancer Res.* **2016**, *18*, 8. [\[CrossRef\]](#)
- Woodward, J. Crossing the endothelium. *Cell Adhes. Migr.* **2008**, *2*, 151–152. [\[CrossRef\]](#) [\[PubMed\]](#)
- Herman, H.; Fazakas, C.; Haskó, J.; Molnár, K.; Mészáros, Á.; Nyúl-Tóth, Á.; Szabó, G.; Erdélyi, F.; Ardelean, A.; Hermenean, A.; et al. Paracellular and transcellular migration of metastatic cells through the cerebral endothelium. *J. Cell. Mol. Med.* **2019**, *23*, 2619–2631. [\[CrossRef\]](#) [\[PubMed\]](#)
- Labelle, M.; Hynes, R.O. The initial hours of metastasis: The importance of cooperative host–tumor cell interactions during hematogenous dissemination. *Cancer Discov.* **2012**, *2*, 1091–1099. [\[CrossRef\]](#) [\[PubMed\]](#)
- Reymond, N.; D’Agua, A.B.B.; Ridley, A. Crossing the endothelial barrier during metastasis. *Nat. Rev. Cancer* **2013**, *13*, 858–870. [\[CrossRef\]](#) [\[PubMed\]](#)
- Haskó, J.; Fazakas, C.; Molnár, K.; Mészáros, Á.; Patai, R.; Szabó, G.; Erdélyi, F.; Nyúl-Tóth, Á.; Györi, F.; Kozma, M.; et al. Response of the neurovascular unit to brain metastatic breast cancer cells. *Acta Neuropathol. Commun.* **2019**, *7*, 133. [\[CrossRef\]](#)
- Strilic, B.; Offermanns, S. Intravascular survival and extravasation of tumor cells. *Cancer Cell* **2017**, *32*, 282–293. [\[CrossRef\]](#)
- Wirtz, P.; Konstantopoulos, D.; Searson, K. Mechanical forces in metastasis. *Biomol. Eng.* **2012**, *11*, 512–522. [\[CrossRef\]](#)
- Leong, H.; Robertson, A.E.; Stoleto, K.; Leith, S.J.; Chin, C.A.; Chien, A.E.; Hague, M.N.; Ablack, A.; Carmine-Simmen, K.; McPherson, V.A.; et al. Invadopodia are required for cancer cell extravasation and are a therapeutic target for metastasis. *Cell Rep.* **2014**, *8*, 1558–1570. [\[CrossRef\]](#)
- Lambert, A.W.; Pattabiraman, D.; Weinberg, R.A. Emerging biological principles of metastasis. *Cell* **2017**, *168*, 670–691. [\[CrossRef\]](#) [\[PubMed\]](#)
- Li, W.; Khan, M.; Mao, S.; Feng, S.; Lin, J.-M. Advances in tumor-endothelial cells co-culture and interaction on microfluidics. *J. Pharm. Anal.* **2018**, *8*, 210–218. [\[CrossRef\]](#) [\[PubMed\]](#)
- Khodarev, N.N.; Yu, J.; Labay, E.; Darga, T.; Brown, C.K.; Mauceri, H.J.; Yassari, R.; Gupta, N.; Weichselbaum, R.R. Tumour-endothelium interactions in co-culture: Coordinated changes of gene expression profiles and phenotypic properties of endothelial cells. *J. Cell Sci.* **2003**, *116*, 1013–1022. [\[CrossRef\]](#)
- Hoffmann, O.I.; Ilmberger, C.; Magosch, S.; Joka, M.; Jauch, K.-W.; Mayer, B. Impact of the spheroid model complexity on drug response. *J. Biotechnol.* **2015**, *205*, 14–23. [\[CrossRef\]](#) [\[PubMed\]](#)
- Wilhelm, I.; Molnár, J.; Fazakas, C.; Haskó, J.; Krizbai, I.A. Role of the blood-brain barrier in the formation of brain metastases. *Int. J. Mol. Sci.* **2013**, *14*, 1383–1411. [\[CrossRef\]](#)
- Mierke, C.T. Role of the endothelium during tumor cell metastasis: Is the endothelium a barrier or a promoter for cell invasion and metastasis? *J. Biophys.* **2008**, *2008*, 183516. [\[CrossRef\]](#)
- Shenoy, A.K.; Lu, J. Cancer cells remodel themselves and vasculature to overcome the endothelial barrier. *Cancer Lett.* **2014**, *380*, 534–544. [\[CrossRef\]](#)
- Feng, S.; Cen, J.; Huang, Y.; Shen, H.; Yao, L.; Wang, Y.; Chen, Z. Matrix metalloproteinase-2 and -9 secreted by leukemic cells increase the permeability of blood-brain barrier by disrupting tight junction proteins. *PLoS ONE* **2011**, *6*, e20599. [\[CrossRef\]](#)
- Rempe, R.G.; Hartz, A.M.S.; Bauer, B. Matrix metalloproteinases in the brain and blood–brain barrier: Versatile breakers and makers. *J. Cereb. Blood Flow Metab.* **2016**, *36*, 1481–1507. [\[CrossRef\]](#)
- Roomi, M.W.; Kalinovsky, T.; Rath, M.; Niedzwiecki, A. Modulation of MMP-2 and MMP-9 secretion by cytokines, inducers and inhibitors in human glioblastoma T-98G cells. *Oncol. Rep.* **2017**, *37*, 1907–1913. [\[CrossRef\]](#) [\[PubMed\]](#)
- Srinivasan, B.; Kolli, A.R.; Esch, M.B.; Abaci, H.E.; Shuler, M.L.; Hickman, J.J. TEER measurement techniques for in vitro barrier model systems. *J. Lab. Autom.* **2015**, *20*, 107–126. [\[CrossRef\]](#)
- Pfaffl, M.W. Relative expression software tool (REST(C)) for group-wise comparison and statistical analysis of relative expression results in real-time PCR. *Nucleic Acids Res.* **2002**, *30*, e36. [\[CrossRef\]](#)
- Kamiloglu, S.; Sari, G.; Ozdal, T.; Capanoglu, E. Guidelines for cell viability assays. *Food Front.* **2020**, *1*, 332–349. [\[CrossRef\]](#)
- Stockert, J.C.; Blázquez-Castro, A.; Cañete, M.; Horobin, R.W.; Villanueva, Á. MTT assay for cell viability: Intracellular localization of the formazan product is in lipid droplets. *Acta Histochem.* **2012**, *114*, 785–796. [\[CrossRef\]](#) [\[PubMed\]](#)
- Romani, A.M. *Physiology and Pathology of Mitochondrial Dehydrogenases*; IntechOpen: London, UK, 2018. [\[CrossRef\]](#)
- Strilic, B.; Yang, L.; Albarran-Juarez, J.; Wachsmuth, L.; Han, K.; Müller, K.H.U.C.; Pasparakis, L.W.M.; Offermanns, S. Tumour-cell-induced endothelial cell necroptosis via death receptor 6 promotes metastasis. *Nature* **2016**, *536*, 215–218. [\[CrossRef\]](#)

28. Strese, S.; Fryknäs, M.; Larsson, R.; Gullbo, J. Effects of hypoxia on human cancer cell line chemosensitivity. *BMC Cancer*. **2013**, *13*, 331. [\[CrossRef\]](#) [\[PubMed\]](#)
29. Al Tameemi, W.; Dale, T.P.; Al-Jumaily, R.M.K.; Forsyth, N.R. Hypoxia-modified cancer cell metabolism. *Front. Cell Dev. Biol.* **2019**, *7*, 4. [\[CrossRef\]](#)
30. Nejad, A.E.; Najafgholian, S.; Rostami, A.; Sistani, A.; Shojaeifar, S.; Esparvarinha, M.; Nedaeinia, R.; Javanmard, S.H.; Taherian, M.; Ahmadi, M.; et al. The role of hypoxia in the tumor microenvironment and development of cancer stem cell: A novel approach to developing treatment. *Cancer Cell Int.* **2021**, *21*, 62. [\[CrossRef\]](#)
31. Muz, B.; de la Puente, P.; Azab, F.; Azab, A.K. The role of hypoxia in cancer progression, angiogenesis, metastasis, and resistance to therapy. *Hypoxia* **2015**, *3*, 83–92. [\[CrossRef\]](#)
32. Petrova, V.; Annicchiarico-Petruzzelli, M.; Melino, G.; Amelio, I. The hypoxic tumour microenvironment. *Oncogenesis* **2018**, *7*, 10. [\[CrossRef\]](#)
33. Eilertsen, M.; Pettersen, I.; Andersen, S.; Martinez, I.; Donnem, T.; Busund, L.-T.; Bremnes, R.M. In NSCLC, VEGF—A response to hypoxia may differ between squamous cell and adenocarcinoma histology. *Anticancer Res.* **2012**, *32*, 4729–4736.
34. Zorova, L.D.; Popkov, V.A.; Plotnikov, E.Y.; Silachev, D.N.; Irina, B.; Jankauskas, S.S.; Babenko, V.A.; Zorov, S.D.; Balakireva, V.; Juhaszova, M.; et al. Mitochondrial membrane potential. *Anal. Biochem.* **2018**, *552*, 50–59. [\[CrossRef\]](#)
35. Gergely, P.; Grossman, C.; Niland, B.; Puskas, F.; Neupane, H.; Allam, F.; Banki, K.; Phillips, P.E.; Perl, A. Mitochondrial hyperpolarization and ATP depletion in patients with systemic lupus erythematosus. *Arthritis Rheum.* **2002**, *46*, 175–190. [\[CrossRef\]](#)
36. Forkink, M.; Manjeri, G.R.; Liemburg-Apers, D.; Nibbeling, E.; Blanchard, M.; Wojtala, A.; Smeitink, J.A.; Wieckowski, M.; Willems, P.H.; Koopman, W.J. Mitochondrial hyperpolarization during chronic complex I inhibition is sustained by low activity of complex II, III, IV and V. *Biochim. Biophys. Acta (BBA) Bioenerg.* **2014**, *1837*, 1247–1256. [\[CrossRef\]](#) [\[PubMed\]](#)
37. Ian, P.; Lanza, R.; Sreekumaran, K.; Nair, M.D. Mitochondrial metabolic function assessed in vivo and in vitro. *Curr. Opin. Clin. Nutr. Metab. Care* **2010**, *13*, 511–517. [\[CrossRef\]](#)
38. Kühlbrandt, W. Structure and function of mitochondrial membrane protein complexes. *BMC Biol.* **2015**, *13*, 89. [\[CrossRef\]](#) [\[PubMed\]](#)
39. Strickland, M.; Stoll, E.A. Metabolic reprogramming in glioma. *Front. Cell Dev. Biol.* **2017**, *5*, 43. [\[CrossRef\]](#) [\[PubMed\]](#)
40. Wong, B.W.; Marsch, E.; Treps, L.; Baes, M.; Carmeliet, P. Endothelial cell metabolism in health and disease: Impact of hypoxia. *EMBO J.* **2017**, *36*, 2187–2203. [\[CrossRef\]](#)
41. Doll, D.N.; Hu, H.; Sun, J.; Lewis, S.E.; Simpkins, J.W.; Ren, X. Mitochondrial crisis in cerebrovascular endothelial cells opens the blood–brain barrier. *Stroke* **2015**, *46*, 1681–1689. [\[CrossRef\]](#)
42. Sweeney, M.D.; Zhao, Z.; Montagne, A.; Nelson, A.R.; Zlokovic, B.V. Blood-brain barrier: From physiology to disease and back. *Physiol. Rev.* **2019**, *99*, 21–78. [\[CrossRef\]](#) [\[PubMed\]](#)
43. Krouwer, V.J.D.; Hekking, L.H.P.; Langelaar-Makkinje, M.; Regan-Klapisz, E.; Post, J.A. Endothelial cell senescence is associated with disrupted cell-cell junctions and increased monolayer permeability. *Vasc. Cell* **2012**, *4*, 12. [\[CrossRef\]](#) [\[PubMed\]](#)
44. Liebner, S.; Kniesel, U.; Kalbacher, H.; Wolburg, H. Correlation of tight junction morphology with the expression of tight junction proteins in blood-brain barrier endothelial cells. *Eur. J. Cell Biol.* **2000**, *79*, 707–717. [\[CrossRef\]](#) [\[PubMed\]](#)
45. Fisher, D.; Mentor, S. Are claudin-5 tight-junction proteins in the blood-brain barrier porous? *Neural Regen. Res.* **2020**, *15*, 1838–1839. [\[CrossRef\]](#) [\[PubMed\]](#)
46. Liu, W.-Y.; Wang, Z.-B.; Zhang, L.-C.; Wei, X.; Li, L. Tight junction in blood-brain barrier: An overview of structure, regulation, and regulator substances. *CNS Neurosci. Ther.* **2012**, *18*, 609–615. [\[CrossRef\]](#)
47. Lee, K.Y.; Kim, Y.-J.; Yoo, H.; Lee, S.H.; Park, J.B.; Kim, H.J. Human brain endothelial cell-derived COX-2 facilitates extravasation of breast cancer cells across the blood-brain barrier. *Anticancer Res.* **2011**, *31*, 4307–4313.
48. Mehner, C.; Hockla, A.; Miller, E.; Ran, S.; Radisky, D.C.; Radisky, E.S. Tumor cell-produced Matrix Metalloproteinase 9 (MMP-9) drives malignant progression and metastasis of basal-like triple negative breast cancer. *Oncotarget* **2014**, *5*, 2736–2749. [\[CrossRef\]](#) [\[PubMed\]](#)
49. Luo, P.-L.; Wang, Y.-J.; Yang, Y.-Y.; Yang, J.-J. Hypoxia-induced hyperpermeability of rat glomerular endothelial cells involves HIF-2 $\alpha$  mediated changes in the expression of occludin and ZO-1. *Braz. J. Med. Biol. Res.* **2018**, *51*, 1–7. [\[CrossRef\]](#) [\[PubMed\]](#)

## CHAPTER 4

**PUBLISHED MANUSCRIPT “The Effect of Normoxic and Hypoxic U-87 Glioblastoma Paracrine Secretion on the Modulation of Brain Endothelial Cells”**



UNIVERSITY *of the*  
WESTERN CAPE

## Article

# The Effect of Normoxic and Hypoxic U-87 Glioblastoma Paracrine Secretion on the Modulation of Brain Endothelial Cells

Mariam Rado <sup>1</sup>, Brian Flepisi <sup>2</sup> and David Fisher <sup>1,\*</sup> 

<sup>1</sup> Medical Bioscience Department, Faculty of Natural Sciences, University of the Western Cape, Robert Sobukwe Road, Bellville 7535, South Africa; 3580480@myuwc.ac.za

<sup>2</sup> Department of Pharmacology, Faculty of Health Sciences, University of Pretoria, 9 Bophelo Road, Pretoria 0002, South Africa; brian.flepisi@up.ac.za

\* Correspondence: dfisher@uwc.ac.za; Tel.: +27-21-959-2185

**Abstract:** Background: Glioblastoma multiforme (GBM) is a highly invasive brain tumour, characterized by its ability to secrete factors promoting its virulence. Brain endothelial cells (BECs) in the GBM environment are physiologically modulated. The present study investigated the modulatory effects of normoxically and hypoxically induced glioblastoma U-87 cell secretions on BECs. Methods: Conditioned media (CM) were derived by cultivating U-87 cells under hypoxic incubation (5% O<sub>2</sub>) and normoxic incubation (21% O<sub>2</sub>). Treated bEnd.3 cells were evaluated for mitochondrial dehydrogenase activity, mitochondrial membrane potential ( $\Delta\Psi_m$ ), ATP production, transendothelial electrical resistance (TEER), and endothelial tight-junction (ETJ) gene expression over 96 h. Results: The coculture of bEnd.3 cells with U-87 cells, or exposure to either hypoxic or normoxic U-87CM, was associated with low cellular viability. The  $\Delta\Psi_m$  in bEnd.3 cells was hyperpolarized after hypoxic U-87CM treatment ( $p < 0.0001$ ). However, normoxic U-87CM did not affect the state of  $\Delta\Psi_m$ . BEC ATP levels were reduced after being cocultured with U-87 cells, or with hypoxic and normoxic CM ( $p < 0.05$ ). Suppressed mitochondrial activity in bEnd.3 cells was associated with increased transendothelial permeability, while bEnd.3 cells significantly increased the gene expression levels of ETJs ( $p < 0.05$ ) when treated with U-87CM. Conclusions: Hypoxic and normoxic glioblastoma paracrine factors differentially suppressed mitochondrial activity in BECs, increasing the BECs' barrier permeability.

**Keywords:** glioblastoma multiforme; U-87 cells; tumour secretome; paracrine effects; tumour hypoxia; brain endothelial cells; bEnd.3 cells; blood-brain barrier



**Citation:** Rado, M.; Flepisi, B.; Fisher, D. The Effect of Normoxic and Hypoxic U-87 Glioblastoma Paracrine Secretion on the Modulation of Brain Endothelial Cells. *Cells* **2022**, *11*, 276. <https://doi.org/10.3390/cells11020276>

Academic Editor: David Qian

Received: 20 December 2021

Accepted: 7 January 2022

Published: 14 January 2022

**Publisher's Note:** MDPI stays neutral with regard to jurisdictional claims in published maps and institutional affiliations.



**Copyright:** © 2022 by the authors. Licensee MDPI, Basel, Switzerland. This article is an open access article distributed under the terms and conditions of the Creative Commons Attribution (CC BY) license (<https://creativecommons.org/licenses/by/4.0/>).

## 1. Introduction

Brain endothelial cells (BECs) are the main functional and regulatory components of the blood-brain barrier (BBB). They are characterized by the presence of continuous apicolateral zones of structural proteins called tight junctions (TJs) which link the BECs together, thus significantly limiting the paracellular flux of solutes and the movement of blood-borne cells into the brain. The regulatory function of BECs is modulated by both astrocytes and pericytes, the former enveloping more than 99% of the external surface of the brain's capillary endothelium with their "endfoot" processes, which provides regulatory feedback from the neuronal environment to the endothelium of brain capillaries [1]. TJs between the cerebral endothelial paracellular spaces have been reported to be more rigorous than in other tight epithelia in the body [2]. Nevertheless, the BBB was reported to be structurally and functionally disrupted by the fast-growing and aggressive brain tumour called glioblastoma multiforme (GBM), also referred to as a grade IV astrocytoma [3,4]. Furthermore, the GBM local environment causes BECs to develop abnormal phenotypes demonstrating hyperplastic and heterogeneous sizes and shapes [5].

GBM is the most malignant type of brain tumour [6], presenting a high mortality rate despite the therapeutic approaches, including surgery, chemotherapy, and radiotherapy.

GBM patients have a median overall survival of approximately 15 months [7] and represent 50% of all malignant, aggressive primary brain tumours in humans [8].

Morphologically, GBM tumours can be differentiated into three zones depending on their proximity to the blood vessels (source of O<sub>2</sub>), including the perivascular zone (GBM surrounded by blood vessels), the hypoxic zone (in the core of the GBM tumour tissue), and the invasive zone (that area of the tumour surrounded the vascular zone) [9]. GBM cells in these zones are functionally different, largely based on the O<sub>2</sub> availability. GBM in the perivascular zone causes an abnormally high rate of angiogenesis due to the increased secretion of paracrine factors that cause disorganized blood-vessel formation. In contrast, GBM cells in the hypoxic zone have a low proliferation level with a high expression of hypoxia-inducible factors (HIF) which modulate cellular homeostasis. In the invasive zone, hypoxic GBM cells infiltrate the surrounding tissue toward the blood vessels to take advantage of nutrition and O<sub>2</sub> availability, and also migrate to other sites in the brain. During this process, GBM cells interact with brain stromal cells, such as astrocytes and endothelial cells [10,11]. Factors expressed in endothelial cells (bradykinin, EphrinB2, and interleukin (IL-8)), and in GBM cells (EGFRvIII and MDGI) are thought to be implicated in the chemotaxis of migratory GBM cells across the brain endothelial cells [12]. Clinically, the main problem of GBM is the formation of oedema and the increase of the intracerebral pressure due to the disruption of the BBB at the level of the brain capillary endothelial cell [3,13].

The interaction between GBM cells and the surrounding stromal cells (particularly BECs) is crucial in developing the tumour environment and for tumour progression [14,15]. Both in vitro and in vivo studies have demonstrated that GBM cells secrete paracrine factors [16]. This interaction of the cellular components in the GBM microenvironment is mediated by the secretion of various factors from GBM [16,17], which have autocrine or paracrine effects [18,19]. Invasive cancer cells are characterized by secreted factors that increase their malignancy. These factors are thought to facilitate invasive events, such as the degradation of extracellular matrix (ECM) components, cell detachment, and migration through the basement membrane. Glioblastoma is reported to secrete various types of proteins. In a comparative study to quantify the proteins in the conditioned media of three glioblastoma cell lines (LN18, U118, and U-87), the number of proteins in the U-87 conditioned media was significantly higher than the other cell lines [20]. Glioblastoma releases extracellular vesicles (EVs), carrying molecules such as proteins and microRNAs (miRNAs), vascular growth factors, and IL-6,8, which play a role in inducing BBB breakdown. [16,21]

Although the GBM-induced pathological features in brain endothelial cell morphology have been extensively reported [22–25], it is still unclear by which mechanisms GBM influences the metabolism of BECs. As it is well known that fast-growing and aggressive tumours outpace tumour angiogenesis and develop various intratumour zones of O<sub>2</sub> deprivation (hypoxia) [26], the current study aimed to evaluate whether glioblastoma U87 cells or their secretome (supernatant) produced under hypoxic (5% O<sub>2</sub>) and normoxic (21% O<sub>2</sub>) conditions would differentially modulate the metabolism in brain endothelial cells, particularly with respect to mitochondrial activity. Using a brain endothelial cell line (bEnd.3 cells), which is well described in the literature [27], the current study investigated the effects of coculturing glioblastoma cells (U-87 cells), and treatment with selected concentrations of their supernatant-derived conditioned media on bEnd.3 cells' mitochondrial activity (dehydrogenase activity, mitochondrial membrane potential, and ATP production), and on the permeability across confluent monolayers of bEnd.3 cells (transendothelial electrical resistance (TEER)).

## 2. Materials and Methods

### 2.1. Cell Culture and Supernatant Collection

The murine brain microvascular endothelial cell line (bEnd.3 ATCC® CRL-2299, Gaithersburg, MD, USA) and the invasive human glioblastoma cell line (U-87 MG, ATCC HTB-14, 10801 University Boulevard, Manassas, VA, USA) were cultured in complete Dulbecco's Mod-



ified Eagle Medium ((DMEM), Gibco, No. 22320022, 8717 Grovemont Cir, Gaithersburg, MD, USA), supplemented with 10% fetal bovine serum ((FBS), Biowest, No. 10493-106, 2 Rue du Vieux Bourg, Nuaille, France), and 100 U/mL penicillin/streptomycin (Gibco, No. 15070063) (Complete DMEM)). TrypLE™ Express Enzyme (Thermo Fisher Scientific, No. A1285901, 168 Third Avenue, Waltham, MA, USA) was used for harvesting the cells.

The U-87 cells' supernatant was collected to prepare the U-87 conditioned medium (U-87CM), as follows: U-87 cells were grown in 75 cm<sup>2</sup> culture flasks ( $1 \times 10^5$ /flask) in a normal, humidified 5% CO<sub>2</sub> incubator at 37 °C until they reached 50% confluence; then, the spent growth media were replaced with a fresh complete DMEM. Cells were further incubated either under hypoxic (5% O<sub>2</sub>) or normoxic (21% O<sub>2</sub>) conditions. The incubation under hypoxic conditions was performed by placing the tissue culture flasks in a sterilized modular incubator hypoxia chamber (MIC 101; Billups–Rothenberg, Inc., Sorrento Valley Blvd, San Diego, CA, USA). The hypoxia chamber is provided with a Greisinger oxygen meter with a sensor (GOX 100-0-CO, No. 600437), which allows for the measurement of O<sub>2</sub> levels during the incubation time. After 48 h of incubation in hypoxic or normoxic conditions, the supernatant was collected in ice-cooled centrifuged tubes, centrifuged at 3500 rpm for 5 min at 4 °C, and then filtered with a GVS filter (0.20 µm) (Bio-Smart Scientific, Park Edge Mews, Edgemoor, Link Way, Edgemoor, Cape Town, South Africa). The supernatants were collected and aliquoted in 2–5 mL cryovials and stored at −80 °C.

## 2.2. bEnd.3 Cells Exposure to U-87 Conditioned Media (CM)

The collected U-87 supernatants were thawed at room temperature (21 °C) and added to fresh complete DMEM at concentrations of 20%, 40%, and 75%. This was subsequently referred to as U-87 conditioned media (U-87CM). The bEnd.3 monoculture cells were seeded at various seeding densities, depending on the assay to be conducted and incubated, in a 5% CO<sub>2</sub> incubator at 37 °C for 24 h to allow the cells to attach. Following 24 h incubation, the spent growth media were removed, cells were then exposed to either 20%, 40%, or 75% U-87CM for 24, 48, 72, and 96 h. All media were replaced daily to ensure the continuity of the concentrations used, and to maintain sufficient metabolic substrates for the normal functioning of the cell cultures.

## 2.3. Experimental Design

The study was designed to study the physiological changes in brain endothelial cells bEnd.3 under the influence of U-87 cells. The experiments were carried out in triplicate as a minimum ( $n = 3$ ) and duplicated to ensure repeatability. The effect of normoxic and hypoxic cancerous factors secreted from U-87 cells was compared by treating cultures or monolayers of bEnd.3 cells with selected concentrations of U-87CM or by growing the bEnd.3 cells in a coculture with U-87 cells (Figure 1).

For the in vitro model of the BBB, the bicameral chamber system was used, where the well assumes the abluminal side of the capillary endothelium, while the apical chamber (the insert) assumes the luminal side of the capillary. This allowed for U-87 cells to be cultured in wells, while a three-legged insert (Merck–Millipore, PIHA01250, 6 Hatters Ln, Watford, UK) was used for growing the brain endothelial cell monolayers. These three-legged inserts also facilitated the movement of inserts between varying treatment conditions, e.g., normoxic versus hypoxic conditions.

To ensure the U-87CM had sufficient metabolic constituents, a minimum of 25% fresh growth media (DMEM) was added to the U-87CM to make up the selected treatment concentrations (20%, 40%, and 75%). Furthermore, the U-87 cell cultures were grown to 50% confluency and exposed for a maximum of 48 h, prior to the collection of supernatants and preparation for experimentation. In addition, media for treating cells were replaced daily to ensure continuity in our treatment process.

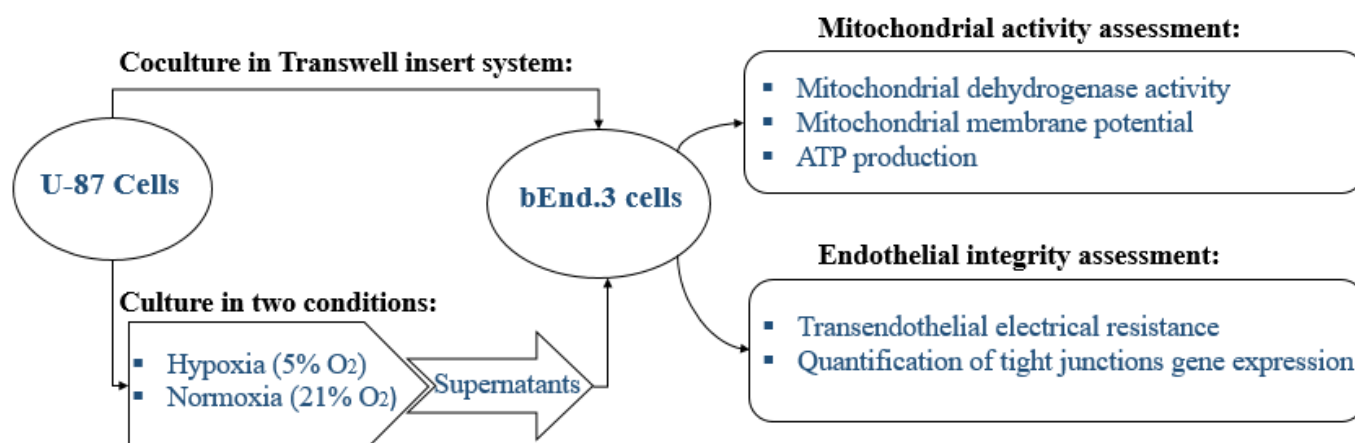


**Figure 1.** A schematic diagram of the research design to study the effect of the paracrine factors secreted by U-87 cells on bEnd.3 cells.

In addition, the lower level of O<sub>2</sub> used in the current study was 5% to avoid compromising the viability of the bEnd.3 cells when cocultured under hypoxic conditions. The current study confirmed that bEnd.3 cell monolayers were indeed sensitive to 5% O<sub>2</sub>, but can recover within 24 h to control levels of permeability.

## 2.4. Experiments

### 2.4.1. Cell Viability Assessment

For the determination of cell viability, the bEnd.3 were seeded on Transwell® inserts (pore size of 0.45 µm, insert diameter of 12 mm, and an effective filtration area of 0.6 cm<sup>2</sup>) (Merck–Millipore, PIHA01250, 6 Hatters Ln, Watford, UK) at a density of  $5 \times 10^5$  cells/insert; the inserts were placed in 24-well plates (Bio-Smart Scientific, No. 30024, Park Edge Mews, Link Way, Edgemoor, Cape Town, South Africa). Growth media (completed DMEM) were added to both the luminal (300 µL) and basolateral sides (800 µL), cells were incubated at 37 °C under 5% CO<sub>2</sub> overnight, allowing them to attach to the surface of the filter membrane. The U-87 cells were separately seeded in 12-well plates (Bio-Smart Scientific, No. 30012) at a density of  $2 \times 10^5$  cells/well on the same day.

Following 24 h of incubation, bEnd.3 cells were cocultured with U-87 cells by placing the inserts with bEnd.3 cells in the 12-well plates containing U-87 cells (NB: 12-well plates were used, as these wells provided a greater surface area for the U-87 cells, and thus potentiated the cancer paracrine effect). Plates were incubated at 37 °C with 5% CO<sub>2</sub> for 96 h. Then, the inserts were removed from the 12-well plates and placed in new 24-well plates. This was important to ensure that only the BECs were assayed for viability and were not cross-contaminated with U-87 cells. In brief, 100 µL of XTT solution was added to each insert, and the cells were incubated for an additional 4 h at 37 °C and 5% CO<sub>2</sub>. Then, the media from the inserts were transferred into 96-well plates (SPL Life Sciences, No. 30096, 26, Geumgang-ro 2047 beon-gil, Naechon-myeon, Pocheon-si, Gyeonggi-do, Korea). The absorbance was measured at 450 nm by using a microplate reader (POLARstar Omega B.M.G. Labtech, Allmendgrün 8, Ortenberg, Germany).

In addition, the bEnd.3 cells were seeded in 96-well plates (SPL Life Sciences, No. 30096) at a density of  $4 \times 10^3$  cells/well, the cells were incubated for 24 h, and treated with U-87CM, as previously described. Following the treatment, the viability of bEnd.3 cells were determined using an XTT assay kit (Roche, No. 11465015001) in 24 h intervals up to 96 h. At each 24 h interval, 50 µL of XTT solution was added to each well, the cells were then incubated for 4 h at 37 °C in a 5% CO<sub>2</sub> incubator. The absorbance was then measured at 450 nm using a microplate reader (POLARstar Omega B.M.G. Labtech).



#### 2.4.2. Mitochondrial Activity Assays

##### Mitochondrial Membrane Potential ( $\Delta\psi_m$ )

Changes in  $\Delta\psi_m$  in bEnd.3 cells after exposure to U-87CM were analysed using tetramethylrhodamine ethylesterperchlorate (TMRE) assay (Thermo Fisher Scientific, No. T669, 168 Third Avenue, Waltham, MA, USA). TMRE is a permeable cationic, lipophilic dye, emitting red-orange fluorescent. It is taken up by active mitochondria into the negatively charged mitochondrial matrix. The intensity of the fluorescent signal obtained is indicative of the  $\Delta\psi_m$ . The higher membrane potential (more polarised) indicates more TMRE accumulation in the mitochondrial matrix [28]. Therefore, the higher red-orange fluorescence would indicate a higher membrane potential (also called hyperpolarisation). In this assay, the bEnd.3 cells were seeded in flasks at a density of  $3 \times 10^4$  cells per flask and treated as previously described. In addition, bEnd.3 were also treated with carbonyl cyanide-3-chlorophenyl hydrazone (CCCP) (Sigma, Eschenstr., Taufkirchen, Germany) as a negative control. The CCCP is a classic oxidative phosphorylation uncoupler, causing the predictable decrease of the  $\Delta\psi_m$  and was, therefore, used as a negative control. Furthermore, CCCP was used to confirm that the uptake of the TMRE was related to the mitochondrial membrane potential. At 24 h intervals, 100  $\mu$ M of CCCP was added and incubated for 10 min before staining with TMRE (at 300 nM for 20 min). The solution stain was then removed, and cells were washed twice with PBS. Cells were then scraped and lysed in a lysis buffer composed of SDS (0.1% v/v) in 0.1 M Tris-HCl buffer. The 150  $\mu$ L of the lysates were loaded in 96-well plates. The fluorescence of TMRE was measured with a multiwell fluorescence plate reader (POLARstar Omega B.M.G. Labtech), with excitation and emission set at  $508 \pm 20$  nm and  $589 \pm 40$  nm, respectively. A total protein concentration was then determined in the remaining lysate samples, corresponding in their lysates using a bicinchoninic acid (BCA) kit (Thermo Fisher Scientific, No. 232225). The fluorescence in each well was normalized for the protein concentration of its corresponding lysate.

##### ATP Generation

Relative intracellular ATP levels were determined using the Mitochondrial ToxGlo™ kit (Promega (G8000), 2800 Woods Hollow Road, Madison, WI, USA). The Mitochondrial ToxGlo™ assay was conducted according to the supplier's protocol. An ATP detection solution was prepared by mixing 10 mL of ATP buffer with an ATP detection substrate. The components were homogenized by vortex to form an ATP detection solution.

To measure the ATP level in bEnd.3 cells cocultured with glioblastoma U-87 cells, bEnd.3 were seeded on Transwell® inserts (pore size of 0.45  $\mu$ m, filtration diameter of 12 mm, and an effective filtration area of 0.6 cm<sup>2</sup>) at a density of  $2 \times 10^3$  cells/insert; the inserts were placed in 24-well plates. Growth media (complete DMEM) were added to both the luminal (300  $\mu$ L) and basolateral sides (800  $\mu$ L), and cells were incubated at 37 °C under 5% CO<sub>2</sub> overnight. The U-87 cells were separately seeded at a density of  $1 \times 10^3$  cells/well on the same day in 12-well plates. Following 24 h incubation, bEnd.3 on the inserts were placed in the 12-well plates where U-87 cells were growing on the well bottoms. The coculture cells were incubated at 37 °C under 5% CO<sub>2</sub> for 96 h. The inserts were then removed from the 12-well plates and placed in new 24-well plates. Then, 100  $\mu$ L of ATP detection solution was added to each insert. Cells were then incubated for an additional 5 min at room temperature in a plate shaker. The mixture from the inserts was transferred into white 96-well plates (SPL Life Sciences, No. 31396). The luminescence was measured using a microplate reader (POLARstar Omega B.M.G. Labtech).

In addition, bEnd.3 cells were seeded ( $1 \times 10^3$  cells/well) in white 96-well plates (SPL Life Sciences, No. 31396) and exposed to the U-87CM, as previously described. At 24 h intervals, 100  $\mu$ L of ATP detection solution was added to each well. Then, the plates were incubated for 5 min at room temperature on a plate shaker. ATP content was measured using a luminescent plate reader (POLARstar Omega B.M.G. Labtech).

#### 2.4.3. Transendothelial Electrical Resistance (TEER)

Brain endothelial monolayer integrity was tested by determining the transendothelial electrical resistance (TEER) using the EVOM TEER measurement system (EVOM: American Laboratory Trading Inc., 12 Colton Road, East Lyme, CT, USA). The bEnd.3 cells were grown on filter membranes (Transwell® inserts with 0.45 µm pore size) at a density of  $5 \times 10^4$  cells/insert. The U-87 cells were seeded in 12-well plates. To evaluate the effect of U-87 cells on the integrity of bEnd.3 monolayer under normoxia (21% O<sub>2</sub>), both cell lines were first grown separately for 96 h; then, the inserts with bEnd.3 cells were placed in the 12-well plates containing the established U-87 cells. The cocultured cells were incubated in normoxic conditions, and TEER was measured daily, starting on day 2.

To evaluate the effect of U-87 cells on bEnd.3 cells under hypoxia, both bEnd.3 and U-87 cells were grown separately in similar conditions as above for 72 h, and the two cell lines were cocultured by placing the bEnd.3 inserts in the 12-well plates containing the U-87 cells. The cocultured cells were incubated in normoxic conditions (21% O<sub>2</sub>) for 24 h, and then incubated under hypoxic conditions (5% O<sub>2</sub>) for the rest of the experimental days. TEER was measured daily, starting from day 3.

To determine the effect of U-87CM on the bEnd.3 monolayer's transendothelial electrical resistance, bEnd.3 cells were seeded on filter membranes (Transwell® inserts with 0.45 µm pore size) at a density of  $5 \times 10^4$  cells/well in 12-well plates for 72 h, and incubated with hypoxic or normoxic U-87CM at concentrations of 20%, 40%, and 75%. Cells were then incubated at 37 °C and 5% CO<sub>2</sub>. TEER measurement started by day 3. In control groups, bEnd.3 cells were grown in inserts and placed in wells with completed DMEM. The measurement was performed by connecting the electrodes to either side of the cell monolayer and measuring the resistance. The resistance of the blank (inserts without cells) was subtracted from the resistance value of the cell monolayer (inserts with cells). The resultant value was multiplied by the surface area of the inserts to give the TEER value. The measurement was performed as described by Srinivasan et al., 2015 [29].

#### 2.4.4. Quantitative PCR (qPCR) Gene Expression Assay

To determine whether the reduction in the endothelial resistance of bEnd.3 cells exposed to U-87CM is associated with tight-junction proteins, qPCR was performed to quantify the gene expression of tight-junction proteins (Occludin and Claudin-5). The bEnd.3 cells were grown in 75 cm<sup>2</sup> flasks and exposed daily to normoxic or hypoxic U-87CM, as previously mentioned. Following the treatment of bEnd.3 cells, a total RNA was extracted using TriPure isolation reagent (Roche, Ref:11667157001, Ground Floor Liesbeeck House River Park, River Lane, Mowbray, Cape Town, South Africa). The first strand of cDNA was synthesized from the total RNA using a Transcriptor first-strand cDNA synthesis kit (Roche, No. 04379012001). The resultant cDNA served as a template for real-time PCR amplification using a SYBR Luna Universal qPCR Master Mix kit (New England bio labs) using the real-time PCR system (Applied Biosystems real-time PCR instrument (Thermo Fisher Scientific, REF 4484643)). To amplify a fragment of Claudin-5, Occludin, and GAPDH (as the housekeeping gene), the primer pairs detailed in Table 1 were used. The amplification was conducted at 95 °C for 1 s, followed by 44 cycles of 95 °C for 15 s, 63 °C for 30 sec, and 95 °C for 15 s. Results were analysed using the Pfaffl method, as described by Pfaffl et al., 2002 [30].

**Table 1.** Primer sequences for quantitative PCR (qPCR) amplification of complementary DNA (cDNA). GAPDH: glyceraldehyde phosphate dehydrogenase.

N	Primers	Primer Pairs (Sequence (5' > 3'))	Product Length	°C
1	GAPDH	Forward: AGGAGAGTGTTTCCTCGTCCC	199	63
		Reverse: TGCCGTTGAATTTGCCGTGA		
2	Claudin-5	Forward: CCCAGTTAAGGCACGGGTAG	126	53–63
		Reverse: GGCACCGTCGGATCATAGAA		
3	Occludin	Forward: TTTCAGGTGAATGGGTCACCG	242	63
		Reverse: ACTTTCAAAAGGCCTCACGGA		

### 2.5. Statistical Analysis

Statistical analysis was performed using GraphPad Prism software (version 6, GraphPad Software, San Diego, CA, USA). Data were expressed as mean  $\pm$  SEM, and the differences between groups were analysed by unpaired Students' *t*-test or one-way ANOVA, followed by Dunnett's multiple comparison test. The significance level was accepted at  $p < 0.05$  for a 95% confidence interval.

## 3. Results

### 3.1. The Effect of U-87 Cells or Their Conditioned Media (U-87CM) on the Viability of bEnd.3 Cells

In the first set of experiments, the effect of coculturing glioblastoma U-87 cells on the viability of bEnd.3 cells were investigated (Figure 2A). Using an XTT cell viability assay, bEnd.3 cell viability was significantly reduced after coculturing with U-87 cells ( $p < 0.04$ ) under normoxic conditions. Following 72 and 96 h of exposure to selected concentrations of U-87CM (produced from U-87 cells cultivated under normoxic or hypoxic conditions), mostly prolonged exposure (72 and 96 h) of both hypoxic and normoxic U-87CM reduced cell viability of bEnd.3 cells, compared to the control (Figure 2B,C). At 24 h of exposure to hypoxic U-87CM, a significant reduction was observed in bEnd.3 cell viability ( $p < 0.05$ ) (Figure 2C). However, treatment with normoxic U-87CM at 24 h produced a slight non-statistical suppression of bEnd.3 cell viability (Figure 2B). At 48 h of exposure to both normoxic- (Figure 2B) and hypoxic- (Figure 2C) derived U-87CM, no statistically significant difference was observed in the viability of bEnd.3 cells. The effects at 96 h were more prominent under normoxic conditions, compared to hypoxic conditions, and the reduction of cell viability depended on both the length of the exposure time to the treatment and the concentration of U-87CM.

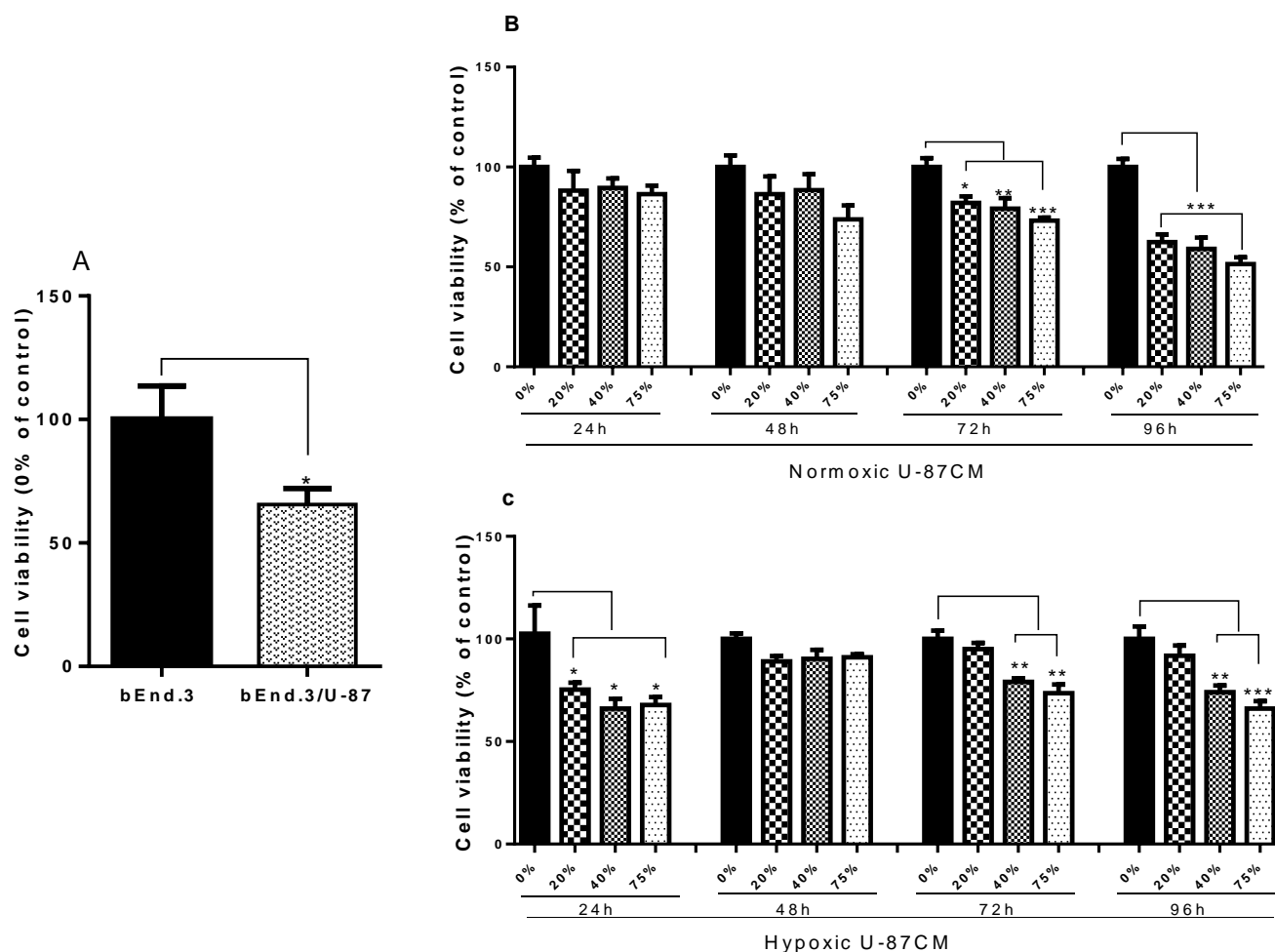


**Figure 2.** Graphs (A–C) show the viability of bEnd.3 cells under the influence of glioblastoma U-87 cells. (A) Shows the viability of monocultured bEnd.3 cells, compared with the bEnd.3 cells cocultured with glioblastoma U-87 cells. Cocultured cells showed a significant reduction in viability (\*  $p < 0.04$ ). (B) Shows cell viability of bEnd.3 cells exposed daily to selected concentrations of conditioned media produced from glioblastoma U-87 cells (U-87CM) cultivated under normoxic incubation (21%  $O_2$ ) (\*  $p < 0.05$ , \*\*  $p = 0.0011$ , \*\*\*  $p < 0.001$ ). The results show that the viability of cells significantly decreased at all concentrations of conditioned media at 72 and 96 h of incubation. (C) Represents cell viability of bEnd.3 cells after daily exposure to U-87CM derived during hypoxic (5%  $O_2$ ) incubation. Viability was significantly reduced at all concentrations of conditioned media after 24 h incubation, and only at 40% and 75% concentrations of conditioned media after 72 and 96 h incubation (\*  $p < 0.05$ , \*\*  $p < 0.01$ , \*\*\*  $p = 0.0008$ ), but showed no significant difference to controls across all concentrations of conditioned media at 48 h of incubation, ( $n = 4$ ).

### 3.2. The Effect of U-87CM on the Mitochondrial Activity of bEnd.3 Cells

The viability experiments showed that bEnd.3 cells were affected by the U-87CM paracrine secretome. In light of these viability data, additional experiments were performed to obtain more detailed data on the mechanism of the observed effect of U-87CM on the mitochondrial activity of bEnd.3 endothelial cells. The ability of U-87CM to affect the mitochondrial activity in bEnd.3 cells were investigated through the evaluation of mitochondrial membrane potential and ATP levels.

#### 3.2.1. Mitochondrial Membrane Potential ( $\Delta\Psi_m$ )

The changes in the mitochondrial membrane potential were measured by using a tetramethylrhodamine ethylesterperchlorate (TMRE) assay. The stain of bEnd.3 cells with

TMRE was performed in parallel with carbonylcyanide-3-chlorophenylhydrazone (CCCP). CCCP was used to produce a decrease in the  $\Delta\Psi_m$  through oxidative phosphorylation uncoupling, and formed the negative control. The exposure of bEnd.3 cells to normoxic U-87CM produced a statistical decrease in the  $\Delta\Psi_m$  activity in all treatment concentrations at 24 h of exposure (Figure 3A) (\*\*  $p < 0.01$ , \*\*\*  $p < 0.001$ ). The decrease in  $\Delta\Psi_m$  indicated depolarization of  $\Delta\Psi_m$ , although the depolarization state was not constant, as cells recovered statistically to control  $\Delta\Psi_m$  at 48, 72, and 96 h exposure. However, bEnd.3 cells exposed to hypoxic U-87CM showed a significant increase in the  $\Delta\Psi_m$  activity after 48 h of treatment, particularly after 48 h exposure (at 40% and 75%;  $p < 0.001$ ), at 72 h (at 75%;  $p < 0.01$ ), and at 96 h, at all treatment concentrations ( $p < 0.0001$ ), compared to the control (Figure 3B).

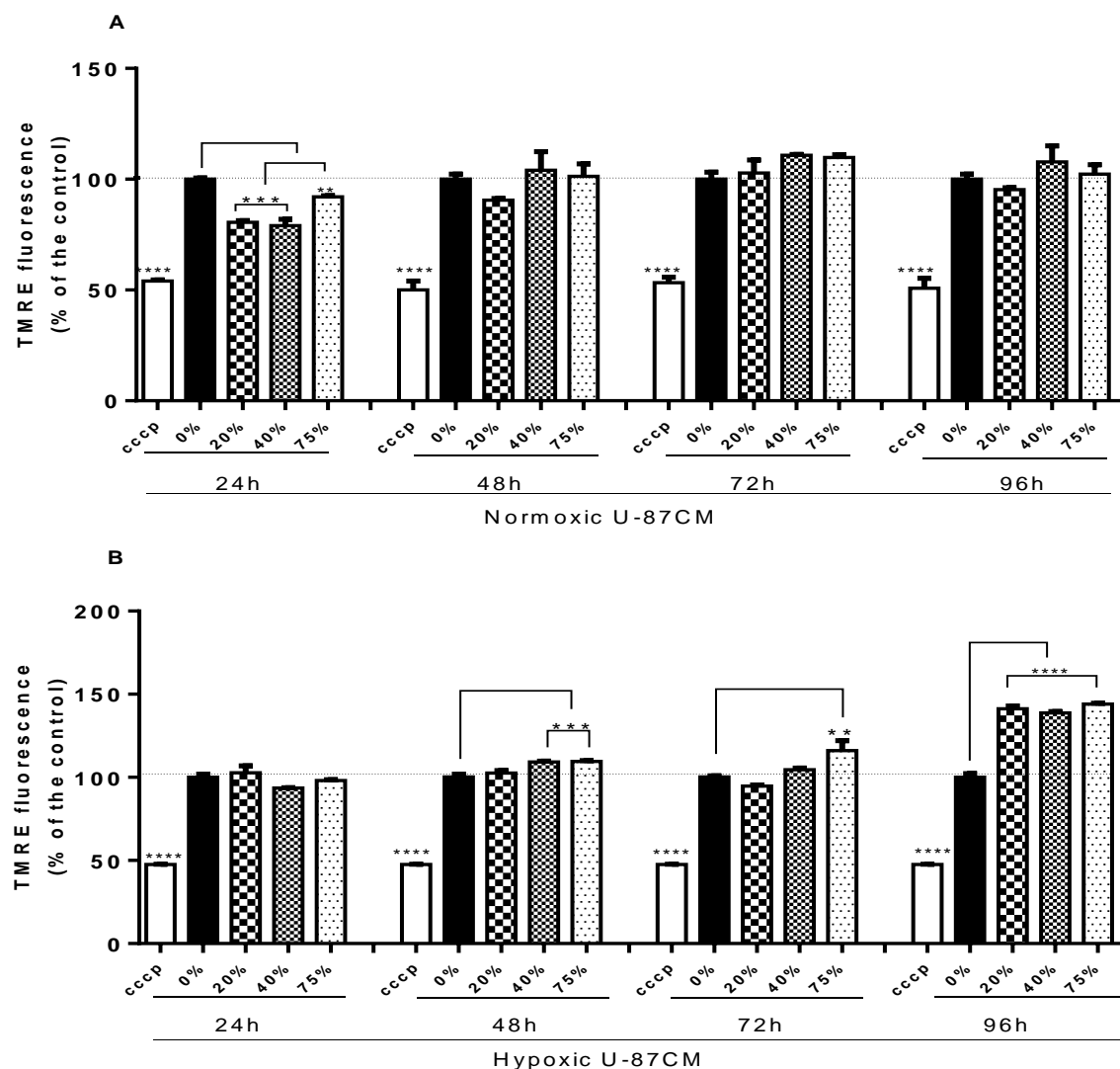


**Figure 3.** Graphs (A,B) show the changes in mitochondrial membrane potential ( $\Delta\Psi_m$ ) in bEnd.3 cells under the influence of glioblastoma U-87 cell-derived CM. (A) Shows mitochondrial membrane potential ( $\Delta\Psi_m$ ) in bEnd.3 cells after daily exposure to selected concentrations of glioblastoma U-87 conditioned media (U-87CM) derived from U-87 cells under normoxic conditions (21%  $O_2$ ). (B) Shows the changes in mitochondrial membrane potential ( $\Delta\Psi_m$ ) in bEnd.3 cells after daily exposure to selected concentrations of conditioned media derived from U-87 cells under hypoxic conditions (5%  $O_2$ ). CCCP: carbonyl cyanide 3-chlorophenylhydrazone, a known  $\Psi_m$  depolarising agent, was used to decrease the mitochondrial membrane potential (negative control) (\*\*  $p < 0.01$ , \*\*\*  $p < 0.001$ , \*\*\*\*  $p < 0.0001$ ), ( $n = 4$ ).

### 3.2.2. ATP Level in bEnd.3 Cells under the Influence of Glioblastoma U-87 Cells

The primary function of mitochondria is to generate ATP through oxidative phosphorylation. ATP levels in bEnd.3 cells cocultured with glioblastoma U-87 cells or their conditioned media (U-87CM) were investigated. Results showed a significant decrease in ATP levels in bEnd.3 cells after being cocultured with U-87 cells (Figure 4A) ( $p < 0.001$ ). Similar results were observed after long-term exposure (for 72 and 96 h) of bEnd.3 cells to both normoxic and hypoxic U-87CM (Figure 4B,C;  $p < 0.0001$ ); the cellular ATP levels were decreased in a dose-dependent manner. However, no significant difference was observed after 24 or 48 h treatment with either normoxic or hypoxic U-87CM (Figure 4B,C), except at 48 h exposure to 75% hypoxically derived U-87CM, which showed a significant decrease in the ATP level, relative to the control ( $p = 0.0385$ ).

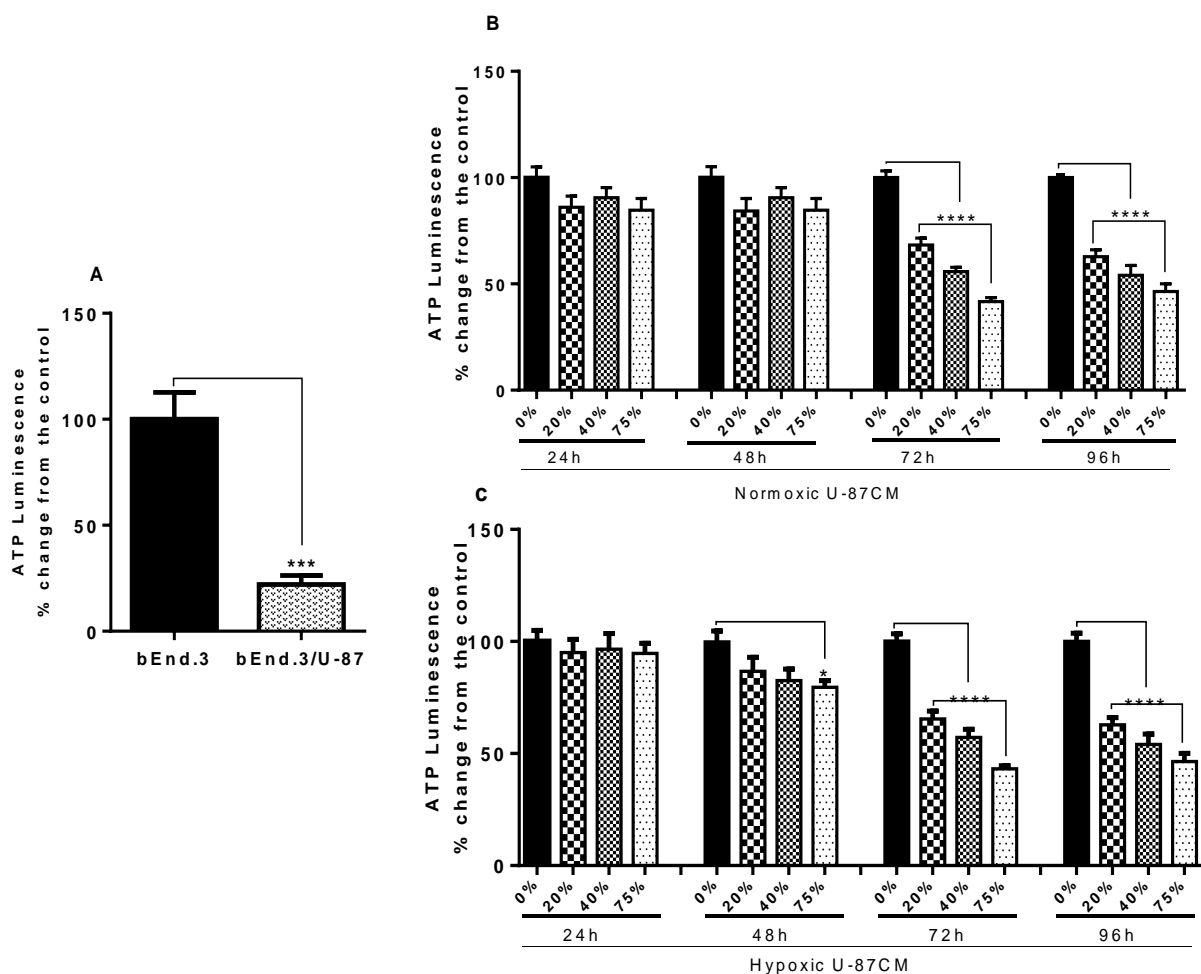


**Figure 4.** Graphs (A–C) show the changes in cellular ATP levels in bEnd.3 cells under the influence of glioblastoma U-87 cells. (A) Shows the significant reduction in cellular ATP level in bEnd.3 cells cocultured with glioblastoma U-87 cells, compared to monocultured bEnd.3 cells (\*\* $p = 0.0004$ ), ( $n = 4$ ). (B) Shows significant reduction in cellular ATP levels in a dose-response manner, compared to the control, after 72 and 96 h in culture in normoxic U-87CM (derived from U-87 cells cultivated in normoxic conditions (21%  $O_2$ ) (\*\*\*\*  $p < 0.0001$ )), ( $n = 4$ ). (C) Shows significant reduction in cellular ATP levels in a dose-response manner, compared to the control, after 72 and 96 h after treatment with selected concentrations of hypoxic U-87CM (derived from U-87 cells cultivated in hypoxic conditions (5%  $O_2$ ) (\*  $p = 0.0385$ ; \*\*\*\*  $p < 0.0001$ ), ( $n = 4$ ).

### 3.3. The Effect of the Coculture of Glioblastoma U-87 Cells on the Permeability of bEnd.3 Cell Monolayer

The ability of U-87 cells or their conditioned media (U-87CM) to perturb the permeability of the bEnd.3 cells monolayer was assessed by measuring the transendothelial electrical resistance (TEER) across confluent monolayers of bEnd.3 cells. The bEnd.3 cells were cocultured with U-87 cells under hypoxic and normoxic conditions using the Transwell system, or cultivated with hypoxic- and normoxic-derived U-87CM at selected concentrations (20%, 40%, and 75%), as previously described.

TEER across bEnd.3 confluent monolayers cocultured with U-87 cells under normoxic conditions is shown in Figure 5A. TEER across monocultured bEnd.3 monolayers (controls) and the cocultured bEnd.3 monolayer (bEnd.3 cells cocultured with glioblastoma U-87 cells) were measured on a daily basis for 8 days.

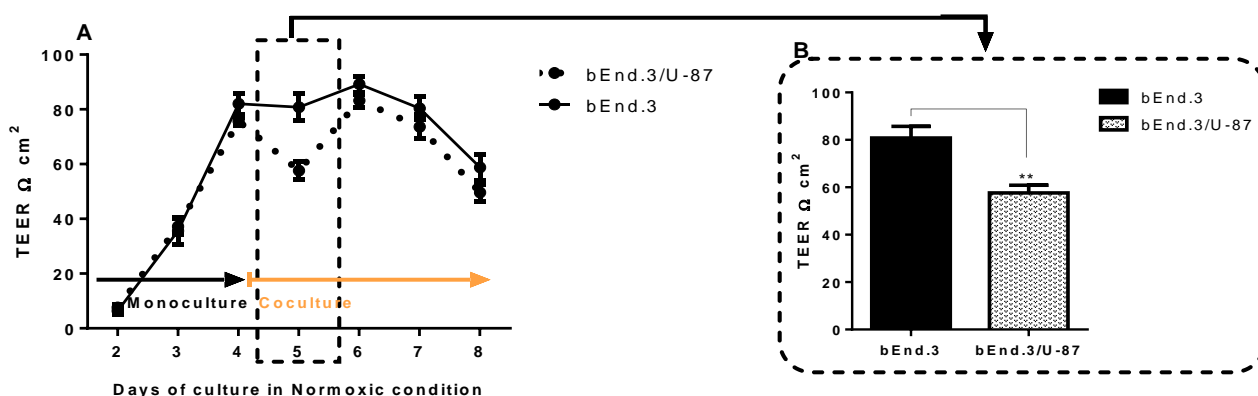


**Figure 5.** Transendothelial electrical resistance (TEER) of bEnd.3 monolayers. **(A)** Confluent monocultures of bEnd.3 cells were cocultured with glioblastoma U-87 cells under normoxic conditions (21% O<sub>2</sub>). TEER was only statistically different to control monolayers on day 5, and on all other days were statistically not different ( $p > 0.05$ ). **(B)** Peak-TEER of bEnd.3 monolayers after 24 h coculture with glioblastoma U-87 cells (\*\*  $p = 0.002$ ), ( $n = 3$ ).

It is important to note that, from days 2–4, both control and experimental groups of bEnd.3 cells were grown as monocultures. Furthermore, TEER readings typically increased with time, and no difference was observed between the two groups of cells. By the end of day 4, cells in the control group were kept as a monoculture. In contrast, the experimental bEnd.3 monolayers were cocultured with U-87 cells. The bEnd.3 monolayers cocultured with U-87 cells had significantly reduced TEER measurements after 24 h, as compared to the controls (Figure 5A,B on day 5) ( $p = 0.002$ ). Interestingly, the reduction of TEER was not constant, as bEnd.3 cells cocultured with U-87 cells recovered their resistance by day 6 and were statistically not different from controls at days 6 to 8.

To compare the effects of coculture of U-87 cells under hypoxic conditions, bEnd.3 monolayers were cultured under normoxic conditions and as monocultures until day 3 (Figure 6). TEER measurements were carried out on these monocultured bEnd.3 cell monolayers incubated under normoxic conditions until day 3, whereafter, experimental bEnd.3 monolayers were cocultured with U-87 cells under normoxic conditions (21% O<sub>2</sub>) for 24 h (Figure 6, day 4). Hypoxic incubation started by the end of day 4, and TEER was measured under these conditions for the rest of the experimental timeframe (Figure 6, 7 days).



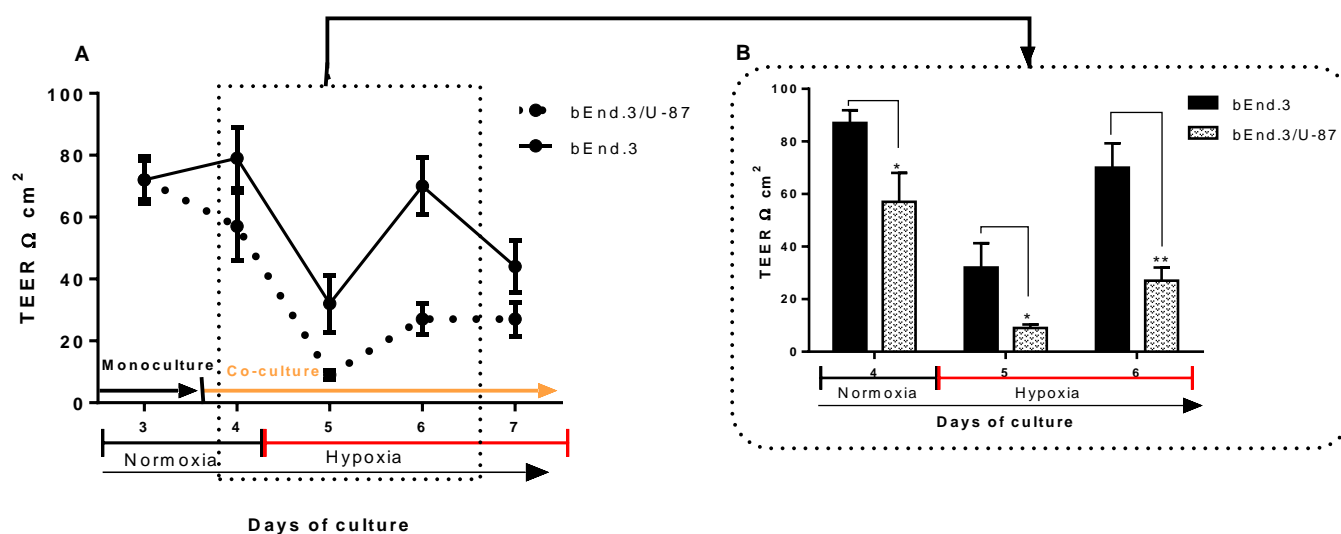


**Figure 6.** Transendothelial electrical resistance (TEER) of bEnd.3 monolayers. **(A)** Transendothelial electrical resistance (TEER) of bEnd.3 cells under hypoxic coculture with U-87 cells. Note that monocultures of bEnd.3 cells were introduced to coculture with U-87 cells after day 3 under normoxic conditions (TEER reading on day 4); thereafter, hypoxic conditions were introduced (after day 4 to the end of the experimental timeframe). **(B)** Illustrates the changes of TEER of bEnd.3 cells from normoxic to hypoxic incubation (\*  $p < 0.05$ , \*\*  $p < 0.002$ ), ( $n = 3$ ).

As shown in Figure 6A, under normoxia, the coculture with U-87 cells significantly decreased compared to the control (Figure 6A,B on day 4) ( $p = 0.032$ ). The reduction in the resistance of the cocultured bEnd.3 monolayer was constantly suppressed on the days after hypoxic incubation (Figure 6A,B on day 5) ( $p = 0.033$ ). Interestingly, the resistance of the bEnd.3 monoculture (control) also decreased in hypoxia, although it recovered by day 6 to normal levels of TEER (Figure 6B, day 6) ( $p < 0.002$ ). Although the TEER of the controls (bEnd.3 cell monolayers) and the cocultured bEnd.3/U-87 cells were suppressed under conditions of hypoxic coculture, both recovered on day 6, but the recovery of the monocultured bEnd.3 cell monolayers were much greater.

### 3.4. The Effect of the U-87CM on the Permeability of the bEnd.3 Cell Monolayer

The exposure of bEnd.3 cells to U-87CM negatively affected the permeability of the bEnd.3 monolayers. The bEnd.3 confluent monolayers were exposed to selected concentrations of normoxically derived U-87CM (Figure 7A). The treatment with normoxic U-87CM started on day 4 of cultivation. On day 5, barrier resistance of the bEnd.3 cell monolayers decreased after 24 h of exposure, particularly at 20% and 75% concentrations ( $p < 0.05$ ). However, the exposure of the bEnd.3 monolayer to the 40% concentration showed a nonstatistical decrease in TEER, in comparison with the control (0%). On day 6, exposed bEnd.3 cell monolayers had significantly decreased TEER measurements at all treatment levels, relative to the control (Figure 7B, day 6) ( $p < 0.001$ ). This statistically significant trend continued on days 7 and 8.

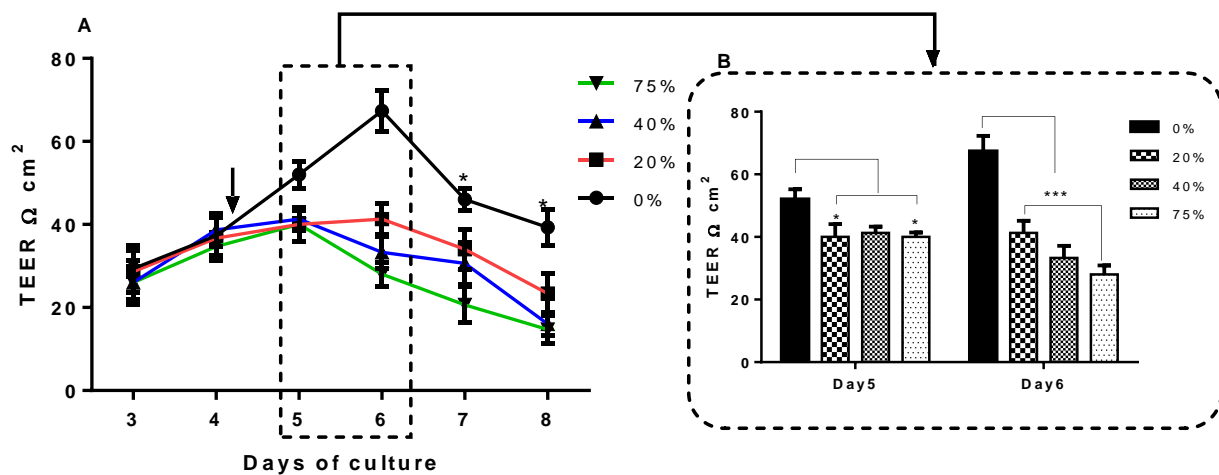


**Figure 7.** TEER of bEnd.3 cells exposed to selected concentrations of U-87CM. **(A)** TEER of bEnd.3 monolayer exposed to U-87CM produced from U-87 cells in normoxic conditions (21% O<sub>2</sub>). The arrow indicates the start of monolayer treatment with U-87CM at the end of day 4. The asterisks (\*) refer to the significant difference between controls (0%) and cells exposed to selected concentration of normoxic U-87CM; on day 7 (at 40% and 75%; \*  $p < 0.05$ , \*\*\*  $p < 0.001$ , respectively); on day 8 (at 20% (\*  $p < 0.05$ ), at 40%, and 75% (\*\*\*  $p < 0.001$ )). **(B)** Compares “peak” TEER values across bEnd.3 monolayers on days 5 and 6 after exposure (for 24 and 48 h, respectively) to U-87CM from the normoxic conditions (\*  $p < 0.05$ , \*\*\*  $p < 0.001$ ), ( $n = 3$ ).

Using the same experimental design as in the normoxia permeability experiments, hypoxic U-87CM also decreased the barrier resistance (Figure 8A). The difference in TEER across the control (0%) and the bEnd.3 monolayers exposed to U-87CM concentrations at day 5 (after 24 h exposure) was a nonstatistical decrease across the treatment concentration range (Figure 8B, day 5). However, 24 h later, on day 6, hypoxic U-87CM had a significant decrease in the barrier resistance in a concentration-dependent manner (Figure 8B) at 40% ( $p < 0.01$ ) and 75% ( $p < 0.0001$ ), respectively. However, the resistance of bEnd.3 monolayers exposed to 20% U-87CM at day 6 was not significant, in comparison to the control.

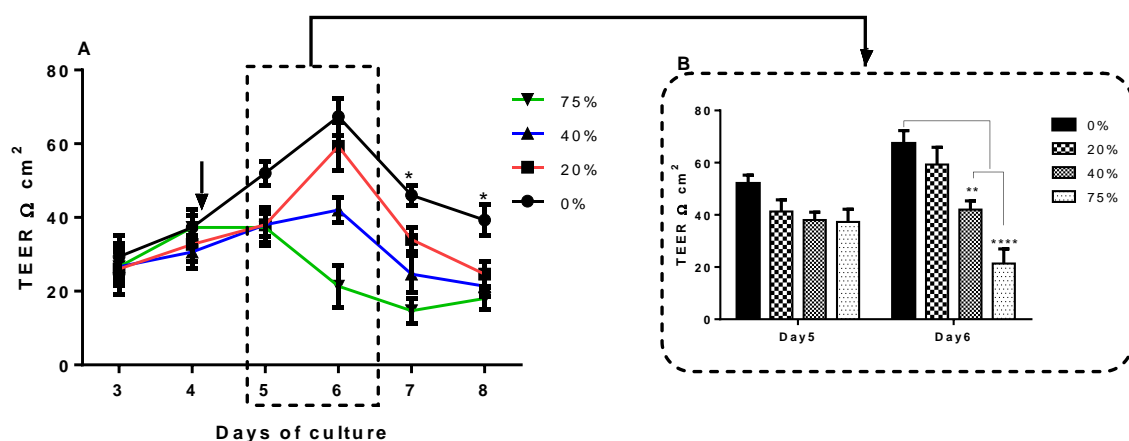


**Figure 8.** TEER of bEnd.3 cells exposed to selected concentrations of U-87CM. **(A)** Shows TEER of bEnd.3 monolayers exposed to hypoxic U-87CM. The arrow indicates the start of treatment of monolayers with U-87CM at the end of day 4. The asterisks (\*) refer to the significant difference between controls (0%) and cells exposed to selected concentrations of hypoxic U-87CM; on day 7 (at 40% and 75%; \*\*  $p < 0.01$ , \*\*\*\*  $p < 0.0001$ , respectively) and on day 8 (at 20%, 40%, and 75%; \*  $p < 0.05$ , \*\*  $p < 0.01$ , \*\*\*  $p < 0.001$ , respectively). **(B)** Compares “peak” TEER on day 5 (24 h exposure) and day 6 (48 h exposure) (\*\*  $p < 0.01$ , \*\*\*\*  $p < 0.0001$ ), ( $n = 3$ ).

### 3.5. qPCR Gene-Expression Analysis

To clarify the mechanism by which glioblastoma U-87CM perturbs the resistance across the bEnd.3 monolayer, gene expression of tight junctions (Occludin and Claudin-5) in bEnd.3 cells exposed daily to U-87CM was evaluated using qPCR. As demonstrated in Figure 9A, the exposure to normoxic U-87CM increased Claudin-5 gene expression in bEnd.3 cells. However, only the high concentration (75%) of normoxic U-87CM significantly elevated the gene expression of Claudin-5 ( $p < 0.03$ ). The expression of the Claudin-5 gene was significantly increased in bEnd.3 cells exposed to hypoxic U-87CM (Figure 9B). However, bEnd.3 cells exposed to a low concentration of hypoxic U-87CM (20%) showed the highest gene expression of Claudin-5, relative to the control ( $p < 0.05$ ), whereas the exposure to the other concentrations (40% and 75%) did not show a significant difference in Claudin-5 gene expression, compared to the control.

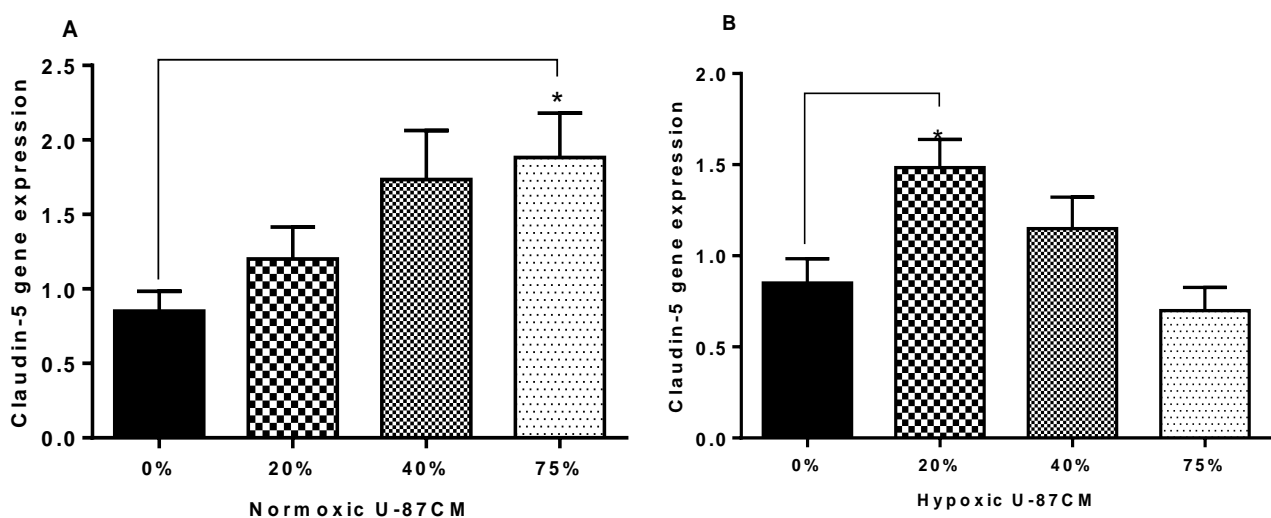


**Figure 9.** Gene expression level for Claudin-5 in bEnd.3 cells under the paracrine influence of glioblastoma U-87 cells. (A) Shows Claudin-5 gene expression in bEnd.3 cells after the exposure to selected concentrations of conditioned media derived from U-87 cells (U-87CM) under normoxic conditions (21% O<sub>2</sub>) (\*  $p < 0.03$ ). (B) Represents Claudin-5 gene expression in bEnd.3 cells after the exposure to selected concentrations of U-87CM were generated under hypoxic conditions (5% O<sub>2</sub>) (\*  $p < 0.05$ ), ( $n = 4$ ).

Occludin gene expression was also quantified in bEnd.3 cells cultivated in U-87CM. The bEnd.3 cells treated with the 75% concentration of normoxic U-87CM had significantly increased levels of Occludin gene expression, as compared to the controls (Figure 10A) ( $p < 0.0047$ ). However, no significant difference was observed in Occludin gene expression in bEnd.3 cells treated with 20% or 40% concentrations of U-87CM, in comparison to the control. The bEnd.3 cells exposed to 40% and 75% concentrations of hypoxic U-87CM showed a significant decrease in Occludin gene expression (Figure 10B) ( $p < 0.05$ ); however, the lowest treatment concentration (20%) of hypoxic U-87CM did not elicit a change in Occludin gene expression in bEnd.3 cells.

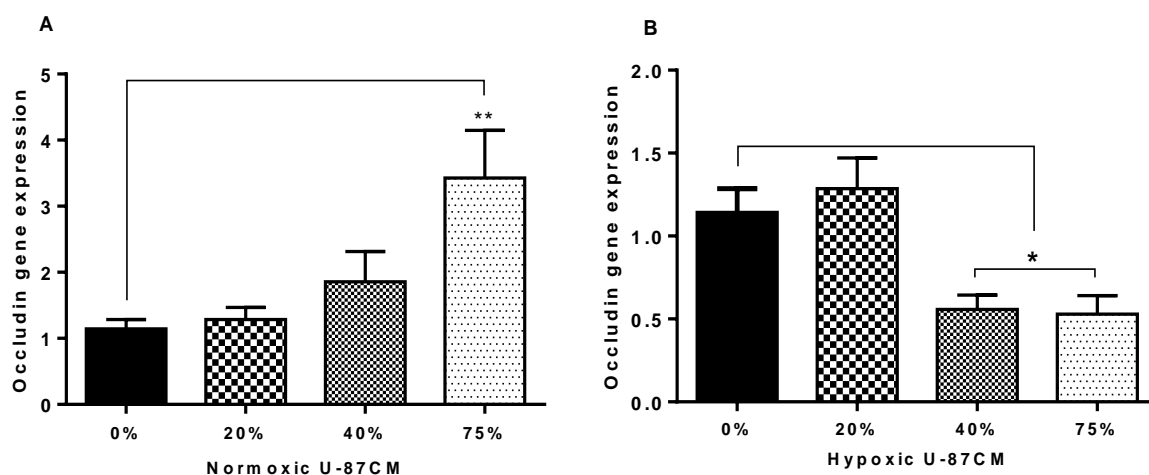


**Figure 10.** Gene expression level for Occludin in bEnd.3 cells after the exposure to selected concentrations of U-87CM. (A) Shows Occludin gene expression in bEnd.3 cells that were exposed daily to U-87CM produced in normoxic conditions (21% O<sub>2</sub>) (\*\*  $p = 0.0047$ ). (B) Represents gene expression of Occludin in bEnd.3 exposed daily to U-87CM produced under hypoxic conditions (5% O<sub>2</sub>) (\*  $p < 0.05$ ), ( $n = 4$ ).

#### 4. Discussion

The brain endothelial cells (BECs) are the anatomical sites governing the transepithelial transport function of the BBB [31]. The regulatory effectiveness of BECs is frustrated by brain tumours, particularly by high-grade brain tumours such as Glioblastoma [24]. Glioblastoma, also called Glioblastoma multiforme (GBM), is the most malignant form of a primary brain tumour [8], characterized by an extraordinary ability to infiltrate the surrounding neural tissue [9]. The GBM microenvironment is composed of other brain cells, including infiltrative immune cells, astrocytes, pericytes, and endothelial cells [21]. The interaction between GBM cells and other cells in the GBM environment occurs via soluble paracrine factors secreted into the GBM environment [32]. Analysis of GBM secretion showed that GBM can secrete approximately 2000 variant proteins into their environment [33]. GBM-secreted factors could transiently alter both normal neural precursor cells [34] and modulate brain endothelial properties [25]. GBM-secreted factors diffuse to the surrounding cells and affect their normal physiological functionality. Constant exposure of brain endothelial cells to the tumour environment induce both phenotypic and functional alterations in BECs [23]. It is well established that, clinically, the most disruptive feature of GBM is the increased BBB permeability, which leads to the formation of oedema and the increase of the intracerebral pressure due to the disruption of the BBB, primarily at the level of the endothelial cell site [3,13].

In the current study, the effect of glioblastoma-secreted paracrine factors on the physiological state of brain endothelial cells (bEnd.3) was investigated. The study aimed to determine whether endothelial cells exposed to glioblastoma U-87 cells are physiologically altered by focusing on the mitochondrial function of BECs. Using the XTT assay, the cell viability of bEnd.3 cells cocultured with glioblastoma U-87 cells or cultivated with conditioned media produced under normoxic (21% O<sub>2</sub>) or hypoxic (5% O<sub>2</sub>) conditions was determined. The XTT cell viability assay reflects the metabolic status of a cell culture population by monitoring the changes in the activity of the mitochondrial dehydrogenase. Current results illustrated that the viability of brain endothelial cells is negatively affected by U-87 cells (Figure 2A) and by conditioned media derived from U-87 cells (Figure 2B,C). Contrary to these results, it has been previously reported that glioblastoma cells release various factors, such as growth factors [20,33], which are known to enhance the survival and angiogenic properties of BECs [35]. In addition, the cytokines that are largely expressed by GBM [36], IL-8, and IL-6 are upregulated [37]. In support of our findings of GBM-induced suppression of BEC viability, these cytokines were found to disrupt the brain endothelial

function, and to induce apoptosis [38] or necroptosis [39] in endothelial cells to facilitate the extravasation of cancer cells. Previous studies focused on the endothelial alteration in the brain tumour environment (in vivo or in vitro) by establishing models that monitor the interaction between cancer cells and endothelial cells, mostly focusing on the molecular and morphological aspects. However, none have focused on the metabolic alteration of BECs under the influence of GBM. In the current study, the endothelial metabolic activity was significantly reduced following daily exposure to glioblastoma U-87 cells and their secretions, as indicated by the reduction in the viability of bEnd.3 cells cultivated with glioblastoma U-87 cells or their conditioned media (U-87CM). As the bEnd.3's suppressed viability was monitored by measuring mitochondrial dehydrogenase activity, it implicated the modulation of BEC mitochondrial function via GBM paracrine factors.

The intact BBB is as rigorous in preventing the efflux of unsolicited cells/substances as it is in preventing their influx into the brain [40]. It is, therefore, in the interest of the metastatic tumour to compromise the integrity of the BBB to relocate to non-neural tissue. The present study showed that these normoxic paracrine factors were not effective within 48 h but only affected BEC viability at 72 h, while having a more pronounced dose effect at 96 h. This alludes to these paracrine factors having an insidious long-term effect on the mitochondrial function, which only becomes statistically evident from 72 h onward.

It appears that under hypoxic conditions that the paracrine effect is more aggressive within 24 h of exposure, and despite a nonstatistical decrease at 48 h, the suppressive trend was clearly present at 72 and 96 h. However, the effects of U-87CM were unexpectedly more pronounced under normoxic conditions, especially in the long-term (at 96 h) treatment. This may allude to the more aggressive GBM secretion of paracrine factors under normoxic conditions, relative to hypoxic conditions. The clear dose-related effect of U-87CM in both normoxic and hypoxic treatments further indicates that blocking this paracrine effect may be a possible avenue for clinical intervention.

To further investigate the mitochondrial activity in bEnd.3 cells under the influence of U-87 glioblastoma cells, we evaluated the mitochondrial membrane potential ( $\Delta\Psi_m$ ) of bEnd.3 cells after daily exposure to normoxic and hypoxic U-87CM, by staining bEnd.3 cells with tetramethylrhodamine ethylesterperchlorate (TMRE). Physiologically, mitochondria use the electrochemical driving force of protons ( $H^+$ ) produced from the reductive transfer of electrons through protein complexes I–IV in the inner mitochondrial membrane to produce ATP [41]. The differential concentration of protons between the outer mitochondrial space and the mitochondrial matrix forms the basis of the mitochondrial membrane potential ( $\Delta\Psi_m$ ). This process accumulates  $H^+$  in the outer intermitochondrial space, which subsequently flows back into the mitochondrial matrix via the ATP-producing F1/F0 ATP-synthase to complete the electron transport chain and to, thereby, generate ATP. A low  $\Delta\Psi_m$  indicates a decreased driving force for ATP and vice versa [28,42].

The bEnd.3 cells exposed to normoxically derived U-87CM showed suppression in the  $\Delta\Psi_m$ , compared to the control, only at 24 h. Thereafter, at 48–96 h, no statistically significant difference was observed, compared to the controls (Figure 3A). In contrast, an increase in the  $\Delta\Psi_m$  (hyperpolarisation) was observed in bEnd.3 treated with hypoxic U-87CM after long-term exposure, particularly 96 h, where all treatments with hypoxically derived U-87CM produced significantly higher  $\Delta\Psi_m$  (Figure 3B). At the cellular level, this indicated an accumulation of TMRE ( $H^+$ ) in the intermitochondrial space, yielding higher fluorescent intensity than in control bEnd.3 cells. The hyperpolarisation state results from the high transfer of  $H^+$  to the outer intermitochondrial inner space or from a compromise of the  $H^+$  driving force via the ATP-synthase. ATP-synthase inhibition reduces the utilization of the electrochemical  $H^+$  gradient, which causes ATP depletion, ADP accumulation, and  $\Delta\Psi_m$  hyperpolarisation [43]. Although the current data implicate hypoxically derived U-87CM in modulating the state of  $\Delta\Psi_m$ , further investigation is recommended to determine the exact mechanism for mitochondrial hyperpolarisation in brain endothelial cells in a GBM cancer environment.

Given the effects of normoxic and hypoxically derived U-87CM on  $\Delta\Psi_m$ , the current study investigated how ATP levels in the bEnd.3 BECs would be affected. Therefore, cellular ATP levels in bEnd.3 cells exposed to glioblastoma U-87 cells (coculture) or their conditioned media (U-87CM) were measured as a further evaluation for mitochondrial function. Data derived from the current study showed a marked reduction of ATP levels in bEnd.3 cells after a daily coculture with glioblastoma U-87 cells (Figure 4A). Similar results were observed after long-term exposure to normoxic and hypoxic U-87CM (Figure 4B,C, respectively), where suppression of ATP levels was nonstatistical at 48 h, but at 72 and 96 h, a clear dose-related suppression of ATP concentration in the BECs was observed. This was in alignment with the decrease in bEnd.3 cell-viability observations (Figure 2), and the elevated  $\Delta\Psi_m$  by hypoxically derived U-87CM seen at 96 h (Figure 3B). Given that the main function of mitochondria is ATP synthesis, and that most physiological activities of the cell are dependent on the availability of ATP, it is an accurate indicator of mitochondrial activity and cell viability [44]. In the current study, the depletion in ATP levels under hypoxic conditions may be associated with a GBM-induced increase in  $\Delta\Psi_m$  in BECs, uncoupling the process whereby the  $H^+$  concentration in the inter-mitochondrial space drives the production of ATP via ATP-synthase [45]. In contrast, the normoxically induced reduction in ATP levels was not related to hyperpolarisation of  $\Delta\Psi_m$ , which suggests that under normoxia, GBM induces decreased ATP levels via another mechanism. Given that ATP levels in the cell are related to the reversible reactions of ATP synthesis and hydrolysis,  $ATP + H_2O \rightleftharpoons ADP + (Pi)$ , we postulate that, in view of the fact that no hyperpolarization/depolarization of the outer-mitochondrial space ( $\Delta\Psi_m$ ) was observed during normoxic conditions (Figure 3A), the hypothetical proton-driven suppression of ATP concentrations at 72 h and 96 h is not valid. It is, therefore, indeed plausible that the mechanism of ATP depletion involved increased hydrolysis of ATP, rather than suppressed proton-driven ATP synthesis. Given the limitations of this study, it is recommended that further study be carried out to elucidate the effect of cancer paracrine factors under normoxic and hypoxic conditions on ATP synthesis and hydrolysis in conjunction with  $O_2$  consumption.

One of the most disruptive features of clinical GBM is increased BBB permeability and brain oedema formation. The disruption in cellular ATP level has also been associated with BBB permeability and tight-junction protein changes in mice [46]. Thus, the current study investigated the effects of coculturing bEnd.3 monolayers with U-87 GBM cells, as well as treating bEnd.3 monolayers with both normoxically and hypoxically derived U-87CM on the transendothelial permeability (using TEER). The coculture experiments conducted under normoxic conditions in the current study demonstrated a statistically transient increase in permeability (decrease TEER) (at 24 h) across bEnd.3 monolayers (Figure 5). However, after 24 h, the permeability returned to TEER levels that were not statistically different from controls. These data are in alignment with our data on normoxic  $\Delta\Psi_m$ , where we also only saw a significant depression at 24 h but not thereafter. This transient decrease in permeability under normoxic conditions may not be sufficient for GBM tumour cells to metastatically escape from neural tissue across the notoriously impermeable BBB, and it may be the reason for the low level of non-neural metastasis observed in patients with GBM tumours (<2%) [47]. However, clinically the progression of GBM is often associated with the migration of GBM tumour cells along nerve tracts and along the outer perimeters of blood vessels within the CNS [48]. Nevertheless, there is clear evidence in the literature that GBM tumours located in the CNS can metastatically cross the BBB (most likely in cases where the BBB has been compromised) and relocate to bone tissue, lung tissue, and muscle tissue [49]; however, this only reflects 2% of all GBM cases. Furthermore, given the demand for supplying nutrients and  $O_2$  to neural tissues, and the high density of blood vessels in brain tissue, where the extravascular space represents only 20% of the neural tissue [48], it is unlikely that the GBM tumour's microenvironment would be in a state of hypoxia. Thus, it may only be under conditions of the rapid growth of the GBM tumour that intratumour



tissue may be hypoxically challenged. It is under these hypoxic conditions that differential modulation of BECs may occur.

In the experiment presented in Figure 6, two sets of bEnd.3 monolayers were cultured for 48 h (2 days) under normoxic conditions, and on day 3, TEER was measured. Immediately afterwards, one set of the bEnd.3 monolayers (on inserts) was introduced to coculture with U-87 cells (here cancer cells were grown on the floor of the well, while the insert with the bEnd.3 monolayers was placed into this well). TEER was measured on day 4, and this allowed for the comparison of the bEnd.3 monolayer's permeability before and after being introduced to the U-87 coculture and also to the bEnd.3 monoculture, which served as a control. Hereafter, both sets of bEnd.3 monolayers were introduced to hypoxic (5% O<sub>2</sub>) incubation for the rest of the experimental timeframe (until day 7), and TEER was measured on a daily basis. This allowed for the comparison of monocultured bEnd.3 monolayers with those cocultured with cancer U-87 cells, under hypoxic conditions.

In contrast to normoxic conditions seen in the coculture experiments in Figure 5, the bEnd.3 monolayers that were cocultured with U-87 cells under hypoxic conditions showed increased permeability (decreased TEER) throughout the hypoxic period (Figure 6). Thus, a clear difference in the modulation of BECs under hypoxic conditions was observed, with bEnd.3 monolayers cocultured with U-87 cells remaining highly permeable throughout the hypoxic conditions. It is unlikely that the increased permeability was related to the decreased levels of O<sub>2</sub>, as it must be pointed out that hypoxia only depressed monocultures of bEnd.3 cells transiently, and after 24 h, these monolayers recovered their TEER values and were always statistically more impermeable, compared to bEnd.3 monolayers cocultured under hypoxic conditions (Figure 6B).

By hypothetical extension, the bEnd.3 monolayers were treated with selected concentrations of U-87CM in the current study and TEER was measured. The exposure of monocultured bEnd.3 monolayers to normoxic U-87CM (Figure 7) significantly decreased TEER in a time-dependent manner after 24 h and 48 h of treatment.

Similarly, the treatment with hypoxic U-87CM (Figure 8) decreased TEER of bEnd.3 monolayers, but only after 48 h of exposure to 40% and 75% hypoxic U-87CM. Interestingly, the resistance of the bEnd.3 monolayer was more compromised after the treatment with normoxic U-87CM (Figure 7). That might reflect the differential metabolic state of GBM cells under normoxia and hypoxia. Such differences were observed by Emily Chen et al., 2018, who reported that U-87 cells reduced their metabolic activity and proliferation under hypoxia [50]. GBM cells, like all cancer cells, actively grow close to the blood vessels due to the high level of O<sub>2</sub>. In addition, cancer cells under aerobic conditions preferentially use glycolysis (Warburg effect) [51]. This suggested that GBM cancer cells were highly active under normoxia, which was reflected in their paracrine secretions. At this point, the identification of factors secreted in U-87 secretions (produced in normoxia and hypoxia) will be helpful, and more research is required to elucidate these mechanisms.

The bEnd.3 cells exposed to normoxic and hypoxic U-87CM (Figures 7 and 8, respectively) were unable to recover their resistance after the treatment; however, the cocultured bEnd.3 cells under normoxia (Figure 5) recovered after 48 h to the control levels of TEER, but not under hypoxia. This may be due to the coculture effect between bEnd.3 cells and U-87 cells. The coculture with endothelial cells ensured the constant cross-talk between U-87 and bEnd.3 cells. This “cross-talk” between both types of cells might lead to the modulation of paracrine or autocrine factors secreted from both cell types. It is, therefore, important to note that U-87CM were produced from monocultured U-87 cells in the absence of intermodulation between U-87 cells and bEnd.3 cells. Therefore, modulatory “cross-talk” paracrine factors between U-87 cells and bEnd.3 cells were not present in the normoxic U-87CM TEER experiments (Figure 7), where the increase in permeability (reduction in TEER) was seen throughout the treatment of U-87CM. Based on this postulate, BECs may be able to respond to U-87 cancer cell paracrine-induced increases in permeability by inhibiting the U-87 cell paracrine effects (Figure 5). In the absence of inhibition by bEnd.3 cells on



U-87 cells, continuous suppression of TEER by paracrine factors in U-87CM occurs, as can be seen in Figure 7.

In the analogous coculture experiments (Figure 6), hypoxic conditions caused an extended reduction in TEER. We suggest that either the reciprocal inhibition by bEnd.3 cells on paracrine factors secreted by U-87 cells (seen in Figure 5) was suppressed under hypoxic conditions, or under hypoxic conditions U-87 cells secrete paracrine factors more aggressively. The former hypothesis is favoured in view of the fact that this paracrine effect was suppressed when U-87 cells were incubated under hypoxic conditions for the following reasons: firstly, in contrast to the analogous normoxia experiments (Figure 7), no statistical suppression of TEER occurred on day 5 (Figure 8). Secondly, in contrast to normoxically derived U-87CM, hypoxically derived U-87CM only caused a significant decrease in TEER, relative to controls, only at higher treatment concentrations (40% and 75%) on day 6. Although a more aggressive hypoxic response from U-87 cells was expected, normoxia tended to produce more prominent or aggressive responses from GBM. This may be because GBM originates from glial CNS cells in a location that is highly vascularized (80% of extracellular CNS tissue is made up of blood vessels) [52]. Therefore, in view of the fact that GBM develops in an environment that is seldom deficient in O<sub>2</sub> and nutrients, it is less likely to be aggressive under hypoxic conditions. In the event of the fast-growing GBM tumour outstripping angiogenesis and developing zones of hypoxia, a process that facilitates intra-CNS metastasis, the metastatic GBM cell will always find itself in a relatively O<sub>2</sub>-rich CNS environment, making aggressive hypoxic paracrine mechanisms superfluous. Furthermore, the short window provided to compromise the BBB permeability under normoxic conditions (Figure 5) supported the clinical case data in that most GBM tumours seldom metastasize to extra-CNS tissue.

Endothelial resistance is maintained by transmembrane tight junctions [53], particularly in Occludin and Claudin-5 [54,55]. These proteins are the most integral tight-junction proteins at the brain endothelial paracellular space [56]. The expression of Claudin-5 and Occludin is critical for endothelial integrity. Downregulation of these proteins would lead to decreased brain transendothelial resistance [57]. A similar effect on the bEnd.3 monolayer was observed when exposed to U-87CM in the current study (Figures 5–8). These results are consistent with a previous study by Schneider et al. (2004) that reported the impairment of the endothelial barrier by glioblastoma cells. The disruption of BBB function was also shown in parallel in vivo and in vitro studies using different types of glioblastoma cell lines [58]. Furthermore, it has been reported that GBM cells release a wide range of vascular growth factors (VGFs) [59], which in turn modulate the expression of Claudin-5, promoting the BBB impairment [60].

As Occludin and Claudin-5 are the anchors of transendothelial cell permeability, the mechanism by which glioblastoma U-87 cells decreased the resistance of the bEnd.3 monolayer was investigated in the current study. The qPCR was used to quantify the gene expression of Occludin and Claudin-5 in bEnd.3 exposed to U-87CM. The results showed statistical upregulation in gene expression for both Claudin-5 and Occludin in bEnd.3 cells exposed to 75% normoxic U-87CM (Figures 9A and 10A). The Claudin-5 gene expression was statistically upregulated in bEnd.3 cells that were exposed to hypoxically derived U-87CM only at 20% concentration (Figure 9B), whereas high concentrations significantly suppressed Occludin gene expression in bEnd.3 cells (Figure 10B), endorsing our TEER data for hypoxically treated bEnd.3 monolayers with U-87CM (40% and 75%) (Figure 8). However, these results did not fully correlate with the TEER results, which engenders the following points: firstly, tight-junction proteins may be degraded by soluble factors secreted by glioblastoma cells, particularly metalloproteinases (MMPs), as it is reported that glioblastoma cells release a wide range of these proteases, degrading the tight-junctional proteins [61]. Secondly, a negative correlation between mRNA and protein expression at the level of transcription can indicate that modulation of TJs occurs post-translationally, affecting and compromising their insertion or functionality at the membrane level [62]. Lastly, the disruption of the endothelial resistance could be via the transcellular way, rather

than the paracellular way. Therefore, further investigation is required to elucidate the exact mechanism whereby endothelial tight junctions and transendothelial permeability is affected by paracrine factors.

## 5. Conclusions

GBM cells modulate the function of brain capillary endothelial cells via paracrine factors differentially under normoxic and hypoxic conditions (Table 2). Furthermore, the differential permeability (TEER) effects between coculturing bEnd.3 cells with U-87 cells, compared to treating them with U-87 conditioned media, suggest cross-modulatory effects between these cell types, which strongly advocate further research. It is clear that U-87 cells and their paracrine secretions modulate ATP generation by uncoupling  $\Delta\Psi_m$  under hypoxic conditions, but do not use the same mechanism to uncouple ATP generation under normoxic conditions. Under normoxic conditions, the authors speculate that increased ATP hydrolysis might be responsible for the suppression of ATP levels in cells exposed to selected concentrations of the U-87 GBM secretome. Nevertheless, the U-87 cell-derived conditional media-induced suppression of ATP levels in the bEnd.3 is correlated with reduced viability of BECs. This long-term mechanism (only achieving statistical resolution in viability after 72 h), together with U-87 GBM cancer-cell paracrine effects causing increased permeability (decrease TEER), may be the mechanism behind the clinical oedema formation, and the subsequent increase of the intracerebral pressure, implicating the disruption of the BBB, primarily at the level of the endothelial cells of the brain capillaries. Lastly, the dose-response effect of treating BECs with different concentrations of U-87CM suggests additional avenues of research with clinical implications for treating GBM cancer patients.

**Table 2.** A summary of U-87CM effects on brain endothelial cells (bEnd.3 cells). CM: conditional media.

The Effects of U-87CM Paracrine Factors		
Endothelial Parameters	Normoxia (21% O <sub>2</sub> )	Hypoxia (5% O <sub>2</sub> )
Mitochondrial dehydrogenase	Suppressed after 72 and 96 h.	Suppressed after 24 h, 72 and 96 h.
Mitochondrial membrane potential	Depolarization after 24 h.	Hyperpolarization after 48, 72, and 96 h exposure to the 75% U-87CM.
ATP production	Decrease after 72 and 96 h.	Decrease after 48 h at 75% concentration, and after 72 and 96 h exposure.
TEER	Decrease after 24 h coculture, then recover to TEER control. Decrease after 24 h exposure to U-87CM.	Decrease after 24 h coculture with U-87 cancer cells but do not recover. Decrease after 48 h exposure to U-87CM at 40% and 75%.

**Author Contributions:** Conceptualization, D.F. and M.R.; methodology, M.R.; software, D.F.; validation, D.F., B.F. and M.R.; formal analysis, M.R. and D.F.; investigation, M.R.; resources, D.F.; data curation, M.R. and D.F.; writing—original draft preparation, M.R.; writing—review and editing, D.F.; visualization, D.F.; supervision, D.F. and B.F.; project administration, D.F.; funding acquisition, D.F. All authors have read and agreed to the published version of the manuscript.

**Funding:** University of the Western Cape Senate grant.

**Institutional Review Board Statement:** The study was conducted according to the guidelines of the Declaration of Helsinki, and approved by the Institutional Review Board of the Research Office of the University of the Western Cape (Project registration no.: 20/5/9; January 2020).

**Informed Consent Statement:** Not applicable.

**Data Availability Statement:** All experimental data collected are archived within the University of the Western Cape (UWC) archives and are available as per UWC data and intellectual property policy guidelines and their associated copyright protection.

**Acknowledgments:** We acknowledge the SA-MRC (Cape Town) for their assistance and use of their laboratory infrastructure. In this regard, we especially want to thank Bianca Sansom for her insightful suggestions regarding our PCR experiments.

**Conflicts of Interest:** The authors declare no conflict of interest.

## References

- Persidsky, Y.; Ramirez, S.; Haorah, J.; Kanmogne, G.D. Blood–brain Barrier: Structural Components and Function under Physiologic and Pathologic Conditions. *J. Neuroimmune Pharmacol.* **2006**, *1*, 223–236. [[CrossRef](#)] [[PubMed](#)]
- Serlin, Y.; Shelef, I.; Knyazer, B.; Friedman, A. Anatomy and physiology of the blood–brain barrier. *Semin. Cell Dev. Biol.* **2015**, *38*, 2–6. [[CrossRef](#)] [[PubMed](#)]
- Wolburg, H.; Noell, S.; Fallier-Becker, P.; Mack, A.F.; Wolburg-Buchholz, K. The disturbed blood–brain barrier in human glioblastoma. *Mol. Asp. Med.* **2012**, *33*, 579–589. [[CrossRef](#)] [[PubMed](#)]
- Hanif, F.; Muzaffar, K.; Perveen, K.; Malhi, S.M.; Simjee, S.U. Glioblastoma Multiforme: A Review of its Epidemiology and Pathogenesis through Clinical Presentation and Treatment. *Asian Pac. J. Cancer Prev.* **2017**, *18*, 3–9. [[CrossRef](#)]
- Urbańska, K.; Sokołowska, J.; Szmidi, M.; Sysa, P. Review Glioblastoma multiforme—An overview. *Współczesna Onkol.* **2014**, *5*, 307–312. [[CrossRef](#)] [[PubMed](#)]
- Brighi, C.; Puttick, S.; Rose, S.; Whittaker, A.K. The potential for remodelling the tumour vasculature in glioblastoma. *Adv. Drug Deliv. Rev.* **2018**, *136–137*, 49–61. [[CrossRef](#)] [[PubMed](#)]
- Hottinger, A.F.; Abdullah, K.G.; Stupp, R. Current Standards of Care in Glioblastoma Therapy. *Glioblastoma* **2016**, 73–80. [[CrossRef](#)]
- Zhang, X.; Zhang, W.; Cao, W.-D.; Cheng, G.; Zhang, Y.-Q. Glioblastoma multiforme: Molecular characterization and current treatment strategy (Review). *Exp. Ther. Med.* **2011**, *3*, 9–14. [[CrossRef](#)] [[PubMed](#)]
- D’alessio, A.; Proietti, G.; Sica, G.; Scicchitano, B.M. Pathological and Molecular Features of Glioblastoma and Its Peritumoral Tissue. *Cancers* **2019**, *11*, 469. [[CrossRef](#)]
- Hambardzumyan, D.; Bergers, G. Glioblastoma: Defining Tumor Niches. *Trends Cancer* **2015**, *1*, 252–265. [[CrossRef](#)] [[PubMed](#)]
- Vollmann-Zwerenz, A.; Leidgens, V.; Feliciello, G.; Klein, C.A.; Hau, P. Tumor Cell Invasion in Glioblastoma. *Int. J. Mol. Sci.* **2020**, *21*, 1932. [[CrossRef](#)]
- Peleli, M.; Moustakas, A.; Papapetropoulos, A. Endothelial-Tumor Cell Interaction in Brain and CNS Malignancies. *Int. J. Mol. Sci.* **2020**, *21*, 7371. [[CrossRef](#)] [[PubMed](#)]
- Dubois, L.G.; Campanati, L.; Righy, C.; D’Andrea-Meira, I.; Porto-Carreiro, I.; Pereira, C.M.; Balça-Silva, J.; Kahn, S.A.; Dos Santos, M.F.; Oliveira, M.D.A.R.; et al. Andrea-meira, Gliomas and the vascular fragility of the blood brain barrier. *Front. Cell. Neurosci.* **2014**, *8*, 418. [[CrossRef](#)]
- Hoelzinger, D.; De Muth, T.; Berens, M.E. Autocrine Factors That Sustain Glioma Invasion and Paracrine Biology in the Brain Microenvironment. *J. Natl. Cancer Inst.* **2007**, *99*, 1583–1593. [[CrossRef](#)] [[PubMed](#)]
- Lorger, M. Tumor Microenvironment in the Brain. *Cancers* **2012**, *4*, 218–243. [[CrossRef](#)]
- Giusti, I.; Delle Monache, S.; Di Francesco, M.; Sanità, P.; D’Ascenzo, S.; Gravina, G.L.; Festuccia, C.; Dolo, V. From glioblastoma to endothelial cells through extracellular vesicles: Messages for angiogenesis. *Tumor Biol.* **2016**, *37*, 12743–12753. [[CrossRef](#)] [[PubMed](#)]
- Charalambous, C.; Hofman, F.M.; Chen, T.C. Functional and phenotypic differences between glioblastoma multiforme—derived and normal human brain endothelial cells. *J. Neurosurg.* **2005**, *102*, 699–705. [[CrossRef](#)]
- Bonnin, D.A.A.; Havrda, M.C.; Israel, M.A. Glioma Cell Secretion: A Driver of Tumor Progression and a Potential Therapeutic Target. *Cancer Res.* **2018**, *78*, 6031–6039. [[CrossRef](#)] [[PubMed](#)]
- Karagiannis, G.S.; Pavlou, M.P.; Diamandis, E.P. Cancer secretomics reveal pathophysiological pathways in cancer molecular oncology. *Mol. Oncol.* **2010**, *4*, 496–510. [[CrossRef](#)]
- Formolo, C.A.; Williams, R.; Gordish-Dressman, H.; Mac Donald, T.J.; Lee, N.H.; Hathout, Y. Secretome Signature of Invasive Glioblastoma Multiforme. *J. Proteome Res.* **2011**, *10*, 3149–3159. [[CrossRef](#)] [[PubMed](#)]
- Simon, T.; Jackson, E.; Giamas, G. Breaking through the glioblastoma micro-environment via extracellular vesicles. *Oncogene* **2020**, *39*, 4477–4490. [[CrossRef](#)]
- Schneider, S.W.; Ludwig, T.; Tatenhorst, L.; Braune, S.; Oberleithner, H.; Senner, V.; Paulus, W. Glioblastoma cells release factors that disrupt blood-brain barrier features. *Acta Neuropathol.* **2004**, *107*, 272–276. [[CrossRef](#)]
- Charalambous, C.; Chen, T.C.; Hofman, F.M. Characteristics of tumor-associated endothelial cells derived from glioblastoma multiforme. *Neurosurg. Focus* **2006**, *20*, E22. [[CrossRef](#)] [[PubMed](#)]
- Ishihara, H.; Kubota, H.; Lindberg, R.L.P.; Leppert, D.; Gloor, S.M.; Errede, M.; Virgintino, D.; Fontana, A.; Yonekawa, Y.; Frei, K. Endothelial Cell Barrier Impairment Induced by Glioblastomas and Transforming Growth Factor  $\beta$ 2 Involves Matrix Metalloproteinases and Tight Junction Proteins. *J. Neuropathol. Exp. Neurol.* **2008**, *67*, 435–448. [[CrossRef](#)] [[PubMed](#)]
- Dwyer, J.; Hebda, J.K.; Le Guelte, A.; Galan-Moya, E.M.; Smith, S.S.; Azzi, S.; Bidere, N.; Gavard, J. Glioblastoma Cell-Secreted Interleukin-8 Induces Brain Endothelial Cell Permeability via CXCR2. *PLoS ONE* **2012**, *7*, e45562. [[CrossRef](#)] [[PubMed](#)]

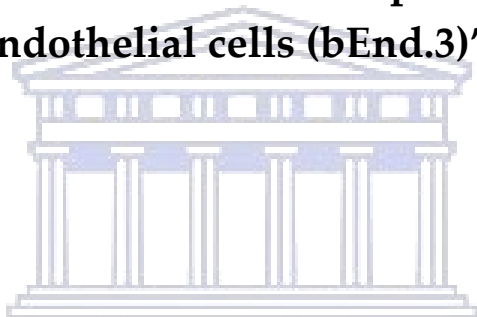
26. Nejad, A.E.; Najafgholian, S.; Rostami, A.; Sistani, A.; Shojaeifar, S.; Esparvarinha, M.; Nedaeinia, R.; Javanmard, S.H.; Taherian, M.; Ahmadlou, M.; et al. The role of hypoxia in the tumor microenvironment and development of cancer stem cell: A novel approach to developing treatment. *Cancer Cell Int.* **2021**, *21*, 62. [\[CrossRef\]](#)
27. Watanabe, T.; Dohgu, S.; Takata, F.; Nishioku, T.; Nakashima, A.; Futagami, K.; Yamauchi, A.; Kataoka, Y. Paracellular Barrier and Tight Junction Protein Expression in the Immortalized Brain Endothelial Cell Lines b, END.3, b, END.5 and Mouse Brain Endothelial Cell 4. *Biol. Pharm. Bull.* **2013**, *36*, 492–495. [\[CrossRef\]](#) [\[PubMed\]](#)
28. Perry, S.W.; Norman, J.P.; Barbieri, J.; Brown, E.B.; Gelbard, H.A. Mitochondrial membrane potential probes and the proton gradient: A practical usage guide. *Biotechniques* **2011**, *50*, 98–115. [\[CrossRef\]](#) [\[PubMed\]](#)
29. Srinivasan, B.; Kolli, A.R.; Esch, M.B.; Abaci, H.E.; Shuler, M.L.; Hickman, J.J. TEER Measurement Techniques for In Vitro Barrier Model Systems. *J. Lab. Autom.* **2015**, *20*, 107–126. [\[CrossRef\]](#)
30. Pfaffl, M.W.; Horgan, G.W.; Dempfle, L. Relative expression software tool (REST(C)) for group-wise comparison and statistical analysis of relative expression results in real-time PCR. *Nucleic Acids Res.* **2002**, *30*, 643. [\[CrossRef\]](#)
31. Profaci, C.P.; Munji, R.N.; Pulido, R.S.; Daneman, R. The blood–brain barrier in health and disease: Important unanswered questions. *J. Exp. Med.* **2020**, *217*, e20190062. [\[CrossRef\]](#) [\[PubMed\]](#)
32. Charles, N.A.; Holland, E.C.; Gilbertson, R.; Glass, R.; Kettenmann, H. The brain tumor microenvironment. *Glia* **2011**, *59*, 1169–1180. [\[CrossRef\]](#)
33. Okawa, S.; Gargica, S.; Blin, C.; Ender, C.; Pollard, S.M.; Krijgsveld, J. Pollard, Proteome and secretome characterisation of glioblastoma- derived neural stem cells. *Stem Cells* **2018**, *35*, 967–980. [\[CrossRef\]](#)
34. Venugopal, C.; Wang, X.S.; Manoranjan, B.; McFarlane, N.; Nolte, S.; Li, M.; Murty, N.; Siu, K.W.M.; Singh, S.K. GBM secretome induces transient transformation of human neural precursor cells. *J. Neuro-Oncol.* **2012**, *109*, 457–466. [\[CrossRef\]](#)
35. Bussolati, B.; De Ambrosis, I.; Russo, S.; Deregius, M.C.; Camussi, G. Altered angiogenesis and survival in human tumor-derived endothelial cells. *FASEB J. Off. Publ. Fed. Am. Soc. Exp. Biol.* **2003**, *17*, 1159–1161. [\[CrossRef\]](#)
36. Albulescu, R.; Codrici, E.; Popescu, I.D.; Mihai, S.; Necula, L.G.; Petrescu, D.; Teodoru, M.; Tanase, C.P. Cytokine Patterns in Brain Tumour Progression. *Mediat. Inflamm.* **2013**, *2013*, 979748. [\[CrossRef\]](#)
37. Motaln, H.; Gruden, K.; Hren, M.; Schichor, C.; Primon, M.; Rotter, A.; Lah, T.T. Human Mesenchymal Stem Cells Exploit the Immune Response Mediating Chemokines to Impact the Phenotype of Glioblastoma. *Cell Transplant.* **2012**, *21*, 1529–1545. [\[CrossRef\]](#)
38. Kebers, F.; Lewalle, J.-M.; Desreux, J.; Munaut, C.; Devy, L.; Foidart, J.-M.; Noel, A. Induction of Endothelial Cell Apoptosis by Solid Tumor Cells. *Exp. Cell Res.* **1998**, *240*, 197–205. [\[CrossRef\]](#)
39. Strilic, B.; Yang, L.; Albarran-Juarez, J.; Wachsmuth, L.; Han, K.; Müller, K.H.U.C.; Pasparakis, L.W.M.; Offermanns, S. Tumour-cell-induced endothelial cell necroptosis via death receptor 6 promotes metastasis. *Nature* **2016**, *536*, 215–218. [\[CrossRef\]](#) [\[PubMed\]](#)
40. Ahishali, B.; Kaya, M. Evaluation of Blood-Brain Barrier Integrity Using Vascular Permeability Markers: Evans Blue, Sodium Fluorescein, Albumin-Alexa Fluor Conjugates, and Horseradish Peroxidase. *Methods Mol. Biol.* **2020**, *2367*, 87–103. [\[CrossRef\]](#)
41. Wikström, M.; Springett, R. Thermodynamic efficiency, reversibility, and degree of coupling in energy conservation by the mitochondrial respiratory chain. *Commun. Biol.* **2020**, *3*, 451. [\[CrossRef\]](#)
42. Zorova, L.D.; Popkov, V.A.; Plotnikov, E.Y.; Silachev, D.N.; Pevzner, I.B.; Jankauskas, S.S.; Babenko, V.A.; Zorov, S.D.; Balakireva, A.V.; Juhaszova, M.; et al. Mitochondrial membrane potential. *Anal. Biochem.* **2018**, *552*, 50–59. [\[CrossRef\]](#)
43. Gergely, P.; Grossman, C.; Niland, B.; Puskas, F.; Neupane, H.; Allam, F.; Banki, K.; Phillips, P.E.; Perl, A. Mitochondrial hyperpolarization and ATP depletion in patients with systemic lupus erythematosus. *Arthritis Rheum.* **2002**, *46*, 175–190. [\[CrossRef\]](#)
44. Aslantürk, Ö.S. In Vitro Cytotoxicity and Cell Viability Assays: Principles, Advantages, and Disadvantages. *IntechOpen* **2018**, *13*, 71923. [\[CrossRef\]](#)
45. Janssen Duijghuijsen, L.M.; Grefte, S.; de Boer, V.; Zeper, L.W.; Van Dartel, D.A.M.; Van Der Stelt, I.; Bekkenkamp-Grovenstein, M.; Van Norren, K.; Wichers, H.; Keijer, J. Mitochondrial ATP Depletion Disrupts Caco-2 Monolayer Integrity and Internalizes Claudin 7. *Front. Physiol.* **2017**, *8*, 794. [\[CrossRef\]](#) [\[PubMed\]](#)
46. Wang, G.; Yuan, Y.; Gao, L.; Tan, X.; Yang, G.; Zhao, F.; Jin, Y. Disruption of Intracellular ATP Generation and Tight Junction Protein Expression during the Course of Brain Edema Induced by Subacute Poisoning of 1,2-Dichloroethane. *Front. Neurosci.* **2018**, *12*, 12. [\[CrossRef\]](#)
47. Kalokhe, G.; Grimm, S.A.; Chandler, J.P.; Helenowski, I.; Rademaker, A.; Raizer, J.J. Metastatic glioblastoma: Case presentations and a review of the literature. *J. Neuro-Oncol.* **2011**, *107*, 21–27. [\[CrossRef\]](#) [\[PubMed\]](#)
48. Lah, T.T.; Novak, M.; Breznik, B. Brain malignancies: Glioblastoma and brain metastases. *Semin. Cancer Biol.* **2020**, *60*, 262–273. [\[CrossRef\]](#)
49. Rosen, J.; Blau, T.; Grau, S.J.; Barbe, M.T.; Fink, G.R.; Galldiks, N. Extracranial Metastases of a Cerebral Glioblastoma: A Case Report and Review of the Literature. *Case Rep. Oncol.* **2018**, *11*, 591–600. [\[CrossRef\]](#)
50. Chen, J.-W.E.; Lumibao, J.; Blazek, A.; Gaskins, H.R.; Harley, B. Hypoxia activates enhanced invasive potential and endogenous hyaluronic acid production by glioblastoma cells. *Biomater. Sci.* **2018**, *6*, 854–862. [\[CrossRef\]](#) [\[PubMed\]](#)
51. Liberti, M.V.; Locasale, J.W. The Warburg Effect: How Does it Benefit Cancer Cells? *Trends Biochem. Sci.* **2016**, *41*, 287. [\[CrossRef\]](#) [\[PubMed\]](#)

52. Kaplan, L.; Chow, B.W.; Gu, C. Neuronal regulation of the blood–brain barrier and neurovascular coupling. *Nat. Rev. Neurosci.* **2020**, *21*, 416–432. [[CrossRef](#)] [[PubMed](#)]
53. Haseloff, R.F.; Dithmer, S.; Winkler, L.; Wolburg, H.; Blasig, I.E. Transmembrane proteins of the tight junctions at the blood–brain barrier: Structural and functional aspects. *Semin. Cell Dev. Biol.* **2015**, *38*, 16–25. [[CrossRef](#)] [[PubMed](#)]
54. Jiao, H.; Wang, Z.; Liu, Y.; Wang, P.; Xue, Y. Specific Role of Tight Junction Proteins Claudin-5, Occludin, and ZO-1 of the Blood–Brain Barrier in a Focal Cerebral Ischemic Insult. *J. Mol. Neurosci.* **2011**, *44*, 130–139. [[CrossRef](#)] [[PubMed](#)]
55. Jia, W.; Lu, R.; Martin, T.A.; Jiang, W.G. The role of claudin-5 in blood-brain barrier (BBB) and brain metastases (Review). *Mol. Med. Rep.* **2013**, *9*, 779–785. [[CrossRef](#)] [[PubMed](#)]
56. Liebner, S.; Kniesel, U.; Kalbacher, H.; Wolburg, H. Correlation of tight junction morphology with the expression of tight junction proteins in blood-brain barrier endothelial cells. *Eur. J. Cell Biol.* **2000**, *79*, 707–717. [[CrossRef](#)]
57. Liu, W.-Y.; Wang, Z.-B.; Zhang, L.-C.; Wei, X.; Li, L. Tight Junction in Blood-Brain Barrier: An Overview of Structure, Regulation, and Regulator Substances. *CNS Neurosci. Ther.* **2012**, *18*, 609–615. [[CrossRef](#)]
58. Leten, C.; Struys, T.; Dresselaers, T.; Himmelreich, U. In vivo and ex vivo assessment of the blood brain barrier integrity in different glioblastoma animal models. *J. Neuro-Oncol.* **2014**, *119*, 297–306. [[CrossRef](#)]
59. Krishnan, S.; Szabo, E.; Burghardt, I.; Frei, K.; Tabatabai, G.; Weller, M. Modulation of cerebral endothelial cell function by TGF- $\beta$  in glioblastoma: VEGF-dependent angiogenesis versus endothelial mesenchymal transition. *Oncotarget* **2015**, *6*, 22480–22495. [[CrossRef](#)]
60. Argaw, A.T.; Gurfein, B.T.; Zhang, Y.; Zameer, A.; John, G.R. VEGF-mediated disruption of endothelial CLN-5 promotes blood-brain barrier breakdown. *Proc. Natl. Acad. Sci. USA* **2009**, *106*, 1977–1982. [[CrossRef](#)]
61. Roomi, M.W.; Kalinovsky, T.; Rath, M.; Niedzwiecki, A. Modulation of MMP-2 and MMP-9 secretion by cytokines, inducers and inhibitors in human glioblastoma T-98G cells. *Oncol. Rep.* **2017**, *37*, 1907–1913. [[CrossRef](#)] [[PubMed](#)]
62. Koussounadis, A.; Langdon, S.P.; Um, I.H.; Harrison, D.; Smith, V.A. Relationship between differentially expressed m, RNA and m, RNA-protein correlations in a xenograft model system. *Sci. Rep.* **2015**, *5*, 10775. [[CrossRef](#)] [[PubMed](#)]



## CHAPTER 5

**PUBLISHED MANUSCRIPT “The paracrine effect of hypoxic and normoxic cancer secretion on the proliferation of brain endothelial cells (bEnd.3)”**



UNIVERSITY *of the*  
WESTERN CAPE

# The Paracrine Effect of Hypoxic and Normoxic Cancer Secretion on the Proliferation of Brain Endothelial Cells (bEnd.3)

Mariam Rado and David Fisher \* 

Medical Bioscience Department, Faculty of Natural Sciences, University of the Western Cape,  
Robert Sobukwe Road, Bellville 7335, South Africa; 3580480@myuwc.ac.za

\* Correspondence: dfisher@uwc.ac.za; Tel.: +27-21-959-2185

**Abstract:** Background: This study aimed to investigate the disruption of cell cycle phases of bEnd.3 cells exposed to cancer paracrine secretion. Cancer cells have been reported to use the secretion of paracrine factors to compromise the endothelial barrier to prepare for their passage into the parenchyma. As cancer cells are known to act differently under conditions of hypoxia, we investigated how conditional media (CM) derived from breast and glioblastoma cells incubated under conditions of normoxia and hypoxia would affect proliferation of brain endothelial cells (bEnd.3). Methods: Brain endothelial cells (bEnd.3) were cultivated with normoxic and hypoxic CM generated from breast cancer MCF7 cells and glioblastoma U-87 cells. Cell proliferation was evaluated using the trypan blue exclusion assay and phases of the cell cycle were evaluated using flow cytometry. Results: bEnd.3 proliferations was suppressed more aggressively with hypoxic CM after 72 and 96 h; cell cycle analysis showed that paracrine treatment tended to prevent BECs from entering the G2 phase, thus suppressing cell division. Conclusions: MCF7 and U-87 cells induce suppressed proliferation of BECs differentially under hypoxia by blocking cell cycle progression to the G2 phase.

**Keywords:** cell division; cell proliferation; brain endothelial cells; cancer secretion; hypoxia; normoxia; U-87 cells; MCF7 cells; bEnd.3 cells



**Citation:** Rado, M.; Fisher, D.

The Paracrine Effect of Hypoxic and Normoxic Cancer Secretion on the Proliferation of Brain Endothelial Cells (bEnd.3). *Cells* **2022**, *11*, 1197.  
<https://doi.org/10.3390/cells11071197>

Academic Editor: David Qian

Received: 11 March 2022

Accepted: 30 March 2022

Published: 2 April 2022

**Publisher's Note:** MDPI stays neutral with regard to jurisdictional claims in published maps and institutional affiliations.



**Copyright:** © 2022 by the authors. Licensee MDPI, Basel, Switzerland. This article is an open access article distributed under the terms and conditions of the Creative Commons Attribution (CC BY) license (<https://creativecommons.org/licenses/by/4.0/>).

## 1. Introduction

Blood vessels are central to the metastatic process of cancer cells. Metastatic breast cancer cells have a preference for brain tissue, and almost 30% of breast cancer cells form tumours in the brain [1]. For breast cancer cells to successfully enter neural tissue, they have to traverse the notoriously impregnable blood–brain barrier (BBB). Brain capillary endothelial cells (BECs) form the primary barrier and have to be compromised to provide entry to cancer cells. Primary glioblastoma (GBM) cancer cells are one of the most aggressive tumours, representing up to 50% of all malignant primary brain tumours in humans. These GBM cells arise from the brain's glial tissue [2]. However, as opposed to breast cancer, which is well known to metastasically enter into the central nervous system (CNS), GBM has a very low rate (<2%) of metastasis [3].

As cancer grows, the invading cancer cells are released from the primary tumour site and migrate towards the blood vessels to access nutrients and oxygen, moving to other anatomical locations more suitable for growth [4]. Paracrine factors and their mechanisms that determine the crossing of blood vessels are still unclear, but the invasive cancer cells indeed interact with vascular cells (particularly the endothelium) during this process. According to the literature, invasive cancer cells either form co-option with the pre-existing blood vessels or initiate the formation of new blood vessels (angiogenesis) from pre-existing vessels in order to survive [5]. Cancer cell co-option is a non-angiogenic process through which tumour cells utilise pre-existing tissue blood vessels to support tumour growth, survival and metastasis [5]. The co-option of cancer cells with the existing blood vessels was observed in many types of cancer. However, it is often observed in organs with high vasculature, such as the brain and lung, and it is suggested that the ineffectuality of



anti-angiogenic therapy is due to the co-option phenomena [6]. Although the mechanism whereby cancer cells co-opt existing blood vessels is not completely understood, cancer–endothelial paracrine interactions are believed to play a key role in initiating the recruitment of metastatic cancer cells to bind with the luminal endothelium. Metastatic cancer cells modulate the capillary endothelium with paracrine factors to facilitate the migration across capillary, both from the primary tumour site into the capillary lumen or from the capillary lumen into new parenchymal tissue [7].

Teuwen et al. (2021) showed that endothelial cells in co-opted vessels have a lower proliferation rate than the angiogenic endothelial cells in normal vessels, although they are transcriptomically similar to quiescent endothelial cells in healthy vessels [8]. In GBM, the co-option with the blood vessel is the preferred pathway to infiltrate the surrounding CNS tissues [7] rather than metastatically migrating to a distal anatomical tissue.

The survival of metastatic cancer cells relies on compromising endothelial cells as tumour cells use blood vessels to access distal anatomical locations for optimum O<sub>2</sub> and nutrition. It is well known that cancer cells modify their metabolism depending on their situation and location [9–11]. Thus, it is expected that detached metastatic cancer cells are metabolically not ready to proliferate. The process of detachment from the tumour body probably affects their metabolism [12] and, therefore, detached cancer cells are physiologically optimised functionally to prioritise their immigration to new locations. Circulating cancer cells have decreased viability due to the harsh circulatory environment with its shear stresses and immunological factors [13]. In contrast, cancer cells in a rapidly growing tumour might use paracrine factors to act on endothelial cells to induce angiogenesis to support their growth with nutrition and O<sub>2</sub> and also remove their waste.

Glioblastoma and breast cancer cells are well-known to produce a high level of growth and other paracrine factors [14,15]. The high level of expression of growth factors from cancer cells was associated with an increase in the permeability at the BBB [16–19] due to the disruption of the tight junction [20].

At the core of GBM tumours, cancer cells have been associated with suppressed proliferation due to low levels of O<sub>2</sub> and have been reported to modulate their metabolism and proliferation rates under these conditions, mostly through the secretion of autocrine and paracrine factors [21].

Mitochondria are an essential regulator of cell proliferation [22]. In our previous studies [23,24], we showed that mitochondrial activity of endothelial cells (bEnd.3) was suppressed after cultivation with paracrine factors secreted from breast and GBM cancer cells. Mitochondria regulate cell signalling pathways, cell death and gene expression, including cell division [25].

Given that cancer cells can modulate their proliferation rates differentially under conditions of normoxia and hypoxia, in this study, we investigated whether paracrine factors secreted from breast and GBM cancer cells incubated under normoxic (21% O<sub>2</sub>) and hypoxic (5% O<sub>2</sub>) conditions could modulate brain endothelial cells, the primary regulatory component of the BBB. Our main hypothesis is that under normoxic and hypoxic conditions, metastatic and non-metastatic cancers might differentially modulate BECs.

## 2. Materials and Methods

### 2.1. Experimental Design

The study is designed to investigate the paracrine effect of conditioned media derived from glioblastoma cells (U-87 (ATCC HTB-14) and breast cancer MCF7 cells (ATCC HTB-22) incubated under normoxic (21% O<sub>2</sub>) and hypoxic (5% O<sub>2</sub>) conditions on the proliferation of brain endothelial cells (bEnd.3 ATCC® CRL-2299, Gaithersburg, MD, USA). The experiments were carried out in triplicate as a minimum ( $n = 3$ ) and duplicated to ensure repeatability. The effect of normoxic and hypoxic cancerous factors secreted by cancer cells in their supernatants was compared by treating bEnd.3 cells with selected concentrations of cancer cells' CM for 24 to 96 h. At each time interval, the cellular proliferation was measured

by counting the cells in culture. Using the same experimental design, cell cycle analysis was also performed using flow cytometry (BD Biosciences, Franklin Lakes, NJ, USA).

## 2.2. Cell Culture and Treatment

Murine brain microvascular endothelial cells line (bEnd.3) were cultured in complete Dulbecco's Modified Eagle Medium (DMEM, Gibco, No 22320022, 8717 Grovemont Cir, Gaithersburg, MD, USA, 20877, United States) supplemented with 10% Fetal Bovine Serum (FBS; Biowest, No 10493-106, 2 Rue du Vieux Bourg 49,340 Nuaillé -France) and 100 U/mL penicillin/streptomycin (Gibco, No 15070063) (Complete DMEM)). TrypLE™ Express Enzyme (ThermoFisher Scientific, No A1285901, 168 Third Avenue, Waltham, MA, USA 0245) was used for harvesting the cells.

Cancer cells were cultured in a normal humidified 5% CO<sub>2</sub> incubator at 37 °C until they reached 50% confluence, then the spent growth media was replaced with a fresh complete DMEM. Cells were further incubated either under hypoxic (5% O<sub>2</sub>) or normoxic (21% O<sub>2</sub>) conditions. The incubation under hypoxic conditions was performed by placing the cells in a sterilised Modular Incubator hypoxia chamber (MIC 101; Billups-Rothenberg, Inc., Sorrento Valley Blvd, San Diego, CA 92121, USA). The hypoxia chamber is provided with a Greisinger oxygen meter with a sensor (GOX 100-0-CO, No 600437, Billups-Rothenberg, Inc., San Diego, CA, USA), which allows for the measurement of O<sub>2</sub> levels during the incubation time. After 48 h of incubation in hypoxic or normoxic conditions, the supernatant was collected in ice-cooled centrifuged tubes, centrifuged at 3500 × g rpm for 5 min at 4 °C and then filtered with a GVS filter (0.20 µm). The supernatants were collected and aliquoted in 2–5 mL and stored at −80 °C. A fresh complete DMEM was added to the cancer supernatant to make up 20%, 40% and 75% concentrations, forming the basis of the conditioned media (CM).

## 2.3. Proliferation Assessment

Cell proliferation in endothelial cells was determined by calculating the increase in the cell number using the trypan blue dye (TB). In this assay, bEnd.3 cells were seeded in 6-well plates at  $5 \times 10^5$  cells per well, each experimental group was seeded in triplicate, the volume of medium was 1.5 mL/well. The plates were incubated at 37 °C and 5% CO<sub>2</sub> for 24 h allowing the attachment of the cells. An inverted microscope (Eclipse-Ts2-Ls, Nikon, Amsterdam, The Netherlands) was used to observe the attachment. Once the attachment was confirmed, the growth medium was removed and replaced with CM produced from U-87 glioblastoma cancer cells supernatant and MCF7 breast cancer cells supernatant under hypoxic and normoxic conditions: the supernatant was diluted with complete DMEM to concentrations of 20%, 40% and 75%. Controls were treated with a fresh, completed DMEM media. The cells were incubated for 24, 48, 72 and 96 h, during which daily exposure with CM was performed. At each time interval, cells in each well were washed, detached by TrypLE™ Express Enzyme (ThermoFisher Scientific, Waltham, MA, USA), centrifuged and resuspended in normal media. Immediately, cells were prepared for cell counting by mixing 10 µL of cells suspension with 10 µL of trypan blue (TB). Then, 10 µL from the cell suspension-TB mixture was added to the counting slides. The count was performed by Countess III specialised cell counter (ThermoFisher Scientific, 168 Third Avenue, Waltham, MA, USA), which eliminates a large margin of human variability, which occurs when conducting a manual count on a hemocytometer. The Countess III utilises standardised algorithms to eliminate debris and takes into account potential cell clusters and cell size.

#### 2.4. Cell Cycle Analysis by Flow Cytometry

In this study, the results obtained from the cell proliferation assay motivated the analysis of the cell cycle of brain endothelial cells after exposure to selected concentrations of conditioned media (CM) using flow cytometry.

bEnd.3 cells were seeded in T<sub>25</sub> flasks at a density of  $5 \times 10^5$  cells/flask, then incubated for 24 h at 37 °C in a 5% CO<sub>2</sub> incubator allowing the cell attachment. The growth medium was replaced by selected concentrations of cancer conditioned media generated under hypoxic (5% O<sub>2</sub>) and normoxic (21% O<sub>2</sub>) culture conditions of U-87 cells and MCF7 cells. Cells were cultivated for 24, 48, 72 and 96 h. For the purpose of flow cytometry, CM was removed, and cell cultures were washed with 1ml PBS. bEnd.3 were then harvested by exposing cell cultures to 700 µL of TrypLE™ Express enzyme for 5 min in a humidified incubator. Cells were then pelleted, washed once with cold PBS. Slowly, 70% of ice-cold ethanol was added to the cell while vortexing to reduce cell clumping to a final volume of 5 mL. The cells were stored at −20 °C for a minimum of 2 h. Before analysis, cells were pelleted at 1000 × g rpm for 5 min. Carefully, ethanol was removed, and cells were centrifuged in 1X cold PBS at 1000 × g rpm for 5 min. After removing the PBS, 0.5 mL of DAPI stain solution was added to each sample, then incubated for 10 min at room temperature (RT). Cell cycle phase distribution was determined by BD (BD Biosciences, Franklin Lakes, NJ, USA) FACS Aria III flow cytometer. Samples were analysed in triplicates, DNA content of 10,000 events was analysed by FlowJo\_v10.6.1 analysis software (Ashland, OR, USA).

#### 2.5. Statistical Analysis

All data were analysed using Graph Pad Prism version 6.0 (San Diego, CA, USA). All data were presented as means ± SEM. Differences between the groups were analysed by one or two-way ANOVA, followed by Dunnett's multiple comparison test. The level of significance was accepted at  $p < 0.05$  for a 95% confidence interval. The number of replicates is indicated in the figure legends.

### 3. Results

#### 3.1. Proliferation of bEnd.3 Cells after Exposure to Cancer Secretion

An equal number of brain endothelial cells were cultured in 6-well plates in triplicates (as described in the methodology). Cell proliferation was measured by counting the cell number after exposure to conditioned media harvested from cancer cells cultured under normoxia and hypoxia.

In Figure 1A, bEnd.3 cells were cultivated in normoxic MCF7 conditioned media (MCF7CM). After 48 h of exposure, bEnd.3 BECs showed no difference in their proliferation rate compared to the control; however, after 72 h, cells exposed to 40% and 75% of normoxic MCF7CM significantly reduced their proliferation ( $p < 0.05$  and  $p < 0.01$ , respectively), and at 96 h, a significant dose-related suppression of cell proliferation was observed at all concentrations ( $p < 0.05$  and  $p < 0.01$ ).

In Figure 1B, bEnd.3 cells were exposed to hypoxic MCF7 conditioned media (MCF7CM). The proliferation of cells after 48 h of cultivation with hypoxic MCF7CM was not different from the control; however, at 72–96 h, a dose-related suppression of proliferation occurred particularly in cells exposed to 40% and 75% (Figure 1B:  $p < 0.05$ ;  $p < 0.01$ ;  $p < 0.001$ ).

In Figure 1C, bEnd.3 cells were cultured with U-87CM generated from U-87 cells cultured under normoxic conditions. Cells in the control groups (0%) demonstrated a gradient increase in their proliferation over time and exposed bEnd.3 cells also showed increased proliferation over time; however, the exposed bEnd.3 cells seemed to proliferate slower than control bEnd.3 cells. At 24 and 48 h of exposure, no difference was observed in the proliferation rate between the control and the exposed cells. However, prolonged exposure for 72 and 96 h caused a significant decrease in the proliferation of bEnd.3 cells treated with 75% of U-87CM ( $p < 0.05$ ), whereas bEnd.3 cells exposed with 20% and 40% at the same time did not show a significant difference in the proliferation rate compared to the control.

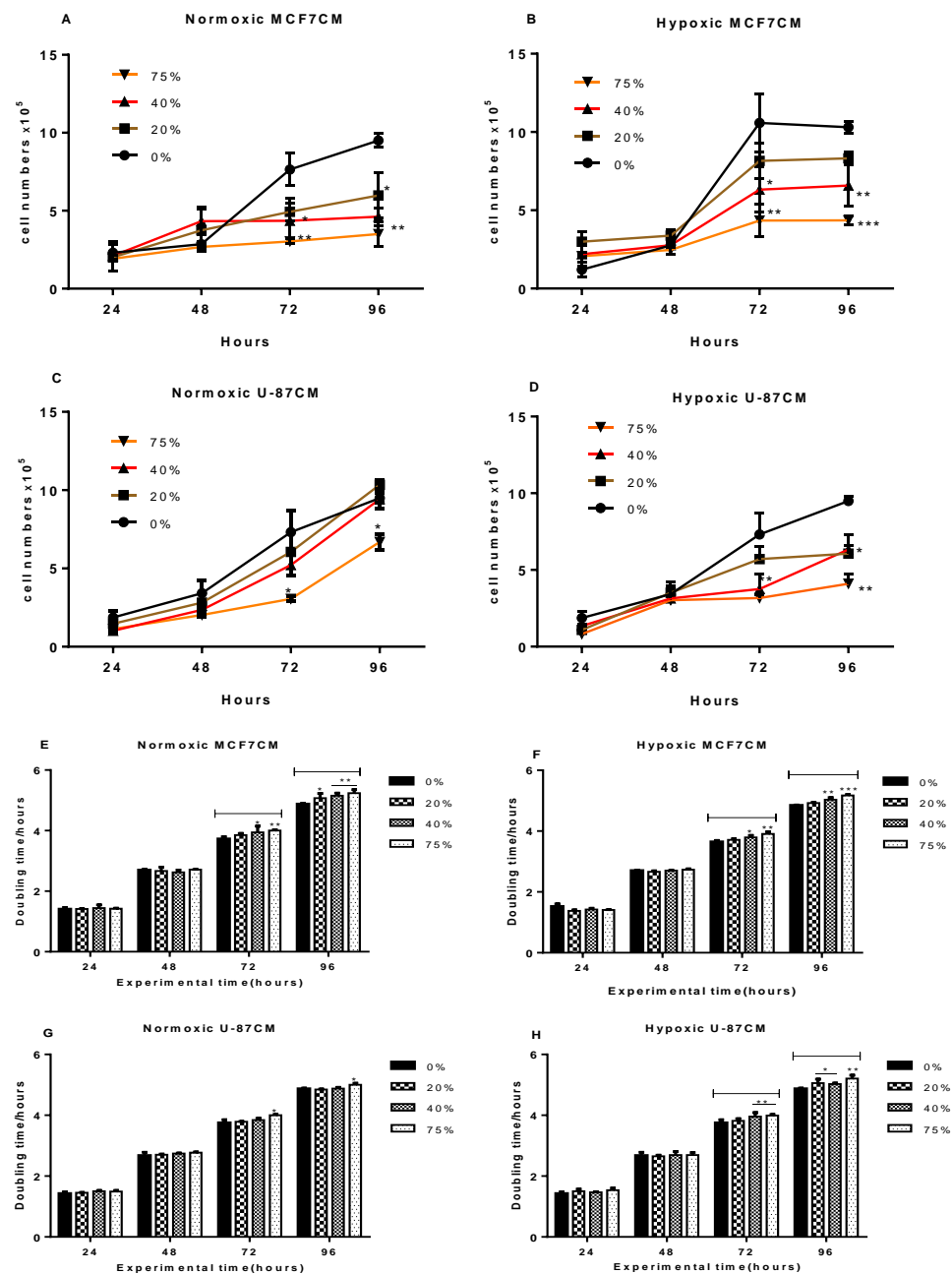


**Figure 1.** Shows the proliferation of bEnd.3 cells that were exposed to conditioned media produced from MCF7 and U-87 cells cultivated under normoxic (21% O<sub>2</sub>) and hypoxic (5% O<sub>2</sub>) conditions: (A) illustrates the proliferation rate of bEnd.3 cells after daily exposure to selected concentrations of normoxic MCF7CM (derived from breast cancer cells). (B) Shows the proliferation rate of bEnd.3 cells after daily exposure to selected concentrations of hypoxic MCF7CM. (C) Shows the proliferation rate of bEnd.3 cells exposed daily to selected concentrations of glioblastoma U-87 cell normoxically derived conditioned media (U-87CM). (D) Shows the proliferation rate of bEnd.3 cells daily exposed to selected concentrations of hypoxic U-87CM. (E–H) show the doubling time for bEnd.3 cells exposed to normoxic and hypoxic cancer secretions. (\*  $p < 0.05$ , \*\*  $p < 0.01$ , \*\*\*  $p < 0.001$ ;  $n = 3$ ).

Figure 1D illustrates the proliferation rate of bEnd.3 cells after exposure to hypoxically derived U-87CM. At 24 and 48 h of exposure, no statistically significant changes were observed in the proliferation rate between the control groups and the treated cells. At 72 and 96 h, bEnd.3 cells exposed to U-87CM (40 and 75% U-87CM) proliferated at a significantly slower rate than the control (Figure 1D:  $p < 0.05$ ;  $p < 0.01$ ).

We use the standard formula for growth rate (GR):  $GR = N2 - N1 / t2 - t1$  (units: cells/h) ( $N1$  is the number of cells at the start of the experiment;  $N2$  is the number of cells at a particular selected timeframe (in our case 24, 48, 72, 96 h)). From these data, we can evaluate the specific growth constant:  $\mu = \text{LOG}_{10} N1 - \text{LOG}_{10} N0 / t1 - t0$ . Because the specific growth constant represents a measure of the ability of the organism to grow under a given set of environmental conditions, doubling times are more easily understood or meaningful. The doubling time is simply the time (in hours) required for the cells to divide. Smaller values of DT indicate rapid growth, while larger doubling times indicate slow growth. The specific growth constant is then used to calculate the doubling time (DT) as follows:  $DT = (\text{Log}_{10} 2) / \mu \times 24$  or  $DT = (0.301 / \mu) \times 24$  (see Figure 1). The DT data closely reflected the proliferation data.

### 3.2. Analysis of Cell Cycle of bEnd.3 Cells after Exposure to Cancer Secretion

The proliferation data illustrated that exposure of bEnd.3 cells to paracrine secretion from cancer cells suppressed the proliferation after 72 and 96 h. Thus, we examined the changes in the cell cycle of bEnd.3 after extended exposure to cancer conditioned media; bEnd.3 cells were cultivated in selected concentrations of glioblastoma U-87 (U-87CM) and breast cancer MCF7 cells conditioned media (MCF7CM) and monitored at 72 and 96 h. Controls (non-treated bEnd.3 cells) were statistically compared to treated bEnd.3 cells and were prepared for cell cycle analysis using the DAPI experimental protocols. The changes in the cell number in cell division phases (G1, S and G2) between exposed bEnd.3 cells and the control were statistically compared.

#### 3.2.1. Cell Cycle Analysis of BECs Exposed to Breast Cancer-Derived Conditioned Media (MCF7CM)

BECs (bEnd.3 cells) were cultured with normoxic MCF7CM and produced no significant changes occurring between 24–48 h. In Figure 2A, at 72 h, the exposure to MCF7CM at all concentrations resulted in the accumulation of cells in the G1 phase relative to the control ( $p < 0.001$  at 20%,  $p < 0.0001$  at 40% and 75%); as a consequence, fewer cells entered the S phase and G2 phase of the cell cycle. The cell number in the S phase for controls was significantly higher than those exposed to 40% and 75% of normoxic MCF7CM ( $p < 0.0001$ ). Similar results are shown in Figure 2B (at 72 h), where bEnd.3 cells exposed to hypoxic MCF7CM, an accumulation of exposed bEnd.3 cells in the G1 phase occurred, delaying the entering of cells into the S and G2 phases compared to the control. The G1 phase of treated bEnd.3 cells at all concentrations were significantly higher than the controls ( $p < 0.01$  at 20% and 40%, and  $p < 0.001$  at 75%). This eventuated in a significant decrease in the number of exposed cells in the S phase ( $p < 0.05$ , and  $p < 0.01$  at 40% and 75%, respectively) and in the G2 phase ( $p < 0.05$ ) compared to the control. Numbers of bEnd.3 cells exposed to 20% hypoxic MCF7CM in the S phase and 40% in the G2 phase were decreased non-statistically relative to the control; however, a significant decrease in cell number was observed in the G2 phase in bEnd.3 cells exposed to 20% and 75% hypoxic MCF7CM ( $p < 0.05$ ).

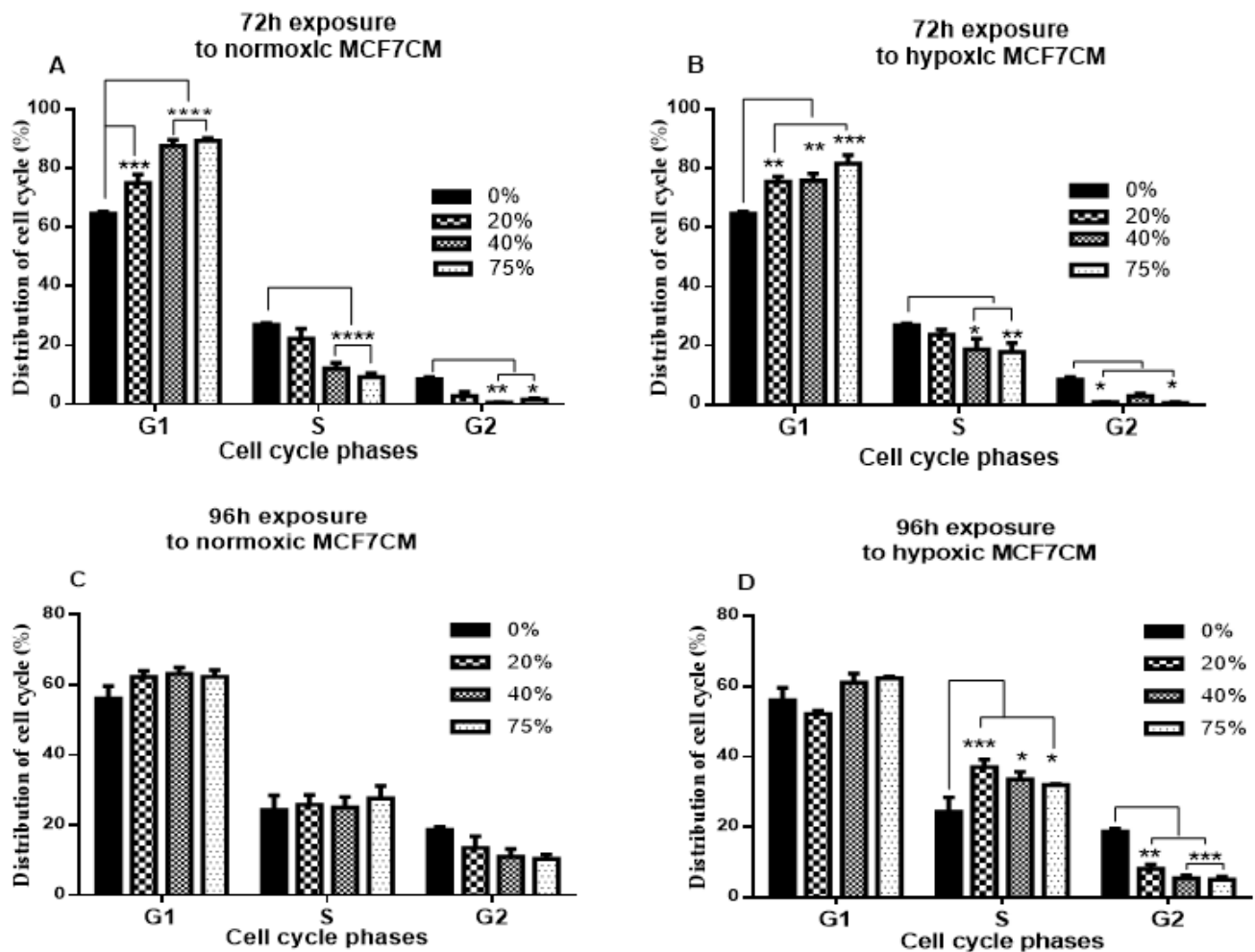


**Figure 2.** Represents a quantification of cell cycle distribution in bEnd.3 cells after exposure to conditioned media generated from MCF7 cells (MCF7CM) under normoxic (21% O<sub>2</sub>) and hypoxic (5% O<sub>2</sub>) conditions: (A) bEnd.3 cells were exposed to normoxic MCF7CM for 72 h. (B) bEnd.3 cells were exposed to hypoxic MCF7CM for 72 h. (C) bEnd.3 cells were exposed to normoxic MCF7CM for 96 h. (D) bEnd.3 cells were exposed to hypoxic MCF7CM for 96 h. (\*  $p < 0.05$ , \*\*  $p < 0.01$ , \*\*\*  $p < 0.001$ , \*\*\*\*  $p < 0.0001$ ;  $n = 3$ ).

As shown in Figure 2C, after 96 h, exposure to normoxic MCF7CM did not show a significant difference in the number of exposed cells relative to the control in all cell cycle phases. However, the exposure to hypoxic MCF7CM for 96 h in Figure 2D shows that, compared to the control, exposed bEnd.3 cells at all concentrations were located in the S phase of the cell cycle relative to the control ( $p < 0.05$  and  $p < 0.001$ ), causing a delay in cells entering the G2 phase ( $p < 0.01$  and  $p < 0.001$ ).

### 3.2.2. Analysis of Cell Cycle of bEnd.3 Cells Exposed to Glioblastoma U-87 Cells Conditioned Media (U-87CM)

In Figure 3A, bEnd.3 cells were cultured with normoxic U-87CM. At 72 h, all concentrations (20%, 40% and 75%) showed that the cell cycle distribution was not statistically different compared to the control. However, at 72 h (Figure 3B), the distribution of cells exposed to hypoxically derived U-87CM in the G1 phase was significantly higher in bEnd.3 cells that were treated with 75% compared to the control ( $p < 0.0001$ ), while the distribution of cells in the S phase was significantly higher in bEnd.3 cells that were exposed to 20% and 75% compared to the control ( $p < 0.01$  and  $p < 0.05$ , respectively). In all concentrations



in the G2 phase, the cell distribution was significantly lower in the exposed bEnd.3 cells compared to the control ( $p < 0.05$ ,  $p < 0.01$  and  $p < 0.0001$ ).

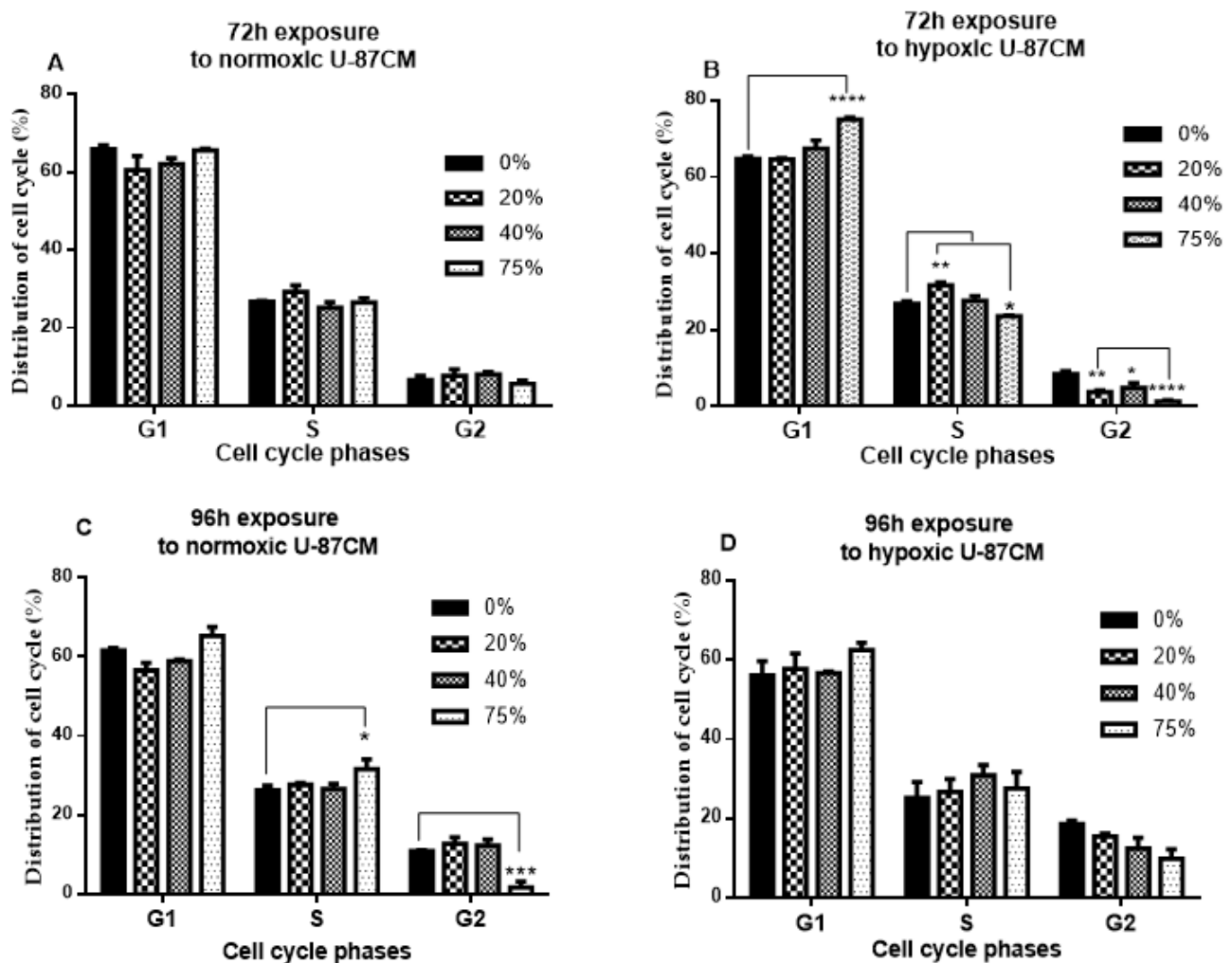


**Figure 3.** Represents a quantification of cell cycle distribution of bEnd.3 cells after exposure to conditioned media generated from U-87 glioblastoma cells (U-87CM) under normoxic (21% O<sub>2</sub>) and hypoxic (5% O<sub>2</sub>) conditions: (A) bEnd.3 cells were exposed to normoxic U-87CM for 72 h. (B) bEnd.3 cells were exposed to hypoxic U-87CM for 72 h. (C) bEnd.3 cells were exposed to normoxic U-87CM for 96 h. (D) bEnd.3 cells were exposed to hypoxic U-87CM for 96 h. (\*  $p < 0.05$ , \*\*  $p < 0.01$ , \*\*\*  $p < 0.001$ , \*\*\*\*  $p < 0.0001$ ;  $n = 3$ ).

Figure 3C demonstrated that after 96 h exposure, the number of cells exposed to 75% of normoxic U-87CM elevated in the G1 and S phases ( $p > 0.05$ ), which resulted in a delay of cells to enter the G2 phase of the cell cycle ( $p < 0.001$ ). Cell cycle phases of bEnd.3 cells exposed to the lower concentrations of U-87CM did not statistically differ from the control. In Figure 3D, bEnd.3 cells that were cultured with hypoxically derived U-87CM were not statistically different from the control.



#### 4. Discussion

Brain and breast cancer are common aggressive cancers due to their extraordinary ability to metastatically invade both local and distal anatomical tissue. Breast cancer is the most common metastatic cancer of the brain after lung cancer [26], seemingly preferring anatomical areas that are highly vascularised and with high  $O_2$  concentrations. To enter the brain, metastatic breast cancer cells must cross the notoriously rigorous BBB endothelial cells. In contrast, brain cancer (glioblastoma) spreads aggressively into different areas in the brain especially relocating along the internal routes of brain blood vessels but is known to rarely metastatically cross the BBB to tissues outside the brain [27,28]. Both brain and breast cancer cells use the endothelial cells of capillaries to metastatically relocate to their new locations.

The high proliferation rate in glioblastoma and breast cancer outstrips angiogenesis to create an area of oxygen deficiency at the core of the tumour. Thus, tumour growth is differentiated into tumour zones depending on oxygen availability. The core area of the tumour is known to become necrotic, where  $O_2$  levels can drop to less than 0.01%; here, most cancer cells become necrotic [29]. Subsequently, these hypoxic cancer cells reduced their proliferation to adapt to the low levels of  $O_2$  and modulated their metabolism to survive. Hypoxic cells tend to detach and emigrate to other ideal areas (high  $O_2$  and nutrient concentration) for their proliferation. Tumour cells surrounding the hypoxic area are mostly normoxic (also called perivascular cells due to their proximity to blood vessels). The area between the tumour body and the blood vessels is called the invasive area. Cancer cells present in the invasive area detach from the hypoxic tumour area; they migrate towards blood vessels, co-opting with them to gain access to nutrition and  $O_2$  while preparing to migrate through the blood vessels [30]. The intravasation of cancer cells into the blood vessel is mediated by proteases mainly secreted from cancer cells such as matrix metalloproteinases (MMPs) [31], acting on the extracellular matrix membrane, which paves the separation of the cell–cell protein junction. Cancer cells spend a short time in the bloodstream as it is perilous due to the immune agents and mechanical shear stresses [32]. Cancer cells attach to the luminal surfaces of small capillaries (arrestation) before metastasis across the capillary endothelium to the new location occurs (this process is also called extravasation). The attachment of cancer cells at the luminal surfaces of small capillaries dramatically slows blood flow (blood flow is proportional to radius). This results in zones of relative capillary hypoxia both proximal and distal to the attachment of the metastatic cancer cell. The formation of capillary hypoxic zones may affect how aggressively the metastatic cancer cell impacts brain endothelial physiology either directly or via paracrine factors (Figure 4) [33]. The interaction between these cancer cells and brain endothelial cells at extravasation and intravasation points is not fully understood.

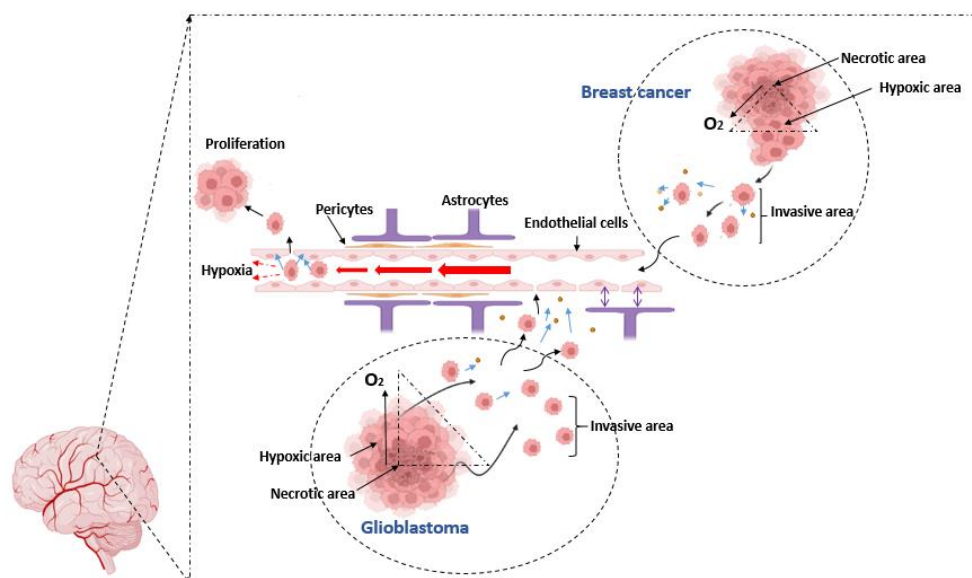


**Figure 4.** Schematic illustration compares our postulates on the metastatic mechanism of brain cancer cells (GBM) and metastatic brain cancer cells (breast cancer) to compromise the brain capillary: Both brain cancer and breast cancer are solid tumours, characterised by tumour zones of low levels of  $O_2$ , facilitating the transformation of primary tumour cells into differentiated metastatic cancer cells. The core of the fast-growing tumour forms a necrotic zone (dying or dead cells) which is surrounded by a hypoxic zone where cancer cells are metabolically modified by the low  $O_2$  level. Hypoxic cells are transformed into invasive cells, which tend to detach from the tumour and migrate to the blood vessels, forming invasive areas. Cancer cells in the invasive area secrete factors (proteases: blue arrows), enhancing their passage into the blood vessel. Cancer cells migrate with the bloodstream and are arrested to the luminal surface of brain capillaries, creating complex interactions with endothelial cells, initially via soluble paracrine factors released from cancer cells before the physical adhesion, to facilitate the movement of cancer cells through the endothelium. Simultaneously, attachment of cancer cells to the lumen drastically reduces blood flow (blood flow rate ( $F$ ) is proportional to the radius ( $r$ ) of the blood vessel:  $F \propto r^4$ ), resulting in the formation of relative hypoxia both proximally and distally to the site of cancer cell attachment. The effect of hypoxia on BECs cause increased permeability, compromising the integrity of the capillary endothelium which facilitate the metastasis of cancer cells into the brain [34–36].

Given that cancer cells are known to modulate their rates of proliferation in response to  $O_2$  concentration, we investigated whether paracrine factors secreted from cancer cells incubated under normoxic or hypoxic conditions would affect the proliferation rates of BECs (bEnd.3 cells). Invasive cancer cells are characterised by the secretion of heterogeneous secreted factors that increase their malignancy. Among the various effects to facilitate invasive events, these factors are thought to affect the degradation of extracellular matrix (ECM) components, cell detachment and migration through the basement membrane. Glioblastoma and breast cancer cells are reported to secrete a variety of paracrine factors: these cancer cells release extracellular vesicles, carrying molecules such as proteins and microRNAs, vascular growth factors, IL-6,8, all of which play a role in inducing the BBB breakdown [37]. In a comparative study to quantify the proteins in the conditioned media of three glioblastoma cell lines (LN18, U118 and U-87), the number of proteins in the U-87 conditioned media was significantly higher than in the other cell lines [38]. We further examined if the cell cycle was implicated in the modulation of BEC (bEnd.3) proliferation treated with selected concentrations of normoxic or hypoxically derived conditioned media.

Proliferation is a measurement of the rate at which cultured cells are dividing. In this brief report, we compared the rate of BEC (bEnd.3 cells) division over 96 h, with those which have been exposed to selected concentrations of conditioned media, which was

derived from cultured cancer cells grown under either normoxic (21% O<sub>2</sub>) or hypoxic (5% O<sub>2</sub>) conditions of incubation. We chose two types of cancers: breast cancer, which has a preference for metastatically relocating to the CNS, and the aggressive glioblastoma cancer, which tends to have a preference for neural tissue with less than 2% metastasis occurring [3].

Our first observation was that BEC (bEnd.3) did not statistically respond to either the normoxically or the hypoxically derived conditional media for 24 and 48 h. Secondly, treatment with paracrine factors derived from the supernatant (conditioned media) of cancer cells affected the long-term suppression of cell division of BEC (bEnd.3 cells) at 72 and 96 h. Breast cancer (MCF7) conditioned media had a dose-related effect on cell proliferation, and under normoxically derived MCF7CM suppressed cell division, while hypoxically derived MCF7CM essentially had a more differentiated dose-related effect which extended from 72 to 96 h. In contrast, only the highest concentration of normoxically-derived U87CM (75%) produced a suppression of proliferation. However, under the hypoxically-derived U87CM conditions, all treatment concentrations suppressed proliferation (except the lowest dose (20%) at 72 h). This indicated that U87 cells incubated under hypoxic conditions generated paracrine factors more aggressively under hypoxic conditions.

The proliferation of bEnd.3 cells exposed to normoxic or hypoxic U-87 or MCF7 conditioned media were not statistically different from the controls after 24–48 h exposure. This indicated that bEnd.3 cells were either able to adapt to the initial cancer paracrine secretion for 48 h of exposure, or the paracrine effects were initially buffered within the BECs (bEnd.3) but thereafter were suppressed or overwhelmed. Previous studies in our laboratory showed that ATP was only suppressed after 72 h of treatment with conditioned media [23]. It is well established that cell division is an energy-intensive process and very sensitive to a lack of ATP. This postulate is in alignment with our proliferation experiments, in which, only after 72 and 96 h, bEnd.3 cells exhibited a slower proliferation than the control (Figure 1). This suggested that cancer secretions suppress proliferation only after long-term exposure. Our results are supported by previous observations of Charalambous (2006), which showed that human brain endothelial cells isolated from brain cancer areas proliferate slower than their normal counterparts [39]; however, another study reported that renal endothelial cells isolated from tumour area proliferated quicker than normal renal endothelial cells [40]. Other studies reported that co-culture of brain cancer cells with HUVEC endothelial cells increased the cell number of endothelial cells due to the higher stimulation by pro-angiogenic factors secreted from cancer cells such as growth factors and cytokines [37,41]. However, these studies only reported experiments carried out under normoxic conditions. The literature seems to provide a consensus that cancer cells tend to increase the proliferation of systemic endothelial cells, while the proliferation of BECs is suppressed. Given that our data showed that cancer-derived paracrine factors affect the rate of BEC proliferation, we further investigated the cell cycle of endothelial cells exposed to cancer hypoxic- and normoxic-induced cancer secretions after long-term exposure (72 and 96 h) using flow cytometry.

However, we also reported on the corresponding doubling time (DT) for these experimental groups. The DT closely reflected our proliferation data, and in general, DT was only significantly different at 72 and 96 h. The increase in DT for treated cells endorsed the proliferation data, in that DT of treated cell cultures had larger DTs, indicating slower rates of BEC cell division.

Flow cytometry is a powerful technique commonly used in cell biology. It allows the analysis of multi-parametric physical and chemical characteristics of millions of cells per second. This makes it a rapid and quantitative method for the analysis and categorisation of cell cycle phases [42].

We used the Fluorescence-activated cells sorter (FACS), a type of flow cytometry that analyses the internal structures of cells and separates them into different groups, to investigate BECs that were exposed to the selected concentration of CM [43,44]. Because

the proliferation of BECs was affected, we wanted to understand at which phase of the BEC's mitotic cycle this occurred.

At the cellular level, proliferated cells pass through sequential phases to complete the cell division (including G1-S-G2); during these phases, the cell has different amounts of DNA, which can be detected and quantified by flow cytometry.

Cell cycle analysis of bEnd.3 cells exposed to normoxic MCF7CM only showed a change in the G2 phase after 72 h exposure (Figure 2A), whereas the distribution of bEnd.3 cells after 96 h exposure with normoxic MCF7CM was not statically different from the control (Figure 2C). In contrast, significant changes were observed in the G1, S and G2 phases after 72 and 96 h of cultivation with 75% of hypoxic MCF7CM (Figure 2B,D). What is consistent throughout cell cycle data is that, compared to controls, treated cells are held up in both the G1 and the S phases, resulting in suppressed cell numbers in the G2 phase. Fewer cells in the G2 phase would result in fewer cells being in preparation to enter into the mitotic phase of active cell division, thus leading to suppression of cell proliferation.

bEnd.3 cells exposed to normoxic U-87CM for 72 h did not show a statistical difference in cell phase distribution compared to the control (Figure 3A). It was surprising that only a non-statistical suppression of the G2 phase of bEnd.3 cells occurred for treatment with normoxic U87CM (75%) at 72 h. However, after 96 h, only the S and G2 phases of normoxic U87CM (75%) exposure were altered significantly (Figure 3C). This was reflected in the proliferation data in which also only cells treated with 75% normoxic U87CM were suppressed. These results were similar to the data observed in the breast cancer study, which saw the suppression of cells entering into the G2 phase of the cell cycle, thus stalling BECs (bEnd.3 cells) from entering into the mitotic phase of cell division.

However, after exposure to hypoxic U-87CM (Figure 3B), the change in G1/S/G2 phases was only observed after 72 h exposure; exposure for 96 h did not statically show a difference in the distribution of cell cycle phases (Figure 3D). Cells exposed to hypoxically derived U87CM tended to be held up from progressing to the next phase in either the G1 or the S phase, resulting in the G2 phase having suppressed numbers of cells. This would result in fewer cells entering into the mitotic phase of cell division, ultimately suppressing cell proliferation. Although at 96 h this trend persists (although not statistically significant), it is firmly supported by our proliferation results, which showed suppression of cell division at 96 h. Furthermore, even though cell phase data at 96 h tended to recover towards normality, the effects of suppressed cell division at 72 h would impact the proliferation data at 96 h.

The mechanism by which CM affects BECs (bEnd.3 cells) via paracrine factors is most likely a result of suppression of ATP generation. Previous results from our laboratory demonstrated that cancer cells and their secretions modulate the mitochondrial activity of endothelial cells, decreasing ATP cellular concentrations [23]. Mitochondria are an essential regulator for cell metabolism and proliferation [22] and any suppression of mitochondrial function, which effectively decreases ATP levels in the cell, would trigger a decrease in the energy-intensive process of mitosis.

## 5. Conclusions

In this brief report, we provide evidence on the differential effects of normoxically-and hypoxically-induced paracrine factors in suppressing the proliferation of BECs. Hypoxic incubation tends to induce cancer cells into a more aggressive secretion of paracrine factors which brings about an increased suppression of BEC division. Our cell cycle data indicate that these paracrine factors tend to prevent BEC (bEnd.3) from entering into the G2 phase, suppressing cell division by preventing these BEC (bEnd.3) from entering into the active mitotic phase of cell division. Our in vitro experimental treatment with paracrine secretions from cancer cells indicates that an important mechanism by which cancer cells manipulate brain capillary endothelial cells is by hampering their normal proliferation in an attempt to compromise capillary integrity. This would ultimately assist either intravasation and/or extravasation of cancer cells during the process of metastasis. The fact that these paracrine

factors show dose-related effects on proliferation suggest an important avenue for further research into the prevention of cancer metastasis.

**Author Contributions:** D.F. and M.R. contributed equally to the conceptualization and drafting of the paper, while the editing was carried out by D.F. Collection of experimental data and statistical analysis was carried out by M.R. All authors have read and agreed to the published version of the manuscript.

**Funding:** Funding received from the University of the Western Cape: SNS funds.

**Institutional Review Board Statement:** Not applicable.

**Informed Consent Statement:** Not applicable.

**Data Availability Statement:** The data is archived according to UWC policies. The data presented in this study are available on request from the corresponding author.

**Acknowledgments:** We acknowledge the services and support of IMBM (UWC) for the use of their FACS flow cytometry infrastructure.

**Conflicts of Interest:** The authors declare no conflict of interest.

## References

- Witzel, I.; Oliveira-Ferrer, L.; Pantel, K.; Müller, V.; Wikman, H. Breast cancer brain metastases: Biology and new clinical perspectives. *Breast Cancer Res.* **2016**, *18*, 8. [\[CrossRef\]](#) [\[PubMed\]](#)
- Zhang, X.; Zhang, W.; Cao, W.-D.; Cheng, G.; Zhang, Y.-Q. Glioblastoma multiforme: Molecular characterization and current treatment strategy (Review). *Exp. Ther. Med.* **2012**, *3*, 9–14. [\[CrossRef\]](#) [\[PubMed\]](#)
- Prabhakaran, N.; Miller, D.C.; Litofsky, N.S.; Frazier, S.R. Extraneural Metastasis of Primary Glioma Occurring in a Setting of Occupational Ionizing Radiation Exposure. *Case Rep. Neurol. Med.* **2019**, *2019*, 1748739. [\[CrossRef\]](#)
- Bockhorn, M.; Jain, R.K.; Munn, L.L. Active versus passive mechanisms in metastasis: Do cancer cells crawl into vessels, or are they pushed? *Lancet Oncol.* **2007**, *8*, 444–448. [\[CrossRef\]](#)
- Zhang, Y.; Wang, S.; Dudley, A.C. Models and molecular mechanisms of blood vessel co-option by cancer cells. *Angiogenesis* **2020**, *23*, 17–25. [\[CrossRef\]](#)
- Donnem, T.; Hu, J.; Ferguson, M.; Adighibe, O.; Snell, C.; Harris, A.L.; Gatter, K.C.; Pezzella, F. Vessel co-option in primary human tumors and metastases: An obstacle to effective anti-angiogenic treatment? *Cancer Med.* **2013**, *2*, 427–436. [\[CrossRef\]](#)
- Seano, G.; Jain, R.K. Vessel co-option in glioblastoma: Emerging insights and opportunities. *Angiogenesis* **2020**, *23*, 9–16. [\[CrossRef\]](#)
- Teuwen, L.A.; de Rooij, L.P.M.H.; Cuyppers, A.; Rohlenova, K.; Dumas, S.J.; García-Caballero, M.; Meta, E.; Amersfoort, J.; Taverna, F.; Becker, L.M.; et al. Tumor vessel co-option probed by single-cell analysis. *Cell Rep.* **2021**, *35*, 109253. [\[CrossRef\]](#)
- Wu, W.; Zhao, S. Metabolic changes in cancer: Beyond the Warburg effect. *Acta Biochim. Biophys. Sin.* **2013**, *45*, 18–26. [\[CrossRef\]](#)
- Pascual, G.; Domínguez, D.; Benitah, S.A. The contributions of cancer cell metabolism to metastasis. *Dis. Models Mech.* **2018**, *11*, dmm032920. [\[CrossRef\]](#)
- Zhang, Y.; Yang, J.M. Altered energy metabolism in cancer: A unique opportunity for therapeutic intervention. *Cancer Biol. Ther.* **2013**, *14*, 81–89. [\[CrossRef\]](#) [\[PubMed\]](#)
- Hawk, M.A.; Schafer, Z.T. Mechanisms of redox metabolism and cancer cell survival during extracellular matrix detachment. *J. Biol. Chem.* **2018**, *293*, 7531–7537. [\[CrossRef\]](#) [\[PubMed\]](#)
- Fan, R.; Emery, T.; Zhang, Y.; Xia, Y.; Sun, J.; Wan, J. Circulatory shear flow alters the viability and proliferation of circulating colon cancer cells. *Sci. Rep.* **2016**, *6*, 27073. [\[CrossRef\]](#) [\[PubMed\]](#)
- Sheen-Chen, S.M.; Chen, H.S.; Sheen, C.W.; Eng, H.L.; Chen, W.J. Serum levels of transforming growth factor  $\beta$ 1 in patients with breast cancer. *Arch. Surg.* **2001**, *136*, 937–940. [\[CrossRef\]](#) [\[PubMed\]](#)
- Tatla, A.S.; Justin, A.W.; Watts, C.; Markaki, A.E. A vascularized tumoroid model for human glioblastoma angiogenesis. *Sci. Rep.* **2021**, *11*, 19550. [\[CrossRef\]](#) [\[PubMed\]](#)
- Dvorak, H.F. Vascular permeability factor/vascular endothelial growth factor: A critical cytokine in tumor angiogenesis and a potential target for diagnosis and therapy. *J. Clin. Oncol.* **2002**, *20*, 4368–4380. [\[CrossRef\]](#)
- Valable, S.; Montaner, J.; Bellail, A.; Berezowski, V.; Brillault, J.; Cecchelli, R.; Divoux, D.; MacKenzie, E.T.; Bernaudin, M.; Roussel, S.; et al. VEGF-induced BBB permeability is associated with an MMP-9 activity increase in cerebral ischemia: Both effects decreased by Ang-1. *J. Cereb. Blood Flow Metab.* **2005**, *25*, 1491–1504. [\[CrossRef\]](#)
- Mendonça, M.C.P.; Soares, E.S.; Stávale, L.M.; Kalapothakis, E.; Cruz-Höfling, M.A. Vascular Endothelial Growth Factor Increases during Blood-Brain Barrier-Enhanced Permeability Caused by Phoneutria nigriventer Spider Venom. *BioMed Res. Int.* **2014**, *2014*, 721968. [\[CrossRef\]](#)
- Jiang, S.; Xia, R.; Jiang, Y.; Wang, L.; Gao, F. Vascular Endothelial Growth Factors Enhance the Permeability of the Mouse Blood-brain Barrier. *PLoS ONE* **2014**, *9*, e86407. [\[CrossRef\]](#)



20. Argaw, A.T.; Gurfein, B.T.; Zhang, Y.; Zameer, A.; John, G.R. VEGF-mediated disruption of endothelial CLN-5 promotes blood-brain barrier breakdown. *Proc. Natl. Acad. Sci. USA* **2009**, *106*, 1977–1982. [\[CrossRef\]](#)
21. Hambardzumyan, D.; Bergers, G. Glioblastoma: Defining Tumor Niches. *Trends Cancer* **2015**, *1*, 252–265. [\[CrossRef\]](#) [\[PubMed\]](#)
22. Arciuch, V.G.A.; Elguero, M.E.; Poderoso, J.J.; Carreras, M.C. Mitochondrial regulation of cell cycle and proliferation. *Antioxid. Redox Signal.* **2012**, *16*, 1150–1180. [\[CrossRef\]](#) [\[PubMed\]](#)
23. Rado, M.; Flepisi, B.; Fisher, D. Differential Effects of Normoxic versus Hypoxic Derived Breast Cancer Paracrine Factors on Brain Endothelial Cells. *Biology* **2021**, *10*, 1238. [\[CrossRef\]](#) [\[PubMed\]](#)
24. Rado, M.; Flepisi, B.; Fisher, D. The Effect of Normoxic and Hypoxic U-87 Glioblastoma Paracrine Secretion on the Modulation of Brain Endothelial Cells. *Cells* **2022**, *11*, 276. [\[CrossRef\]](#) [\[PubMed\]](#)
25. Zhang, J.; Han, X.; Lin, Y. Dissecting the regulation and function of ATP at the single-cell level. *PLoS Biol.* **2018**, *16*, e3000095. [\[CrossRef\]](#) [\[PubMed\]](#)
26. Leone, J.P.; Leone, B.A. Breast cancer brain metastases: The last frontier. *Exp. Hematol. Oncol.* **2015**, *4*, 33. [\[CrossRef\]](#)
27. Watkins, S.; Robel, S.; Kimbrough, I.F.; Robert, S.M.; Ellis-Davies, G.; Sontheimer, H. Disruption of astrocyte-vascular coupling and the blood-brain barrier by invading glioma cells. *Nat. Commun.* **2014**, *5*, 4196. [\[CrossRef\]](#)
28. Lah, T.T.; Novak, M.; Breznik, B. Brain malignancies: Glioblastoma and brain metastases. *Semin. Cancer Biol.* **2020**, *60*, 262–273. [\[CrossRef\]](#)
29. McKeown, S.R. Defining normoxia, physoxia and hypoxia in tumours—Implications for treatment response. *Br. J. Radiol.* **2014**, *87*, 20130676. [\[CrossRef\]](#)
30. D'Alessio, A.; Proietti, G.; Sica, G.; Scicchitano, B.M. Pathological and molecular features of glioblastoma and its peritumoral tissue. *Cancers* **2019**, *11*, 469. [\[CrossRef\]](#)
31. Mehner, C.; Hockla, A.; Miller, E.; Ran, S.; Radisky, D.C.; Radisky, E.S. Tumor cell-produced matrix metalloproteinase 9 (MMP-9) drives malignant progression and metastasis of basal-like triple negative breast cancer. *Oncotarget* **2014**, *5*, 2736–2749. [\[CrossRef\]](#) [\[PubMed\]](#)
32. Labelle, M.; Hynes, R.O. The initial hours of metastasis: The importance of cooperative host-tumor cell interactions during hematogenous dissemination. *Cancer Discov.* **2013**, *2*, 1091–1099. [\[CrossRef\]](#) [\[PubMed\]](#)
33. Cao, H.; Yu, D.; Yan, X.; Wang, B.; Yu, Z.; Song, Y.; Sheng, L. Hypoxia destroys the microstructure of microtubules and causes dysfunction of endothelial cells via the PI3K/Stathmin1 pathway. *Cell Biosci.* **2019**, *9*, 20. [\[CrossRef\]](#) [\[PubMed\]](#)
34. Engelhardt, S.; Huang, S.; Patkar, S.; Gassmann, M.; Ogunshola, O.O. Differential responses of blood-brain barrier associated cells to hypoxia and ischemia: A comparative study. *Fluids Barriers CNS* **2015**, *12*, 4. [\[CrossRef\]](#)
35. Cohen, E.B.; Gecki, R.C.; Toker, A. Metabolic pathway alterations in microvascular endothelial cells in response to hypoxia. *PLoS ONE* **2020**, *15*, e0232072. [\[CrossRef\]](#)
36. Baldea, I.; Teacoe, I.; Olteanu, D.E.; Vaida-Voievod, C.; Clichici, A.; Sirbu, A.; Filip, G.A.; Clichici, S. Effects of different hypoxia degrees on endothelial cell cultures—Time course study. *Mech. Ageing Dev.* **2018**, *172*, 45–50. [\[CrossRef\]](#)
37. Giusti, I.; Monache, D.S.; di Francesco, M.; Sanit, P.; D'Ascenzo, S.; Gravina, G.L.; Festuccia, C.; Dolo, V. From glioblastoma to endothelial cells through extracellular vesicles: Messages for angiogenesis. *Tumor Biol.* **2016**, *37*, 12743–12753. [\[CrossRef\]](#)
38. Formolo, C.A.; Williams, R.; Gordish-Dressman, H.; MacDonald, T.J.; Lee, N.H.; Hathout, Y. Secretome signature of invasive glioblastoma multiforme. *J. Proteome Res.* **2011**, *10*, 3149–3159. [\[CrossRef\]](#)
39. Charalambous, C.; Hofman, F.M.; Chen, T.C. Functional and phenotypic differences between glioblastoma multiforme—derived and normal human brain endothelial cells. *J. Neurosurg.* **2005**, *102*, 699–705. [\[CrossRef\]](#)
40. Bussolati, B.; Deambrosis, I.; Russo, S.; Deregibus, M.C.; Camussi, G. Altered angiogenesis and survival in human tumor-derived endothelial cells. *FASEB J.* **2003**, *17*, 1159–1161. [\[CrossRef\]](#)
41. Khodarev, N.N. Tumour-endothelium interactions in co-culture: Coordinated changes of gene expression profiles and phenotypic properties of endothelial cells. *J. Cell Sci.* **2003**, *116*, 1013–1022. [\[CrossRef\]](#) [\[PubMed\]](#)
42. McKinnon, K.M. Flow cytometry: An overview. *Curr. Protoc. Immunol.* **2019**, *120*, 5.1.1–5.1.11. [\[CrossRef\]](#) [\[PubMed\]](#)
43. Liao, X.; Makris, M.; Luo, X.M. Fluorescence-activated cell sorting for purification of plasmacytoid dendritic cells from the mouse bone marrow. *J. Vis. Exp.* **2016**, *2016*, e54641. [\[CrossRef\]](#) [\[PubMed\]](#)
44. Bonner, W.A.; Hulett, H.R.; Sweet, R.G.; Herzenberg, L.A. Fluorescence activated cell sorting. *Rev. Sci. Instrum.* **1972**, *43*, 404–409. [\[CrossRef\]](#)



## CHAPTER 6

### General conclusions and recommendations

#### 6.1. General conclusion

The current study investigated the modulatory effect of cancer secretion derived from glioblastoma cells (U-87) and breast cancer cells (MCF7) on brain endothelial cells (bEnd.3).

This study considered the high ability of cancer cells to alter their metabolic characteristics depending upon the surrounding environmental conditions (such as the availability of Oxygen), increasing their malignancy and resistance to therapeutic methods. Invasive cancer cells are characterized by their high ability to secrete variant substances to invade the surrounding tissues and spread to new places in the other organs. Thus, the study focused on the paracrine effect of the soluble factors secreted in the condition media of glioblastoma U-87 cells and breast cancer MCF7 cells in different physiological conditions (normoxia and hypoxia) on the brain endothelial features. A non-direct coculture system was established to maintain the cross-talk between cancer cells and brain endothelial cells.

Both glioblastoma and breast cancer cells use blood vessels to spread. The mechanism to overcome the endothelial barrier at the blood-brain barrier (BBB) is always discussable. Previous studies showed that the endothelial cells in cancer environments were subjected to morphological and structural changes associated with their functional properties. The current study showed that cancer cells, through their secretions, can disrupt the function of the brain endothelial cells.

The current study showed that cancerous secretions from breast cancer cells and brain cancer cells could negatively affect brain endothelial cells by disrupting

mitochondrial function and ATP generation, decreasing cell viability, integrity, and proliferation.

Our data showed that hypoxic metastatic breast cancer cells severely affect brain endothelial cells. The endothelial mitochondrial activity decreased irreversibly after 48hr of exposure, whereas the effect of normoxic breast cancer cells was mostly shown after 96hours. That was reflected in the endothelial tightness of the brain endothelial cells. Normoxic cancer cells disturb the endothelial monolayer integrity for only 24hours before it recovers to the control level. In contrast, the hypoxic breast cancer effect in disturbing the endothelial integrity was permanent.

Brain cancer cells differentially induced the brain endothelial modulation. Brain cancer cells under hypoxia could affect the viability of brain endothelial cells after 24 hours of coculture. In contrast, brain cancer cells needed 72 hours to affect the viability of brain endothelial cells under normoxia. After exposure to hypoxic brain cancer, the uncoupling of  $\Delta\Psi_m$  modulated the mitochondrial ATP generation in brain endothelial cells. The brain endothelial integrity was depressed after exposure to normoxic and hypoxic brain cancer cells. Only hypoxic cause irreversible disruption in the integrity of the endothelial monolayer.

Both breast and brain cancer cells negatively affected endothelial proliferation through their hypoxic and normoxic secretions. However, Hypoxic cancerous cells tend to induce cancer cells into a more aggressive secretion of paracrine factors, which brings about an increased suppression of BEC division.

Overall, Data suggest that cancer secreted factors are the mediators to modulate the brain endothelial cell function; thus, the manipulation of cancer- endothelial cells cross-talk may be a base to develop a therapeutic target for cancer and the BBB disruption

## 6.2. Recommendations

The study showed the paracrine effect of U-87 glioblastoma cells and MCF7 breast cancer secretion on the modulation of the mitochondrial activity of brain endothelial cells; however, the study can be expanded to include identification and quantification of possible active compounds cancerous factors secreted from these cancer cells, and that by using LC-MS/MS. Western blotting could also be done in lieu of qPCR profiling to assess protein expression of the endothelial tight junction. Ultrastructural changes in the bEnd.3 exposed to cancer secretion could be studied using scanning and transmission electron microscopic techniques. Lastly, an appropriate *in vivo* model could be used to study the influence of cancer secretion on the BBB in a living system.

